





Dra. Pilar Campins Falcó, Catedrática, y Dra. Yolanda Moliner Martínez, Profesora Titular, ambas del Departamento de Química Analítica de la Universitat de València,

**CERTIFICAN**

Que la presente memoria, titulada “New strategies for improving the sustainability of analytical methods in different matrices”, constituye la Tesis Doctoral de Lusine Hakobyan para optar al grado de Doctora en Química, y que ha sido realizada en los laboratorios del Departamento de Química Analítica de la Universitat de València, bajo nuestra dirección y supervisión.

Y para que así conste a los efectos oportunos, firman el presente certificado en València, a 15 de enero de 2021.

Fdo. Dra. Pilar Campins Falcó

Directora de Tesis

Fdo. Dra. Yolanda Moliner Martínez

Codirectora de Tesis





***Lo que importa verdaderamente en la vida no son los objetivos que nos marcamos sino los caminos que seguimos para lograrlos.***

***(Peter Bamm)***



## **AGRADECIMIENTOS**

En primer lugar, me gustaría agradecer a Pilar por aceptarme en el grupo de investigación Mintota, por darme la oportunidad de volver a retomar el camino académico y así poder lograr el objetivo que tuve que dejar en su día en Armenia. Su profesionalidad y constancia me han transmitido los valores necesarios para mejorar mis aptitudes dentro de este campo.

Además, quisiera mostrar mis agradecimientos a Yolanda y Carmen por guiarme durante el doctorado y transmitirme sus conocimientos en investigación. Me han enriquecido tanto a nivel personal como profesional.

También quisiera mencionar a Rosa y Jorge, los cuales han sabido ayudarme en los momentos en los que los he necesitado.

De entre todas las cosas que me ha aportado el grupo, quisiera destacar el ambiente de compañerismo existente que me ha permitido desarrollar mi trabajo de la mejor forma posible. Así se puede lograr cualquier objetivo.

Y por supuesto no podría olvidarme de mis compañeros doctorandos: María, Anabel, Pascu, Javi, Neus, Rodrigo, Sara, Ana, Lorenzo, Adri, Henry, Sergio, Héctor, Rocío, David y Camila. Gracias por vuestros ánimos, vuestro apoyo y sobre todo por las risas compartidas. Además, tampoco puedo olvidarme de Amparo, con la cual he compartido grandes momentos en comidas, cenas y viajes.

También me gustaría agradecer a los miembros del grupo de investigación GICAPC, especialmente a Juanlu, Lori, Cristian, Víctor, Laura, Pepe y Pablo por los momentos divertidos que hemos compartido durante las comidas y en los congresos.

Por último, doy las gracias a mi familia, mi gran apoyo en los momentos más difíciles y quien me ha dado fuerza para seguir adelante. Una parte de este gran trabajo os lo dedico a vosotros.



## RESUMEN

El concepto “sostenible” apareció en los años 70 con el objetivo de relacionar el desarrollo económico y la conservación de los ecosistemas. La palabra sostenibilidad se debe al informe Brundland realizado en 1987 en el marco de la Comisión de las Naciones Unidas para el Medio Ambiente. Este informe advirtió sobre las consecuencias ambientales negativas del desarrollo económico y la globalización, tratando de ofrecer soluciones a los problemas derivados del crecimiento demográfico y la industrialización. *La sostenibilidad persigue garantizar el equilibrio entre crecimiento económico, cuidado del medio ambiente y bienestar social.*

Esta definición da lugar a la idea de desarrollo sostenible, progreso que no compromete los recursos futuros dándole un carácter multidisciplinar. La sostenibilidad asume que la naturaleza y el medio ambiente son fuentes agotables de recursos, siendo necesarios su protección y uso racional en todos los ámbitos. La calidad de vida de una sociedad depende en gran medida de su calidad ambiental y del bienestar económico. Se requiere por tanto un equilibrio entre tres elementos: medio ambiente, economía y sociedad, logrando el desarrollo en cada uno de ellos sin repercusiones negativas en los demás.

**Particularizando en la Química**, el calificativo sostenible aporta un enfoque holístico, que establece políticas y objetivos medibles para un proceso continuo de mejora. En este contexto, la Química Verde aparece directamente relacionada con la Química Sostenible.

*“La Química Verde se define como la química que se centra en el diseño, obtención, fabricación y uso de productos químicos que tengan un potencial de contaminación reducido o nulo”.* Nació a principios de la década de 1990 en Estados Unidos a través de la Agencia de Protección Ambiental como herramienta conceptual para la protección del medio ambiente y fue expresada en 12 principios establecidos por Paul Anastas y John Warner en 1998.

*“La Química Sostenible no solo incluye los conceptos de Química Verde, también amplía la definición para considerar el proceso químico y también sus efectos, materiales, energía y economía”.* Un proceso químico sostenible es aquel que no produce impactos ambientales y residuos, aporta eficiencia en la reacción

considerada en su caso, utiliza cantidades mínimas de energía y es económicamente justificado en el marco del problema a resolver.

La **Química Analítica Sostenible** une la Química Analítica Verde, cuyos 12 principios definidos por Galuzca et al. se basan en los de la química verde, y los principios socio-económicos. La Química Analítica tiene un papel importante en el desarrollo de la sostenibilidad, a través del seguimiento de contaminantes en el medio ambiente y de procesos y a su vez disminuyendo el impacto medioambiental de sus propias metodologías. Reducir la cantidad de disolventes necesarios en la etapa de pretratamiento de la muestra, la cantidad y toxicidad de los disolventes y reactivos utilizados para la medición mediante su automatización y/o miniaturización y desarrollar metodologías analíticas alternativas que no requieran de disolventes ni reactivos son posibles medidas a adoptar.

Por otra parte, existe una necesidad creciente de utilizar métodos para evaluar la sostenibilidad de un proceso o producto en general, con la finalidad de categorizar su impacto. En esta Tesis se ha propuesto la huella de carbono como medida directa de impacto ambiental de metodologías analíticas y se ha utilizado la herramienta hexágono propuesta por nuestro grupo de investigación MINTOTA-UV para medir la sostenibilidad de procedimientos analíticos. Se contribuye a la Química Analítica Sostenible desde dos estrategias diferentes:

1. Pretratamiento de la muestra en línea y miniaturización mediante el desarrollo de la técnica microextracción en tubo acoplada a cromatografía líquida capilar (IT-SPME-CapLC).
2. Desarrollo de dispositivos colorimétricos para análisis in situ.

El pretratamiento de la muestra suele ser necesario para extraer, aislar y concentrar los analitos de interés. Este paso aumenta por tanto la selectividad y la sensibilidad. Sin embargo, implica un alto grado de manipulación de la muestra, que conduce a métodos no eficientes en términos de impacto ambiental y económico. La extracción en fase sólida (SPE) es una de las técnicas más utilizadas. Se basa en el uso de columnas empaquetadas con una fase sólida adsorbente capaz de retener los analitos cuando la muestra pasa a través de ella o está en contacto con la fase extractante.

Arthur y Pawliszyn en 1990 introdujeron la microextracción en fase sólida (SPME), como alternativa miniaturizada a la SPE. En 1997 Eisert y Pawliszyn propusieron la microextracción en fase sólida en tubo (IT-SPME). Esta técnica es de gran interés desde el punto de vista de la Química Analítica Sostenible ya que es automatizable y es fácil de acoplar a cromatografía líquida (LC). Además de facilitar y simplificar en gran medida la etapa de pretratamiento de la muestra, IT-SPME es una técnica respetuosa con el medio ambiente, ya que minimiza el uso de disolventes, reduce la generación de residuos y, finalmente, se puede acoplar en línea a LC.

Los principales parámetros relacionados con la eficiencia de extracción en IT-SPME son la fase extractiva, el caudal, el volumen de muestra procesada y la longitud de la columna capilar. Por tanto, deben tenerse en cuenta a la hora de diseñar el procedimiento IT-SPME. La selección de la fase de extracción es un parámetro clave ya que el éxito en la eficiencia de extracción depende de la interacción entre los analitos objetivo y la fase.

La miniaturización de los sistemas de cromatografía líquida (LC) fue propuesta en 1967 considerando la disminución del diámetro interno (i.d.) de la columna analítica. Su disminución conlleva un menor flujo de fase móvil, reduciendo el consumo de disolventes y por tanto la cantidad de residuos generados. Según Nazario et al. 2015, la disminución en el flujo de la fase móvil posibilita además nuevos mecanismos de interacción entre la fase móvil y los analitos, lo que conduce a una mayor selectividad. Por otro lado, la reducción del diámetro interno de la columna analítica también disminuye el volumen de muestra requerido. Los efectos señalados son factores positivos para la química analítica sostenible.

Esta Tesis demuestra que un sistema miniaturizado como CapLC acoplado en línea a IT-SPME es una herramienta eficaz y versátil para el análisis de una gran variedad de analitos en diferentes matrices: ambientales, biológicas, alimentarias y forenses, entre otros.

Otro de los retos que aborda la Tesis es el desarrollo de dispositivos que permitan realizar determinaciones in situ, es decir, en el lugar donde se encuentra el compuesto de interés y se produce el problema. Además de evitar el transporte de la muestra al laboratorio, que conlleva tiempo, costes y recursos, también se

minimiza el riesgo de contaminación o degradación de la muestra. Los dispositivos de análisis in-situ deben cumplir una serie de características, como portabilidad, bajo costo, simplicidad y rapidez, dichas características los hacen especialmente atractivos desde el punto de vista de la Química Analítica Sostenible.

Los sensores químicos son dispositivos formados por un elemento de reconocimiento que está en contacto directo con un elemento de transducción, siendo capaces de proporcionar información química específica. Los sensores colorimétricos presentan ventajas ya que se basan en cambios de color y la lectura puede ser realizada de distintas formas:

- ✓ En un laboratorio con un Instrumento óptico o in situ con un instrumento óptico portátil.
- ✓ Mediante análisis de imágenes digitalizadas para medición in situ.
- ✓ Por inspección visual para realizar mediciones in situ (semi)cuantitativas.

En esta Tesis se han desarrollado composites poliméricos de polidimetilsiloxano (PDMS), pudiendo contener tetraetilortosilicato (TEOS), nanopartículas de sílice ( $\text{SiO}_2$  NPs), líquidos iónicos (IL), y sensores sólidos plasmónicos soportados en nylon. Se han propuesto dispositivos basados en PDMS dopados con 1,2-naftoquinona-4-sulfonato (NQS). El cambio de color se produce por reacción de sustitución nucleofílica entre los grupos amino y el grupo sulfonato del NQS. Otro caso estudiado es el atrapamiento del reactivo de Griess (sulfanilamida y N-(1-naftil) etilendiamina) en el soporte polimérico PDMS. La derivatización se basa en la formación de compuestos azoicos entre el reactivo de Griess y nitrito. Se ha extendido su uso para la medida de nitrato proponiendo una dispersión de nanopartículas de zinc (ZnNPs) inmovilizada o no en nylon. También se ha propuesto un soporte PDMS dopado con reactivo colorimétrico azul sólido BB (FB). El cambio de color se basa en la formación del complejo azo entre FB y alquilresorcinoles (AR). La respuesta de los sensores sólidos plasmónicos, concretamente las nanopartículas de plata (AgNPs) retenidas en nylon, se basa en la banda de resonancia de plasmón superficial que se modifica por la agregación de los AgNPs en presencia de compuestos sulfurados.

Cabe destacar que en la actualidad existen varias aplicaciones gratuitas y disponibles que se pueden utilizar para el análisis de imágenes. Software como Adobe Photoshop, GNU, GIMP, ImageJ, entre otros, son capaces de convertir una



señal de color en diferentes parámetros numéricos. Existen varios modelos de descomposición de color (RGB, HSV, CMYK, CIELAB), que pueden posibilitar información analítica.

**RGB** (Rojo, Verde, Azul): Los colores se crean a partir de la combinación de sus tres colores primarios (rojo, verde y azul), las intensidades pueden variar entre 0 y 255.

**HSV** (Matiz, Saturación, Valor): Es una combinación de tres valores: matiz, saturación y brillo. Por tanto, este modelo proporciona información sobre la cantidad y brillo del color.

**CMYK** (Cyan, Magenta, Yellow y Key): es un modelo de color sustractivo, utilizado en la impresión en color.

El espacio de color **CIELAB**, también conocido como  $L^* a^* b^*$ , es un espacio de color definido por la Comisión Internacional de Iluminación (abreviado CIE) en 1976.

Estos modelos son herramientas para el análisis de imágenes. Sin embargo, la etapa de adquisición de la imagen juega un papel fundamental, ya que de ella dependen los resultados derivados de su posterior tratamiento. Uno de los parámetros que más puede influir en la calidad de la imagen obtenida es la iluminación, de acuerdo con Chaplan et al. (2014).

Se han propuesto diferentes opciones para minimizar el impacto de la luz externa. En esta Tesis se emplearon el software GIMP y el modelo RGB para descomposición de color de las imágenes de los sensores realizadas con un teléfono móvil.

El objetivo general de esta Tesis ha sido el desarrollo de metodologías analíticas sostenibles que resuelvan diferentes problemas en diferentes campos. Los objetos específicos han sido:

1. Desarrollar herramientas analíticas para abordar la sostenibilidad y la química analítica mediante el uso de dos estrategias:
  - ✓ IT-SPME – Cap LC DAD
  - ✓ Dispositivos sólidos de análisis in situ

2. Evaluar el IT-SPME acoplado CapLC-DAD como una herramienta sostenible basada en la miniaturización del pretratamiento de muestra y del proceso cromatográfico.
3. Desarrollar dispositivos dopados en diferentes soportes (PDMS, nylon) para realizar análisis in situ.
4. Realizar pruebas de concepto de los procedimientos propuestos para varios analitos de interés (orgánicos e inorgánicos) en distintas matrices tales como ambientales, biológicas, alimentarias y forenses.

### **Matrices ambientales**

Se ha abordado la determinación de herbicidas (irgarol-1051 y diuron) en aguas superficiales mediante técnicas IT-SPME-CapLC y, por otro lado, la de nitrato y nitrito en aguas ambientales mediante dispositivos in situ basados en PDMS como soporte sólido dopado con el reactivo Griess.

- Para la determinación de irgarol -1051 y diuron en aguas superficiales, se optimizó la naturaleza de la fase sorbente, la longitud de la columna capilar y el volumen de muestra procesada. Los límites de detección (LD) fueron 0.015 y 0.2 µg /L para irgarol-1051 y diuron utilizando detector de fila de diodos (DAD), por lo que se puede utilizar para evaluar el cumplimiento de la normativa europea. Se estimó la precisión de los tiempos de retención y los valores de RSD para diurón e irgarol-1051 fueron de 0,3 y 0,5%. Esta estrategia no solo fue evaluada en términos de parámetros analíticos básicos, sino también en términos de impacto ambiental, comparándola con otras metodologías propuestas en la literatura sobre el tema. Para ello, se propuso y evaluó la huella de carbono. Los resultados indicaron que la metodología más sostenible para determinar irgarol-1051 y diurón es el IT-SPME-CapLC-DAD. Por lo tanto, puede ser una metodología alternativa fácilmente aplicable y respetuosa con el medio ambiente para estimar los dos analitos en muestras de agua ambientales. Los resultados mostraron que irgarol-1051 y diurón estaban por debajo de los LDs y, por lo tanto, las muestras de agua ensayadas cumplían con los estándares de calidad europeos establecidos.
- Para determinar nitrito o nitrato en muestras de agua, se ha desarrollado una membrana de PDMS modificado con líquido iónico (IL) y dopada con el reactivo de Griess La determinación de nitrito y nitrato en muestras de

agua se realizó mediante análisis in situ. Se estudió la influencia de algunos compuestos dopantes, sobre las propiedades de las membranas de PDMS, como el TEOS, y/o líquidos iónicos. El IL hexafluorofosfato de 1-metil-3-octilimidazolio (OMIM-PF<sub>6</sub>) proporcionó los mejores resultados. En esta membrana el reactivo de Griess es más estable que en disolución y se libera a la disolución para llevar a cabo la reacción de derivatización. Para aplicar el procedimiento al nitrato se propuso una dispersión de nanopartículas de Zn (ZnNPs) en una mezcla de tensioactivos (SDS/CTAB). Se estudió la adición de ZnNP y se comparó con la de polvo de Zn. También se estudió la capacidad de reducción de ZnNPs utilizando dos enfoques: (i) en disolución y (ii) inmovilización de ZnNPs en membranas de nylon. Finalmente, las respuestas analíticas se obtuvieron midiendo la absorbancia o utilizando los componentes RGB de imágenes digitales. Los resultados indicaron una buena precisión (RSD <8%) y una estabilidad satisfactoria. El límite de detección alcanzado fue de 0.01 y 0.5 mg/L para nitrito y nitrato. La aplicación práctica se demostró mediante el análisis de diferentes aguas ambientales. Los resultados obtenidos fueron satisfactorios y estadísticamente comparables con los obtenidos mediante electrodo selectivo de nitrato o espectroscopía UV-Vis. Por lo tanto, se puede decir que este estudio ofrece una nueva metodología sostenible para la determinación in situ de nitrito y nitrato en matrices de agua.

### **Matrices biológicas**

Se han estudiado cuatro casos de potencial uso. Determinación de antibióticos como meropenem en tubos endotraqueales mediante IT-SPME-CapLC, sulfuros en cardiomiocitos y en aire exhalado mediante sensor plasmónico sólido basado en la inmovilización de AgNPs sobre membrana de nylon. Finalmente, se ha propuesto un dispositivo dopado de PDMS y también IT-SPME-CapLC para la determinación de alquilresorcinolos (AR) en muestras de orina.

- Cuantificar la concentración de antibiótico en dispositivos médicos invasivos puede dar información sobre su capacidad de penetrar en el biofilm que se genera y, por tanto, sobre la eficacia ofrecida en el tratamiento de la infección. Con ese objetivo se ha propuesto IT-SPME

acoplado en línea a CapLC-DAD para determinar la concentración de meropenem en tubos endotraqueales de pacientes en unidad de cuidados intensivos que fueron tratados con este antibiótico. Se estudió la extracción de meropenem de los ETT. Se ensayó la extracción directa, extracción asistida por agitación y extracción por ultrasonido. Los resultados indicaron resultados de recuperación similares y, por lo tanto, se eligió la extracción directa. La aplicación del procedimiento propuesto ha dado lugar a límites de detección muy bajos (3ng/mL) y precisión satisfactoria (RSD <4%). Se encontró meropenem en concentraciones del orden de ng/mL en los tubos ETT. La validación del procedimiento se llevó a cabo mediante un estudio de recuperación. Los valores de recuperación mostraron resultados satisfactorios (94-103%). El nuevo enfoque propuesto en este trabajo ha demostrado ser una alternativa no solo por la sensibilidad y precisión, sino también por la sencillez, la rentabilidad, minimización del uso de reactivos y disolventes y el tiempo de análisis, contribuyendo por tanto a la química analítica sostenible.

- La determinación de compuestos de sulfuro volátiles (VSC) en el aliento humano se determinó mediante el uso de un sensor plasmónico de AgNPs. El mecanismo de retención y agregación de AgNPs se ha confirmado mediante espectroscopía UV-vis, TEM, SEM y espectroscopia Raman. Además, se demostró la agregación de AgNPs debido a la presencia de sulfuro a partir del aumento en el diámetro hidrodinámico, estimado usando la técnica analítica de fraccionamiento en flujo mediante campo de flujo asimétrico (AF4) acoplado en línea a dispersión dinámica de luz (DLS). Otra característica importante que se estudió es el tamaño de partícula de los AgNPs que puede afectar a la sensibilidad, eligiendo AgNPs de 20nm para el diseño del sensor. En presencia de compuestos de sulfuro a niveles de ppbv las membranas plasmónicas cambiaron el color del amarillo a naranja/marrón. La espectrofotometría de reflectancia difusa y las imágenes digitales procesadas obtenidas con un teléfono inteligente se han utilizado como medidas para análisis cuantitativo. Se alcanzó un intervalo lineal para sulfuro de hidrógeno de 150 a 1000 ppbv y un límite de detección (LD) de 45 ppbv,

midiendo después de 10 min de exposición del sensor a la atmósfera de sulfuro de hidrógeno (2 L) para porcentajes de humedad entre 50 y 96% y temperatura ambiente. El límite de detección se puede mejorar aumentando el tiempo de exposición, si es necesario. También se obtuvieron resultados satisfactorios en términos de precisión (<10%) y selectividad. Finalmente, las membranas se aplicaron para la determinación de compuestos sulfurosos volátiles en el aliento exhalado de 10 voluntarios humanos sanos. Los niveles de H<sub>2</sub>S detectados en el aliento humano exhalado podrían servir como marcadores para algunas enfermedades, tales como la halitosis. Sus valores se encontraron en el intervalo de concentración de 70 a 210 ppbv, por debajo del límite de diagnóstico de periodontitis o gingivitis (250 ppbv). El sensor colorimétrico plasmónico propuesto es estable y presenta una sensibilidad óptima. Además, es económico, desechable, seguro y fácil de usar y se ha aplicado con éxito para determinar los VSC expresados como sulfuro de hidrógeno en muestras de aliento a diferentes volúmenes de muestreo entre 2 L y 250 mL, como prueba de concepto.

- Para la detección de H<sub>2</sub>S en muestras biológicas (cardiomiocitos) mediante análisis in vitro se ha desarrollado una tecnología para preparar un multisensor colorimétrico en fase sólida (hasta 96 dispositivos). Aparte de la simplicidad en la fabricación, también es rápido de preparar y el costo de fabricación es muy bajo. La placa de multisensor se prepara en 3 min. Se optimizó el volumen necesario de dispersión de AgNPs en el nylon, eligiendo 110 µL como valor óptimo para cada sensor unitario. También se estudió la precisión con y sin glicerol midiendo la reflectancia difusa de una placa con 14 y 24 sensores respectivamente, siendo los valores de RSD (%) obtenidos inferiores al 5%. Como señales analíticas se proponen los espectros normalizados a 500 nm obtenidos usando la técnica analítica de espectrofotometría de reflectancia difusa. El intervalo lineal para H<sub>2</sub>S fue 0.34 – 8 µM y el límite de detección fue de 0.13µM, se estimaron en condiciones de incubación a 37 ° C y 95% de humedad durante 8 horas. Se realizó una evaluación mediante la herramienta hexágono de evaluación y selección de métodos analíticos. Dicha herramienta

permite indicar que el método presenta ventajas como alta sensibilidad, menor costo económico y mayor sostenibilidad que otros métodos analíticos recientes propuestos en la literatura. La estrategia propuesta es energéticamente eficiente, no requiere pretratamiento de la muestra, portátil, rápido y de fácil manejo por personal no especializado y ofrece la ventaja de análisis simultáneo con alta sensibilidad para la determinación de sulfuro de hidrógeno en muestras biológicas como células, y también es aplicable para otro tipo de matrices como plasma o saliva, entre otras.

- Se han propuesto los alquilresorcinoles (AR) como biomarcadores sensibles y específicos del consumo de gluten. El dispositivo colorimétrico propuesto se sintetizó dopando un composite PDMS/TEOS con el reactivo azul sólido (Fast Blue B salt, FB). El ensayo se basó en la liberación de FB a la solución que contiene AR y la formación del complejo azo que se midió a 520 nm. La respuesta se evaluó por espectroscopia UV-vis y IT-SPME-LC-DAD para aislar la señal del ácido 3,5-dihidroxihipocinámico (DHCA). Los resultados indicaron que el análisis espectroscópico se puede utilizar como una herramienta de detección para diferenciar muestras positivas y negativas. El ensayo cromatográfico permite aislar la respuesta de AR en muestras positivas. En las condiciones experimentales óptimas, el valor de LD fue de 60 ng/mL al agregar un paso de extracción en fase sólida (cartuchos C18) antes del análisis, la precisión fue del 7 %. Los estudios realizados en muestras de orina muestran que DHCA puede usarse como biomarcador de la ingesta de gluten. Las principales ventajas de la metodología propuesta son el desarrollo de una herramienta de preselección previa al análisis cromatográfico y la miniaturización de éste último y por tanto la simplificación de la evaluación de la transgresión dietética y ello a través de metodologías sostenibles.

## Matrices alimentarias

Se ha desarrollado la determinación de nitrito y nitrato en aguas obtenidas de verduras frescas y enlatadas, además de la determinación de la frescura de muestras de carne a partir de la medida de la liberación de amoníaco, desarrollando composites dopados de PDMS para su uso in situ.

- La determinación de nitrato y nitrito en aguas de muestras de vegetales (acelgas y espinacas) frescos y enlatados se realizó empleando sensores colorimétricos basados en la membrana polimérica de PDMS/TEOS-IL dopada con el reactivo de Griess (SA-NEDD), descrita anteriormente. En el caso del nitrato, se utilizó la dispersión de ZnNPs como agente reductor. La respuesta analítica se obtuvo midiendo la absorbancia o las coordenadas RGB de la imagen digital obtenida de la membrana. Las aguas de verduras frescas y enlatadas se procesaron directamente. Las ventajas del método propuesto están relacionadas con las figuras de mérito obtenidas, la portabilidad, el bajo costo y el corto tiempo de análisis.
- La determinación del amoníaco en atmósferas se realizó empleando sensores basados en PDMS dopados con líquidos iónicos (LI) particularmente con OMIMPF<sub>6</sub>, con la hipótesis de que los IL pueden proporcionar cambios en la morfología del composite, que permiten lograr sensores más sensibles. Además, se demostró la naturaleza másica del sensor y se estableció su cinética. La capacidad de adsorción está de acuerdo con la isoterma de Langmuir y por tanto los sitios de adsorción son homogéneos en el sensor y el mecanismo de respuesta es quimisorción. La calibración es flexible y es función del tiempo de muestreo, la temperatura y el volumen de muestreo. Además, se observó que el sensor IL-NQS-PDMS es capaz de discriminar entre grupos aminos primarios y secundarios en atmósferas. Una prueba de concepto indicó que se obtiene una respuesta significativa de amoníaco, principal nitrógeno básico volátil para la evaluación de la frescura, cuando la muestra de carne envasada se mantiene hasta diez días a 4°C. El amoníaco liberado fue  $20 \pm 4 \mu\text{g}/\text{kg}$  y  $18 \pm 3 \mu\text{g}/\text{kg}$  empleando reflectancia difusa y %R obtenida a partir de las fotos de sensores tomadas por un teléfono inteligente. La evolución hasta 12 días del sensor dentro del paquete que contenía la carne se siguió a partir de las

imágenes captadas por el teléfono inteligente, mostrando un perfil diferente con respecto a los estándares ensayados, lo que puede deberse a una liberación progresiva del amoníaco de la carne. Por lo tanto, el empleo del sensor PDMS-NQS-IL podría ser una nueva alternativa potencialmente sostenible para el análisis in situ de la frescura de la carne en referencia a las aportaciones de la literatura. También se ha demostrado que la presencia de sulfuro no interfiere en la respuesta de amoniaco del sensor.

### **Matrices forenses**

- Se ha estudiado la toma de muestra, así como la determinación de residuos orgánicos (OGS) y residuos inorgánicos (IGSR) de disparos en las manos de policías tras efectuar sendos disparos. La microextracción en fase sólida en tubo (IT-SPME) acoplada en línea a cromatografía líquida capilar con detector de fila de diodos (CapLC-DAD) permite evaluar la presencia de OGSR, mayoritariamente difenilamina (DPA) y la microscopía electrónica (SEM-EDX) se ha utilizado para IGSR. Se ha optimizado el procedimiento de extracción de DPA de las manos de los tiradores, ensayando distintos muestreadores. La mejor eficiencia de extracción se logró utilizando un hisopo de algodón seco seguido de extracción del mismo asistida por vórtex con agua en segundos. Cabe mencionar que se emplearon la mínima cantidad de disolventes no tóxicos y materiales de bajo coste. De esta forma, se obtuvieron LD satisfactorios (0,3 ng) y buena precisión (RSD 9%). Se encontró DPA en el 81% de las muestras analizadas y residuos inorgánicos tratados.



# INDEX



<b>CHAPTER 1 INTRODUCTION .....</b>	<b>1</b>
1.1 Sustainability.....	3
1.2 Sustainability and Chemistry .....	9
1.3 Sustainability and Analytical Chemistry.....	13
1.4 In-tube solid phase microextraction coupled to capillary liquid chromatography (IT- SPME - CapLC).....	16
1.4.1 IT - SPME modalities in LC.....	17
1.5 In-situ analysis devices.....	22
1.5.1 Chemical sensors .....	25
1.5.2 Analytical response.....	31
1.6 Matrices and analytes.....	33
1.6.1 Environmental samples .....	33
1.6.2 Biological samples.....	42
1.6.3 Forensic matrices.....	55
1.6.4 Food matrices .....	60
<b>CHAPTER 2 OBJECTIVES.....</b>	<b>67</b>
<b>CHAPTER 3 MATERIALS AND METHODS.....</b>	<b>75</b>
3.1 Reagents .....	77
3.2 Instrumentation.....	78
3.2.1 Spectroscopic techniques .....	78
3.2.2 Microscopic techniques.....	79
3.2.3 Chromatographic techniques: Capillary liquid chromatography (CapLC).....	81
3.3. Sensor preparation .....	82
3.3.1 PDMS based sensors.....	82
3.3.2. Nanoparticle-based sensors .....	85
3.4. Standard atmospheres preparation and humidity measurement...	87
3.5. Analysis of real samples.....	89

3.5.1 Sampling .....	92
3.5.2 Sample pre-treatment .....	95
3.5.3 Analytical matrices.....	98
Environmental samples .....	98
Forensic samples.....	98
Biological samples.....	99
Food samples .....	99
3.6 Procedures and experimental condition .....	100
3.6.1 Chromatographic conditions .....	100
3.6.2. Sensor response: In-situ analysis.....	102
<b>CHAPTER 4 RESULTS AND DISCUSSION .....</b>	<b>107</b>
4.1 Environmental samples .....	109
4.1.1 A sustainable on-line CapLC method for quantifying antifouling agents like irgarol-1051 and diuron in water samples: estimation of the carbon footprint.....	109
4.1.2 Improving sustainability of the Griess reaction by reagent stabilization on PDMS membranes and ZnNPs as reductor for nitrates: Application to environmental water matrices.....	118
4.2 Biological samples.....	128
4.2.1. Nylon-supported plasmonic assay based on the aggregation of silver nanoparticles. In-situ determination of hydrogen sulfide like compounds in brea samples.....	129
4.2.2 Determination H <sub>2</sub> S in live cardiac cells samples using AgNPs multisensor sheet .....	148
4.2.3 Fast Blue B Functionalized silica-polymer composite to evaluate DHCA as biomarker of gluten intake.....	157
4.2.4 Determination of antimicrobials in invasive medical devices by in-tube solid phase microextraction as preconcentration tool: application to endotracheal tubes .....	167
4.3 Food samples .....	174

4.3.1 Ionic-liquid doped polymeric composite as passive colorimetric sensor for meat freshness as a use case.....	174
4.3.2 New approach for Griess reaction based on reagent stabilization on PDMS membranes and ZnNPs as reductor of nitrates. Application to waters from canned and fresh vegetable samples.....	194
4.4 Forensic samples.....	197
4.4.1 Estimating diphenylamine in gunshot residues from a new tool for identifying both Inorganic and organic residues in the same sample .....	197
<b>CHAPTER 5 GENERAL CONCLUSIONS .....</b>	<b>217</b>
<b>REFERENCES .....</b>	<b>225</b>
<b>ANNEX .....</b>	<b>263</b>
<b>A1 Abbreviations .....</b>	<b>265</b>
<b>A2 Figure list .....</b>	<b>271</b>
<b>A3 Table list.....</b>	<b>283</b>
<b>A4 PhD contributions to publication.....</b>	<b>289</b>



# **CHAPTER 1. INTRODUCTION**





## 1.1 Sustainability

The concept “sustainable” is related with the idea of reconciling economic development and the conservation of natural ecosystems. It was first appeared in 70`s and was enunciated in various reports and in different ways [1]. However, the expression with the most acceptance success was the term sustainability reached in 1987. The current concept of sustainability first appeared in the Brundland report (also known as Our Common Future Report) in 1987 by the **World Commission on Environment and Development** [2]. This report warned about the negative environmental consequences of economic development and globalization, trying to offer solutions to the problems derived from population growth and industrialization. From then until today, the term sustainability sounds more and more frequently and is linked to many areas as **Figure 1.1** shows, which was obtained from the data base Web of Science (Clarivate Analytics). Different organizations expressed their own definition of the concept of sustainability too.

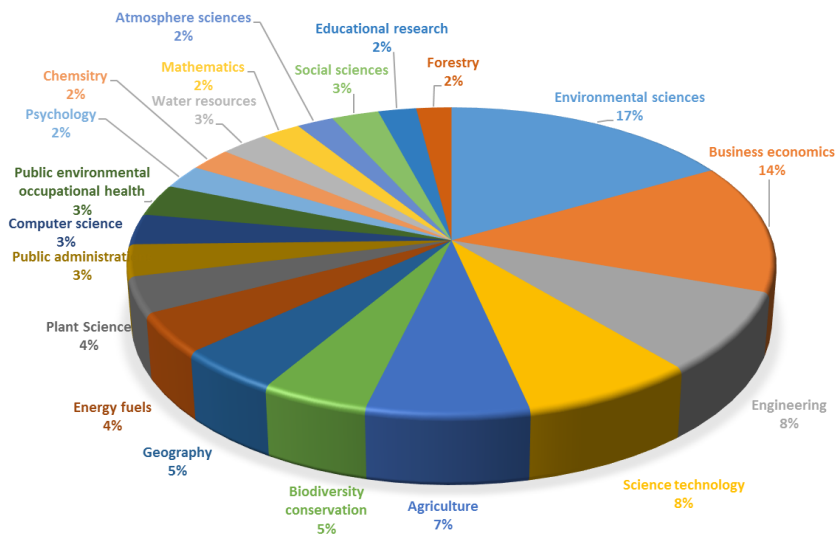


**Figure 1.1** Weight of sustainability in different scientific areas expressed in percentages with respect to the total publications that contain this item. Web of Science source by searching sustainability (December 2020).

According to The World Conservation Union (United Nations Environment Program and World Wide Fund for Nature, 1991) [3], sustainable development implies the improvement of the life quality within the ecosystem limits. According to the International Council of Local Environmental Initiatives (ICLEI) (1994) the definition of sustainability offers basic environmental, social and economic services to all members of a community without endangering the viability of the natural, built and social systems on which the supply of services depends [4].

*Sustainability refers to the satisfaction of current needs without compromising the ability of future generations to satisfy theirs, guaranteeing the balance between economic growth, care for the environment and social well-being.*

This definition gives rise to the idea of sustainable development, being a mode of progress that maintains the delicate balance today, without endangering future resources. Sustainability assumes that nature and the environment are not exhaustible sources of resources, their protection and rational use being necessary.

On the other hand, the quality of life of a given society depends largely on environmental quality and economic well-being. Finally, a balance is required between three elements: environment, economy and society, that is, to achieve development in each of the three elements without negative repercussions between them [5,6]. **Figure 1.2** shows the principles and approach of the three elements mentioned above. To understand the sustainability concept related to chemistry it is important to understand the fundamentals of sustainability. **Table 1.1** summarizes the main topics.

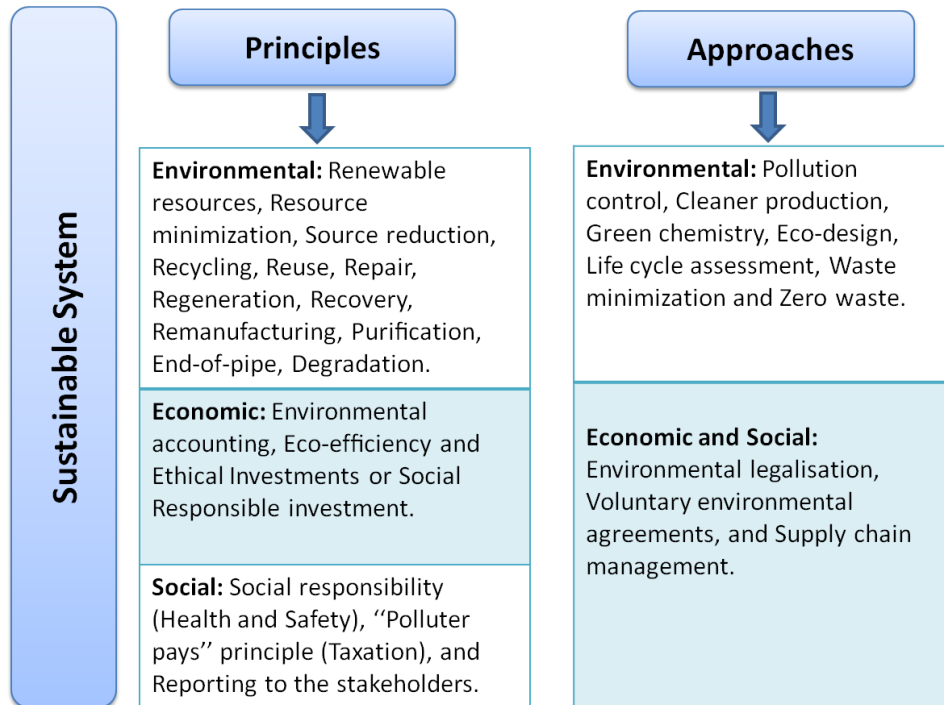


Figure 1.2 Sustainable systems: principles and approaches.

Table 1.1 Summary of the principles and approaches in sustainability

**PRINCIPLES**

**ENVIRONMENTAL**

**Renewable resources**      The resources that are available are treated in a continuously renewed way [7].

**Resource minimization**      Conservation of natural resources. Concerns about resources such as energy, raw materials, and water supply.

**Source reduction** Reduction of energy and quantity of materials entering a waste stream[8].

**Recycling** Collection and treatment of waste products and its use as raw material [7].

**Reuse** Use of waste as raw material in a different process without any structural change.

**Repair** Improvement of a product to increase its quality and usefulness before its reuse.

**Regeneration** Material renewal to return it in its primary form for use in the same or a different process.

**Recovery** Energy waste found in the waste stream for beneficial use[7].

**Remanufacturing** Reconstruction or reconditioning of machines, mechanical devices to reuse then [9].

**Purification** Removal of unwanted particles like mechanical also organic compounds and other impurities.

**End-of-pipe** Treatment of polluting substances at the end of the production process [8].

**Degradation** Biological, chemical or physical process that results in the loss of productive potential [7].

## **ECONOMIC**

***Environmental Accounting*** Reduce cost improvement of the environmental quality and profitability of the organization [8].

***Eco-efficiency*** Delivery of competitively priced goods and services that satisfy human needs and bring quality of life [8,10,11].

***Ethical investments*** Financial instruments stimulate responsible corporate practices.

## **SOCIAL**

***Social responsibility*** Safe, respectful, liberal, equitable and equal human development.

***Health and safety*** Working environment including responsibilities and standards.

***Polluter pays*** According to Environmental Protection Agency (EEA), environmental damage is paid in the form of cleaning and taxes that pollute it [7].

***Reporting to stakeholders:*** Global Reporting Initiative create a framework and report on the economic, environmental and social performance of all organizations [12].

## APPROACHES

### *ECONOMIC and SOCIAL*

***Environmental Legalization*** Group of laws, regulations, directives that influence both the environment and the life to improve the environment protection and the quality of life.

***Voluntary Environmental Agreements*** Agreements between the corporations, government and/or non-profit sectors [13].

***Supply Chain Management*** Plans, implement and control the operations of the supply chain to meet the consumer requirements.

### *SOCIAL*

***Pollution control*** Reduce the impacts of the pollutants, before they are released into the environment, through some type of treatment[11].

***Cleaner production*** Systematically organized approach to production activities, which has positive effects on the environment (minimization, improvement of eco-efficiency and sources reduction) [14,15].

***Eco-design*** Product development process that takes into account the complete life cycle of a product

	and considers environmental aspects at all stages of a process [8,11]
<b><i>Life cycle assessment</i></b>	Stages and the life span of products, their environmental impacts and services, manufacturing processes and decision [7,8]. Carbon footprint estimation.
<b><i>Waste minimization</i></b>	Techniques that reduce the amount of waste generated during industrial processes (according EPA).
<b><i>Zero waste</i></b>	Minimizes waste and maximizes recycling, reducing consumption and ensuring that products are reused, regenerated, repaired and recycled internally or back to nature or to the marketplace.

---

## 1.2 Sustainability and Chemistry

The importance of the chemical process sustainability is evidenced by the numerous reports in the literature that begin to address this issue [16–22]. As it can be seen in **Figure 1.3**, the citations that related with chemical sustainability were increased progressively during the last 10 years.

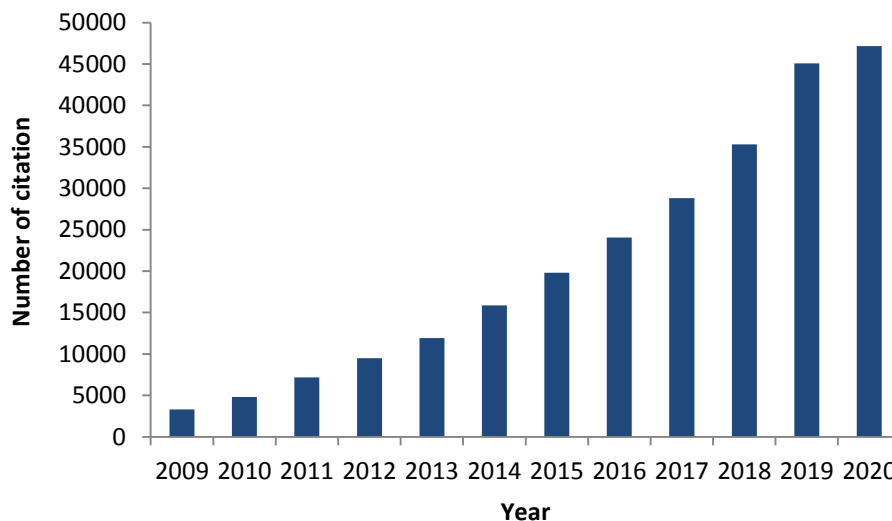


**Figure 1.3** Evolution of the citation number of published papers in Web of Science for matching the search terms “sustainable chemistry” in a period of 12 years (December 2020).

Through new approaches and technologies, sustainable chemistry stimulates technical and social innovations. It develops and creates products and services [23]. Sustainable chemistry is based on a holistic approach, setting policies and measurable objectives for a continuous process of improvement. This implies the development of networks with interdisciplinary scientific research and education. By encompassing all the information, the development of alternative processes fulfils the following needs: recycling concepts, supporting the recovery and efficiency of resources avoiding rebound effects, damages and deterioration as in human beings as also in ecosystems and natural resources. Summarizing, by means of a series of parameters, the adequacy of chemical processes is evaluated by:

- Preparation of a chemical process.
- Environmental impact.
- Resources used.
- Generated wastes.

In this context, Green Chemistry appears directly related with sustainable chemistry, however these are not synonyms.



*“Green chemistry can be defined as a chemistry that is focused on the design, manufacture and use of chemicals that have decreased or no pollution potential”. “Sustainable chemistry” not only includes the concepts of green chemistry, it also expands the definition to include a larger system than just the reaction. Sustainable chemistry also considers the effects of processing, materials, energy, and economics (Figure 1.2).*

Green chemistry was born in the Environmental Protection Agency (EPA) in USA in the early 1990s as an approach and a conceptual tool for environmental protection to pollution caused by industry chemistry, and was expressed by 12 principles established by Paul Anastas and John Warner in 1998. Green chemistry is the design, development and implementation of chemical processes or products to reduce or eliminate the use and generation of dangerous and toxic substances.

**Table 1.2** *The 12 principles of Green Chemistry*

<b>GREEN CHEMISTRY 12 PRINCIPLES</b>	
<b>1.Prevention</b>	<i>Minimization of residue formation.</i>
<b>2.Atomic economy</b>	<i>Synthetic methods must be designed to obtain the maximum incorporation in the final product of all subjects used in the process.</i>
<b>3.Less harmful synthesis</b>	<i>Whenever possible, must design synthetic methodologies with low or no human and environmental toxicity.</i>
<b>4.Safe chemical reagents</b>	<i>Chemicals must be selected to preserve their efficiency of their function in the process and to toxicity.</i>
<b>5.Solvents and other safe auxiliary substances</b>	<i>The use of auxiliary substances (solvents, separation, etc.) should be avoided whenever possible and be innocuous when used.</i>
<b>6.Energy efficiency</b>	<i>Energy needs must be considered in relation to their environmental and economic impacts, and should be minimized. Synthetic methods should be carried out at room temperature and atmospheric pressure if possible.</i>

<b>7. Renewable raw materials use:</b>	<i>Raw materials must be renewable and non-extinguishable.</i>
<b>8. Derivatives reduction</b>	<i>Unnecessary derivatives (blocking of groups, protection/unprotection, temporary modification of physical /chemical processes) should be avoided as far as possible. Because these measurements require additional reagents and can generate waste.</i>
<b>9. Catalysis</b>	<i>Catalytic reagent (as selective as possible) are higher than stoichiometric reagents.</i>
<b>10. Degradation</b>	<i>The chemicals used will be chosen so that at the end of their function they decompose into harmless and non-persistent degradation products in the environment.</i>
<b>11. Real-time analysis for pollution prevention</b>	<i>Substances and ways to use it in a chemical process should be chosen in a way that minimizes the possibility of accidents.</i>
<b>12. Safe chemistry for accident prevention</b>	<i>Substances and ways to use it in a chemical process should be chosen in a way that minimizes the possibility of accidents.</i>

---

As we have discussed earlier, achieving sustainable chemical processing requires a rather complex balance between resources use, economic growth and environment impact. Green chemistry becomes one of the tools to characterize chemical sustainability.

In summary, a sustainable chemical process is that one that does not produce environmental impacts or waste, offers high levels of sustainability in reaction efficiency, uses minimal amounts of energy and is cost-effective.

### 1.3 Sustainability and Analytical chemistry

The relevance of sustainable analytical chemistry has increased in the last years, as it can see in **Figure 1.4**.

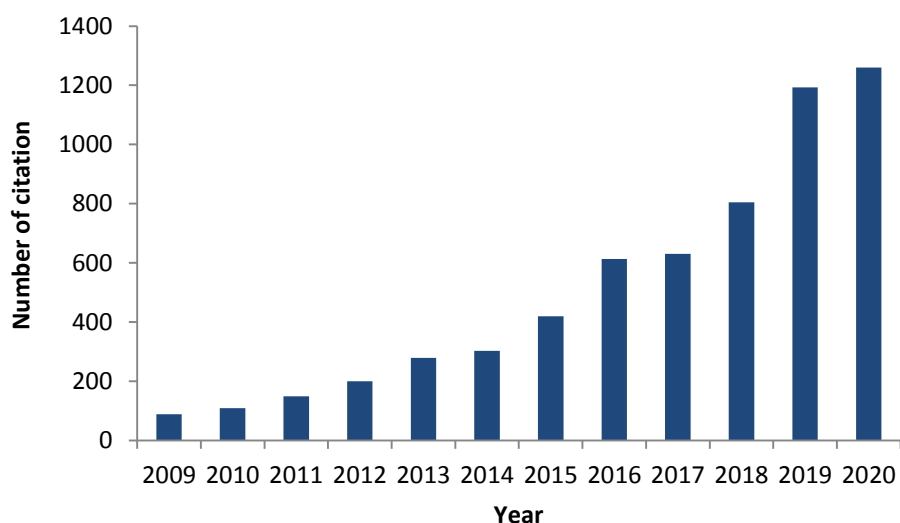


**Figure 1.4** Evolution of the number of citation in Web of Science for matching the search sustainable analytical chemistry for the last 12 years (December 2020).

Sustainability in analytical chemistry combines the components of Green analytical chemistry (**Figure 1.5**) with the principles corresponding to the socio-economic factor (discussed in **Figure 1.2**). Directly related with sustainability is green analytical chemistry, its characteristics are described in the 12 well-know principles introduced by Galuzca et al., starting from those corresponding to Green Chemistry [24].

1. Apply direct analysis techniques to avoid sample treatment
2. Minimize the volume and number of samples
3. Carry out in-situ determinations
4. Integrate analytical processes and operations to reduce consumption of reagents and energy
5. Select miniaturized and automated methods
6. Avoid derivatization stages
7. Reduce waste generation and implement management measures

8. Give preference to multicomponent analysis over individual ones
9. Minimize energy consumption
10. Promote the use of reagents obtained from renewable sources
11. Eliminate or substitute reagents
12. Increase operator safety

Thus, the principles of sustainable analytical chemistry include green analytical chemistry principles, economic and social principles as **Figure 1.5** indicates.

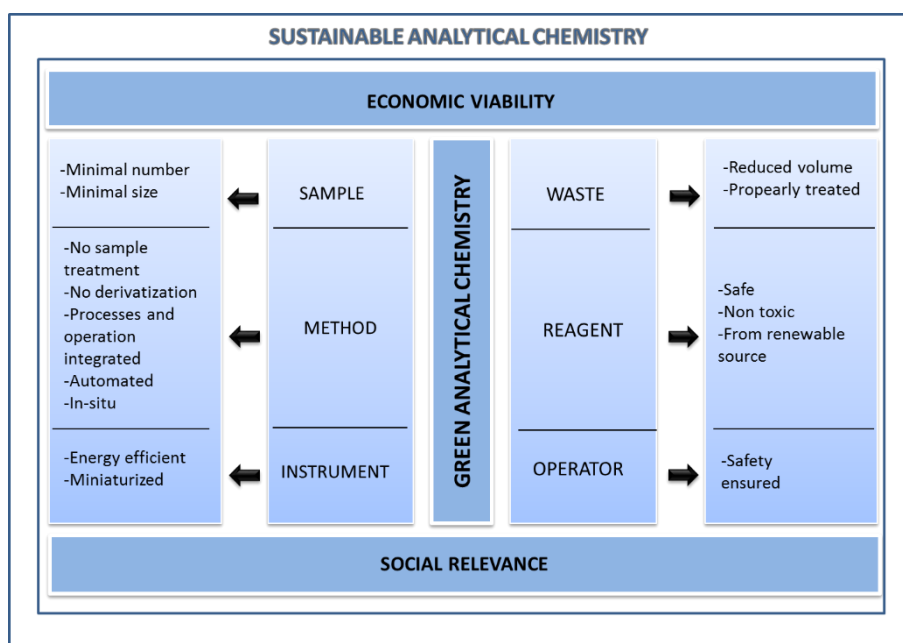


**Figure 1.5** Sustainable analytical chemistry scheme

Analytical chemistry has an important role in the development of sustainability, due to monitorization of pollutants and development of more sustainable processes. The environmental impact of analytical methods can be reduced by:

- ✓ Reducing the amount of solvents required in the sample pre-treatment stage.
- ✓ Reducing the amount and toxicity of solvents and reagents used in the measurement step, especially through automation and miniaturization.

- ✓ Developing alternative direct analytical methodologies that do not require solvents or reagents.

On the other hand, there is an increasing need to use methods for evaluating the sustainability of a process or product in general. There are several "green chemistry metrics" tools to calculate environmental impact such as carbon footprint [25]; atomic economics [26]; environmental factor E [27]; environment, health and safety index (EHS) [28]; and LCA [29,30]. Three multi-criteria methods have been compared recently [31] in the analytical chemistry field, one of them, hexagon tool, proposed by our research group MINTOTA [32,33].

The carbon footprint estimation (CFP) is a metric tool to evaluate the methodology negative environmental impact. CFP represents the net emissions of greenhouse gases (GHG) emitted by an individual, organization, event or product measured as CO<sub>2</sub> equivalents [34]. Thus, CFP can be understood as an awareness tool about the environmental cost associated with a product or process, in a way that influences decision-making that contribute to the reduction of GHG emissions.

Hexagon tool [31-33] is proposed for evaluating the optimal selection and/or testing of sustainable analytical methods. Besides, it allows a quick and easy to use visual inspection of the characteristics of an analytical procedure by means of the regular hexagonal pictogram (**see Figure 1.6**). The pictogram is formed by six equilateral triangles, it accounts for the variables of the analytical method that are evaluated and quantified, such as the figures of merit, toxicity and safety, waste, environmental impact and economic cost. The existence of metrics is widely encouraged not only in research labs but also in industries, as green is a contemporary driving force promoting the development of more environmental-friendly analytical scenarios. Hexagon tool can be a guide to evaluate and/or select analytical procedures that are in line with the philosophy of sustainable analytic chemistry, taking into account the needs of green chemistry and cost-effective aspects.

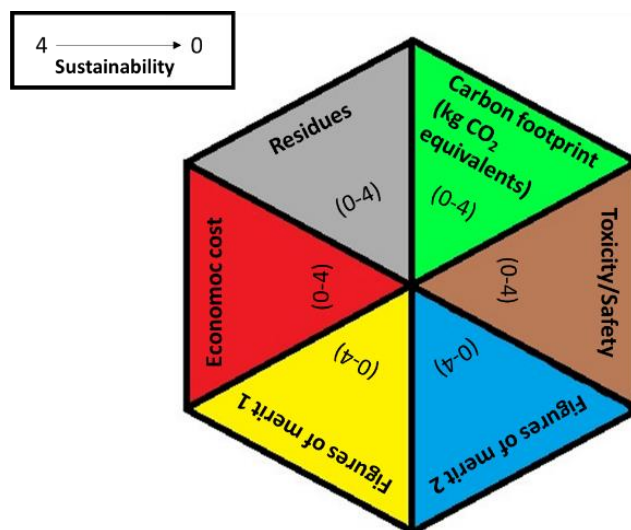


**Figure 1.6** Pictogram to evaluate and quantify the sustainability of an analytical procedure (Figures of merit 1: Sample treatment, method characteristics and calibration. Figures of merit 2: Quality control and Accuracy).

This Thesis contributed to sustainable analytical chemistry by using two strategies:

- ✓ Coupling on-line the sample pre-treatment with the separation and determination step and miniaturization
- ✓ Developing solid colorimetric devices for in-situ analysis

These two approaches were evaluated in terms of environmental, economic and social impact.

#### 1.4 In-tube solid phase microextraction coupled to capillary liquid chromatography (IT - SPME - CapLC)

Sample pre-treatment is often necessary to extract, isolate and concentrate the analytes of interest [35,36]. This step increases selectivity and sensitivity [37]. However, this involves a high degree of sample manipulation, which leads to non-efficient methods in terms of environmental and economic impacts.

Solid phase extraction (SPE) is one of the most widely used techniques for sample pre-treatment. It is based on the use of columns packed with a solid. In the recent decades new miniaturized extraction techniques have been proposed [38]. Microextraction based techniques emerged as alternative tools to develop more sustainable techniques by reducing reagents wastes, extractive phases and if possible energy, their on-line coupling with separation system is an added value for some of them. Liquid and solid microextraction based techniques have been proposed. Liquid phase microextraction (LPME) is carried out by using immiscible solvents with water at low  $\mu\text{L}$ . There are different LDME modalities such as drop microextraction (SDME) [39,40], liquid-dispersive liquid microextraction (DLLME) [41–43], hollow fiber liquid phase microextraction (HFLPME), among others [44–46].

Solid phase microextraction (SPME) was proposed by Pawliszyn et al in 1990, focussed at the beginning, mainly to gas chromatography (GC) [47]. It is performed by immersing a fiber coated with the extractive phase in the sample solution or in its headspace or even in solid samples. After extraction time, the analyte is desorbed by using an organic solvent or thermally by direct injection in the GC system. The main advantage is miniaturization of the sample step, since sampling extraction and preconcentration are carried out in one step. Later in 1997, Eisert and Pawliszyn proposed in-tube solid-phase microextraction (IT-SPME), thereby solving the problems associated with fiber brittleness and long desorption times [48]. In addition to the advantages mentioned, this technique is of great interest from the point of view of analytical green chemistry since it is automatable and it is easy to couple on line with liquid chromatography (LC) too. Among the different SPME techniques, in tube–SPME (IT-SPME) has shown advantages in the context of sustainable analytical process and LC.

### 1.4.1 IT-SPME modalities in LC

IT-SPME now can be performed using two different modalities: draw/eject and in-valve.

**In draw/eject mode**, the capillary column is coupled between the needle and loop of a programmable autosampler. Next, a fraction of the sample is repeatedly aspirated and ejected through the capillary column until reaching equilibrium between analytes and extractive phase [49]. Finally, analytes are transferred to the analytical column by static extraction, with appropriate solvent, or by dynamic

extraction, through the mobile phase. **(Figure 1.7)**. In this technique, high recoveries can be achieved by increasing the number of draw/eject cycles. In general, this modality is usually used for complex matrices with low volume availability (biological samples).

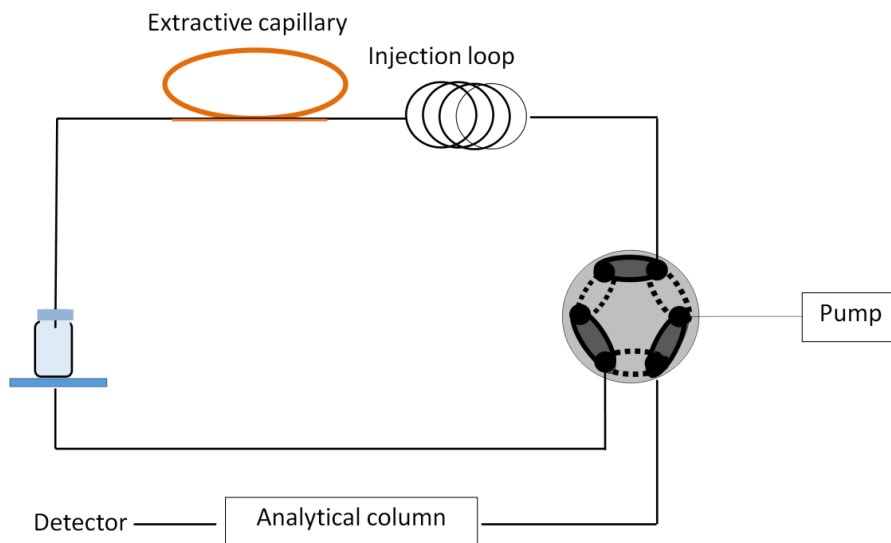


**Figure 1.7.** Schematic representation of the draw/eject configuration.

**In valve IT-SPME.** The most common configuration is to use the IT-SPME capillary column as injection loop of the valve of the liquid chromatographic system. The analytes are retained on the surface of a capillary column during the sample loading process and, later, are transferred to the analytical column by means of a change of the valve to the inject position **(Figure 1.8)**.

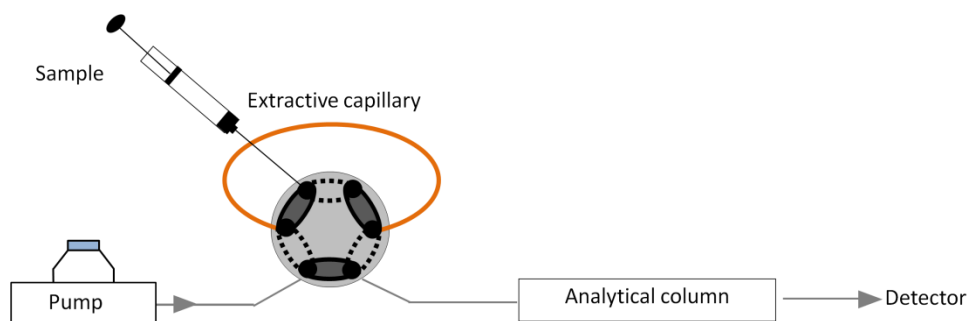


**Figure 1.8.** Schematic representation of the in-valve IT-SPME system.



Although, the absolute extraction efficiency is low, sensitivity can be increased by passing relatively high volumes of sample. In this technique, the IT-SPME capillary columns go from commercial GC columns to synthesized capillary coatings. This modality can also be performed with a system based on two valves system [50,51] (see **Figure 1.9**) or other similar configurations.

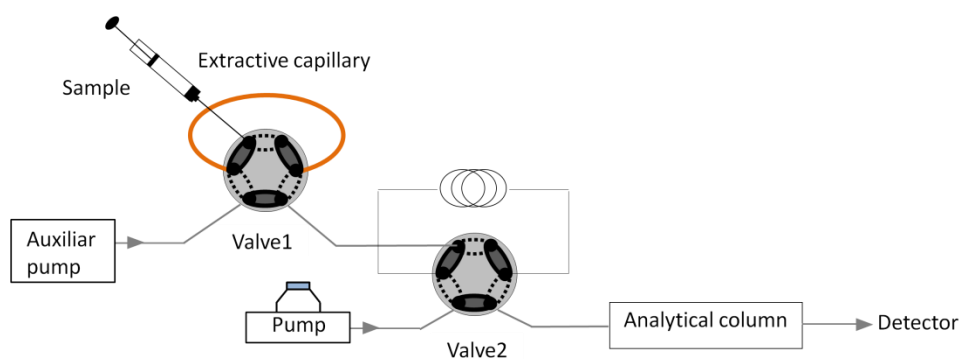


**Figure 1.9** Schematic representation of a IT-SPME system in circulation mode with two valves.

The main parameters related with the extraction efficiency are: extractive phase, flow rate, processed sample volume and capillary column length. Therefore, they should be taken into account when designed the IT-SPME procedure.

The selection of the extraction phase is a key parameter since the success on the extractive efficiency depends on the interaction between the target analytes and the phase. The main commercial phases used in the literature are: polydimethylsiloxane (PDMS) based extractive phase (TRB 5, 20, 35, 50), porous divinylbenzene columns (Supel-Q Plot) and CP - Pora Plot amine and polyethylene glycol (PEG).

In this Thesis PDMS based extractive phases have been proposed for environmental, biological and forensic samples. These extractive phases are advantageous since the polarity can be turned as a function of the diphenyl groups. **Table 1.3** summarized the main PDMS column tested in this Thesis.

**Table 1.3** PDMS<sub>2</sub>-based capillary columns used in this Thesis

Extractive capillary	Coating
TRB-5	5% diphenyl-95% polydimethylsiloxane
TRB-20	20% diphenyl-80% polydimethylsiloxane
TRB-35	35% diphenyl-65% polydimethylsiloxane
TRB-50	50% diphenyl-50% polydimethylsiloxane

Besides the commercial extractive phases, alternative IT-SPME capillary columns have been proposed for providing more sensitivity, selectivity and stability. Some examples are: modified capillaries coated with multi-walled carbon nanotubes (MWCNTs)[52] for analysis of substituted anilines and for quantification of polar triazines and degradation products [53]; synthetic polymers that present specific regions for the recognition of certain compounds (MIPs) to determine 4-nitrophenol in environmental samples [54], drug monitoring [55] and antibiotic analysis [56]; metal oxides NPs have been also proposed to modify coated phases, which were applied in the determination of acetylsalicylic acid, acetaminophen, atenolol, diclofenac and ibuprofen [57], triazines [58] and organophosphate compounds [59].

The volume of sample processed is a relevant factor, since processing larger volumes implies a greater amount of retained analytes (until the saturation of the adsorbent phase). Depending on the need of each case, the injected volumes can vary from  $\mu\text{L}$  [60] to up to mL [61,62].

Length of the capillary column can be also used to improve extractive efficiency since the amount of solvent phase depends on the capillary length. Longer lengths imply more surface area of sorbent material available to extract the analytes. There have been publications in which capillary column lengths of 20 cm [63], 30 cm [64], 60 cm [65], 70 cm [66] or 80 cm [67] were employed.

Flow rate is adjusted according to the analysis. The flow rates used can be of the order of  $\mu\text{L}/\text{min}$  [53,62,68] or higher flows (mL/min) [67,69] according to the type of LC used.

In addition, clean-up can be also performed when complex samples are analysed. This step is carried out by passing a volume of the adequate solvent through the

capillary column. Therefore, cleaning solvent as well as its volume are parameters that should be optimized [62,64].

Finally, desorption is carried out to transfer the analyte to the analytical column. The desorption of the analytes can be carried out by using a solvent by the static mode or by means of the mobile phase, which is the dynamic mode, the latter being the most common. In the case of static desorption, the variables that affect are the volume of solvent and the extraction time, in the case of dynamic desorption, its effectiveness depends on the composition of the phase mobile and flow rate.

This technique is versatile when adapting to different chromatographic systems such as NanoLC [70] UHPLC [50,51] or CapLC [58,60–62,64,71,72]. One of the characteristics that differentiates the aforementioned chromatographic systems is the diameter of analytical columns, which establishes mobile phase flow. **Table 1.4** shows a classification of LC systems based on column dimensions and mobile phase flows.

**Table 1.4** General classification of LC systems taking into account the dimensions of the column and the flow.

LC system	Analytical column i. d. (mm)	Mobile phase flow ( $\mu\text{L} / \text{min}$ )
Preparative	> 10	> 5000
Conventional	4.0 - 4.6	2000
Narrow bore	2.1	500
Microbore	1	100
Capilar	0.1 – 0.5	1 – 20
Nano	< 0.1	< 1

The miniaturization of LC systems was proposed in 1967, it was based on minimizing the internal diameter (i.d.) of the analytical column. Later, different works were published that used analytical columns of 1 mm i.d. filled with particles of different sizes and covered by different materials [73,74]. Currently, there are commercial columns for LC ranging from 2.1 mm to 75  $\mu\text{m}$  i.d. [75,76]. Another parameter involved in the miniaturization of the LC is the particle size of the stationary phase. In recent decades, the diameter of the particles used as

stationary phase has been reduced, obtaining greater efficiency [77] due to pumps working at higher pressures (UHPLC) have been introduced.

The reduction of the internal diameter of the analytical column leads to a decrease in the flow of mobile phase, reducing the consumption of solvents and therefore the amount of waste generated. According to Nazario et al. in 2015 [75], the decrease in the flow of mobile phase makes possible new mechanisms of interaction between mobile phase and analytes, which leads to improved selectivity. On the other hand, reducing the internal diameter of the analytical column also reduces the volume of the sample required. It should be noted that reducing the diameter decreases the dispersion of the analytes within the analytical column. The decrease in chromatographic dilution improves the signal-to-noise ratio, which leads to a significant increase in sensitivity compared to the conventional technique. Therefore, the miniaturized chromatographic systems are in accordance with the principles of sustainable analytical chemistry.

In this Thesis a miniaturized system such as CapLC coupled on line to IT-SPME and diode array detection (DAD) with low economic cost and environmental impact satisfied the requirements of sustainable analytical chemistry, making it effective and versatile tool for the analysis of a great variety of analytes in different matrices such as environmental, biological, food and forensic, among others.

## 1.5 In-situ analysis devices

As above mentioned, sustainability is directly related with environment, economy and social impact. An economically sustainable analytical chemistry method means that it has to be cost effective, which often means high-throughput, fully automated systems. Portable devices can be a cost-effective alternative [78].

One of the great challenges of Analytical Chemistry is the development of devices that allow to carry out determinations in situ, that is, in the place where the compound of interest is found and the problem is produced [79,80]. Therefore, apart from avoiding transport of the sample to the laboratory, which entails time, costs and resources [81], the risk of contamination or degradation of the sample is also minimized.

Two types of analysis are classified according to the site where analytical process is developed: off-line and In-situ (**Figure 1.10**). In an off-line process, the sample is transported to the laboratory for analysis and the analysis is carry out there, while in in situ analysis is carried out by introducing the device at the sampling site (in-line) or it can be carried out near the sampling site (on -line). Also, on-site devices can be classified as passive or active depending on the type of sampling. Active devices require a power source for sampling (for example, a pump). However, passive devices do not require energy consumption, so sampling is done mainly by diffusion.

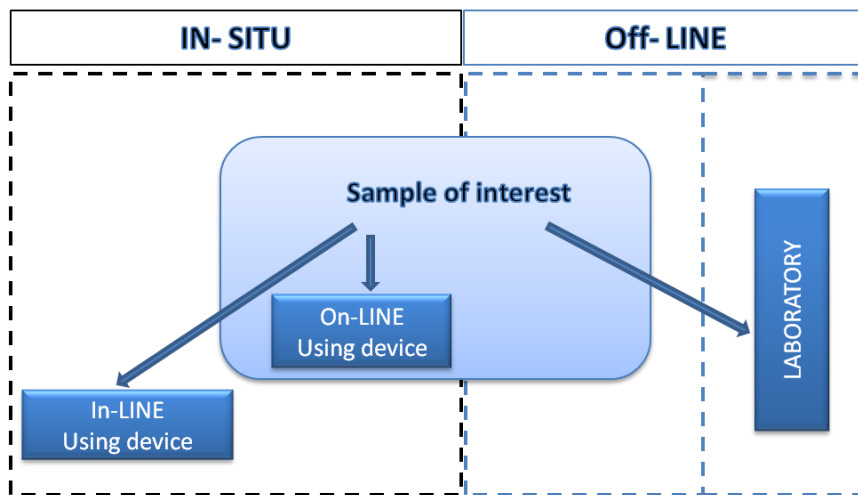


**Figure 1.10** Schematic representation of in-situ and off-line analysis.

In-situ analysis devices must meet a number of characteristics, such as portability, low cost, simplicity and rapidity, [82]. Currently, different devices that meet these characteristics are already available on the market, such as glucometers, pregnancy tests, alcohol or bad breath meters in exhaled air and several probes, among others. Another advantage is the level of simplicity when handling these devices, which allows the analysis to be carried out by non-specialized personnel. However, the need to advance in the knowledge of these devices is still a challenge. As can be seen in **Figure 1.11** the number of publication has increased exponentially in the last years showing the interest on this topic.

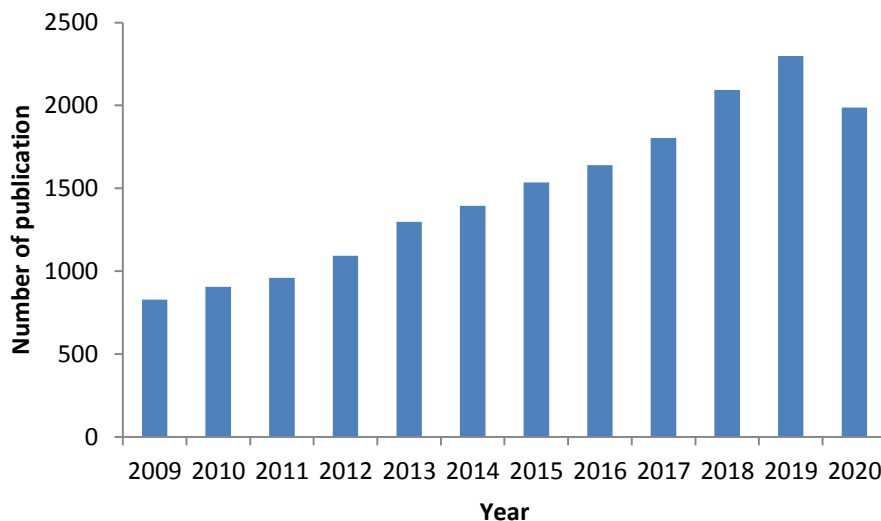


**Figure 1.11** Number of publications in Web of Science for matching the following search term “sensors” and “in-situ analysis” in the 2000-2020 periods.

The main devices reported can be classified as optical devices, portable instruments, electrochemical devices and remote stations. **Figure 1.12** shows the advantages and disadvantages of these devices.

Optical devices offer interesting properties such as low cost, portability, low energy consumption, simplicity that make them especially attractive from the point of view of analytical chemical sustainability [80]. The vast majority of optical devices are colorimetric, which allows us to perform a (semi)quantitative analysis by visual inspection, without the need for instrumentation [83,84]. Kits, test strips, microfluidic platforms, solid and plasmonic sensors, colorimetric tubes, colorimetric supports have been proposed for this aim.

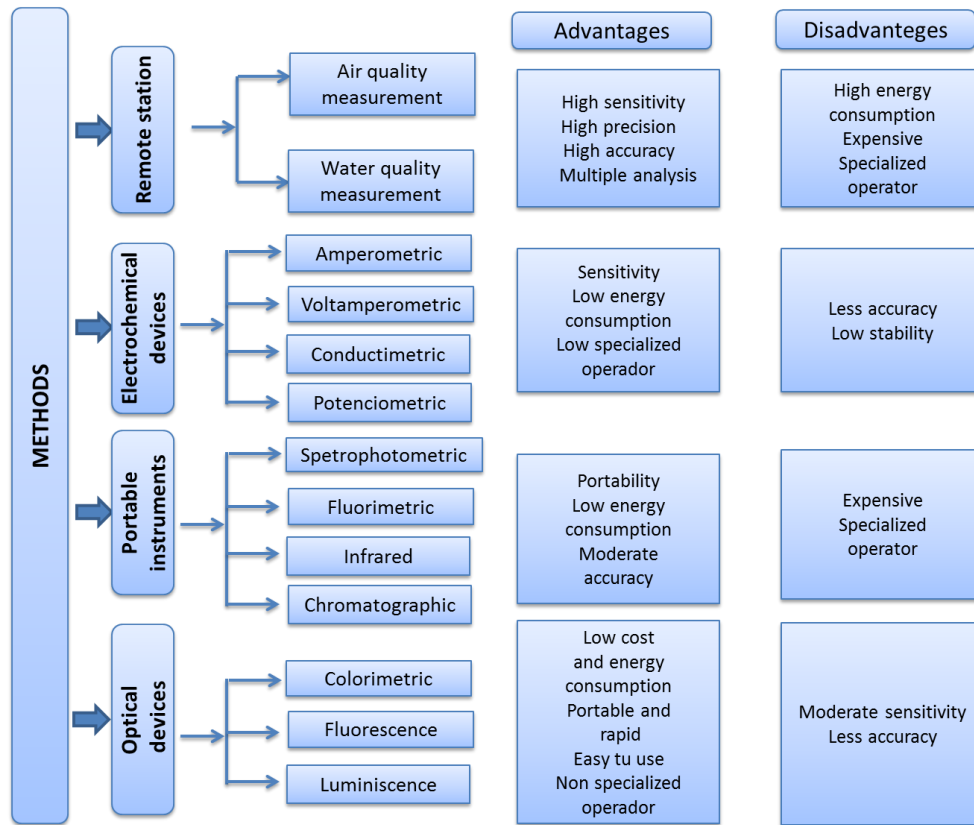


Figure 1.12 In-situ devices classification with some of their characteristics.

### 1.5.1 Chemical sensors

According to the IUPAC definition, a chemical sensor is a device that transforms chemical information into a useful readout signal. Chemical sensors are devices formed by a recognition element that is in direct contact with a transduction element, being capable of providing specific quantitative or semi-quantitative chemical information [85].

Among the different strategies to develop chemical sensors, and related to sustainable devices, colorimetric sensors show advantages since they are based on colour changes and therefore, the readout can be performed by:

- Optical instrument for quantitative purposes at laboratory or in-situ with portable optical instrument.

- Analysis of images for quantitative measurement for in-situ analysis.
- Simple visual inspection to perform semiquantitative estimations for in-situ analysis.

In a colorimetric device, the property to readout is the change of colour when the sensing device is generally in contact with the target analyte. These optical properties are obtained through a derivatization procedure of the target analyte. Among the different options, the use of colorimetric reagents deposited, embedded or immobilized in a solid-support, that in contact with the analyte gives rise to a change of colour. This change can be inside of in the solid support or in the solution (liquid sensing). The read-out in solution or in solid support depends on the solid support composition, analyte and reaction medium.

Traditional colorimetric reagents have been used for this purpose, however, new responses based on optical signals have been recently reported. This is the case of surface plasmon resonance based sensor obtained for noble metallic nanoparticles (MNPs). MNPs such as AgNPs and AuNPs are characterized by a surface plasmon band that is produced by the oscillation of electrons on the metal surface when they come into resonance with electromagnetic radiation [86–88]. Plasmonic sensors, specifically silver nanoparticles (AgNPs), which the current thesis will be about, are based on the colour change produced by the aggregation of AgNPs in the presence of target analyte. AgNPs have an intense colour (yellow) in the visible region due to the plasmon band, while their aggregation provides different colours (orange/brown) due to displacement of the plasmon band. The development of this type of sensor has experienced a considerable increase [88,89] with applications for the analysis of compounds in areas such as food [90,91] medicine [92–95] or environmental pollution [96–98]. Designing a solid-phase colorimetric plasmonic sensor should consider several factors such as:

- ✓ Avoiding rigid chemicals attached to the support that can cause spatial reorganization/ aggregation of NPs against the analyte [99].
- ✓ The immobilization can cause surface modification on NPs and promote their aggregation too.
- ✓ The immobilization should guarantee the access of the analyte to the NPs surface.

There are not many works on this topic; for example, Heli et al. [100], described a simple and sensitive plasmonic solid sensor based on nanoparticles embedded in



bacterial cellulose for ammonia exposure. Also, Colombelli et al. [101] reported an optochemical sensor based on double decker terbium (III) bis (phthalocyaninato) complex TbPc<sub>2</sub> thin films for sensing volatile organic compounds.

A key point on the development of these sensing devices is the solid support used to perform the sensing reaction. Paper, silica and polymers based on PDMS and nylon are some of the materials proposed as solid supports for the design of in-situ sensors. One of the materials as support that arouses great interest is paper due to its low cost, versatility, abundance, simplicity and compatibility [102].

Whatman paper was one of the most widely used to carry out analytical applications. These devices based on the use of paper as a solid support have been widely used to carry out qualitative and semi-quantitative analysis, since the simplicity of the technique allows detecting the colour change by simple visual inspection. These sensors were applied in different fields as diverse as medicine [103] the environment [104–109] or food [110].

Among the different solid supports, in this Thesis polymeric and nylon supports have proposed as efficient alternatives.

**Polydimethylsiloxane** (PDMS) is a linear polymer of dimethylsiloxane Si(CH<sub>3</sub>)<sub>2</sub>. It belongs to the group of organosilicon compounds, substances commonly known as silicones (**Figure 1.13 A**). PDMS is a widely employed polymer since it shows low manufacturing cost, easy fabrication, optical transparency, low toxicity, non-flammability, flexible/stretch ability and gas permeability. The PDMS matrix has been employed to develop a smart strategy for preparing colorimetric sensing devices [111–113]. To this end the derivatizing reagent is entrapped in this polymer. For this reason, different authors have used PDMS material to develop colorimetric sensors based on the high hydrophobic polymeric matrix, thus the performance for more polar analytes is limited. Therefore, the use of matrix modifiers has been proposed for increasing polarity. Tetraethyl orthosilicate (TEOS) and SiO<sub>2</sub>NPs have been proposed to modify hydrophobicity. They combine the mutual advantages of both, organic and inorganic parts to obtain novel nano structured materials with different extra functionalities. **Figure 1.13B** shows the structure of TEOS.

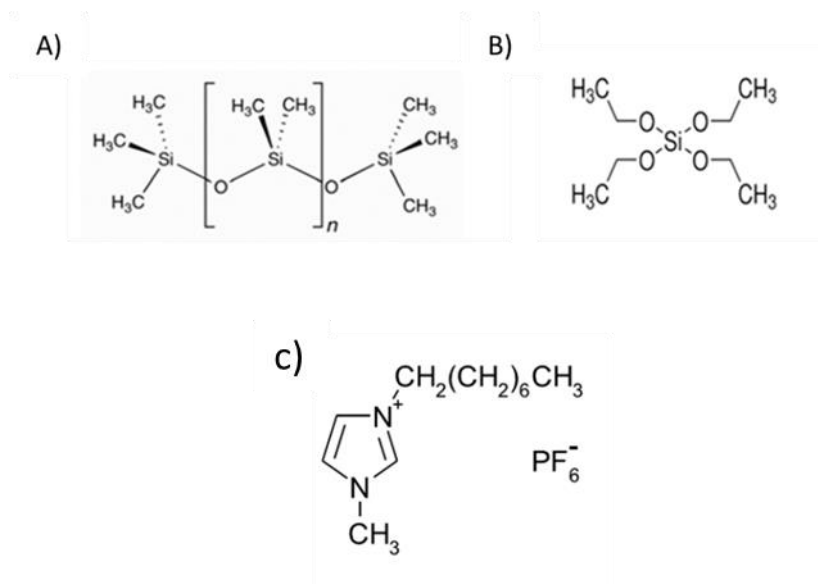


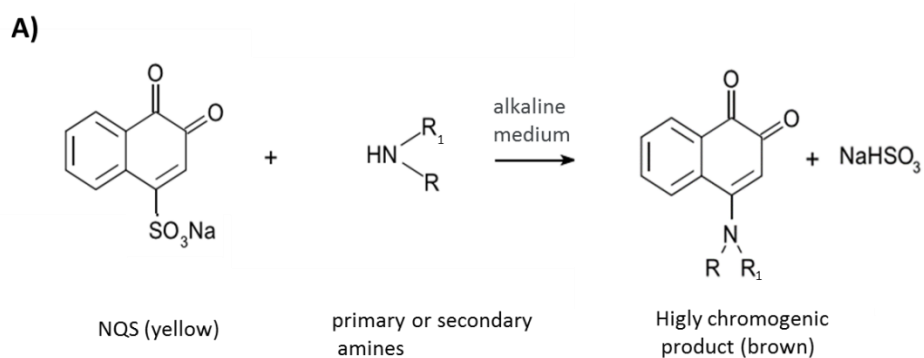
**Figure 1.13** A) PDMS, B) TEOS, C) OMIMPF<sub>6</sub> structures

A.I. Argente et al, in 2016 reported, that the presence of TEOS in the polymeric matrix leads to an increase in the hydrophilicity of the PDMS sensing device while maintaining the stability and inertness of the polymeric solid support, additionally, improving the homogeneity of the sensing device. The addition of NPs SiO<sub>2</sub> in the PDMS/TEOS matrices improved the pore size of the polymer matrix [112].

By another hand, there is a growing interest in using Ionic liquids (ILs) in the materials field since the presence of organic cations and anions places, with their unique structural and physiochemical characteristics lead to design and tune the properties of the materials [114,115]. ILs are also interesting materials to improve PDMS matrix. In particular, the hybrid organic-inorganic ILs endow an improvement on the mechanical properties of the materials maintaining the flexibility and tractability. In addition, these additives can increase the permeability of the polymeric matrices. The presence of ILs also yields to specific interactions inside of the membrane [116–118]. In this Thesis the ionic liquid 1-methyl-3-octylimidazolium hexafluorophosphate (OMIMPF<sub>6</sub>) has been used. The structure is show in **Figure 1.13D**.

Entrapping of a responsive colorimetric derivatizing reagent as a smart strategy to develop colorimetric sensing devices is proposed [79,111–113,119]

This is the case of 1,2-naphthoquinone-4-sulfonate NQS-doped PDMS based sensors [111,120][4,5]. In this thesis several entrapments have been demonstrated: NQS for nucleophilic substitution reactions between the primary and secondary amine groups and the sulfonate group of NQS reagent (**see Figure 1.14A**) [121–123]; entrapment of Griess reagents (sulphanilamide and N-(1-naphthyl) ethyldiamine) in the PDMS polymeric support for azo compounds formation between Griess reagents and nitrite (**see Figure 1.14B**) [124,125]. And finally, PDMS doped with fast blue B (FB) colorimetric reagent for azo complex formation between FB and alkylresorcinols (1.3 dihydroxy-5-pentylbenzene (PR)) (**Figure 1.14C**).



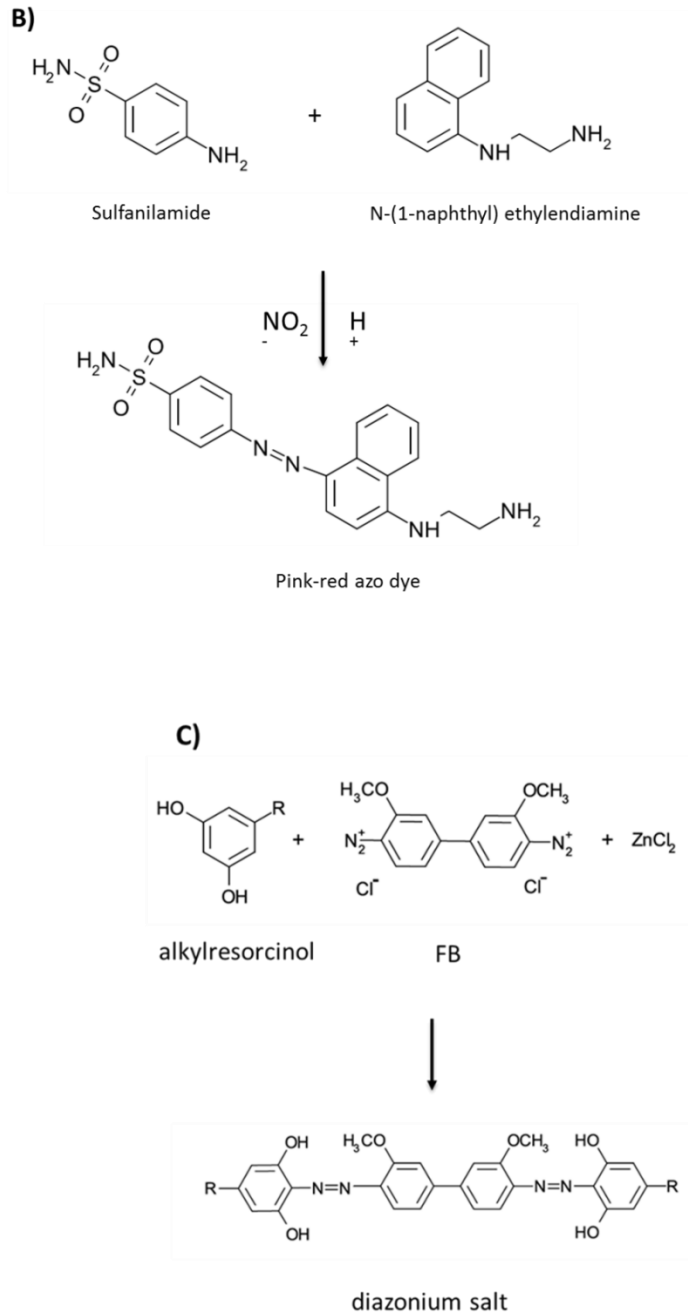


**Figure 1.14** Derivatization reactions **A)** Reaction of NQS in the presence of primary, secondary amines or ammonia in an alkaline medium. **B)** Griess reaction in the presence of nitrites. **C)** Chemical reaction between AR and FB reagent.

**Nylon** is a synthetic polymer that belongs to the group of polyamide. It is formed by two monomers, each with 6 carbon atoms: hexamethylenediamine and adipic acid. The polymeric structure is shown in **Figure 1.15**

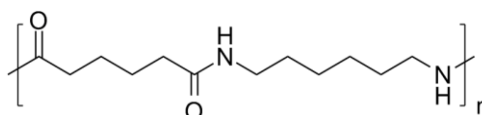


**Figure 1.15** Structure of Nylon.

Nylon membranes are hydrophilic, flexible and resistant in nature, with a regular microporous structure. Depending on the size of the pore there are nylon of 0.1, 0.22, 0.45 microns, the last two sizes have been used in this Thesis. Nylon membranes are widely used in different fields thanks to their inherent characteristics such as hydrophilicity, excellent physical and thermal resistance and good compatibility with aqueous samples. According to the mentioned characteristics, a variety of applications can be found such as diagnostic kits, biosensors, drug filtration, bacteria and particle retention. Regarding particle retention, there are several articles dealing with synthesis of nanoparticles in concrete of silver in nylon-nanofiber [126,127]. Considering this characteristic, it was used for the preparation of plasmonic sensors of AgNPs individual or multi-sensors attachable for 96-well plates. Multi-sensors allow simultaneous multi-analysis and they are in great need in the clinical field, where many samples are treated on a daily basis. Therefore, a sustainable technique including portability, simplicity, cost-effectiveness and ease of use arouses great interest in the clinical field. Our group had already developed another multisensory for simultaneous analysis in 96 wells [128], where the high importance of multisensory in the clinical field was emphasized, also cost-effectiveness, and simplicity of the method.

### 1.5.2 Analytical response

In Analytical Chemistry, colorimetric techniques are widely used in, since they provide both qualitative and quantitative information about a solution or a

coloured support. It is a simple technique, however, to obtain and quantify the analytical signal, specific equipment such as UV-vis spectrophotometers (in dissolution case) and diffuse reflectance equipment (in solid support case) are needed, among others. In this context, smart technology can provide solutions for in situ measurement and without qualified personnel. Currently, there are sophisticated smartphone, high resolution cameras, powerful processors with storage capacity, which can replace conventional equipment [104,129].

The relevance of this topic is demonstrated by the increase in the number of publication about smartphones as an example (see **Figure 1.16**).

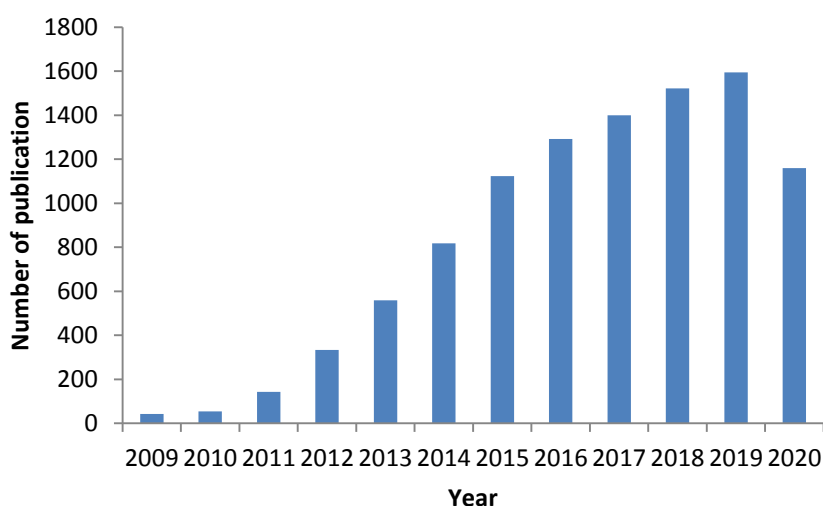


**Figure 1.16** Number of publication evolution in Web of Science on Smartphone used with analytical applications.

Currently there are several free and available applications that can be used for image analysis. Software such as Adobe Photoshop, GNU Image Manipulation Program (GIMP), Inkscape, Krita or ImageJ, are capable of converting a colour signal to different numerical parameters. There are several models for colour decomposition (RGB, HSV, CMYK, CIELAB), that allows to provide analytical information.

**RGB (Red, Green, Blue):** The colours are created from the combination of their three primary colours (red, green and blue), the intensities can vary between 0

and 255. The black colour is obtained when the value of the three components is 0, while the white occurs when all three parameters take the value 255.

**HSV** (Hue, Saturation, Value): It is a combination of three values: hue, saturation and brightness. Therefore, this model provides information on the quantity and brightness of the colour.

**CMYK** (Cyan, Magenta, Yellow y Key): Is a subtractive colour model, used in colour printing.

**CIELAB colour space** also referred to as  $L^*a^*b^*$  is a colour space defined by the International Commission on Illumination (abbreviated CIE) in 1976.

These models are tools for image analysis. However, the image acquisition stage plays a critical role, since the results derived from its subsequent treatment depend on it. One of the parameters that can most influence the quality of the image obtained is lighting reported by Chaplan et al. [130].

In order to solve this problem, some authors have proposed several techniques when taking the image, to eliminate any possible interference from external light that could influence the acquisition of the images [129,131,132]. On the other hand, other publications have chosen to insert reference points (black and white) aimed at correcting the interference factor [104,133]. In this Thesis RGB colour mode was used to perform images analysis.

## 1.6 Matrices and analytes

In this Thesis, IT-SPME- Cap-DAD and sensor devices have been proposed as sustainable tools to determine of different analytes of interest in environmental, biological, forensic and food sample.

### 1.6.1 Environmental samples

Humans are totally dependent on the environment for living. Therefore, it is important to take care and monitor the environment, through analytical techniques that allow qualification and quantification of different hazard analytes existing in the environment system. Environmental samples are air, water (aquifers, well water, coastal water, rain, among others), soil and sediments and

biota. The pre-treatment of environmental samples is a fundamental and essential step due to the complexity of the matrix [134].

Organic and inorganic compounds are of environmental interest, and therefore, the methodologies must be adequate to their requirements. In this Thesis, biocides such as irgarol, diuron, nitrite and nitrate have been studied as use cases of organic and inorganic compounds.

**Biocides: Irgarol-1051** belongs to compounds of the triazine family. **Diuron** is an herbicide from the phenylurea group. Irgarol-1051 and diuron, has been widely employed as booster biocides in antifouling paints to prevent the fouling on surfaces submerged in water [135]. The use of antifouling paints is an effective method to control invasive species, from microbes such as algae and bacteria to barnacles and shellfish that can adhere to the hull of ships, thus reducing the speed of ships and increasing fuel consumption [136]. These coatings, in addition to combating the formation and settlement of biofouling communities on surfaces exposed to water, are also intended to protect against chemical and biological corrosion. Normally these antifouling paints are applied to commercial and pleasure boats, underwater pipelines, dam gates, oil rigs, aquaculture facilities, among others. These biocides are added to antifouling products due to their high effectiveness as a growth inhibitor of marine and freshwater algae through interactions with their photosynthetic system. However, both compounds show harmful effects to the marine ecosystem [137] at a concentration level given. Irgarol and diuron accumulate in areas where they are intense boating activities. This is mainly due to the fact that both biocides are relatively persistent in sea water and not widely divided into other environmental matrices such as sediments.

In seawater, Irgarol-1051 has a half-life ( $t_{1/2}$ ) of between 100 and 350 days [138–140] whilst being very persistent in anaerobic sediments [141]. Irgarol-1051 as it does not easily degrade in water which may explain its persistence once released from painted surfaces [139] (Scarlett et al. 1999). Diuron also persists in seawater, but is less persistent in marine sediments with a half-life of 14 days [142].

Additionally, these compounds can be degraded to different transformation products that are potential contaminants as secondary pollution [143–145].

**Figure 1.17** shows the structure of iragrol - 1051 and diuron as well as their main degradation products and maximum allowable concentrations (MAC) expressed [146] from the environmental quality standards (EQS)[147].



Both biocides do not present the same toxicity for all types of aquatic beings. For example, diuron has extremely high toxicity for phytoplankton organisms, however it has lower levels of toxicity for aquatic invertebrates. Therefore, data on possible effects on environmental matrices are very important in the general assessment of the risks that these biocides can cause to the aquatic environment. Therefore, is necessary to control their levels in environmental matrices to avoid harmful environmental effects.

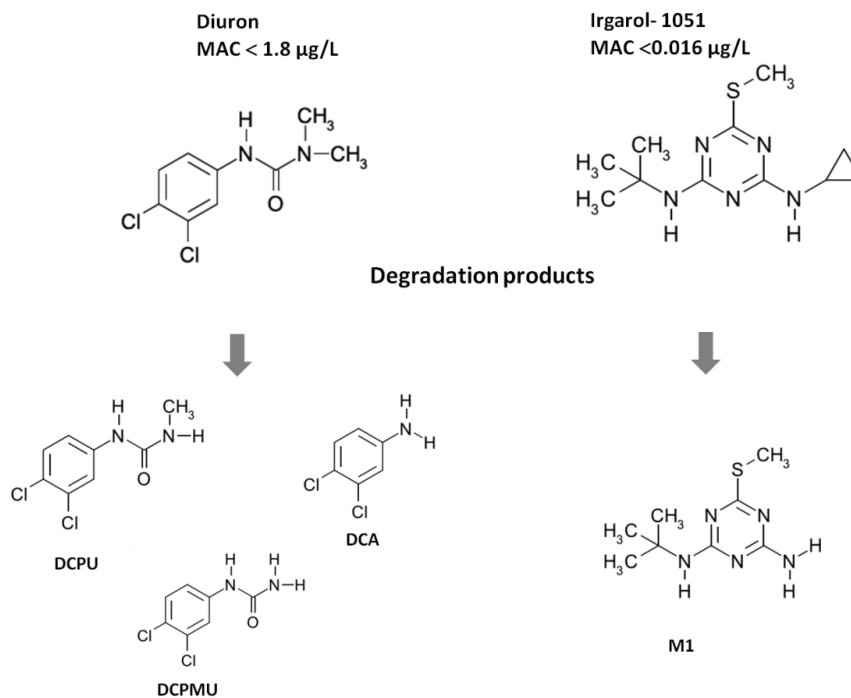


**Figure 1.17** Diuron and irgarol-1051 chemical structure with their main degradation products DCPU (3, 4-Dichlorophenylurea), DCPMU (1-(3, 4-Dichlorophenyl)-3-methylurea), DCA (3,4 - dichloroaniline) and M1 (2-methylthio-4-tert-butylamino-6-amino-s-triazine) respectively.

Consequently, the determination of these compounds in water involves extraction, clean-up and preconcentration before the chromatographic analysis. Solid phase extraction (SPE) coupled with HPLC-UV detection or HPLC-MS detection have been reported to determine booster biocides in environmental matrices [148,149]. Fully automated procedures such as SPE coupled on-line with LC-MS have also been investigated [150,151]. These systems showed high sensitivity, reproducibility and selectivity not only for biocides but also for multiresidue analysis. Giraldez et al. evaluated stir bar sorptive extraction (SBSE) and thermal desorption (TD)-GC-MS to determine these compounds in sea water with successful results [152]. In addition, microwave assisted extraction followed by SPE (MAE-SPE) and combined with LC-MS/MS have also been proposed to estimate booster biocide in environmental matrices [153]. Microextraction based techniques are other alternatives as pre-treatment step to extract and preconcentrate booster biocides from environmental samples. Headspace solid phase microextraction (HS-SPME), SPME and single drop solid phase microextraction (SDSPME) were first utilized [154–156]. More recently, microfunnel-supported liquid-phase microextraction (MF-LPME) coupled to HPLC-UV detection has been described to determine irgarol-1051 and diuron in water samples [157]. Moreover, dispersive liquid-liquid microextraction (DLL-ME)-HPLC-MS/MS has also been proposed for these biocides [158]. In all cases, these techniques are carried out in off-line mode, which yield to long analysis times, especially if the number of samples is high. Therefore, in this context, the use of on-line SPME techniques, such as in-tube solid phase microextraction (in-tube SPME), can be advantageous compared with off-line SPME modalities since extraction, preconcentration, injection, separation and detection are carried out in a single step. Thus, analysis time is reduced and sensitivity and precision can be improved.

**Nitrite and Nitrate ( $\text{NO}_2^-$ ,  $\text{NO}_3^-$ )**

In environmental samples, such as water, nitrite and nitrate are widely present. The high risk of nitrate and nitrite contamination is due to the use of fertilizers, animal waste, and wastewater disposal. Due to their high solubility in water, nitrate and nitrite migrate from the soil to groundwater and as they do not volatilize, therefore, they are likely to remain in the water until consumed by plants or other organisms [159]. Nitrate is consumed in a variety of bacterial processes such as the anaerobic denitrification, dissimilatory nitrate reduction to ammonium or nitrous oxide, being a potent greenhouse gas [160]. The amounts of nitrate in waters and soil contribute to their amounts in vegetables and fruits. Therefore, elevated concentrations of nitrate in water systems pose a significant risk to both the environmental and to human health [161]. In **Table 1.5** are summarized the main regulations about nitrate concentration in water.

**Table 1.5** Concentrations limits of nitrate or nitrite established by different regulations.

Sample	Limit $\text{NO}_3^-$	Limit $\text{NO}_2^-$	Regulation
<b>Drinking water</b>	50 mg/L	0.5 mg/L	Council Directive 98/83/EC of 3 November 1998 [162] EPA - United States Environmental Protection Agency [163] WHO – World Health Organization [164]
<b>Groundwater</b>	50 mg/L	-	Directive 2006/118/EC of the European Parliament and of the Council of 12 December 2006 [165]
<b>Sewage treatment plant</b>	25 mg/L	-	Spanish regulation, Royal Decree 1620/2007 of 7 December [166]

Because of this concern, during the past 15 years, numerous methods have been reported for the detection and determination of nitrite and/or nitrate including spectrophotometric, chemiluminescent, electrochemical, chromatographic, capillary electrophoresis, spectrofluorimetric and electrochemiluminescent methods [167]. From among these methods, the spectroscopic methods have excellent detection limits and have facile protocols. These methods are far the most widely used due to its simplicity and cheapness. The well-known

spectrophotometric method for analysis of nitrite is based on the Griess reaction [168]. Often the protocols described for this determination indicate that the procedure should be carried out in the laboratory either in batch or continuous mode (flow injection analysis). These methodologies are far away from the actual needs of analytical methods that combine high sensitivity, accuracy and rapid analysis with simplicity, portability, low cost and accessible to non-qualified personal. Thus, in order to develop in situ procedures, the Griess reaction presents some weak points, such as i) the reagents are added in solution and ii) the determination of nitrate required its reduction to nitrite. Concerning to Griess reagents, these are rather unstable and usually need to be keeping at low temperatures as individual solutions. An option to stabilize reagents is to embed them in solid supports; material such as polymers can be used as an inert matrix support [111,169]. This scheme is increasingly used for the development of optical sensors and microfluidic devices [112,113,128,170]. These strategies generally allow miniaturization, reduce reagent and waste, cost, non-required any external forces, and they can be used for in situ analysis by non-trained personal. It should be noted, the reagent entrapment during the polymeric gelation process has certain advantages such as greater resistance of the membrane or a better preservation of the reagent against environmental conditions. For the  $\text{NO}_3^-$  reductors such as Zn and Cd have been used. After a literature search we found the following nitrate reduction approaches: using a column of Zn granules or a copper-coated cadmium column [171,172] and hydrazide with copper catalyst [173] photoinduced device. Also vanadium III chloride as a reducing agent was proposed [174,175]. Many of these procedures were performed online using flow injection analysis (FIA) to monitor the reduction process and the derivatization step. In reference to the in situ procedures Martínez-Cisneros et al. [176] proposed a laboratory procedure on a chip using a cadmium column and Griess reaction. M. Jayawardane et al [177], used immobilized Zn powder for the reduction reaction and developed a procedure based on microfluidic paper. In recent years, the use of nanoparticles aroused great interest due to their special properties. To our knowledge, any work has been published using NP as a nitrate reductor combined with the Griess reaction. In this Thesis, PDMS based membranes have been proposed to determine  $\text{NO}_2^-$  and  $\text{NO}_3^-$  in fresh and preserved spinach and chard matrices. **Table 1.6** summarizes some methods for determining  $\text{NO}_2^-$  and  $\text{NO}_3^-$ .

**Table 1.6** Main analytical properties of different procedures described in the literature for  $\text{NO}_2^-/\text{NO}_3^-$  determination (\*related with higher complexity of the parameter).

Analyte/ sample	Procedure	Evaluation					Ref.
		Analytical parameters		Green points	Economical points		
		Analytical time/ Robustez	Figures of merits LODs/Dynamic range	Foot print Kg $\text{CO}_2/100$ muestras	Waste	Reagent consumption Personal time consumed Instrumentation	
$\text{NO}_3^-$ (water)	<b>Nitrate Reduction</b> – column Zn granules (0,15-0,40 mm) 8cm- 3 min. <b>Derivatization Griess-</b> solution <b>Analytical signal-</b> Absorbance	FIA in lab or in situ (40 samples/h)	1,3 ug/L 3-700 ug/L	0.25	High amount of waste (continous flow)	Reagents:*** Personal: ** Instrumentation: ***	[171]
$\text{NO}_2^-/\text{NO}_3^-$ (water and food samples)	<b>Nitrate Reduction</b> – Zn powder (0,1 g/sample)- 5 min volume 100 mL <b>Derivatization Griess-</b> 10 min <b>Analytical signal-</b> Absorbance	Batch	3 to 5 mg/Kg	5.99	High volumes used	Reagents:*** Personal: *** Instrumentation: **	[178]

NO <sub>3</sub> <sup>-</sup> (water)	<b>Nitrate Reduction –</b> Zn powder (150 μm) (25 mg/sample)-10 min <b>Derivatization Griess</b> - solution <b>Analytical signal-</b> Absorbance	Batch	0,5 mg/L 0,5-45 mg/L	0.23	10 mL sample/1 min reagent	Reagents:** Personal: *** Instrumentation: **	[179]
<sup>a)</sup> NO <sub>2</sub> <sup>-</sup> / <sup>b)</sup> NO <sub>3</sub> <sup>-</sup> (Synthetic, tap, pond and mineral water)	<b>Inkjet printing with</b> <b>AKD</b> Zn suspension prepared by mixing 500 mg of Zn dust (<10 μm); 1mg /sample (75seconds) <b>Derivatization Griess</b> - μPAD paper support (3-7 min) <b>Analytical signal-</b> scanned images processed	In situ Microfluidic Sensor Stable for 30 days Stored in vacuum at ≤- 20°C )	<sup>a)</sup> 1,0/ <sup>b)</sup> 19 μM 10-150 μM <sup>a)</sup> 50-1000 μM <sup>b)</sup>	9.45 In the fabrication of the sensor /scanner	Low consumption of reagents (μl)	Reagents:* Personal: * Instrumentation: **	[174]
Reference methods							
NO <sub>3</sub> <sup>-</sup>	<b>Electrode Nitrate</b> 10 mL sample 10 mL of buffer ( (Al <sub>3</sub> SO <sub>4</sub> ) <sub>3</sub> 17 mg ; Ag <sub>2</sub> SO <sub>4</sub> 34.3 mg; H <sub>3</sub> BO <sub>4</sub> 18.6 mg, H <sub>2</sub> SO <sub>3</sub> H 25.4 mg/per sample)	In situ o in the lab Interference s: Cl <sup>-</sup> , CO <sub>3</sub> <sup>-2</sup> , NO <sub>2</sub> <sup>-</sup> , CN <sup>-</sup> , S <sup>2-</sup> , Br <sup>-</sup> , I <sup>-</sup> , ClO <sub>3</sub> <sup>-</sup> ,	LODs: 10 <sup>-5</sup> M Range: 10 <sup>-5</sup> M- 10 <sup>-1</sup> M	1.8*10 <sup>-4</sup>	High volumes	Reagent:** Time/sample: 3min Instrumentation: ***	[180]

	<b>Analytical signal-</b> Electrochemical	$\text{ClO}_4^-$					
$\text{NO}_3^-$	Absorbance measurement at 220 nm and 275 nm <b>Analytical signal-</b> Absorbance	In situ (probes) In the lab (batch or FIA) Interference s: soaps, $\text{NO}_2^-$ , $\text{Cr}^{6+}$	LODs: 0.02 mg/L Range: 0.07 a 7 mg/L	0.025		Reagent: Time/sample: 1min Instrumentation: ***	[180]
$\text{NO}_3^-$	<b>Nitrate Reduction –</b> Cd column <b>(Derivatización Griess</b> - solution <b>Analytical signal-</b> Absorbance	FIA Column innactivation , Cd toxicity	LODs: 0.002 mg/L Range: 0 a 10 mg/L	0.082	Waste of Cd	Reagent: *** Time/sample: 15min Instrumentation: ***	[180]
$(\text{NO}_3^-, \text{NO}_2^-)$ $(\text{Cl}^-, \text{F}^-, \text{PO}_4^{3-}, \text{SO}_4^{2-})$	<b>Ionic Chromatography</b> Anionic column, mobil phase $\text{Na}_2\text{CO}_3$ 5.2 mM/ $\text{NaHCO}_3$ 1 mM Injection 20 $\mu\text{l}$	In the lab	Intervalo: 0.2— 50 mg/L LODs 0.02 $\mu\text{g/L}$	3.3		Reagent:* Time/sample: 20 min Instrumentation: ****	[180]

### 1.6.2 Biological samples

Regarding to biological samples, the aim of quantitative analytical method is to provide accurate and reliable results of the amount of a targeted or untargeted analyte, usually a pharmaceutical or drug, a metabolite or a biomarker. Biological samples such as organs, tissues, cells, DNA, RNA, proteins, exhaled breath or body fluids like urine, saliva, blood, sweat, cerebrospinal fluid, breast milk, sweat, gastric fluid, among other [181] can be considered. The development of biological sample analysis methods has become more and more challenging over the past years due to very demanding requirements in terms of method reliability, sensitivity, speed of analysis and sample throughput.

In this Thesis different biological samples have been studied to develop new sustainable strategies. Mucosa samples, breath samples and urine samples have been analysed to determine different analytes of interest. Both, in-tube SPME-DAD and PDMS and nylon based in-situ devices have been proposed.

**Endotracheal tubes (ETTs)** are catheters that are inserted into the trachea with the purpose of establishing and maintaining a patent airway and to ensure adequate exchange of O<sub>2</sub> and CO<sub>2</sub>. Therefore, it is an increasing source of healthcare-associated infections due to colonization of these appliances by microbes[182]. The surface of these devices acts as a substrate which allows the attachment of microorganisms, resulting in the formation of a dense multicellular communities of bacteria embedded in a self-produced extracellular matrix that imbibes and protects them, known as biofilm [183,184]. The formation of a biofilm in medical devices is of particular concern due, once the device is colonized, infection is such difficult to be eradicated that, in most clinical practice guidelines, the withdrawal of a device related to the infection is recommended. However, in many occasions, the devices removal is not possible and the treatment with an antimicrobial therapy is needed, making the biofilm an object of great interest in many investigation fields. Although, there are several approaches for the biofilm prevention, traditional treatment with antimicrobials is generally used [185]. In this Thesis meropenem has been studied.

**Meropenem (Figure 1.18)**, chemically (4R,5S,6S)-3-[(3S,5S)-5-(dimethylcarbamoyl)pyrrolidin-3-yl]sulfanyl-6-[(1R)-1-hydroxyethyl]-4-methyl-7-oxo-1-azabicyclo[3,2,0]hept-2-ene-2-carboxylic acid, is a carbapenem ( $\beta$ -lactam) antibiotic with broad-spectrum to a wide range of gram positive, gram negative



and anaerobic bacteria. These type of  $\beta$ -lactams are often used as last resort when patients with infections become gravely ill or are suspected of harboring resistant bacteria [186]. Carbapenems, like all  $\beta$ -lactam antibiotics, inhibit bacterial cell wall synthesis by inactivating penicillin-binding proteins [187–189]. Moreover,  $\beta$ -lactams are time-dependent antibiotic, which means that, to ensure a bactericidal effect, the concentration of free drug must be maintained above the minimum inhibitory concentration between two consecutive doses [190–193]. Meropenem has shown clinical efficacy in the treatment of a wide range of serious infections such as lower respiratory tract, intra-abdominal infection, obstetric/gynecological, urinary tract, meningitis, cystic fibrosis and in febrile neutropenia [194,195]. Therefore, the estimation of the concentrations in patients and in particular, in invasive medical devices, such as ETTs is of great importance in order to evaluate the effectiveness of treatments.

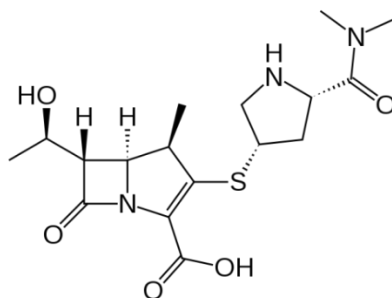


**Figure 1.18** Chemical structure of meropenem.

Traditionally, the determination of antibiotics in biological fluids has been carried out using microbiological procedures [6]. Nevertheless, the literature survey reveals different analytical methods for quantitative estimation of antimicrobials in biological fluids and in pharmaceutical formulations, including high-performance liquid chromatography [189,196–199], capillary zone electrophoresis [200] or ultraviolet spectrophotometry [196], among others (**see Table 1.7**). As can be observed, the analysis by HPLC with UV–vis [192,196] or MS/MS detection [188] remains the main analytical technique for the determination of antimicrobials. HPLC methods usually involve a sample pre-treatment step before the analysis, which generally is the most time-consuming part of the chemical analysis. As described in-tube SPME is a potential alternative method, and therefore, it was studied to determine meropenem in mucosa sample from endotracheal tube.

**Table 1.7** Main analytical properties of different analytical methods proposed for Meropenem and other antimicrobials in the bibliography.

Analyte	Matrix	Sample treatment	Method	LOD	LOQ	RSD (%)	Linear range	Ref.
<b>Meropenem</b>	Pharmaceutical dosage	-	Microbiological assay			0.94	1.5-6 µg/mL	[187]
<b>Meropenem</b>	Bacterial media	Centrifugation (centrifugal filter device)	LC-MS/MS			6.91	50-25,000 ng/mL	[188]
<b>Cefepim</b>	Human plasma	SPE (with tubes vacuum manifold Macherey-Nagel)	HPLC-UV		0.5, µg/mL	6.8	2.5–60 µg/mL	[192]
<b>Ceftazidim</b>					0.5, µg/mL	8.4	2.5–60 µg/mL	
<b>Cefuroxim</b>					0.5, µg/mL	12.2	2.5–60 µg/mL	
<b>Meropenem</b>					0.5, µg/mL	3.5	2.5–60 µg/mL	
<b>Piperacillin</b>					0.5, µg/mL	5.6	2.5–60 µg/mL	
<b>Meropenem</b>	Pharmaceutical dosage	-	HPLC-UV	4.24 ng/mL	12.85 ng/mL	0.85	10-70 ng/mL	[196]
			UV spectrophotometric method	19.41 ng/mL	59.09 ng/mL	0.89	5-35 ng/mL	
<b>Meropenem</b>	Serum and bronchial secretions	SPE(HPLC-integrated-extraction system) (extraction column)	HPLC-UV/vis	0.5 µg/mL	0.5µg /mL	6	0.5 to 40 µg /mL	[197]
<b>Amikacin</b>	Water	SPE(laboratory-made exchange columns packed)	SCX- HPLC-CL	0.7 µg/L		3.1	2.5-50 µg/L	[201]
<b>Streptomycin</b>				7.5 µg/L		4.9	25-500 µg/L	
<b>n</b>				10.0 µg/L		5.4	30-750 µg/L	
<b>Kanamycin B</b>				1.0 µg/L		2.7	3.5-75 µg/L	

<b>Paromomycin</b>				1.5 µg/L		3.6	5.0-100 µg/L	
<b>Neomycin B</b>	plasma	Centrifugation	HPLC-UV	0.01 µg/ml	0.05 µg/ml	7.17	0.05-100µg/ml	[202]
<b>Meropenem</b>								
<b>Meropenem</b>	Plasma	SPE(HLB cartridges used in a Varian vacuum manifold)	MEKC	0.2 µg/mL			0.5–50µg/mL	[203]
<b>Linezolid</b>	Cerebrospinal fluid	Without sample pretreatment		0.3 µg/mL				
<b>Meropenem</b>	Bacterial growth médium (spiked sample)	1.Precipitation(centrifugation) with direct injection	HPLC-DAD		0.5 µg/mL			[204]
<b>Vancomycin</b>		2.Precipitation and solvent evaporation			2 µg/mL			
					0.5 µg/mL			
<b>Amoxicilin</b>	Human plasma	Precipitate of proteins and centrifugation.	UPLC-MS/MS	-	1.05 mg/L	16.7	1-100 mg/L	[205]
<b>Cefuroxime</b>	Bovine serum				0.62 mg/L	11.9	1-100 mg/L	
<b>Ceftazidime</b>					0.81 mg/L	7.1	0.5-80 mg/L	
<b>Meropenem</b>					0.52 mg/L	11.4	0.5-80 mg/L	
<b>Piperacillin</b>					1.09 mg/L	8.1	1-150 mg/L	
<b>Ertapenem</b>	Urine (spiked sample)	-	LC-UV	2.362 µg/mL	7.156 µg/mL	1.354	15-50 µg/mL	[206]
<b>Meropenem</b>				0.943 µg/mL	2.858 µg/mL	0.909	20-50 µg/mL	
<b>Doripenem</b>				1.137 µg/mL	3.445 µg/mL	1.391	20-50 µg/mL	

				µg/mL	µg/mL			
<b>Meropenem + 10 β-lactams</b>	Human plasma	Centrifugation	HPLC-UV		0.1 µg/mL	4.7	0.1- 50 µg/mL.	[207]
<b>Doripenem</b>	Human plasma	Centrifugation of human plasma adding internal standart solution. Evaporation	UPLC-UV		0.50 mg/L	6.6		[208]
<b>Ertapenem</b>					0.50 mg/L	12.2		
<b>Imipenem</b>					0.50 mg/L	5.08		
<b>Meropenem</b>					0.50 mg/L	2.9		
<b>Ampicillin</b>	Human Plasma	Centrifugation	LC-MS/MS		300 ng/mL	6.97	0.3-150 µg/mL	[209]
<b>Piperacillin</b>					300 ng/mL	8.20	0.3-150 µg/mL	
<b>Tazobactam</b>					150 ng/mL	7.02	0.15-75 µg/mL	
<b>Meropenem</b>					50 ng/mL	7.81	0.1-50 µg/mL	
<b>Acyclovir</b>					100 ng/mL	9.06	0.1-50 µg/mL	
<b>Metronidazole</b>					100 ng/mL	9.44	0.05-25 µg/mL	
<b>Meropenem + 11 β-lactams</b>				Human plasma	Proteins precipitation with ACN and centrifugation	HPLC-UV		5 µg/mL
<b>Meropenem + 8 β-lactams</b>	Human serum (spiked sample)	SPE (using Waters Oasis HLB cartridges)	HPLC-MS/MS	0.05 µg/mL	0.10 µg/mL		0.1–50 µg/mL	[211]
<b>Meropenem Biapenem</b>	Peritoneal fluid	Centrifugation (Nanosep 10K centrifugal filter device)	HPLC-UV		0.01 µg/mL	0.05 µg/mL	0.05–100 µg/mL	[212]
	Human Bile				0.02 µg/mL	0.1 µg/mL	0.1–100 µg/mL	

**Volatile sulfure compounds (VSCs)**

The composition of human breath can provide relevant information about health status, thus, it is an interesting biological sample. Many volatile organic compounds (VOCs), mainly alkanes and benzene derivatives, in the breath report lung cancer [213]. On the other hand, Broza et al. report a respiration-based classifier for gastric cancer that uses a nanomaterial-based sensor array [214]. Early detection of kidney lesions can also be performed using breath samples [215]. Finally, volatile sulfur compounds (VSCs) such as hydrogen sulfide ( $\text{H}_2\text{S}$ ), methyl mercaptan ( $\text{CH}_3\text{SH}$ ), and dimethyl sulfide ( $(\text{CH}_3)_2\text{S}$ ) have interest in many analytical fields; one of the most monitored gas is  $\text{H}_2\text{S}$  [216]. Specifically, VSCs are primarily produced by anaerobic bacteria and are considered to be the major gases associated with halitosis and have demonstrated a high correlation with breath malodour, which is also termed as halitosis [217]. Halitosis is one of the common problems that affect people in their day to day life, and it is an important negative factor in social communication. It has been reported that about 20% of the general population are suffering from halitosis, and about 50% was estimated that will suffer from it once in their lives [218]. In addition, some studies reported that halitosis or bad breath can be associated with the presence of plaque, tongue coating [219] and periodontal diseases [220]. According to several studies is not considered halitosis if VSCs levels are between 80-160 ppb, considered weak halitosis if  $[\text{VSCs}] = 160\text{-}250$  ppbv (malodor at a close distance) and halitosis strong- $[\text{VSCs}] > 250$  ppbv (malodour at a greater distance) [220,221]. Commercial measurement tools for the quantification of mouth odours are the halitometer [222] and CG and GC-MS [223]. These are expensive and relatively complex instrumentation and requires warm-up times and yearly maintenance and they are not accessible to the general population. Also, there is an Oral microbial BANA [224] test, which quantifies salivary levels of an enzyme, correlating this value with sulfide levels (see **Table 1.7**). Other methods for determination of sulfur compounds frequently used are electrochemical devices [225] and optical methods such as the commercial lead acetate paper strips 48 or the colorimetric tubes of  $\text{Hg}^{+2}$  [226]. These methods have some disadvantages, for example, lead, its toxic and colorimetric tubes need active sampling with a pump; and in addition, the sensitivity of these methods often are low ( $>1000$  ppbv), which is not suitable for sensitive sulfur detection in, for example, breath samples. An iodometry coupled to a photometric detector [227] was also proposed with a good limit of detection. A disposable sensor based on  $\text{Bi}(\text{OH})_3$  coated on paper and

wetted in alkaline media responded also to H<sub>2</sub>S in 30 min [228]. This sensor has been tested in breath samples, however, it needs to be stored under a nitrogen atmosphere to avoid reactivity with CO<sub>2</sub>. Plasmonic colorimetric sensors have been also reported for sulphide detection but these were performed in solution [229–231]. **Table 1.8** shows a summary of the analytical methods for determining VSCs.

**Table 1.8** Summary of existing methods for the in situ sulphide determination.

Analytical method	Concentrations (LOD, range in ppbv)	Response (time, linear conditions)	Selectivity	Stability	Matrix	Applications (samples)	Green Process <sup>a</sup>	Cost <sup>b</sup>	Ref./ Commercial brand
<b>1) INSTRUMENTAL</b>									
<b>Halitometer (electrochemical sensor)</b>	LOD = 10 10 - 3000	10 min	Affected by humidity, alcohol and other gases	1 year	Gaseous	Breath (Halitosis)	x	***	[222] Commercial
<b>OralChroma (Gas chromatography)</b>	LOD = 10 50-1000	8 min	Separately determination of H <sub>2</sub> S, metyl and dimethyl mercaptano	2 years	Gaseous	Breath (Halitosis)	x	***	[223] Commercial
<b>2) INDIRECT</b>									
<b>Enzymatic test BANA:</b>	Semi-cuantitativo	15 min, 55°C	Affected by humidity and light	-	Aquesos	Saliva	xx	**	[224] Commercial
<b>3) ELECTROCHEMICAL</b>									
<b>In<sub>2</sub>O<sub>3</sub>@CuO</b>	300-10000 LOD = 300	5 sec RT	Detection of H <sub>2</sub> S and NH <sub>3</sub>	30 days	Gaseous	-	xx	**	[225]
<b>4) OPTIC</b>									

<b>Lead acetate paper strips</b>	3525- 35250	< 1 min	-	-	Gaseous Aqueous	Employment security and others	x	*	[232] Commercial
<b>Colorimetric tube of Hg<sup>+2</sup> and a pump</b>	LOD = 2·10 <sup>3</sup> (2 - 50)·10 <sup>3</sup>	6 min	SO <sub>2</sub> , HCl, Ethyl mercaptane	-	Gaseous	Employment security and others	x	**	[226] Commercial
<b>Iodometry. Sampler and fotometric detector</b>	LOD = 3.6 150 – 705	12 min	-	-	Gaseous	Breath (n=10)	xx	*	[227]
<b>Bi(OH)<sub>3</sub> on paper (sock it in buffer before use)</b>	LOD > 30 30-200	30 min	Can react with CO <sub>2</sub>	1 month (under N <sub>2</sub> )	Gaseous	Breath (n=1)	xx	**	[228]
<b>AgNO<sub>3</sub> and 3,3',5,5'-tetramethylbenzidiea nanoparticles of Ag<sub>2</sub>S</b>	LOD = 5 24 – 1922	5 min, 30°C, pH=4	Selective to cations and anions	Prepara tion before use	Aqueous	Water samples	xxx	*	[230]
<b>AgNP-tanic acid-benzoquinones</b>	LOD: 4.8·10 <sup>3</sup> (4.8 – 4.8) ·10 <sup>3</sup>	10 min	Selective to thiosulfate against other anions	In solution	Aqueous	Tap and lake water	xxx	*	[231]

<sup>a</sup> Greenest process correspond to xxx, <sup>b</sup> higher cost corresponds to \*\*



In recent years interest in methods of detecting H<sub>2</sub>S in biological matrices has increased, as it is a modulator of the fundamental physiological and pathophysiological functions in different organs such as the brain [233,234], the kidney [235] and the gastrointestinal tract [236,237]. H<sub>2</sub>S has also been reported to be involved in the pathogenesis of a variety of disorders, including Alzheimer's disease and Down syndrome [238,239]. Its physiological actions have also been shown to include regulation of inflammation[240], blood pressure [241], energy production [242] and oxidative stress [243]. Experimental studies reveal that H<sub>2</sub>S is produced enzymatically at  $\mu$ M levels in mammals and exerts a series of physiological actions on the cardiovascular system[240,244]. In previous years cardiovascular research had focused mainly on two endogenously produced gas signaling molecules: nitric oxide and carbon monoxide. However, a third endogenously produced gas signaling molecule, H<sub>2</sub>S, has become a potentially important mediator in such research [245]. In summary, we can say that the accurate and reliable measurement of H<sub>2</sub>S concentrations in biological matrices can provide critical information on the relationship of amounts of H<sub>2</sub>S with various normal or abnormal biochemical processes. Due to many H<sub>2</sub>S-mediated physiological processes discovered in recent years, the search for new methods of detecting H<sub>2</sub>S in biological matrices is at the centre of scientific research.

The properties of the previous method, showed difficulties to be applied for some biological samples such as living cells due to their destructive nature. Therefore, it would be interesting to develop a sensitive, non-invasive, simple, inexpensive, and easy to prepare sensor for in situ analysis for detection of H<sub>2</sub>S, in vitro live cell assays. Therefore, a non-invasive sensor, with high sensitivity and selectivity, inexpensive and easy to prepare for H<sub>2</sub>S in situ analysis in live cell assays in vitro will be an alternative satisfactorily accepted.

### **Alkylresorcinols**

Urine is a biological matrix widely used to determine the health status by obtaining information biomarkers. In this Thesis **alkylresorcinols** in urine samples have been studied as biomarkers to evaluate an adequate gluten-free diet in celiac patients.

Celiac disease is an immune-mediated systemic disorder elicited by gluten and related prolamines present in genetically susceptible individuals. It is characterized by the presence of different clinic symptoms, specific antibodies (SA), haplotypes HLC DQ2 and/or DQ8 and enteropathy. The only efficient therapy is to follow a gluten free diet (GFD), however there are several drawbacks limiting its efficiency, since their compliance with the gluten-free diet is not always adequate, and thus low adherence is achieved and many food products contain low concentrations of gluten. The serologic biomarkers have a limited utility to detect food transgressions, since last more than 24 months to obtain a negative response and afterwards, low transgressions do not produce immunologic response. By another hand, dietary reports are also used, however their low reliability have been demonstrated.

Therefore, and given the relevance of this health problem, there is an important need of a good biomarker that can estimate the gluten intake in the evaluation of celiac patients. Thus, alkylresorcinols (AR) is potential biomarkers to estimate little variations of GFD. These compounds are present in gluten containing grain, hence they can be used as biomarkers of gluten intake of individuals with GFD. The main benefits of the monitoring are directly related with the diet control, preventing patients from involuntary transgressions improving the diagnostic and the medical prognosis, which would be translated in socio-economic benefits in the health system. Therefore, RA and its metabolites can be considered as possible biomarkers in biological samples. In this Thesis 3,5-dihydroxyhydrocinnamicacid (DHCA) and 1,3-dihydroxy-5-pentylbenzene (PR) has been studied (see **Figure 1.19**).

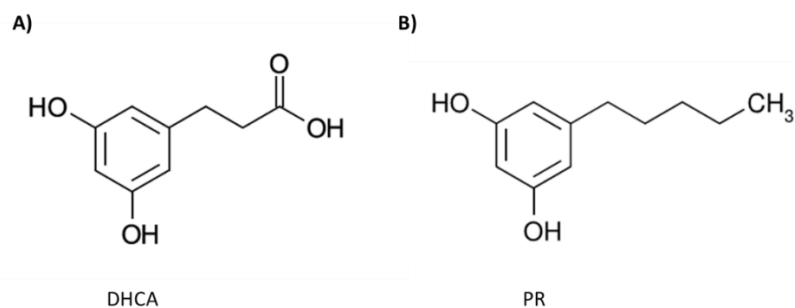


**Figure 1.19. A) DHCA and B) PR structures.**

From an analytical point of view, the methods described to study these compounds are based on chromatographic, HPLC or GC methods with a previous pre-treatment step of the sample. In the case of biological samples, solid phase extraction has been the most widely used technique to extract and preconcentrate analytes. On the other hand, detection has been carried out by UV-vis, fluorescence or EM [246–253]. These reports have shown the possible application of AR as a dietary biomarker of gluten ingestion, however from a practical point of view, there is a need for simplified devices that allow the estimation of these biomarkers for medical services and patients, mainly to obtain a rapid response to possible food offenses.

**Table 1.9** Previously proposed techniques for the determination of AR.

Analysis technique	Extraction	Matrix	Analyte	LOD	RSD (%)	Ref
<b>GC-MS</b>	EFS	Biological fluid	AR	35 nmol/ L	< 15	[254]
<b>GC-MS</b>	EFS	Biological fluid	AR	0.1 µmol/L	< 11.5	[247]
<b>HPLC - DAD - MS</b>	Ultrasound assisted extraction	Food	AR	1.18 – 8.38 ng	< 4.99	[247]
<b>UHPLC - UV-vis</b>				1250 pg	< 10	[248]
<b>UHPLC -Fluorescence</b>	Lixiviation	Food	Heptadecylresorcinol Nonadecylresorcinol Tricosylresorcinol Pentacosylresorcinol	2 pg	< 10	
<b>UHPLC – electrochemical detector</b>				20 pg	< 10	
<b>HPLC - fluorescence</b>	EFS	Biological fluid	Total alkylresorcinol	1.1-1.8 nmol/ L	< 3.1	[249]
<b>Spectrophotometer – UV-Vis</b>	Maceration	Food	Olivetol Catechin	0.253 µg/mL 0.768 µg/mL	< 9.7	[251]

### 1.6.3 Forensic matrices

Forensic science is considered as an alternative for the administration of justice to assist in the resolution of conflicts between members of the community. Forensic samples provide the scientific truth for the administration of justice. Analysis of these samples can take weeks or even months to complete due to the technical requirements of different forensic tests, the limited availability or integrity of some samples and their complexity, and finally, the extensive collection of data in the records required for legal proceedings, makes these tests slower. Therefore, the development of forensic analysis methods has become more and more challenging due to the very demanding requirements mentioned above, such as method reliability, sensitivity and analysis speed.

Chemical and physical evidence such as **gunshot residues (GSRs)** from firearms discharge may provide valuable forensic information [255,256]. GSRs are organic and inorganic components in nature, which can be deposited on a shooter's body, mainly onto the index fingers and thumbs of the hands, after discharging a firearm [257]. A suspect can be successfully identified if GSRs are reliably analyzed. Thus, the detection of these compounds plays an important role in the field of forensic science. Inorganic gunshot residues (IGSRs) are usually spherical particles mainly composed of Ba, Pb, and Sb [258]. Other elements such as Ca, Al, Cu, Fe, Zn, Ni, Si, and K can also be found [259], although they are more prevalent in the environment than Pb, Ba, and Sb [260]. The size of these particles is usually from 0.5  $\mu\text{m}$  to 10  $\mu\text{m}$ , although sizes up to 100  $\mu\text{m}$  have also been reported [261]. The presence of these metallic particles has been traditionally confirmed by scanning electron microscopy coupled to the energy dispersion X-ray (SEM-EDX) technique due to its non-destructive capability to perform both morphological and elemental analyses [262]. However, the analysis of IGSRs has its limitations. False positive results can be produced from inorganic particles derived from environmental and occupational sources [263–265], which is a problem when considering IGSRs as evidence in judicial proceedings in the forensic field. The analysis of organic gunshot residues (OGSRs) in the same sample could provide complementary information that could strengthen the probative value of a forensic sample. Organic components originate mostly from the propellant, and their composition depends on the commercial brand and ammunition type. An important component of gun propellants is diphenylamine (DPA).

**DPA** is an organic compound with the structure presented in the **Figure 1.20**, is an important component of weapon propellants, used as a stabilizer to prevent the decomposition of explosive products such as nitrocellulose and nitroglycerin, both of which are present in many smokeless powders used as propellants[266] Therefore, this stabilizer may remain on a shooter's hands, and it may be used as an indicator of gunshot residues [267]. DPA detection could provide valuable evidence of firearm discharge for the identification of suspects in firearm-related crimes. The low amount of DPA remaining on a shooter's hands requires highly-sensitive analytical techniques for its detection. In order to improve the sensitivity, many methods include off-line sample treatment, which involves time-consuming and tedious steps. **Table 1.10** presents several methods used for extraction and determination of DPA that remains on the hands. The main drawback of the reported methods is the low detection limit required, taking into account the sampling and extraction process, time of analysis, and greenness of the procedure.

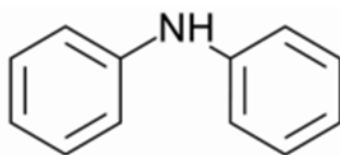


**Figure 1.20** Chemical structure of DPA

As mentioned in section 1.4 on-line sample pre-treatment has become an interesting alternative as sustainable analytical chemistry indicates. Although mass spectrometry (MS) coupled to gas chromatography (GC) or liquid chromatography (LC) offers suitable sensitivity, the chromatographic techniques can present issues. Thermal degradation of DPA can occur by GC and the wide range of polarities of compounds present in GSRs can limit LC. Some methods have also successfully identified DPA using several MS techniques without any chromatographic system such as tandem mass spectrometry (MS-MS) [268], desorption electrospray ionization-mass spectrometry (DESI-MS) [269], nanoelectrospray ionization mass spectrometry (nESI-MS) [270], and ion mobility spectrometry (IMS)[271]. However, IT-SPME coupled to capillary liquid chromatography (CapLC) contributes to increase the sensitivity and sample clean-

## Chapter 1. Introduction

up in an on-line way. Additionally, the miniaturization of the LC technique (i.e., low column dimensions, low flow rates, low amount of wastes) contributes also to achieve improved sensitivity, which can permit the use of diode array UV-detectors (DAD), which cost less than an MS detector.

**Table 1.10** Comparison of reported methods for DPA on a shooter's hands The method proposed in this work was also included for comparison (On-line in-tube solid phase microextraction coupled to capillary liquid chromatography with diode array detection (IT-SPME-CapLC-DAD)).

Analysis Technique	DPA extraction	LOD	DPA amount on hands	Mobile phase; Flow;Injection volume	Organic solvents	Ref.
HPLC-MS	DPA extracted with cotton swab soaked with acetone, wich was evaporated and dissolved in 0.1mL methanol	0.3 ng/mL (solution)	< LOQ	Methanol-water (90:10) 800µL/min; 10µL	Methanol and acetone as extractive solvent and movile phase	[267]
GC-MS	DPA extracted with cotton swab moistened in water , the swab was heated and capillary microextraction made	3 ng	≈1 ng < LOQ	-	Water as extractive solvent	[258]
MS	Cotton swab soaked with methanol to extract DPA from the hand and dilution to 1mL of methanol	1 ng/mL solution	Not studied	-	Methanol as extractive solvent	[268]
MS	Dabbing an adhesive coated aluminium stub over the hands	-	Not detected	4 µL/min	Water:methanol 0.1% formic acid as solvent spray	[272]
HPLC-MS	Cotton swab moistened with isopropyl alcohol:water, 75:25, which was introduced in a tube with 3.2 mL of the mixture and centrifuged. The aliquot was diluted five times with deionized water. SPEC C18 cartridges were	34 ng	0.29-83nmol/L	Acetonitrile: methanol: water, acidified by 0.1% of formic acid; 200 µL/min; 20 µL	Isopropylalcohol as extraction solvent, methanol and acetonitrile for mobile phase	[273]



	conditioned with 250 µL of isopropyl alcohol and deionized water. 5000 µL of aqueous samples were loaded. The sorbent was rinsed with 250 µL of deionized water and dried. The analytes were eluted in acetonitrile:water:methyl alcohol, 80:10:10; 200 µL				
CE	Hands were swabbed by a cotton swab embedded in a solvent. The analyte was recuperated by sonication into 2 mL of solvent. Liquid extraction was carried out with 2 mL of ethyl acetate and 50 µL of ethylene glycol; the solvent was evaporated under dry nitrogen. The residues were reconstituted with diaminocyclohexane tetraacetic acid, and borate	2387 ng/mL (solution)	Not detected	-	Diaminocyclohexane tetraacetic acid and sodium dodecyl sulfate as sampling solvents [259]

### 1.6.4 Food matrices

The evaluation of the food quality and authenticity has been and will be of great importance to guarantee the safety of food in accordance with the legislation. It includes the control of technological processes and their effect on food, the characterization of the food composition, determination of food nutritional value, among others. The complex combination of objectives mentioned above can only be addressed thanks to the large number of advanced analytical technologies available today.

#### Nitrite and Nitrate ( $\text{NO}_2^-$ , $\text{NO}_3^-$ )

Elevated concentrations of nitrate in food matrices suppose a significant risk to human health [161]. Nitrate can be reduced to nitrite even in the human digestive system causing several serious health problems, for example when nitrate can oxidize iron in hemoglobin thus leading to methemoglobinemia. Nitrite forms carcinogenic nitrosamines under the acidic conditions of the stomach which can cause gastric cancer [274].

Vegetables are the most important source of nitrate exposure in the human diet and contribute to the intake of more than 80% of nitrates [275]. The amount of nitrates in environmental samples such as waters and soil contribute to the amount in vegetables and fruits. The main regulations about nitrate concentration in fresh and preserved spinach and in two types of fresh lettuce are summarized in **Table 1.11**.

**Table 1.11** Concentrations limits of nitrate or nitrite established by different regulations.

Sample	Limit $\text{NO}_3^-$	Limit $\text{NO}_2^-$	Regulation
Fresh spinach	2500-3000 mg/Kg	-	Commission Regulation (EC) N° 1881/2006 of 19 December 2006 [276]
Preserved, deep-frozen or frozen spinach	2000 mg/Kg	-	Commission Regulation (EC) No 1881/2006 of 19 December 2006 [276]
Fresh lettuce	2500-4500 mg/Kg	-	Commission Regulation (EC) N° 1881/2006 of 19 December 2006 [276]
Iceberg-type lettuce	2000-2500 mg/Kg	-	Commission Regulation (EC) N° 1881/2006 of 19 December 2006 [276]

The maximum nitrate amount to be ingested daily is less than 3.65 mg/kg by body weight [277]. Therefore, it is essential to design sustainable analytical methods to be able to measure these analytes reliably and at low cost. As we discussed in section 1.6.1 there are several methods (spectrophotometric, chemiluminescent, electrochemical, chromatographic, capillary electrophoresis, spectrofluorimetric and electrochemiluminescent) to measure nitrate and nitrite in environmental and in food samples. [167]. As discussed earlier (in section 1.6.1) a device based on Greiss reagent embedded on PDMS supports has been proposed as a sustainable solution. **Table 1.6** summarizes some methods to determine  $\text{NO}_2^-$  and  $\text{NO}_3^-$  in food and in environmental water.

### **Ammonia and amines**

Meat products are commercially important and widely consumed foods, so ensuring their quality and safety are very essential. The quality of the meat is assessed by the following attributes, such as texture, colour, tenderness and freshness. Therefore, determining meat quality parameters are very essential in all food industry processes because consumers always demand superior quality of meat and meat products [278,279]. The meat freshness is a very important parameter to assess quality and safety [280,281] and it degrades due to microbial deterioration and biochemical reactions during storage. The main ingredients, such as carbohydrates, proteins and fats over time are broken down by enzymes and bacteria, producing many volatile organic compounds (VOCs): carbohydrates break down into hydrocarbons, alcohols, ketones and aldehydes; the protein will break down into **ammonia, amines**, hydrogen sulfide, ethyl mercaptan, etc.; the fat will break down into aldehydes and acid aldehydes [282]. Ammonia and aliphatic amines are colorless gases with a distinctive odor. Ammonia like aliphatic amines has become important pollutants due to their toxic and odorous characteristics. Ammonia and aliphatic amines found in air in considerable concentrations are the result of their extensive use throughout the chemical industry, in which these compounds are applied in the production of fertilizers, pesticides, surfactants, drugs, polymers, colorants. Hence, it is important to monitor these analytes. Ammonia is also produced naturally in the environment, in the air, soil, and water, in plants and animals, including humans. For example, the human body produces ammonia when it breaks down protein-containing foods into amino acids and ammonia, and then converts the ammonia into urea [283]. On the other hand, as commented above, during spoilage, protein-rich foods (meat chicken, pork, beef, mutton and fish) can release organic amines such as dimethylamine ( $C_2H_7N$ ), trimethylamine ( $C_3H_9N$ ), and ammonia ( $NH_3$ ) etc., as a result of microbial degradation. Total volatile basic nitrogen (TVBN) has been used as an index of decomposition in meats and fish since 1952. In meat, TVBN consists mainly of ammonia, with only traces of trimethylamine [284] and other amines. Some methods of evaluation of meat spoilage status determined by ammonia [285–288] and amine compounds [289–295] [21–30] are given in the literature. For amine compounds, generally a separation method was employed [25–30]. It is of great significance for rapid, accurate and nondestructive detection of meat freshness, increasing interest in developing in-situ analysis devices has risen for

aiding to the consumer. In this regard, the development of chemical sensor technology [79,111,285–287,296–298] has acquired great scientific impact. Below in the **Table 1.12** some sensors designed in recent years are discussed to monitor meat contamination and spoilage by determining ammonia and aliphatic amines. In this Thesis, NQS-ILs doped PDMS membranes have been proposed as a sustainable alternative to in-situ determination of ammonia and amines.

**Table 1.12** Different procedures described in the literature for TVBM quantification in meat matrix.

Type of sample	Analyte	Calibration lineal slope/ LOD	Sensor design	Reagent	Sensor response	Measurement	Ref.
<b>Pork and chicken</b>	Triethylamine	-	Intelligent film (Based on cassia gum containing Bromothymol Blue-anchored cellulose fibers)	Bromothymol Blue – pH indicator	colorimetric	portable colorimeter	[287]
<b>Beef (sirloin steak) Chicken (thigh)</b>	Trimethylamine Cadaverine	-/LOD <35ppbv	Combination of a disposable colorimetric sensor array from the printing of various chemically sensitive dyes	Various chemically sensitive dyes	Colorimetric	RGB colour model	[298]
<b>Fish (cod fillet),</b>	H <sub>2</sub> S						
<b>Pork (loin chops)</b>	(CH <sub>3</sub> ) <sub>2</sub> S						

<b>Shrimp</b>				with a handheld device				
<b>Cod and chicken breast</b>	NH <sub>3</sub> , Trimethylamine, H <sub>2</sub> S, CO <sub>2</sub> and CO	-	Paper-based electrical gas sensor (PEGS)	-	Electrochemical	Single PEGS consisting of two carbon electrodes with three fingers and a spacing of 1 mm between each finger.	[285]	
<b>Chicken, beef, fish and pork</b>	Trimethylamine Putrescine Cadaverine	~7ppm	Force Spun polydiacetylene (PDA) nanofibers	PDA	Colorimetric, fluorescence		[289]	





## **CHAPTER 2. OBJECTIVES**



Analytical information is important in different areas of the society towards more sustainable and respectful practices. Indeed, in the last decade, an exponential growth on the development of sustainable analytical method has been observed. This fact implies to follow the principles of sustainable analytical chemistry to develop reliable analytical method, environmental friendly and cost effective that solves the social problem addressed.

The objective of this Thesis has been the development of sustainable analytical methodologies for solving different problems in the environmental, biological, food and forensic analysis. The specific objectives have been:

1. To develop analytical tools to address sustainability in Analytical Chemistry by using two strategies
  - Coupling on-line several steps and miniaturization by IT-SPME – Cap LC DAD
  - Providing new in-situ analytical solid colorimetric devices
2. To evaluate in-tube SPME coupled on-line to CapLC-DAD as a sustainable tool based on the miniaturization of sample pre-treatment.
3. To develop sensing membrane based on different supports to perform in – situ analysis.
4. To validate the proposed procedures for several analyts (organic and inorganic) in environmental, biological, food and forensic matrices.

*Environmental matrices:* the determination of herbicides in surface waters using IT-SPME-CapLC techniques and, on the other hand, nitrate and nitrite in environmental waters using in situ devices based on the embedding of derivatizing reagents in PDMS as a solid support.

*Biological matrices:* the determination of antibiotics such as meropenem in endotracheal tubes using IT-SPME-CapLC and, on the other hand, sulfides in cardiomyocyte cells and in exhaled air using a solid plasmonic sensor based on the immobilization of AgNPs on nylon membrane. Finally, using IT-SPME-CapLC and PDMS based solid support for alkylresorcinols determination in urine samples.

*Food matrices:* The determination of nitrite and nitrate in waters from canned and fresh vegetable samples and ammonia in meat samples using solid PDMS based sensors.

*Forensic matrix:* the determination of diphenylamine in hand gunshot residues by means of IT-SPME-CapLC.

5. Evaluating practical application of the proposed procedures by carrying out proofs of concept.

The development of this Thesis has been possible thanks to the research projects:

- Project PROMETEO 2012/045, granted by Generalitat Valenciana - Programa Prometeo para grupos de investigación de Excelencia, *“Desarrollo de nuevas estrategias para el diseño de dispositivos de análisis in situ”*. (4 years)
- Project CTQ2014-53916-P granted by Spanish Ministry of Economy and Competitiveness and EU from FEDER – Programa Estatal de Fomento de la Investigación Científica y Técnica de Excelencia Subprograma Estatal de Generación de Conocimiento, *“Desarrollo de nuevas estrategias para el diseño de técnicas de cromatografía líquida miniaturizada en línea: nanopartículas, contaminación secundaria”*. (3 years)
- Project PROMETEO2016/109, granted by Generalitat Valenciana - Programa Prometeo para grupos de investigación de Excelencia, *“Desarrollo de nuevas estrategias para el diseño de dispositivos de análisis in situ: nano y biomateriales”*. (4 years)
- Project CTQ2017-90082-P, granted by Ministry of Science, Innovation and Universities, *“Microextracción en fase sólida en tubo acoplada en línea a nanocromatografía líquida: nuevas oportunidades para/desde la nanoescala y cromatografía líquida”*. (4 years)

The results of this Thesis have given rise to scientific articles, 5 published, 1 submitted and 2 in draft forms.

1. J. Pla- Tolós, P. Serra-Mora, **L. Hakobyan**, C. Molins-Legua, Y. Moliner-Martinez, P. Campins Falcó. A sustainable on-line CapLC method for quantifying antifouling agents like irgarol-1051 and diuron in water samples: Estimation of the carbon footprint. *Science of the Total Environment* 569-579,611-618, 2016. Impact Factor (2019): 6.551.

2. **L. Hakobyan**, J. Plá - Tolos, Y. Moliner-Martinez, C. Molins-Legua, P. Campíns-Falcó, Jesús Ruiz Ramos, Paula Ramirez - Galleymore. Determination of antimicrobials in invasive medical devices by in-tube solid phase microextraction as preconcentration tool: application to endotracheal tubes. *Journal of Pharmaceutical and Biomedical Analysis* 151(2018) 170-177. Impact Factor (2019): 3.209
3. A. Argente-García, **L. Hakobyan**, C. Guillem, P. Campíns-Falcó, A new method for estimating diphenylamine in gunshot residues as a new tool for identifying both, inorganic and organic ones, in the same sample. *Separations* **2019**, 6, 16. Open Access.
4. N. Jornet-Martínez, **L. Hakobyan**, A. I. Argente-García, C. Molins-Legua, P. Campíns-Falcó, Nylon-Supported Plasmonic Assay Based on the Aggregation of Silver Nanoparticles: In Situ Determination of Hydrogen Sulfide-like Compounds in Breath Samples as a Proof of Concept. *Journal ACS Sensors*. **2019**, 4, 2164–2172. Impact Factor (2019): 6.944.
5. A. Ballester-Caudet, **L. Hakobyan**, Y. Moliner-Martinez, C. Molins-Legua, P. Campíns-Falcó, Ionic-liquid doped polymeric composite as passive colorimetric sensor for meat freshness as a use case. *Journal Talanta*. **2021**, 223, 2, 121778. Impact Factor (2019): 5.339.
6. **L. Hakobyan**, Y. Moliner Martínez, C. Molins-Legua, P. Campíns-Falcó, New approach for Griess reaction based on reagent stabilization on PDMS membranes and ZnNPs as reductor of nitrates. Application to environmental waters and waters from canned and fresh vegetable samples. Submitted
7. **L. Hakobyan**, M.C. Prieto-Blanco, Maria Roca Llorens, C. Molins-Legua, M. Fuster-García, Y. Moliner-Martinez, P. Campíns-Falcó, Carmen Ribes-Koninckx, Fast Blue B Functionalized Silica-Polymer Composite to Evaluate DHHC as Biomarker of Gluten Intake. Submitted.

8. **L. Hakobyan**, A. Ballester-Caudet, C. Molins-Legua, P. Campins-Falcó, Colorimetric multiplatform for determination of endogenous H<sub>2</sub>S emitted by living cells: application to cardiomyocytes. Submitted

The results have been also presented in conferences. Poster or oral communication have been performed.

1. Y. Moliner-Martínez, A. Argente-García, J. Pla-Tolos, P. Serra-Mora, **L. Hakobyan**, Campins-Falcó, P. Evaluation of in-tube solid phase microextraction coupled to capillary LC with mass spectrometry for the estimation of irgarol-1051 and its polar transformation products in water. *NET-SCARCE International Conference. Rivers under water scarcity: threats and challenges*, International congress. Póster communication. Barcelona, Spain - 2016.
2. Y. Moliner-Martínez, P. Serra-Mora, **L. Hakobyan**, R. Herráez-Hernández, J. Verdú-Andrés and P. Campins-Falcó. New extraction phases for IT-SPME. *2<sup>nd</sup> Caparica Christmas Conference on Sample Pretreatment*, International congress. Oral communication. Caparica, Portugal - 2016.
3. Argente-García, **L. Hakobyan**, Y. Moliner-Martínez and P. Campins-Falcó. Optimization of sampling and treatment of forensic samples for fast and sensitive estimation of diphenylamine using on-line in-tube solid phase microextraction coupled to capillary liquid chromatography. *2<sup>nd</sup> Caparica Christmas Conference on Sample Treatment*, International congress. Poster communication. Caparica, Portugal - 2016.
4. C. Molins-Legua, P. Campins-Falcó, Y. Moliner-Martínez, J. Plá-Tolos, N. Jornet - Martínez, **L. Hakobyan**. Solid biodevice for sensing in microplate supports: application to glucose determination. *18<sup>th</sup> International Symposium on Advances in Extraction Technologies & 22<sup>nd</sup> International Symposium on Separation Scienc.* International congress. Oral communication. Torun Polonia - 2016.

5. M. Muñoz-Ortuño, **L. Hakobyan**, Y. Moliner-Martínez, R. Herráez-Hernández, J. Verdú-Andrés and P. Campins-Falcó. A new tool for direct estimation of chlorophyll by using diffuse reflectance measurements. *NET-SCARCE International Conference*. International congress. Poster communication. Barcelona, Spain - 2016.
6. Y. Moliner-Martínez, **L. Hakobyan**, P. Serra-Mora, C. Molins-Legua, R. Herráez-Hernández, J. Verdú-Andrés and P. Campins-Falcó. High performance extractive phase for IT-SPME. *19<sup>th</sup> International Symposium on Advances in Extraction Technologies*, International congress. Oral presentation. Santiago de Compostela, Spain – 2017.
7. **L. Hakobyan**, Y. Moliner Martinez, C. Molins Legua and P. Campins- Falcó. Ionogel based colorimetric sensor to determine NH<sub>3</sub> in atmospheres. *XXI Reunión de la Sociedad Española de Química Analítica*, National congress, Poster presentation. Valencia, Spain – 2017.
8. C. Molins Legua, D.L. Palacios- López, M.C. Prieto – Blanco, N. Jornet-Martínez, **L. Hakobyan**, S. Bocanegra-Rodríguez, P. Campins- Falcó. Solid sensor supported in PDMS for derivatizing carbonyl compounds in several matrices. *32<sup>nd</sup> International Symposium on Chromatography*. International congress. Poster communication. Cannes-Mandelieu, France – 2018.
9. **L. Hakobyan**, C. Molins Legua, Y. Moliner - Martínez, P. Campins Falcó. New assay for the Griess reaction based on the use of stable Zn nanoparticles dispersions and doped PDMS membranes: application to water analysis. *International Congress on Analytical Nanoscience and Nanotechnology – IX NyNA.*, International congress. Poster presentation. Zaragoza, Spain - 2019.
10. Ballester – Caudet, **L. Hakobyan**, C. Molins Legua, P. Campins Falcó. Solid-phase colorimetric sensors for monitoring meat freshness. *XXII Reunión de la Sociedad Española de Química Analítica*, National congress, Poster communication. Valladolid, Spain – 2019.

11. Y. Moliner – Martinez, M. Fauster- Garcia, **L. Hakobyan**, C. Molins Legua, P. Campins Falcó, M. Roca Llorens, C. Ribes- Koninckx. *XXII Reunión de la Sociedad Española de Química Analítica*, National congress, Poster communication. Valladolid, Spain – 2019.
12. **L. Hakobyan**, C. Molins Legua, P. Campins Falcó, P. Sepulveda Sanchis, A. Dorronsoró – Gonzalez, S. Tejedor – Gascón. *XXII Reunión de la Sociedad Española de Química Analítica*, National congress, Poster communication. Valladolid, Spain – 2019.
13. **L. Hakobyan**, C. Molins Legua, P. Campins Falcó. Different analytical methodologies cleaning in place (CIP) process control. *XXII Reunión de la Sociedad Española de Química Analítica*, National congress, Poster communication. Valladolid, Spain – 2019.
14. C. Molins Legua, **L. Hakobyan**, N. Jornet - Martinez, P. Campins Falcó. Study of the aggregation of silver nanoparticles in solid supports: development of several assays for determination of sulphur compounds in several matrices. *International Congress on Analytical Nanoscience and Nanotechnology – IX NyNA.*, International congress. Oral presentation. Zaragoza, Spain - 2019.









## **CHAPTER 3. MATERIALS AND METHODS**



### 3.1 Reagents

**Table 3.1** shows all the reagents (analytical grade) used during the experimental part of the Thesis, including the commercial suppliers and GHS (Globally Harmonized System of classification and labelling of chemicals) hazard pictograms according to Regulation (EC) No 1272/2008 - classification, labelling and packaging of substances and mixtures (CLP).

**Table 3.1** Summary of reagents with their commercial suppliers and GHS pictograms, were  - (GHS02) flammable,  - (GHS05) corrosive,  - (GHS06) toxic,  - (GHS07) harmful,  - (GHS08) health hazard,  - (GHS09) environmental hazard.

Chemical compound	Supplier						
Acetone	MERK	x			x		
Acetonitrile	VWR	x			x		
Ammonium chloride	Probus				x		
Anhydrous citric	Panreac				x		
<b>C18particles(50µm 65A)</b>							
Cetyltrimethylammonium bromide	Sigma		x		x	x	x
Diphenylamine	Sigma	x	x	x	x		
Diurón	Sigma				x	x	x
Ethanol	Sharlau	x			x		
Fast Blue B salt	Sigma				x		
Glycerol	Sigma				x		
Hydrochloride acid	Scharlab		x		x		
Irgarol®-1051	Sigma				x		x
Methanol	VWR	x		x		x	
Meropenem					x		
N - 1-Naphtyl ethylene diamine dihydrochloride	Sigma				x		
Phosphoric acid	Scharlau		x		x		
Polydimethylsiloxane Sylgard®184 Kit	Dow corning						
Potassium carbonate	Probus				x		
Potassium nitrate	Panreac	x					
Silver nanoparticle dispersion (20 nm)	Sigma						x
Silver nitrate	Scharlab	x	x				x

Sodium dodecyl sulfate	Sigma	x	x	x	
Sodium hydroxide	Sigma		x		
Sodium 1,2- naphthoquinone 4-sulfonate	Sigma			x	
Sodium sulfide	Sigma		x	x	x
Sulphanilamide	Guinama			x	
SiO <sub>2</sub> NPs (20 nm)	Sigma			x	
Tetraethyl orthosilicate	Sigma	x		x	
Trichloroacetic	Scharlab		x	x	x
Zn powder	Probus				x
Zn NPs (60 nm)	Sigma				x
1-butyl-4-methylpyridinium hexafluorophosphate	Sigma			x	
1,3-Dihydroxy-5-pentylbenzene	Sigma		x	x	x
3,5-dihydroxyhydrocinnamic acid	Sigma			x	

## 3.2 Instrumentation

Throughout the development of the Thesis, spectroscopic, chromatographic and microscopic techniques have been used.

### 3.2.1 Spectroscopic techniques

#### UV-Vis spectrophotometry

UV-Vis spectra were registered using a Cary 60 UV-vis spectrophotometer (Agilent Technologies, Santa Clara, CA, USA) (**Figure 3.1A**). For measurement, quartz or plastic cuvettes with 10 mm light path were used. Data acquisition and subsequent processing were performed with the Carry WinUV software. The full UV-vis spectra were registered between 200 and 1000 nm.

#### Diffuse reflectance spectroscopy

Colorimetric measurement of solid support (such as PDMs and nylon-AgNPs) by using diffuse reflectance measurements sensors was carried out using Carry 60 spectrophotometer coupled to a diffuse reflection probe (Harrick Scientific

Products, New York, USA) (**Figure 3.1B**). It was equipped with a video camera and a built-in light that makes it easy to view the sample in real time. GrabBee software, for data acquisition and processing was used CarryWinUV software. Measurements were made in the range of 200 to 800 nm.



**Figure 3.1** A) Cary 60 UV-Vis Spectrophotometer with B) Remote Diffuse Reflectance Accessory (DRA) accessory.

### 3.2.2 Microscopic techniques

#### Optical microscopy

A Nikon ECLIPSE E200LED MV series microscope (Nikon Corporation, Tokyo, Japan) with Nis-Elements 4.20.02 software (Nikon) was used to take microscopic images. The instrument, equipped with 3 objective lenses of different magnifications (10x, 50x and 100x), is shown in **Figure 3.2**.



*Figure 3.2* Optical microscopy ECLIPSE E200LED MV.

### Scanning Electron Microscope (SEM)

For the characterization of tested solid sensors, a Hitachi S-4800 (Tokyo, Japan) scanning electron microscope was used at an acceleration voltage of 20 keV, on samples metallized with a mixture of gold and palladium for 30 s. Image capture and processing were performed with QUANTAX 400 software (Hitachi) (**Figure 3.3**).



*Figure 3.3* SEM - Hitachi S-4800.

### 3.2.3 Chromatographic techniques: Capillary liquid chromatography (CapLC)

Miniaturized liquid chromatography systems have been employed for the chromatographic measurements performed in this Thesis. The capillary chromatographic system (CapLC) consisted on a LC capillary pump (Agilent 1100 Series, Waldbronn, Germany) equipped with a UV-Vis diode array detector (Agilent, 1200 series), equipped with a 80-nL flow cell. The system was linked to a data system (Agilent, HPLC ChemStation) for data acquisition and calculation. Spectra were recorded between 190 and 400nm. **(Figure 3.4)**. The CapLC system was on-line coupled with in-tube SPME to perform the on-line sample pretreatment of samples. Experimental details are summarized in section 3.3.

The chromatographic measurements were carried out to determine irgarol-1051, diuron, diphenylamine, meropenem and DHCA. In all cases, the detection system was a DAD detector. The wavelength was set at 226nm, 254 nm, 280 nm for irgarol-1051, diuron and diphenylamine, respectively and the meropenem absorbance signals were registered at 300 nm. Finally, DHCA derivatives registered at 520nm.



*Figure 3.4 CapLC-DAD system, Agilent 1200 Series with binary pump.*

In addition to the instrumentation described above for the development of the experimental procedure of this Thesis, the following instruments and materials

have also been used: Ultrasonic bath Sonitech (TerraTech, Spain), magnetic stirrer (450 W) (Stuart Scientific), nanopure II water system (Barnstead, UK), ZX3 vortex mixer (VELP Scientifica, Italy), thermostat LT200 (Hagh Lange United for water quality, Sapin), nylon membranes (0.45 and 0.22  $\mu\text{m}$ ) (Teknokroma, Spain), double-sided carbon adhesive tape (8 mm wide x 0.16 mm thick x 1 cm long) (Ted Pella Inc. Redding, US), tape lift kit (Sirchie Finger Print Laboratories, USA), plastic well-plates (Sharlau, Spain), plastic bag from Hardiron store (China), incubators (Forma™ Series II 3110, ThermoFisher), pH-meter Crison micro pH 2001, (Crison Instruments S.A., Barcelona Spain), vacuum pump system (Sharlab, Barcelona, Spain), Malvern Zetasizer Nano ZS from Malvern Panalytical Ltd (UK), thermo – hygrometer Derta OHM HD 9216(Laselle di Selvazzano, Italy) and centrifuge EBA 20 from Hettich (Tuttlingen, Germany).

### 3.3. Sensor preparation

During the development of the Thesis, two different sensing membranes, have been developed: PDMS based sensors and devices based on silver or zinc nanoparticles retained in Nylon, the preparation procedures are detailed below.

#### 3.3.1 PDMS based sensors

- **Preparation of PDMS /TEOS-SiO<sub>2</sub>NPs-SA-NEDD**

The fabrication of the PDMS /TEOS-SiO<sub>2</sub>NPs-SA-NEDD sensing device was carried out following the procedure proposed in[111] with some modifications. Firstly, the reagents sulphanilamide (SA) (4.18%) and N - 1 - Naphthyl ethylenediamine dihydrochloride (NEDD) (1.14%) were added to TEOS (39.77%) and SiO<sub>2</sub>NPs (0.11%) dispersion previously prepared. Achieve homogeneity an ultrasonic bath was used for 5 min. After, the final mixture was added to the elastomer base (49.82%) and the new mixture was vigorously stirred for 15 min at room temperature to obtain a homogeneous suspension. Subsequent, the curing agent (4.98%) was added to the previous solution leaving 5 minutes under stirring. The standard mixing ratio for PDMS was 10:1 elastomer and curing agent, respectively. This ratio provides the desirable and optimum mechanical properties. The gelation procedure was carried out at 30 °C for 8 h. After 200 $\mu\text{l}$  of



the mixture were deposited in the well plate (d=1.5 cm). In case of using microplate wells, 20  $\mu$ l were doped in each well.

- **Doped of PDMS /TEOS-SiO<sub>2</sub>NPs-SA-NEDD-OMIM-PF<sub>6</sub>**

The preparation of the supported IL-based (**Figure 3.5**) PDMS device was performed by mixing the reagents that form the azo compound, such as SA (4.176%) and NEDD (1.145%), with the OMIM-PF<sub>6</sub> (6.187%). The mixture was stirred during 10 min. After, the elastomer base (44.191%) was added to the previous mixture and the resulting combination (combination 1) was stirred during 10 min more to get a homogeneous dispersion. Then, a mixture of TEOS-SiO<sub>2</sub>NPs was prepared by mixing SiO<sub>2</sub>NPs (0.11%) with TEOS (39.772%) (combination 2). Finally, combination 1 and 2 were mixed and stirred vigorously to obtain homogenous mixture. After adding the curing agent (4.419%), the mixture was stirred for 2 min. Finally, the drying procedure was carried out as previously described previously.

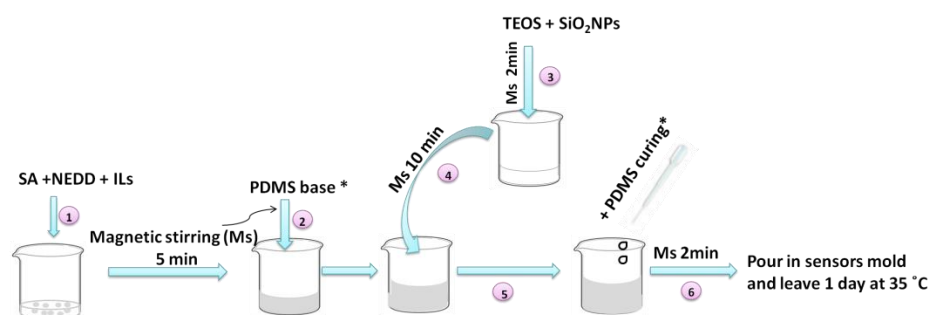


**Figure 3.5** Steps for PDMS /TEOS-SiO<sub>2</sub>NPs-SA-NEDD-ILs sensing devices preparation.

- **Preparation of PDMS /TEOS- SiO<sub>2</sub>NPs-NQS- OMIM-PF<sub>6</sub>**

Synthesis of these sensing membranes (**Figure 3.6**) was performed by mixing the recognition element, NQS (0.325%-0.352%), with the IL (0.2%-7.8%). The mixture was then stirred during 10 min. After, the elastomer base (33.89% - 36.69%) was added to the previous mixture and the resulting mixture was stirred during 10 min to get a homogeneous dispersion (dispersion 1). Then, a mixture of TEOS-SiO<sub>2</sub>NPs was prepared by mixing SiO<sub>2</sub>NPs (0.381% – 0.41%) with TEOS (54.22% - 58.71%)

(dispersion 2). Finally, dispersion 1 and 2 were mixed and stirred vigorously to obtain a homogeneous mixture. Then, the curing agent (3.39% - 3.52%) was added. 200  $\mu\text{L}$  of the resulting solution was deposited on a plastic-well plate and was cured at 35  $^{\circ}\text{C}$  during 24 h.

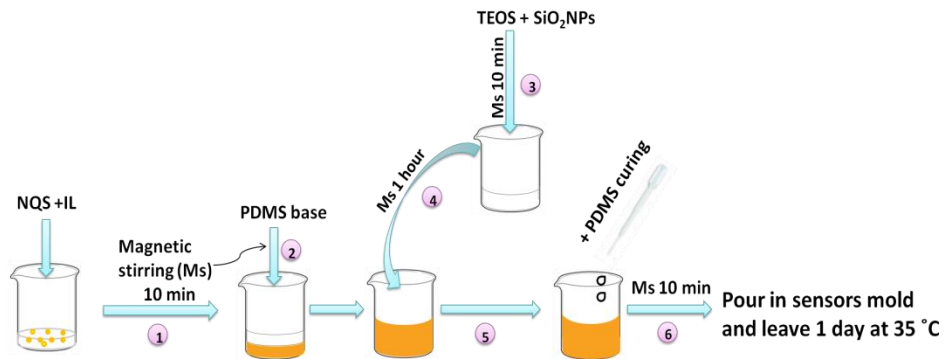


**Figure 3.6** Steps for PDM/TEOS-ILs-NQS-SiO<sub>2</sub>NPs sensing devices preparation.

- **Preparation of PDMS /TEOS- FB**

FB doped PDMS membranes were synthesised based on previously works, [79,112,113]. Briefly, FB (0,35 g) were mixed with PDMS (36.0-90.6 %) and stirred during 5 min to obtain a homogenous mixture. Before the addition of the curing agent, three matrix modifiers were studied: TEOS (58,5-59.1%), C18 (5-20%) and the ionic liquid OMIMPF<sub>6</sub> (0,59%). Finally, curing agent (ratio 1:10 curing-PDMS) was added to the previous mixture and stirred. Once, the homogenous mixture was obtained, 200  $\mu\text{L}$  were place in 1-cm plastic mold and heated at 40 $^{\circ}\text{C}$  for 24 h.

**Table 3.2** summarized the different membrane compositions tested.

**Table 3.2** Composition of PDMS/TEOS-FB sensing membrans.

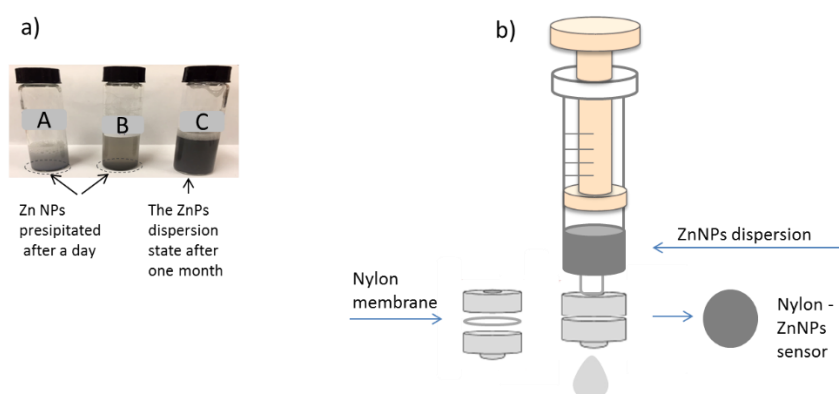
SENSING MEMBRANE COMPOSITION						
MEMBRANE	FB (%)	PDMS (%)	TEOS (%)	IL (%)	C18 (%)	Curing (%)
PDMS	0.35	90.59	-	-	-	9.06
PDMS -TEOS	0.35	36.91	59.05	-	-	3.69

PDMS - C18 (5%)	0.35	86.04	-	-	5.00	8.60
PDMS - C18 (10%)	0.35	81.50	-	-	10.00	8.15
PDMS - C18 (20%)	0.35	72.41	-	-	20.00	7.24
PDMS – IL(*)	0.35	90.05	-	0.59	-	9.01
PDMS - TEOS – IL(*)	0.35	36.91	58.46	0.59	-	3.69

### 3.3.2. Nanoparticle-based sensors

- Preparation of ZnNPs dispersion and Nylon –ZnNPs sensor

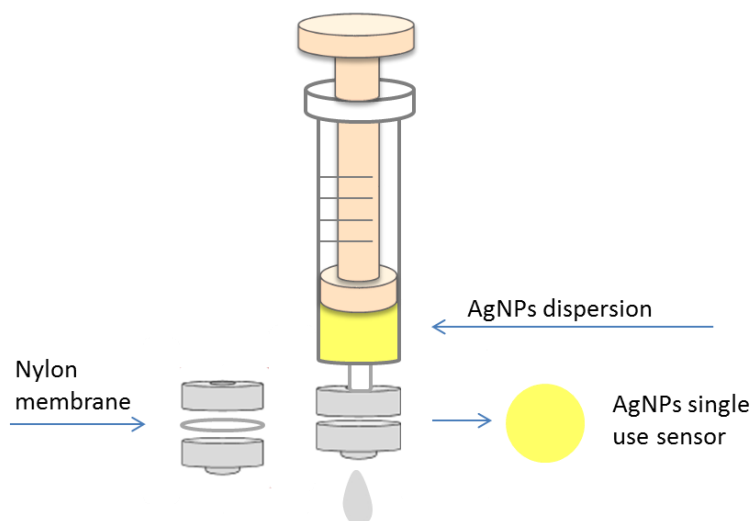
Solutions of surfactants in water were prepared by weighing the appropriate amounts of CTAB and SDS to get final concentrations 15mM and 17.3mM, respectively. Mixtures of CTAB and SDS were prepared by mixing the proportions CTAB 70% -SDS 30% and CTAB 30% -SDS 70%. The solutions and mixtures of surfactants were added to 30 mg of ZnNPs. ZnNPs dispersion were obtained by sonicating the mixture for 15 min. (Figure 3.7A). The suspensions were then aged overnight at room temperature. For the preparation of ZnNPs - Nylon sensors, an appropriate amount of dispersed ZnNP solution was passed through a nylon filter (1 cm diameter) (Figure 3.7B).



**Figure 3.7 A)** Zn NPs in different proportions of surfactants A – CTAB 30% - SDS 70%; B – SDS 100%; C- CTAB 70% - SDS 30%. **B)** ZnNPs sensor preparation scheme.

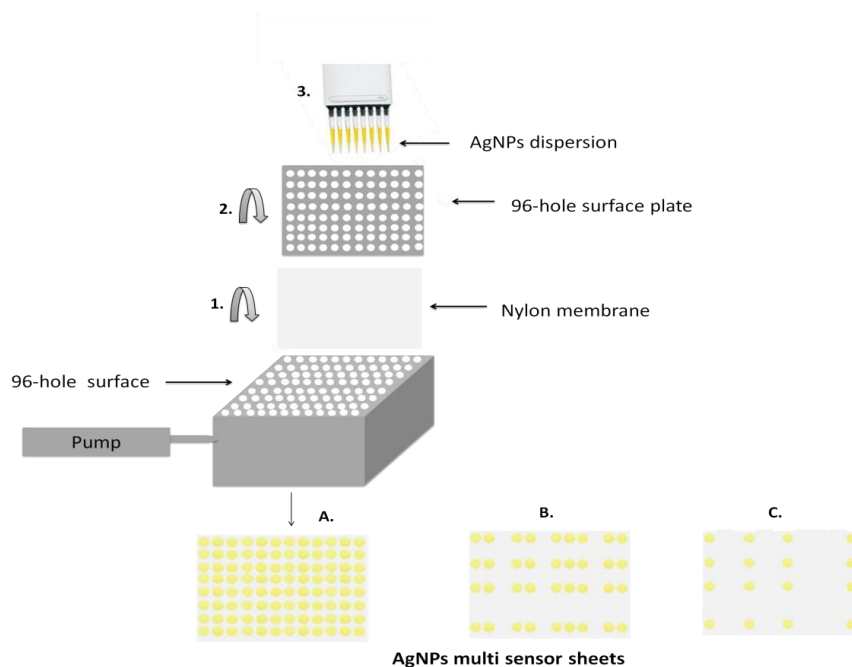
- **AgNPs multisensor and single use sensor preparation**

For AgNPs sensor preparation 200  $\mu\text{L}$  of AgNPs dispersion was passed through a nylon filter (1 cm in diameter) for AgNPs adsorption (**Figure 3.8**).



**Figure 3.8** Scheme of AgNPs sensor preparation

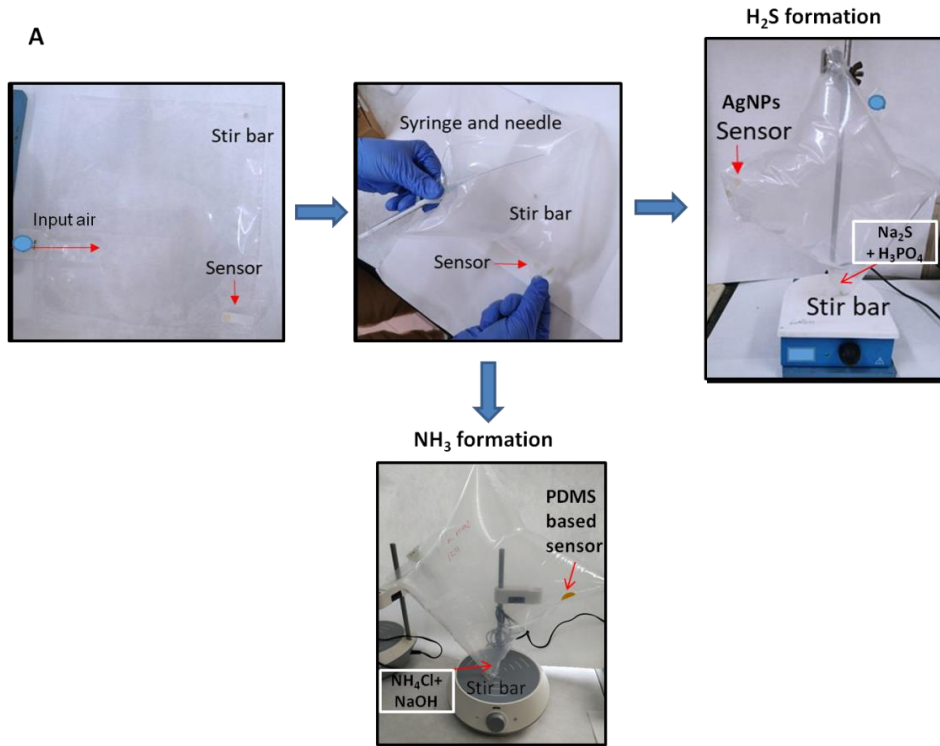
The multisensory sheet consisted of 96 circles of silver nanoparticles retained in a rectangular nylon membrane plate of (11cm by 7,5cm). Each device in a circle form was 0.7 cm in diameter. **Figure 3.9 A** shows the steps of the plasmonic multisensory sheet preparation. In the first step, the nylon membrane was placed between the two plates with 96-hole surfaces, and by means of a micropipette the appropriate amount of AgNPs was added. The system was connected to the pump system, allowing the liquid part of the dispersion to pass through membrane and thus the retention of NPs on the nylon surface without surface functionalization, avoiding chemical reagents, solvents, or complex instrumentation. The multisensory laminate is coupled perfectly with 96-well microplates, which allows testing for 96 wells at a time. Nylon plates with different amounts and positions of silver sensors were prepared by filling the corresponding holes of the system (as needed) of AgNPs and the other holes were filled with nanopure water (**Figure 3.9 B, C**).



**Figure 3.9** AgNPs multisensory sheet preparation scheme. **A)** corresponds to the multisensory sheet with 96 sensors, **B)** – 36 sensors, **C)** – 16 sensors.

### 3.4. Preparation of air standard and humidity measurement

The standard atmospheres ( $\text{H}_2\text{S}$  and  $\text{NH}_3$ ) were prepared in plastic bags (0.25-2L). First, the plastic bag was cutted, then the sensor and a stir bar were introduced. Finally, the bag was sealed by heating the bag **Figure 3.10A**.  $\text{NH}_3$  and  $\text{H}_2\text{S}$  atmospheres were generated in the plastic bags by introducing the standard solutions of  $100\mu\text{L}$   $\text{NaOH}$  (2M) +  $100\mu\text{L}$   $\text{NH}_4\text{Cl}$  and  $100\mu\text{L}$   $\text{Na}_2\text{S}$  +  $100\mu\text{L}$   $\text{H}_3\text{PO}_4$  (95%) respectively by using syringe. The concentrations of  $\text{NH}_4\text{Cl}$  and  $\text{Na}_2\text{S}$  were varied according to the objective set. Finally, the mixtures were stirred for monitoring target analytes. Humidity measurements were carried out by introducing the thermo-hygrometer in the plastic bag **Figure 3.10B**. The humidity of several meat samples atmosphere was also measured with the probe of the Thermo-Hygrometer when meat samples were preserved in a 100 mL plastic bag under refrigeration conditions at  $4^\circ\text{C}$  **Figure 3.10B**.



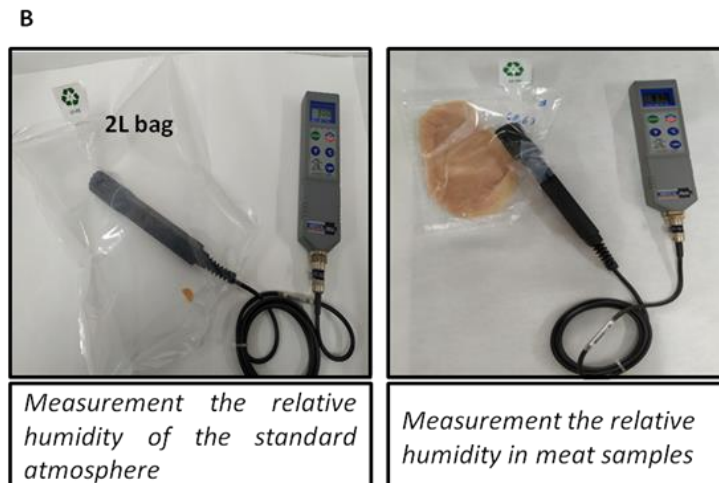


**Figure 3.10** A)  $\text{NH}_3$  and  $\text{H}_2\text{S}$  standard atmospheres preparation steps B) Humidity measurement using termo-hygrometer device.

### 3.5. Analysis of real samples

In this Thesis, different types of matrices have been analyzed: biological, environmental, forensic and food samples. **Table 3.3** summarizes the matrices studied in this Thesis and the analytes determined in each sample.

**Table 3.3** Types of matrices and the analytes determined.

	<b>Sample</b>	<b>Analyte</b>	<b>Sampling</b>	<b>Sample pre-treatment</b>	<b>Techniques used</b>	<b>Section</b>
<b>ENVIRONMENTAL</b>	<b>Port water</b>	Irgarol-1051 and diuron	Direct sampling from ports of region of Valencia	Filtered by nylon membrane, IT-SPME	In tube-SPME - Cap LC	4.1.1
	<b>Canal water</b>	Nitrite, nitrate	Direct sampling from irrigation canal of region of Valencia	Filtered by nylon membrane	PDMS /SA-NEDD-OMIM-PF <sub>6</sub> sensor	4.1.2
	<b>Wells water</b>	Nitrite, nitrate	Direct sampling from well of region of Valencia	Filtered by nylon membrane		
<b>FORENSIC</b>	<b>Shooter hands</b>	DPA	Collecting with swab (21 hands) and with tape(6 hands)	Vortex and IT-SPME	In tube-SPME - Cap LC	4.4.1
<b>BIOLOGICAL</b>	<b>Breath</b>	Hydrogen sulfide	Direct sampling of the exhaled buccal and alveolar air from 10 volunteers	Without pre-treatment	Nylon - AgNPs sensor	4.2.1
	<b>Cells</b>	Hydrogen sulfide	Human ventricular cardiomyocytic cell line AC10	-	Nylon - AgNPs multisensor	4.2.2
	<b>Urine</b>	AR	Direct sampling	SPE –Clean-up	PDMS/TEOS-FB-OMIMPF6 sensor	4.2.3
	<b>ETTs</b>	Meropenem	Direct sampling from 5 patients from	Vortex, IT-SPME	In tube-SPME - Cap LC	4.2.4



		intensive care				
<b>FOOD</b>	<b>Chicken meat</b>	Ammonia	Sampling of packing chicken meat buying from commercial local	Without pre-treatment	PDMS/NQS-OMIMPF <sub>6</sub> sensor	4.3.1
	<b>Spinach</b>	Nitrite, nitrate	Sampling of 1 ml of liquid solution from boiled spinach canned and fresh	Filtration (nylon) membrane, dilution 1:10	PDMS /SA-NEDD-OMIM-PF <sub>6</sub>	
	<b>Chard</b>	Nitrite, Nitrate	Sampling of 1 ml of liquid solution from boiled chard canned and fresh	Filtration (nylon) membrane, dilution 1:10		4.3.2

### **3.5.1 Sampling**

#### **Collection of forensic samples from the hands shot**

To collect GSR, two techniques were used: rubbing with a dry swab the palm and back two hands (right and left) of each policeman and with adhesive tape. Samples were collected immediately after unloading the firearm. The tape lift kit consisted of a metal stub equipped with a carbon adhesive tape inserted in a plastic vial with a tightly fitted cap. For the sampling, the metal stub was passed over the surface of the hand and then was returned to the vial. Finally, all the samples taken in their corresponding vials were transported to the laboratory and stored at room temperature until their analysis (**See section 3.4.2 Figure 3.14**). A total of 21 shooters were sampled by swab and 6 other shooters by adhesive tape. Police hands were also analyzed before firing the shot and without washing their hands. These swabs served as targets to get blank responses.

#### **Sampling of endotracheal tubs (ETTs)**

ETTs were obtained from five patients, three of them diagnosed with nosocomial pneumonia treated with meropenem treatment. Three ETTs from patients with antimicrobial treatment and two ETTs from patients without meropenem treatment were analysed. In addition, control ETTs (not used) were also analysed as blanks. In all cases, sections of 2-cm length of the tip region were cut (**See section 3.5.2 Figure 3.13**) and frozen at  $-18\text{ }^{\circ}\text{C}$  until analysis. At this temperature, the growth of bacterial flora was suppressed in order to avoid health issues during the analysis.

#### **Cardiomyocyte cell samples preparation**

Human ventricular cardiomyocyte cells line AC-10 was cultured in Dulbecco's Modified Eagle's Medium-F-12 (DMEM-F12, Gibco-Invitrogen®) supplemented with 10% fetal bovine serum (FBS, Gibco-Invitrogen®) and 1% penicillin/streptomycin (P/S, Millipore). Cell culture medium used for ischemia-reperfusion experiment was Dulbecco's Modified Eagle's Medium without D-Glucose (Gibco-Invitrogen®) supplemented with 1% penicillin/streptomycin (P/S, Millipore).

### Collecting breath samples

Collection of breath samples were carried out by inserting the AgNPs membrane into the bag and closing it, incorporating the mouthpiece, and exhaling the mixture of mouth and alveolar air into the bags. After 10 min, the membrane was removed from the bag and analysed by digital image colour coordinates and diffuse reflectance. The breath samples were collected from 10 volunteers in 0.25L - 2L plastic bags (**Figure 3.11**).



*Figure 3.11 Collecting human oral breath samples process in image.*

### Chard and spinach sampling

**Canned chard and spinach** were purchased from the local supermarket. 1 ml of liquid part was taken to dilute in 10 ml of nanopure water. Said dilution formed was used for future tests.

To prepare samples from fresh chard and spinach, 280g and 140g were weighed respectively. 140g of **fresh spinach** was boiled in 350 ml of water for up to 20 minutes and 280 g **fresh chard** was boiled in 350 ml of nanopure water, leaving the same time as the spinach. Then 1 ml of liquid part of each species was taken and diluted in 10 ml of nanopure water. These dilutions were used for future tests.

### Sampling of chicken meat

Chicken meat samples preparation was carried out by inserting the purchased meat (from the local supermarket) and the **PDMS /TEOS- SiO<sub>2</sub>NPs-NQS- OMIM-PF<sub>6</sub>** membrane into the bag and sealing it by heat. The samples were stored in the refrigerator at 4-7 °C for up to 14 days as needed (**Figure 3.12**).

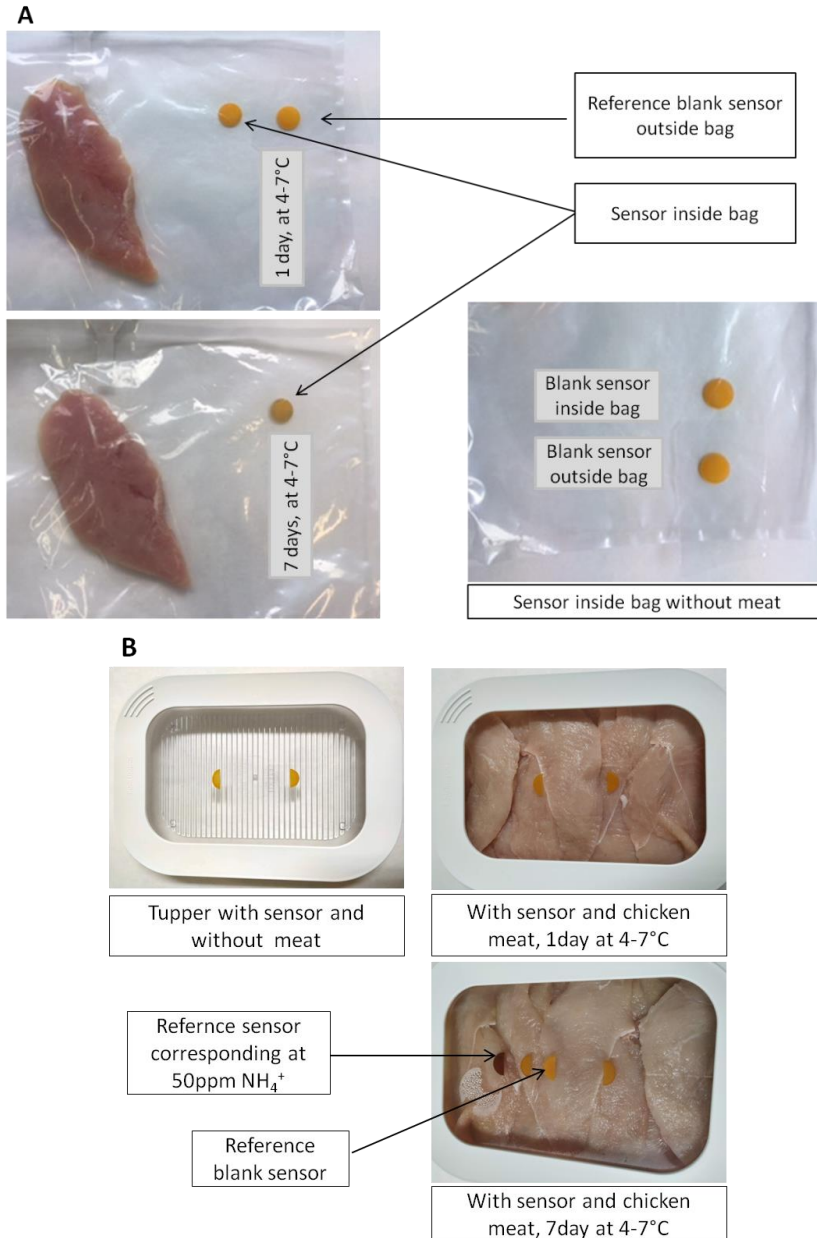


**Figure 3.12** Chicken meat samples preparation in 2 different packaging **A)** plastic bag and **B)** tupper.

### Urine samples

Urine samples were collected during three different days where the gluten intake was controlled. In the first two days, there was no gluten intake and on the third day, the volunteers consumed gluten. Once the samples were taken, they were stored at 4°C. The samples were processed following the SPE procedure described in section 3.4.2. and the AR content was determined by the proposed method described in section 4.2.3. In addition, these samples were analysed by using the chromatographic method. Three replicates of the samples were analysed in all cases.

### 3.5.2 Sample pre-treatment

On-line and off-line techniques have been used for the sample pre-treatment during the development of the Thesis.

#### On-line extraction

- **In-tube SPME procedure**

In-tube SPME device consisted in a conventional six-port injection valve in which loop was replaced by a segment of a gas chromatographic capillary column TRB-50, TRB-35, TRB-20 and TRB-5 (0.32mm i.d. 3µm thickness). Capillary connections to valve were facilitated by the use of 2.5 cm sleeves of 1/16 in. PEEK tubing; 1/16-in. PEEK nuts and ferrules were used to complete the connections. With the valve in load position, aliquots of standards or samples were manually processed into the system employing a 0.1 - 1.0 mL precision syringe. After sample loading, the valve was rotated to the inject position, allowing the desorption of the compounds retained on the coating of the extractive capillary by the mobile-phase and their subsequent transference to the analytical column for separation and detection [299] (**Figure 3.13**). The quantity of the standard or sample injected and the dimensions of the capillary column varied according to the analyte.

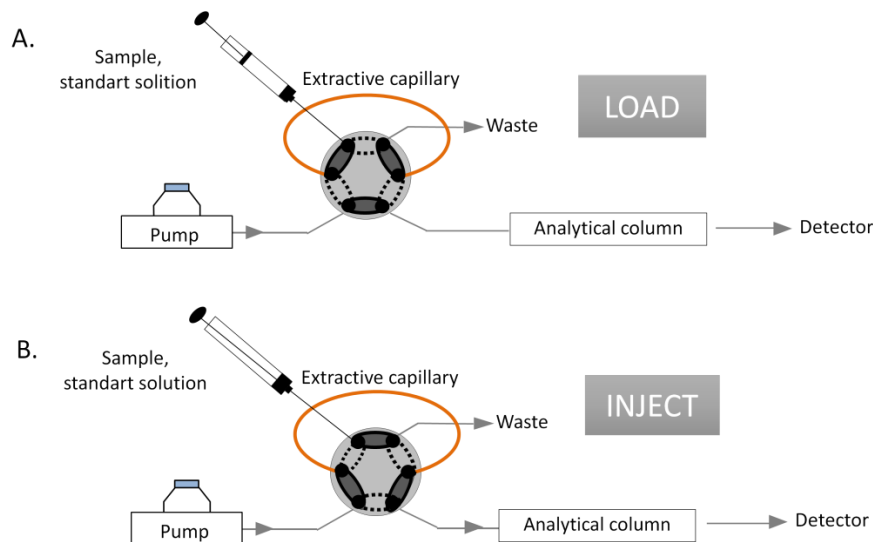


**Figure 3.13** Schematic representation of in valve IT-SPME coupled to a CapLC system. **A)** Load position **B)** Inject position.

### Off –line extraction

- **Vortex assisted extraction (VAE)**

Vortex assisted extraction was used for the extraction of meropenem from the endotracheal tubes, and for the detection of DPA in hands.

### MEROPENEM:

To analyze the endotracheal tubs (ETTs) used in patients, a section of 2 cm was fragmented from the tip region and were placed into a storage vial containing 2 mL of water nanopure as solvent. The extraction was carried out using VAE in each case. The next step was to centrifuge the sputum extracted from the ETTs at 2500 rpm for 15 min, the supernatant was filtered through a 0.45  $\mu\text{m}$  (e.d. 2.5 cm) nylon membrane syringe filter. In addition, direct extraction was studied as a comparative, which was obviously slower. In order to obtain the standard solutions, a volume of meropenem solution was deposited on a ETTs cut fragment (not used in patient), then the solvent was evaporated to dryness at room temperature and carry out the same extraction procedure indicated above. It was

also verified that the analyte is not lost when passing through the Nylon filter. Finally, 500 $\mu$ L of the final solution was loaded into the IT-SPME capillary. The procedure of meropenem extraction is shown in **Figure 3.14**.

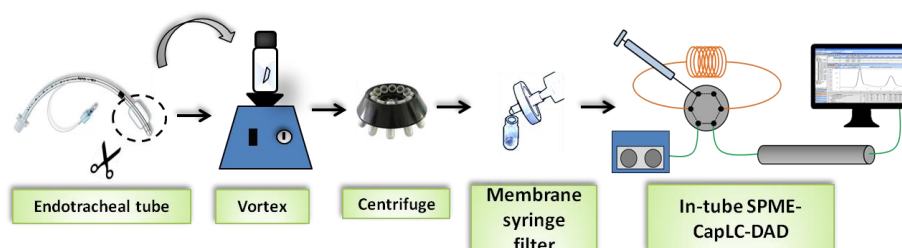


**Figure 3.14** Steps for meropenem extraction and detection from ETTs.

**DIPHENYLAMINE (DPA):** For the detection of DPA in the hands shot, using a cotton swab, the palm and back parts of the two hands (left and right) were rubbed (**Figure 3.15**). The standard DPA solutions were obtained by drying at room temperature a DPA solution and finally collecting with a swab. After sample collection, the tip was placed in a storage vial containing 2 ml of water, so that the cotton was totally wet. DPA was then extracted from the swab under in vortex conditions for 20 sec at room temperature. Finally, 1800  $\mu$ l of the solution was loaded from the solution with extracted DPA into the IT-SPME capillary. Different solvents, samplers, and extraction techniques were tested to optimize the sampling procedure.

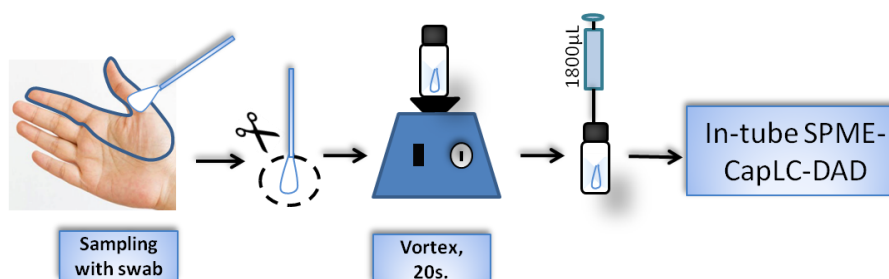


**Figure 3.15** Sampling, extraction and detection process for DPA from shooting hands.

- **Solid phase extraction (SPE)**

First, C18 silica cartridges (200 mg) were conditioned with methanol (1 mL) and water (2 mL). Then, 2 mL of working standard solution or urine sample previously derivatized were passed through the cartridge. Then, a wash step was included by using 0,1 M HCl (1 mL). Finally, AR was eluted with methanol. Urine pretreatment was carried out using SPE.

### 3.5.3 Analytical matrices

#### Environmental samples

- **Port water:** Sampling was carried out monthly during the period from March to June 2014 in the following ports of the Region of Valencia: Port of Valencia, marina Port Saplaya (Alboraya) and marina of Siles (Canet d'En Berenguer). Water samples were collected in brown glass flasks previously cleaned with ultrapure water at a depth of 1 m. After the arrival to the laboratory, samples were filtered through 0.45 mm nylon membranes and stored in the dark at 4 °C until analysis. Storage time was less than one week after the sampling.
- **West and canal water:** The collection of the west and well water samples were carried out in the Valencian Community. Water samples were collected in brown glass flasks previously cleaned with ultrapure water. After the arrival to the laboratory, samples were stored in the dark at 4 °C until analysis. Storage time was less than one week after the sampling.

#### Forensic samples

- **Shooter hands:** Police officers fired test shots at a shooting range at the Valencian Community Police Headquarters (Valencia, Spain) under typical shooting practice conditions. The shots were fired with Heckler & Koch 9 mm pistols, model USP Compact (Oberndorf / Neckar, Germany), which are the most widely used firearms among the police forces in Spain. Each volunteer fired a total of 25 shots (regulation number of shots) and with his own firearm and without touching other surfaces to avoid any



contamination. Only one of these policemen fired 12 shots due to a fault that emerged. A total of 27 shooters were sampled.

### **Biological samples**

In this Thesis biological samples have been analyzed to determine VSCs in breath, cells, also analyzed meropenem in tubs endotracheal, and finally AR in urine.

- **Endotracheal tubes (ETT):** Samples of ETT were provided by the research team of the Intensive Care Unit of the Hospital La Fe (Valencia, Spain). ETTs were obtained from patients diagnosed with nosocomial pneumonia treated with meropenem at dose of 1 g each 8 hours during at least 72 hours.
- **Breath:** Human oral breath samples of 10 volunteers were collected by exhaling air into plastic bags. Prior to collecting the sample, the membrane was put into the empty bag and the bag was closed by heat. For spiked breath samples, a suitable volume of Na<sub>2</sub>S solution and orthophosphoric acid (85%) were placed on the bottom of the bag before sampling. After 10 min of sampling, the sensor was removed from the bag and the response was registered by diffuse reflectance spectrometry, and digital images were taken using a smartphone.

### **Food samples**

- **Spinach:** Canned and fresh spinach were used for sample analysis. **Canned spinach** was purchased from the local supermarket. 1 ml of liquid part was taken to dilute in 10 ml of nanopure water. Said dilution formed was used for future tests. For analysis of **fresh spinach** 140g was boiled in 350 ml of water for up to 20 minutes. Then 1 ml of liquid part of each species was taken and diluted in 10 ml of nanopure water. These dilutions were used for future tests.

- **Chard:** As in the case of spinach, they also analyzed fresh and canned chard. **Canned chard** was purchased from the local supermarket. 1 ml of liquid part was taken to dilute in 10 ml of nanopure water. Said dilution formed was used for future tests. For analysis of **fresh chard**, 280 g was weighed and boiled in 350 ml of nanopure water, leaving the same time as the spinach.
- **Chicken meat:** To control freshness, 0.5 kg of chicken breast was purchased from the local supermarket. The sliced breast was packed under refrigeration conditions for 10 days. The food packaging used is a rectangular shaped commercial Tupper with 100 mL of free space between the meat and the Tupperware lid.

### **3.6 Procedures and experimental conditions**

In this Thesis CapLC-DAD and in-situ analytical devices were employed for determination of target analytes in biological, environmental, food, forensic, samples.

#### **3.6.1 Chromatographic conditions**

**Table 3.4** includes the experimental conditions proposed in the different studies that use that use IT-SPME coupled to CapLC – DAD. In all cases, the mobile phase was filtered before use through nylon filters of 0.45 µm pore size.

**Table 3.4** Experimental conditions used in the analysis of different matrix by IT-SPME-Cap-DAD.

	Matrix	Analyte	Capillary column	Analytical column	Injection volume (μL)	Mobil fase	Elution ACN %	Flow μL/min	λ nm	Section	
IT-SPME CapLC-DAD	Environmental	Port water	Irgarol – 1051	TRB-35	Zorbax SB C <sub>18</sub> (150mmx0.5mm, i.d. 5μm)	4000	CH <sub>3</sub> CN:H <sub>2</sub> O	Isocratic	20	226	4.1.1
		Port water	Diuron	TRB-35	Zorbax SB C <sub>18</sub> (150mmx0.5mm, i.d. 5μm)	4000	CH <sub>3</sub> CN:H <sub>2</sub> O	Isocratic	20	254	4.1.2
		ETTs	Meropenem	TRB-35	Zorbax SB C <sub>18</sub> (150mmx0.5mm, i.d. 5μm)	500	CH <sub>3</sub> CN:H <sub>2</sub> O	Gradient 10%-10min 15%-2min 10%-1min	8	300	4..2.4
	Biological	Urine	AK	TRB-35	Zorbax SB C <sub>18</sub> (50mmx0.5mm, i.d. 5μm)	(+20μL ACN) 15 (+15μL H <sub>2</sub> O)	CH <sub>3</sub> CN:H <sub>2</sub> O	Gradient 30% up 100%- 10min 100%- 6 min	10	520	4.2.3
		Forensic	Hands	DPA	TRB-5 TRB-20 TRB-35 TRB-50 PEG	Zorbax SB C <sub>18</sub> (150mmx0.5mm, i.d. 3.5 μm)	1800 (+20uL water)	CH <sub>3</sub> CN:H <sub>2</sub> O	Gradient 70%- 12min 100%- 4min 70%- 4min	10	280

### 3.6.2. Sensor response: In-situ analysis

In-situ analysis for different matrices includes the use of PDMS sensors and sensors based on silver nanoparticles (AgNPs-Nylon). **Table 3.5** Summarises experimental condition for each procedure developed in this Thesis.

**Table 3.5** Experimental conditions used in the in-situ analysis of compound by PDMS-sensor and AgNPs-sensor.

	Matrix	Sensor	Analyte	Reagent	Sample volume or masa	t <sub>R</sub>	λ (nm)	Section
Environmental	Cannal water	PDMS - SA- NEDD- OMIM- PF <sub>6</sub>	Nitrite	anhydrous citric acid, ZnNPs dispersion	1000μL	8 min	520-540	4.1.1
			Nitrate					
Environmental	West water	PDMS - SA- NEDD- OMIM- PF <sub>6</sub>	Nitrite,	anhydrous citric acid, ZnNPs dispersion	1000μL	8min	520-540	4.1.1
			Nitrate					
Biological	Cells	AgNPs- Nylon	Hydrogen sulfide	-	≈200μL	8 hours	500 norm.	4.2.2
	Breath	AgNPs- Nylon	Hydrogen sulfide	-	250-1000ml	10min	500 norm.	4.2.1
	Urine	PDMS- FB- OMIM- PF <sub>6</sub>	AR	10μL K <sub>2</sub> CO <sub>3</sub>	2000μL	10min	520	4.2.3
Food	Chicken meat	PDMS- NQS- OMIM- PF <sub>6</sub>	Ammonia	-	0.5kg	7 days	590	4.3.1
	Fresh spinach	PDMS - SA- NEDD- OMIM- PF <sub>6</sub>	Nitrite	anhydrous citric acid, ZnNPs dispersion	1000μL	8min	520-540	4.3.2
			Nitrate					
Fresh chard	PDMS - SA- NEDD- OMIM- PF <sub>6</sub>	Nitrite	anhydrous citric acid, ZnNPs dispersion	1000μL	8min	520-540	4.3.2	
		Nitrate						

Canned spinach	PDMS - SA- NEDD- OMIM- PF <sub>6</sub>	Nitrite	anhydrous citric acid, ZnNPs dispersion	1000μL	8min.	520-540	4.3.2
		Nitrate					
Canned chard	PDMS - SA- NEDD- OMIM- PF <sub>6</sub>	Nitrite	anhydrous citric acid, ZnNPs dispersion	1000μL	8min.	520-540	4.3.2
		Nitrate					

\*- 8 hours, is the time when the cell grows and emits H<sub>2</sub>S.

### PDMS - sensor response

- **PDMS /TEOS-SiO<sub>2</sub>NPs-SA-NEDD-OMIM-PF<sub>6</sub> sensor response**

The measurement of nitrites by using the synthesized PDMS /TEOS-SiO<sub>2</sub>NPs-SA-NEDD-OMIM-PF<sub>6</sub> sensor was performed by introducing the PDMS-membranes in a vial containing 0.5 mL of citric acid (330 mM) and adding the 0.5 ml of standard solution of NO<sub>2</sub><sup>-</sup>. To determine nitrates, previously to the Griess reaction, the appropriate volume of dispersed ZnNPs or nylon membrane with ZnNPs as a reducing agent was added (**Figure 3.16**). The pink color formed was measured using a UV-vis spectrophotometer. Spectra were recorded from 200 to 1000 nm.

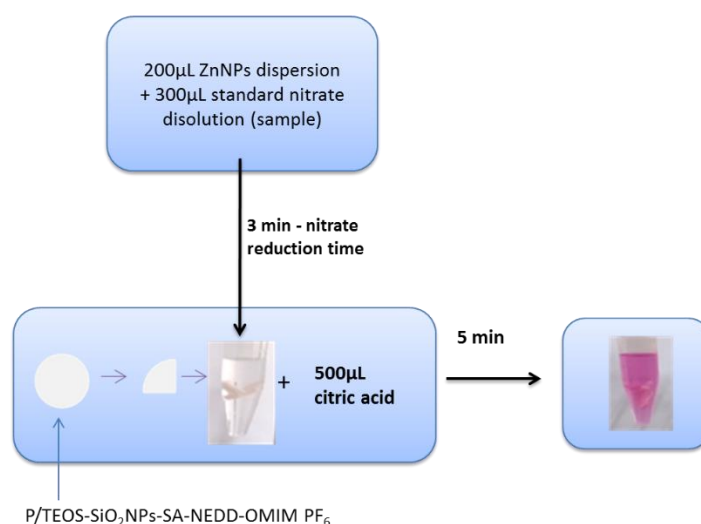


**Figure 3.16** Nitrite or Nitrate detection scheme using PDMS /TEOS-SiO<sub>2</sub>NPs-SA-NEDD-OMIM-PF<sub>6</sub> sensor, based on the Griess reaction.

- **PDMS /TEOS-SiO<sub>2</sub>NPs-NQS-OMIM-PF<sub>6</sub> membrane response**

Gaseous standards of ammonia were generated into 2 L static dilution glass flask (or in other container with different volumes). The PDMS /TEOS-SiO<sub>2</sub>NPs-NQS-OMIM-PF<sub>6</sub> sensor device was hanged up into the static dilution flask. Aliquots of amine standard solutions were injected on the bottom of the flask and 100  $\mu$ L of 2 M NaOH in order to facilitate volatilization. The presence of generated NH<sub>3</sub> produced a change in the colour of the membrane from yellow to brown (**Figure 3.17**). The intensity of the colour is related to the concentration of NH<sub>3</sub> in air and the quantitative analysis was carried out by measuring diffuse reflectance at 590 nm.

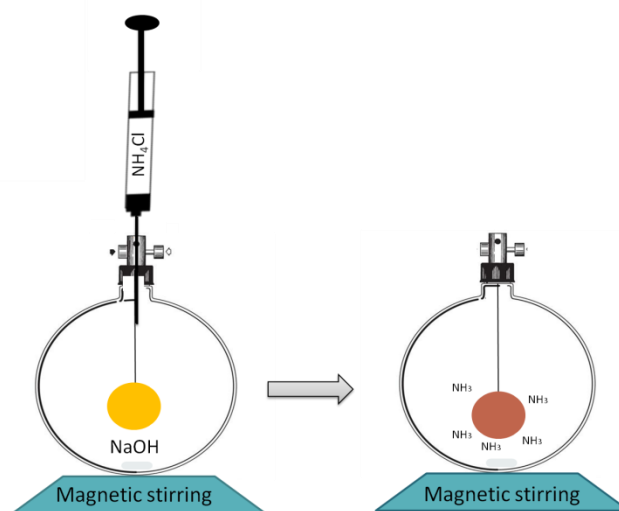


**Figure 3.17** Gaseous ammonia standards generation scheme in the static dilution glass flask.

### AgNPs- nylon sensors and multisensor response

Hermetically sealed bags of different volumes (0.25-2L) and standard dilution flasks (2L) were used for the generation of H<sub>2</sub>S atmospheres. First, the AgNPs – nylon sensor was hung in the standard dilution flask (**Figure 3.18 A**) or sealed in the case of bags (**Figure 3.18 B**) then by using a syringe, 100μL phosphoric acid of 85% and 100μL Na<sub>2</sub>S of the standard solution were added 10 minutes. The sensor was then removed and covered with glycerol. The analytical response was measured by diffuse reflectance. In addition, the interferences of ammonia, ethanol, acetone methanol, propanol, formaldehyde and toluene were tested. And finally, the amount of H<sub>2</sub>S generated in the container was studied through the formation of methylene blue, which has been chosen as a colorimetric reaction widely used for the determination of dissolved sulphur in water [300].

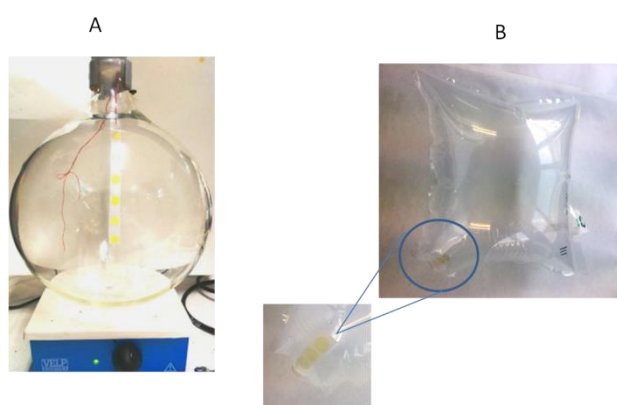


**Figure 3.18** Images of standard dilution flask (**A**) and plastic bag (**B**) with AgNPs sensors.

For the estimation of H<sub>2</sub>S in the **well plats** using AgNPs-Nylon multisensor sheet, the standard solution of Na<sub>2</sub>S in nanopure water was prepared. The working solutions were prepared by diluting the stock solution in liquid culture medium with pH 7, which allowed the growth of cells under favourable conditions of pH and temperature. Well assays for standards and for cells are schematically described in 3 steps (**Figure 3.19**). Step 1: The plate wells were filled with 190 μL of standard cell culture (DMEM with 3 mg/ml glucose, 2.5 mM L-glutamine, and

10% fetal calf serum, pH 7) and appropriate amounts of solution Na<sub>2</sub>S (in the case of cell assays instead of the Na<sub>2</sub>S solution, cell cultures). Step 2: The wells were covered with the AgNPs multisensor plate. Step 3: Finally, the set was taken to the incubator during 8h in adequate conditions for cell growth. **Figure 3.19** shows the AgNPs multisensor sheet before and after H<sub>2</sub>S exposure. The presence of generated H<sub>2</sub>S produced a change in the colour of the sensor from yellow to brown, as function as a concentrationconcentration.

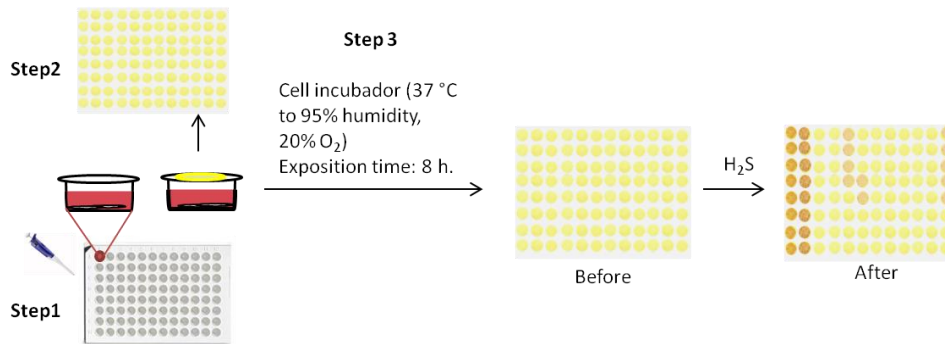


**Figure 3.19** Cells or standard assays steps and multisensor sheet image before and after exposure to different H<sub>2</sub>S concentrations.



## **CHAPTER 4. RESULTS AND DISCUSSION**



## 4.1 Environmental samples

In this section, new sustainable strategies have been proposed for environmental samples, in particular water samples from different sources: coastal, irrigation canals and wells samples were analysed. The determination of organic compounds, such as pesticides (irgarol and diuron) and inorganic compounds (nitrate and nitrite) have been addressed. Two strategies were studied: evaluation of IT-SPME-CapLC-DAD to determine the pesticides and PDMS based sensors to estimate nitrite and/or nitrate concentration.

### 4.1.1 A sustainable on-line CapLC method for quantifying antifouling agents like irgarol-1051 and diuron in water samples: estimation of the carbon footprint

IT-SPME-CapLC-DAD was studied as the analytical strategy to determine biocides such as diuron and irgarol-1051 in water samples (included in Water Frame Directive 2013/39/UE (WFD)). This configuration allows us to process relatively large sample volumes (up to 4 mL). First, optimization of the extraction parameters was studied, and subsequently the analytical parameters were estimated. Finally, the proposed methodology was applied to water samples in order to evaluate the real performance of the proposed strategy [37].

#### IT-SPME procedure optimization

Nature of the sorbent phase, length of the capillary column and volume of the processed sample were optimized. First, PDMS-based GC capillary columns with different percentages of diphenyl groups (5%- TRB5, 20% -TRB20, 35% - TRB35, and 50%- TRB50) were investigated. **Figure 4.1.1A** shows the response as a function of the diphenyl group in the extractive phase. The results indicated that the analytical response (peak area) for irgarol-1051 (2.5 µg/L) and diuron (25 µg/L) employing 1 mL as processed volume, increased with the increment of the diphenyl group percentage. However, the sorbent with 50% diphenyl groups provided a significant decrease in the peak area. Probably, due to the increase in the polarity of the absorbent phase, that resulted in a decrease of the affinity towards the target analytes. Therefore, the TRB-35 sorbent phase was selected

for further experiments. To optimize the length of the capillary column, 1 ml of a standard solution of irgarol-1051 (2.5  $\mu\text{g/L}$ ) and diuron (25  $\mu\text{g/L}$ ) was processed in capillary columns of 30, 60 and 100 cm in length. Compared with the 30 cm capillary, the analytical response for irgarol-1051 improved by 18% and 57% with the 60 and 100 cm capillary columns, respectively. In the case of diuron, that improvement was of 36% and 75% with capillary columns of 60 and 100 cm, respectively. As optimal capacity of the capillary column, 100 cm was chosen, as no improvement was detected for the higher lengths.

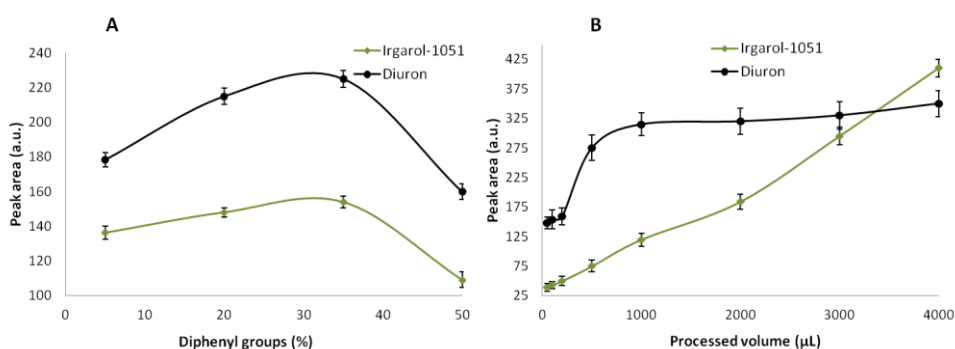


**Figure 4.1.1.** Variation of the analytical response with **A)** The percentage of diphenyl groups in the PDMS based extractive phase; **B)** the processed sample volume (2.5  $\mu\text{g/L}$  of Irgarol-1051 and 25  $\mu\text{g/L}$  of diuron).

The volume of the processed sample was then optimized. To this end, increasing volumes from 50  $\mu\text{L}$  to 4 mL of standard solution of irgarol-1051 and diuron of the concentrations already indicated above were processed. As can be seen in **Figure 4.1.1B**, a greater analytical response was obtained as the sample volume increased. However, in the case of the diuron, this increase was not very significant. This may be due to the autoelution of the analyte as the sample is loaded [301]. Finally, 4 mL was selected as the optimal sample volume.

As In-tube SPME is a non-exhaustive and continuous flow technique, high extraction efficiencies are not expected. However, the analytical response obtained was greatly improved by being able to process large volumes of sample. The extraction efficiencies were estimated through values obtained from the total amount of analyte processed by the capillary column and the amount of analyte extracted. To calculate the amount of analyte extracted, 2  $\mu\text{L}$  of standard solutions were injected and from the areas of the peaks in the resulting

chromatograms and the calibration equations constructed, the estimation of the amount of analyte extracted was performed. The extraction efficiencies obtained were 3 and 19% for diuron and irgarol-1051, respectively. These values are in accordance with the technique. **Figure 4.1.2** shows the chromatogram obtained for a mixture of irgarol-1051 and diuron under the optimum conditions. Retention times and UV-vis spectra were used for the screening and the quantification of the target analytes in water samples.

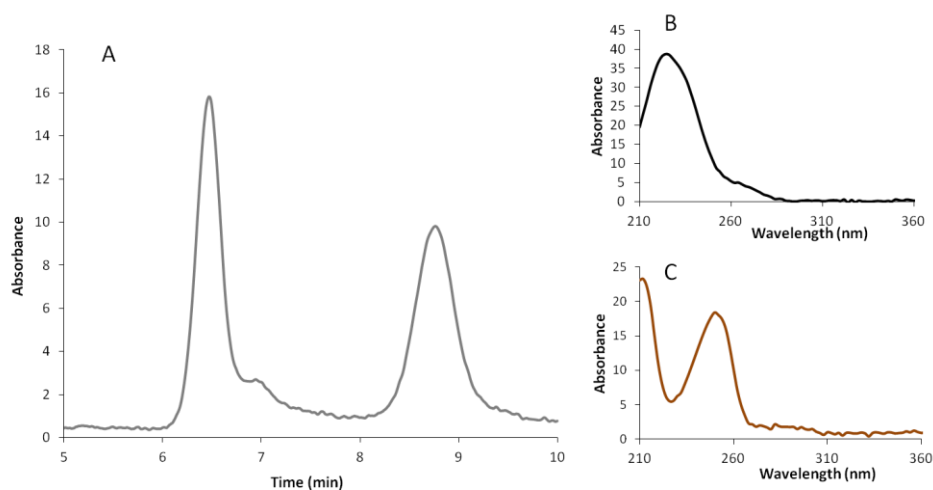


**Figure 4.1.2** A) Chromatogram obtained for a mixture of target analytes under the optimum conditions B) UV-vis spectrum of diuron and C) UV-vis spectrum of irgarol- 1051.

### Analytical performance

Calibration equations, linear working range, LOD, LOQ and precision data are shown in Table 1 for irgarol-1051 and diuron at 226 and 254 nm, respectively. The results indicated satisfactory analytical performance in the lineal interval 0.05–15  $\mu\text{g/L}$  and 0.7–15  $\mu\text{g/L}$  for irgarol-1051 and diuron, respectively. LOD and LOQ for irgarol-1051 were 0.015 and 0.05  $\mu\text{g/L}$ , respectively.

**Table 4.1.1** Analytical parameters obtained with the proposed method to determine diuron and irgarol-1051.

Analytes	Lineal range (µg/L)	Calibration curve $y=a+bx$ (µg/L)		$R^2$	LOD (µg/L)	LOQ (µg/L)	RSD (%)
		$a\pm s_a$	$b\pm s_b$				
Diuron	0.7-15	6±4	11±1	0.998	0.200	0.70	1.5
Irgarol-1051	0.05-10	7±70	188±14	0.995	0.015	0.05	3.2

According to the results obtained the sensitivity achieved with the proposed procedure is suitable for regulatory purposes because the LODs are below the maximum levels fixed by the European regulations for diuron and irgarol-1051 in water samples (Directive 2013/39/EU). The precision for retention times was estimated, and the RSD values for diuron and irgarol-1051 were 0.3 and 0.5%, respectively. The precision of the analytical response was also calculated. As can be seen in **Table 4.1.1**, the intraday RSDs were up to 4% ( $n=3$ ), which are acceptable values at the working concentration levels.

### Carbon footprint and environmental performance

The carbon footprint is calculated by means of GHG emissions produced by an activity and is expressed in kg CO<sub>2</sub> eq. From a qualitative point of view, the in-tube SPME-CapLC-DAD is respectful with the environment since it reduces the consumption of solvents and the use of toxic reagents[53]. However, the lack of a quantitative environmental indicator prevents real estimation of environmental impact and comparison with other methodologies. To calculate the carbon footprint, the equation  $\text{kgCO}_2\text{eq} = \Sigma (\text{amount of electricity consumed (kWh)} \times \text{electricity emission factor (kg CO}_2\text{/kWh)})$  was used. To calculate the carbon footprint, the energy consumed for the analysis of 100 samples has been taken into account, also including the analysis times of each study described. The results indicated that the carbon footprint significantly varied as a function of the sample pretreatment and the separation/detection technique (**Table 4.1.2**). The lowest carbon footprint (1.10 KgCO<sub>2eq</sub>) was achieved with in-tube SPME-CapLC-DAD. The carbon footprints for SPE-HPLC-DAD were 2.20 and 1.8 KgCO<sub>2eq</sub>. These values are higher than the in-tube SPME-CapLC-DAD carbon footprint because SPE based procedures require an additional preconcentración step (evaporation) to reach

the LODs, and so the energy consumption increased. Moreover, analysis times, and especially solvents and wastes significantly increased with SPE based procedures, approximately 200-300 mL/100 samples in the sample pretreatment. Meanwhile, in-tube SPME completely eliminates the solvent consumption in this step. GC-MS combined with SBSE and HS-SPME were the procedures which provided a high amount of emissions, especially HS-SPME-GC-MS due to the need of fiber conditioning, water bath and stirrers during the sample pretreatment. MF-SPME coupled to SPE also provided a high value of carbon footprint, and also due to long sample pretreatment time and lack of multi-sample pretreatment. From these results, it can be concluded that the more sustainable analytical procedure to determine the antifouling biocides is in-tube SPME CapLC-DAD not only because the analytical parameters adequate but also because the environmental performance is also improved. The success of in-tube SPME-CapLC-DAD is maintaining the reliability of the performance parameters, such as sensitivity, precision and accuracy but reducing the environmental impact of the analytical methodology.

**Table 4.1.2** Estimation of carbon footprints Kg CO<sub>2</sub>/100 samples of different analytical procedures proposed for antifouling biocides in water samples.

Analyte	Sample pretreatment		Sample Volume (mL)	Separation / Detection	Analysis time (min)	Carbon footprint KgCO <sub>2</sub>	Analytical performance			Ref
	Off-line	On-line					LOD (µg/L)	RSD (%)	Recovery (%)	
Irgarol-1051 Diuron Chlorothalonil Dichlofluanid TCMTB Thiram	SPE	-	100	HPLC-DAD	17	1.80	0.007-0.415	<11	68-103	[153]
Irgarol-1051 Diuron Derivates	SPE	-	500	HPLC-DAD	60	2.30	0.005-0.011	<14	97-116	[302]
Chlorothalonil Dichlofuamid Sea-Nine 211 Irgarol-1051 TCMTB	SBSE	-	10	TD-GC-MS	110	16.90	0.005-0.900	<30	82-118	[152]
Chorotalonil Dichlofluanid Sea Nine 211	SDE	-	10	GC-ECD	55	26.30	0.0002-0.003	<8.5	78-104	[156]
Irgarol-1051	HS-	-	15	GC-MS	80	220.00	0.010-	<9	82-118	[154]



<b>Sea Nine 211</b>	SPME						0.030			
<b>Irgarol-1051 Diuron</b>	MF- SPME	-	300	HPLC-DAD	100	<b>23.80</b>	0.0014 - 0.0048	<12	-	[157]
<b>Diuron TCMTB Irgarol-1051 Chrothalonil</b>		SPE	100	LC-APCI-MS	25	<b>19.60</b>	0.005- 0.01	5-10	96-111	[303]
<b>Diuron Irgarol-1051 Folpet Dichlofluanid</b>		SPE	100	LC-APCI-MS	21	<b>17.80</b>	0.005- 0.2	<8	88-92	[304]
<b>Multiresidue: Biocidal pesticides and Pharmaceuticals</b>		SPE	20	LC-ESI- MS/MS	26	<b>41.10</b>	0.003- 0.1	<32	62-104	[151]
<b>Irgarol-1051 Diuron</b>	-	IT- SPME	4	CapLC-DAD	10	<b>1.10</b>	0.015 0.200	<4	92-113	<b>Prop osed proce dure</b>

### Water samples analysis

Water samples were collected in different ports of the Region of Valencia at different periods. Retention times, as well as UV-vis spectra, were used for the screening the samples. Finally, if necessary, quantification of the positive samples was also carried out. **Table 4.1.3** shows the samples screened and the quantification results determined by in-tube SPME-CapLC-DAD procedure. As shown in **Table 4.1.3**, the concentration of diuron was below the LOD in all the ports at any sampling period. Therefore, these sampling points satisfied the European standards regarding with diuron. As can be seen in **Table 4.1.3**, irgarol-1051 was below the LODs except in the case of samples 1 and 2 in Port of Valencia, where the concentrations were 0.02 mg/L, which was near to the value of the LODs for this compound (**Figure 4.1.3** shows the chromatogram obtained for sample 1). However, in all cases, it can be considered that these waters met the European standards. The presence of irgarol-1051 in these water samples can be understood taking into account that the Port of Valencia is the main port of the Valencian Community and one of the main ports of Spain and that it handles a large maritime traffic. On the other hand, in the case of Port Saplaya, and Port of Siles, they are marinas and the presence of the analytes would be, more likely, due to a high number of boats and the low recirculation of water.

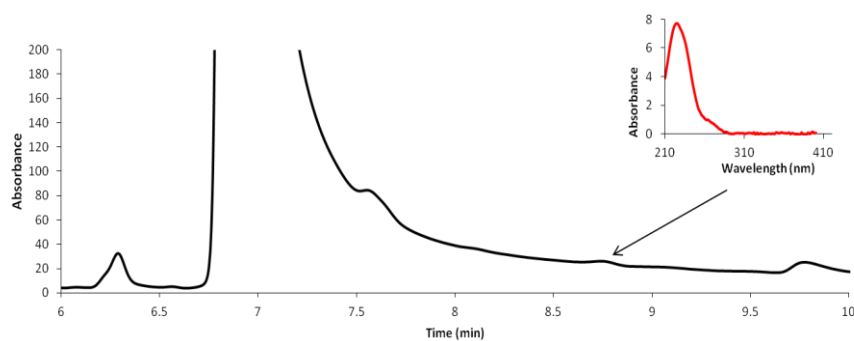


**Figure 4.1.3** Chromatogram obtained for sample 1. Inset: UV-vis spectra of peak  $t_r = 8.7$  min corresponding to irgarol-1051.

In order to validate the results obtained, a recovery study was carried out spiked samples. **Table 4.1.3** summarizes the recovery values obtained. The values were between 92-105 % for all the samples. It should be remarked that these values were within the acceptable range for environmental analysis. These results indicated the absence of matrix effects and so the determination of irgarol-1051

and diuron can be carried out with in-tube SPME-CapLC-DAD procedure employing external standards.

**Table 4.1.3** Samples screened quantification results and recoveries from water samples determined by in-tube SPME-CapLC-DAD.

			Concentration ( $\mu\text{g/L}$ )		Recovery (%)	
			Irgarol-1051	Diuron	Irgarol-1051	Diuron
<b>Port of Valencia</b>	Sample 1	March	0.02	<LOD	102 $\pm$ 9	96 $\pm$ 4
	Sample 2	April	0.02	<LOD	110 $\pm$ 5	100 $\pm$ 5
	Sample 3	June	<LOD	<LOD	104 $\pm$ 6	105 $\pm$ 6
	Sample 4	July	<LOD	<LOD	102 $\pm$ 4	99 $\pm$ 7
<b>Marina Port Saplaya</b>	Sample 5	March	<LOD	<LOD	92 $\pm$ 5	99 $\pm$ 4
	Sample 6	April	<LOD	<LOD	108 $\pm$ 3	103 $\pm$ 6
	Sample 7	June	<LOD	<LOD	113 $\pm$ 3	96 $\pm$ 5
	Sample 8	July	<LOD	<LOD	115 $\pm$ 6	100 $\pm$ 8
<b>Port of Siles</b>	Sample 9	March	<LOD	<LOD	93 $\pm$ 5	92 $\pm$ 7
	Sample 10	April	<LOD	<LOD	98 $\pm$ 4	105 $\pm$ 6
	Sample 11	June	<LOD	<LOD	91 $\pm$ 8	94 $\pm$ 8
	Sample 12	July	<LOD	<LOD	103 $\pm$ 5	98 $\pm$ 6

## Conclusion

In this work, a new strategy based on IT-SPME - CapLC - DAD to determine diuron and irgarol-1051 in environmental water samples has been proposed. The LODs were 0.015 and 0.2  $\mu\text{g/L}$  for irgarol-1051 and diuron, respectively and so, it can be used to achieve the quality standards established by the European regulations. In addition, precision was also satisfactory.

This strategy not only was evaluated in terms of basic analytical parameters, but also in terms of environmental performance. For this aim, the carbon footprint of the proposed procedure has been calculated and compared with the carbon footprint of the previously proposed procedures. This parameter has been proposed as a quantitative indicator of the environmental friendliness of a methodology. For regulatory purposes, the results indicated that the most sustainable methodology to determine irgarol-1051 and diuron is in-tube SPME-CapLC-DAD. Hence, in-tube SPME-CapLC-DAD can be an alternative methodology easily implementable and environmental friendly to estimate irgarol-1051 and diuron in environmental water samples. The new methodology has been applied to evaluate water samples from different ports or marinas in the Region of Valencia. The results showed that irgarol-1051 and diuron were below the LODs and so, water samples met the European quality standards.

### **4.1.2 Improving sustainability of the Griess reaction by reagent stabilization on PDMS membranes and ZnNPs as reductor for nitrates: Application to environmental water matrices**

In this work, a IL modified-PDMS membrane doped with the Griess reagent (NEDD and SA) was proposed as a new strategy to determine nitrite or nitrate in water samples. The determination of nitrite and nitrate in water samples was carried out by in situ analysis. The solid sensor was based on the use of polydimethylsiloxane (PDMS) membranes doped with Griess reagent. The influence of some doping compounds, on the properties of the PDMS membranes, such as tetraethyl orthosilicate (TEOS), or/and ionic liquids has been studied. Griess reagents are entrapped in confined composites of PDMS and ionic liquids, in particular 1-Methyl-3-octylimidazolium hexafluorophosphate (OMIM-PF<sub>6</sub>).

In this membrane the reagents are stable on time and they can be delivered to a solution in order to carry out the derivatization reaction. Better reagent diffusion was obtained using doped PDMS membranes than undoped PDMS. In order to apply the procedure to nitrate, dispersed nanoparticles of Zn (ZnNPs) were employed. The addition of ZnNPs was studied and compared with the addition of powder of Zn. ZnNPs dispersed in surfactants were required in order to increase the control over the reduction reaction. The analytical responses were obtained by measuring the absorbance or by using the RGB components from digital images. The results indicated good precision (RSD <8%) and satisfactory stability of the sensing membrane. The detection limit achieved was 0.01 or 0.5 mg/L for nitrite or nitrate, respectively. The practical application of the sensing devices was demonstrated by analysis of different environmental waters, and waters from canned vegetables and fresh vegetables (these will be studied latter in food section). The results obtained were statistically comparable with those provided by using nitrate ISE or UV-vis measurement. This study offers a new sustainable methodology for on-site determination of nitrite and nitrate in several matrices.

### **Doping study of the composite PDMS/TEOS-SiO<sub>2</sub>NPs-SA-NEDD-OMIM-PF<sub>6</sub> in function of the sensor response.**

In a first step of experiments, the response of composites of PDMS doped with Griess reagents to the NO<sub>2</sub><sup>-</sup> concentration was evaluated. It was observed that when a sensor was introduced into a solution, the reagents (NEDD and SA) atraped in the sensor were released from the solid to solution. In presence of NO<sub>2</sub><sup>-</sup>, the resulting solution presented a maximum between 520 and 540 nm, which indicated that the azo compound derivative was formed. In order to obtain similar sensitivity to that obtained by performing this reaction in solution, the composition of the membrane was assayed. One of the possible drawbacks of PDMS membranes can be the low reagent diffusion; therefore, with the purpose of increasing diffusion, the membranes were doped with TEOS and OMIM-PF<sub>6</sub>.

The addition of TEOS to the membrane improved its hydrophilic character. The amount of OMIM-PF<sub>6</sub> added to the PDMS was less than 7%, providing total gelation. In **Figure 4.1.4** the SEM images corresponding to the PDMS-TEOS and PDMS-TEOS-OMIM-PF<sub>6</sub> membranes are shown. In presence of OMIM-PF<sub>6</sub> the SEM image shows sponge structures. These images are comparable with similar results

obtained by A. I. Horowitz and M. J. Panzer [118] who obtained an asymmetric structure of PDMS polymer with high permeability caused by a decrease in the polymer rigidity backbone and an increasing in void volume available for the diffusion of the permeate molecules.

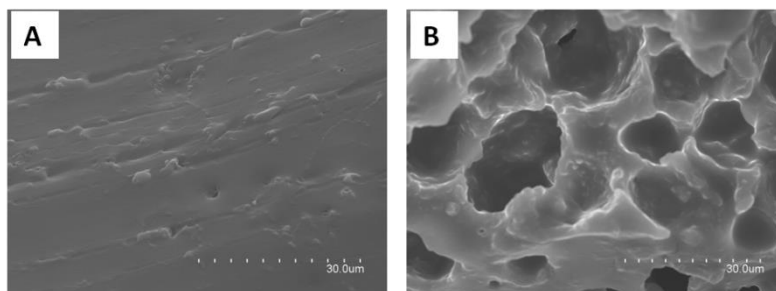


**Figure 4.1.4** SEM micrographs for **(A)** PDMS-TEOS and **(B)** PDMS-TEOS- OMIM-PF<sub>6</sub> solid sensors.

The performance of the different synthesized membranes (PDMS /TEOS-SiO<sub>2</sub>NPs-SA-NEDD and PDMS/TEOS-SiO<sub>2</sub>NPs-SA-NEDD-OMIM-PF<sub>6</sub>) in terms of reagent release was evaluated and compared. As can be seen in **Figure 4.1.5 A**, the release of the reagent (SA-NEDD) depended on the membrane composite and so the analytical signal. The results showed that the analytical responses were 1.5 times higher with the OMIM-PF<sub>6</sub> modified PDMS-TEOS membrane than PDMS-TEOS membrane more likely due to the higher reagent release. Therefore, based on these results, PDMS-TEOS-OMIM-PF<sub>6</sub> doped with SA and NEDD was chosen for further experiments.

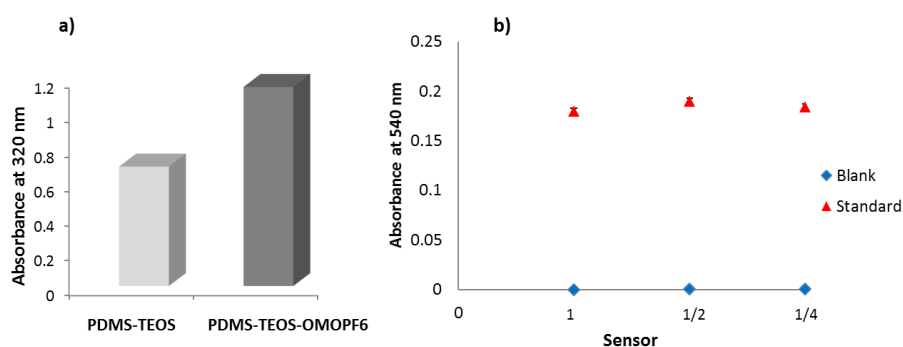


**Figure 4.1.5 A)** Analytical signals obtained with PDMS-TEOS and PDMS-TEOS-OMIMPF<sub>6</sub> membranes doped with SA and NEDD. **B)** Analytical response study for different sensor sizes.

In order to evaluate the diffusion of the reagent, the sensing membranes (diameter =1.5 cm) were cut in different sizes and added to the nitrite solution. The results indicated that the response did not depend on the size. Therefore,  $\frac{1}{4}$  of a sensor, with  $0.44 \text{ cm}^2$  area, was used for each experiment. **(Figure 4.1.5B)**. On the other hand, the nitrite analysis time was optimized by carrying out a kinetic study in order to determine the time necessary to reach a plateau. As we can see in **Figure 4.1.6A** at 5 min the analytical signal was maximum and this time was selected for further experiments.

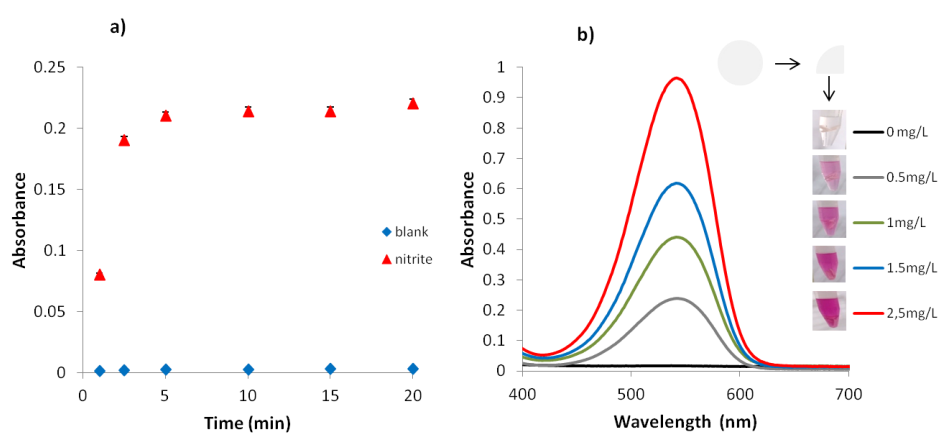


**Figure 4.1.6 A)** Griess reaction time optimization employed PDMS sensing devices for 0.5mg/L nitrite concentration. **B)** Vis spectra of different  $\text{NO}_2^-$  solutions employing Griess reagents entrapped in PDMS membranes.

The use of OMIM- $\text{PF}_6$  improved sensibility and response time owing to increase the accessibility and the porosity of the membrane. As illustrative example, in **Figure 4.1.6B** are shown the spectra obtained for different nitrite solutions, as well as a picture of the corresponding solutions in presence of the sensor.

On the other hand, the PDMS/TEOS- $\text{SiO}_2$ NPs-SA-NEDD-OMIM- $\text{PF}_6$  sensor stability in time and several environmental conditions were studied. According to the results achieved, they were stable for 60 days in storage conditions at room temperature and protected from air exposition.

#### Application to the determination of nitrate in water samples

Several procedures have been described in the bibliography to reduce nitrate to nitrite using power Zn either in batch mode [178] or in FIA mode by using a Zn

column [171]. In order to perform batch procedures, the reduction reagents of nitrate have to be added to the solution. The insolubility of Zn powder in water solution affects the nitrate reduction reaction, and the precision of the results. Thus we have proposed the use of a dispersion of ZnNPs in order to provide a robust reduction. Assuming the possibility to transform nitrite in nitrate, in this section, the possibility to apply the proposed sensing devices to determine nitrate in water samples was evaluated. For this aim, the reduction step was studied. Nitrate reduction can be achieved by adding reduction agents such as Zn powder, however, one of the main drawbacks is the limited solubility in aqueous samples which results in a poor precision of the results. With this in mind, ZnNPs was proposed in this work. However, ZnNPs agglomeration due to Van der Waals forces must be taken into account. Based on previous studies, sonication was tested to prepare stable dispersions, however, results were not satisfactory, and therefore, we studied the addition of surfactants to obtain stable dispersions. Cationic surfactant (CTAB) and anionic surfactant (SDS) were selected. Mixtures at different proportions (0: 100, 30:70, 70:30, 100: 0) of SDS:CTAB were studied. The ZnNPs were dispersed in all these solutions except in a solution of CTAB (100:0). A solution with 30% SDS-70% CTAB was chosen in order to obtain a ZnNPs dispersion with the highest stability (more than 1 month), see **Figure 3.7A (section 3.3.2)**. Zn powder did not provide a dispersion mixture (see **Figure 4.1.7A**).

Hydrodynamic diameter of the proposed ZnNPs in 30% SDS-70% CTAB was established by Dynamic light scattering (DLS). As can be seen in **Figure 4.1.7B** the hydrodynamic size of ZnNPs was around 100 nm.

The reduction potential of ZnNPs was studied by using two approaches: (i) in solution and (ii) ZnNPs immobilization on the surface of nylon membranes.

In the first approach, the effect of the amount of ZnNPs in the reduction reaction and in the Griess reaction was evaluated. As can be seen in **Figure 4.1.8A** 0.12 mg/per assay (or 200  $\mu$ L solution of ZnNPs dispersion) were needed to reach a plateau. This amount of NPs was much lower to that required without dispersion (0.625 mg). Concerning to the time required for the reduction reaction, in **Figure 4.1.8B**, the variation of the response with time is shown. The results indicated that the reaction was completed within 3 min and the absorbance was constant. ZnNPs dispersion did not interference in the subsequent Griess reaction. In this



approach 0.2 mL of ZnNPs dispersion were added to the standard  $\text{NO}_3^-$  solutions or samples. After 3 min, the reagent membrane was added to the solution and the total time to carry out both reactions was 8 min. The reaction product (azo compound formation) was stable with time, since the response was constant with time.

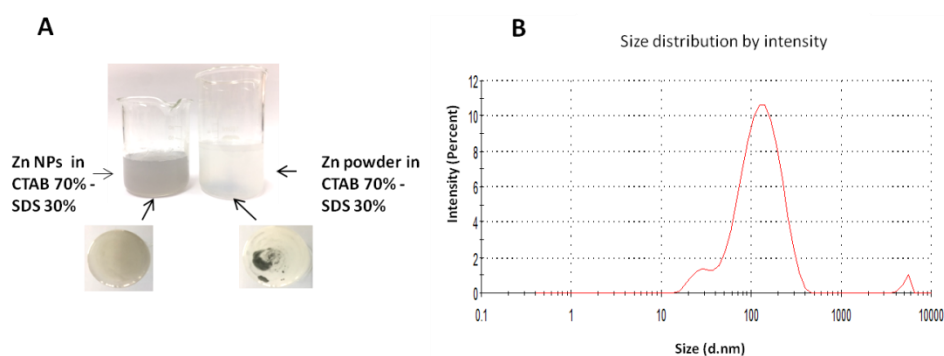


**Figure 4.1.7. A)** ZnNPs and Zn powder in CTAB-SDS surfactant mixture. **B)** Intensity size distribution of the ZnNPs dispersed (in the 30%SDS - 70%CTAB).

In the second approach, ZnNPs were deposited on a Nylon membrane (0.45  $\mu\text{m}$ ). For this aim, 200  $\mu\text{l}$  of ZnNPs(CTAB-SDS) dispersion was passed through the membrane (**Figure 4.1.7B, section 3.3.2**). The resulting membrane was then added to the solution and the reduction took place by releasing ZnNPs in the nitrate solution. Similar results were obtained with both approaches, however, the second approach introduced some advantages, since no reagents are required (**Figure 4.1.8C**). It is important to remark that ZnNPs deposited on the nylon membrane were stable at least 1 month, and therefore, they can be directly used to the nitrate reduction.

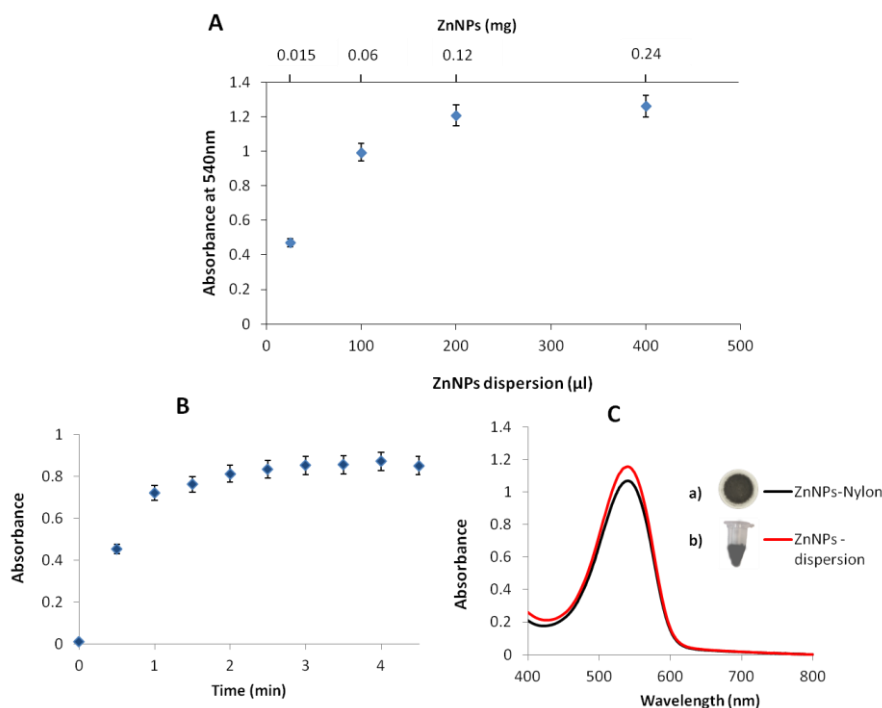


**Figure 4.1.8** A) ZnNPs amount optimization in the reduction reaction of nitrate (24mg/L) to nitrite B) Reduction reaction time optimization of nitrate (20mg/L) to nitrite C) Analytical responses comparison using ZnNPs-Nylon and ZnNPs-dispersion.

### Analytical performance

The calibration equations for nitrate or nitrite determination were established under the different methodologies used. Linear range, sensitivity, precision LODs and LOQs are shown in **Table 4.1.4**. The obtained values indicate that this procedure provides adequate linearity in the working concentration interval 0.04-2.5 mg/L and 1.61-30 mg/L for the nitrite and nitrate, respectively. The detection limit was calculated as  $3 \cdot s / \text{sensitivity}$ , where  $s$  is the blank standard deviation [305], being 0.01 and 0.5 mg/L for nitrite and nitrate, respectively. The limit of quantification was calculated as  $10 \text{ Sa/b}$  and it is also listed in **Table 4.1.4**. Interday and intraday relative standard deviation (%RSD) were calculated using sensors synthesized in the same batch. Using the solution method, the intraday

%RSD were 0.12 and 0.2, for nitrite and nitrate, respectively, while they were 0.4 and 0.7 using the sensor membrane. These results indicate satisfactory %RSD values. In addition, a batch-to-batch precision study was performed. For this aim, the responses of the three sensors prepared in three different batches under identical conditions were obtained. The batch-to-batch interday %RSD values were 1.6 and 6.2 for nitrite and nitrate, respectively. The low %RSD values obtained give evidence that the proposed composites are precise for their practical application.

Additional, analysis of images was also performed by RGB coordinates. The proposed assay allows determining the concentration quantitatively by measuring the RGB components (**Table 4.1.4**) or semiquantitatively by visual observation and comparing the color solution with a color comparison chart.

The responses of the method to mixtures of nitrite/nitrate were also evaluated. In order to determine both analytes, the response of the nitrite was evaluated first using one aliquot of the sample. A second sample aliquot was required to determine nitrate. When both analytes were determined in the same sample aliquot no interference of the ZnNPs was detected in the nitrite response, and the responses of nitrite and nitrate (as nitrite) were additive.

**Table 4.1.4.** Figures of merit obtained using the different methodologies proposed for detection of nitrites and nitrates. <sup>(a)</sup> Assay carried out by adding the conventional Griess method <sup>(b)</sup> Assay performed by using the synthesized PDMS sensor and ZnNPs – dispersion. <sup>(c)</sup> Assay carried out by using PDMS sensor and ZnNPs-Nylon for reduction reaction.

	Linearity ( $y=a+bx$ ) (mg/L <sup>1</sup> )			Linear interval (mg/L)	Precision RSD(%)		LOD (mg/L)
	$a \pm s_a$	$b \pm s_b$	$R^2$		Intraday (n=3)	Interday (n=3)	
<b>NITRITE</b>							
<sup>(a)</sup> Conventional Griess method	0.007±0.003	0.661±0.004	0.99	0.018-1.5	0.12	0.9	0.005
<sup>(b)</sup> Sensing membrane	0.0035±0.009	0.523±0.007	0.99	0.04-2.5	0.4	1.6	0.01
<b>NITRATE</b>							
<sup>(a)</sup> Conventional Griess method	0.028±0.013	0.056±0.001	0.99	4.6-30	0.2	4.3	0.1
<sup>(b)</sup> ZnNPs dispersion reduction. Sensing membrane	0.034±0.007	0.0409±0.0005	0.99	1.6-30	0.7	5.8	0.5
<sup>(c)</sup> ZnNPs –Nylon reduction. Sensing membrane	0.031±0.008	0.038±0.0004	0.99	1.6-30	0.2	6.2	0.5
RGB (green)	0.114±0.013	0.052±0.004	0.99	2.8-25	1.1	7.2	0.8

### Water sample analysis

The potential utility of the proposed methodology for the determination of nitrate or nitrite in real environmental samples such as well water and irrigation water have been tested. Firstly, due to the samples contained particulate matter, the effect of filtering the samples on the nitrite or nitrate response was studied. For this purpose, aliquots of samples previous filtered or not were processed. The results obtained indicated that the sample filtration did not affect the results. According to these results, the samples that have particles in suspension were filtered. In **Table 4.1.5** are shown the concentrations obtained for real water samples, as can be seen  $\text{NO}_2^-$  concentration was very little, while higher concentrations were obtained for  $\text{NO}_3^-$ . These results were in concordance with those obtained by using the reference nitrate ISE electrode method.

**Table 4.1.5** Detected concentrations of  $\text{NO}_3^-$  and  $\text{NO}_2^-$  in different water samples using PDMS sensor.

Samples	Found concentration (mg/L)	
	$\text{NO}_3^-$	$\text{NO}_2^-$
	Method A	Method A
Irrigation canal	69.2±0.9	0.0564±0.0019
Well water 1	21.42±0.05	0.0848±0.0013
Well water 2	2.79±0.01	0.0524±0.0013

### Conclusions

In this work a new approach was proposed for the determination of nitrite and/or nitrate in waters. The method was based on the use of PDMS-TEOS-OMIMPF<sub>6</sub> membrane doped with SA-NEDD, to derivatize nitrite in aqueous solution. If  $\text{NO}_3^-$  determination is required, we proposed a ZnNPs-(CTAB-SDS)-modified nylon membranes as reduction device. The reagent entrapment on PMDS membranes, characterization of ZnNPs dispersions and its reactivity for the reduction of  $\text{NO}_3^-$  to  $\text{NO}_2^-$  have been studied. ZnNPs dispersions were stable at room temperature for more than 1 months, as well as Griess reagent in PDMS-TEOS-OMIM-PF<sub>6</sub> support. The analytical response was obtained by measuring the absorbance or

RGB coordinates of the digitalized image. The results were satisfactory reached at the detection limit of 0.01 and 0.5 mg/L for nitrite and nitrate, respectively, and with good precision (RSD <8%). Based on these results a quick assay for quantitative determination of nitrate or nitrite in real samples has been developed. Nitrite was directly determined by using the Griess reagent membranes while nitrate required the reduction step with ZnNPs. Environmental water samples were processed directly without requiring any sample treatment. The proposed method has advantages compared to other methods known in the literature where unstability of Griess reagent is remarked. This strategy was acceptable to stabilize Griess reagents by embedding them on polymeric solid support such as PDMS. On the other hand, this strategy improves the sustainability of the analytical method in terms of miniaturization, reagent, waste reduction and low cost. Furthermore, this approach does not require external forces and can be used for on-site analysis by untrained personnel. The successful results obtained indicated that the method would be very competitive in routine on-site analysis for water samples. For future trends several formats can be performed; these sensors can be used as a single assay or can be adapted to a microplate assay. In the last case, the amount of membrane used was reduced according to the volume used (20  $\mu$ L). In this case, the absorbance could be measured by a microplate reader or by RGB coordinates obtained from the digital images captured by using a smartphone [128].

### **4.2 Biological samples**

In this section we study the determination of volatile sulfide compounds (VSCs) in biological samples such as breath and human cardiovascular cells. A plasmonic solid sensor based on silver nanoparticles retained on Nylon was proposed. The studies were performed as for the individual sensor as well as for the multisensor sheet that fits the 96-well plate. On the other hand, we determined meropenem in the endotracheal tubes and alkylresoncinol in the urine.

#### **4.2.1. Nylon-supported plasmonic assay based on the aggregation of silver nanoparticles. In-situ determination of hydrogen sulfide like compounds in breath samples.**

The determination of volatile sulfide compounds (VSCs) in human breath was determined by using a solid-phase colorimetric plasmonic sensor based on the retention of AgNPs on a Nylon membrane support, patented by MINTOTA [306]. Depending on the VSCs concentration, the AgNPs – nylon sensor changes from yellow to brown color with different intensities. AgNPs behavior in the membrane has been studied by UV–vis diffuse reflectance spectrometry, Raman spectrometry, high-resolution transmission electron microscopy (HR-TEM), and scanning electron microscopy (SEM). The aggregation of AgNPs in solution was demonstrated by an increase in the hydrodynamic diameter, estimated by both, asymmetric flow field - flow fractionation (AF4) coupled on-line to DLS and batch DLS, and is achieved when sulfide is added to AgNPs covered with citrate. Diffuse reflectance spectrophotometry and processed digital images obtained with a smartphone have been used as measurements for quantitation; a linear concentration range of hydrogen sulfide from 150 to 1000 ppbv and a detection limit (LOD) of 45 ppbv were achieved, measuring after 10 min of the sensor exposition to the hydrogen sulfide atmosphere (2 L) for humidity percentages between 50 and 96% and room temperature. Satisfactory results in terms of precision (<10%) and selectivity were obtained. The new sensor reported was stable, sensitive, inexpensive, disposable, safe, and user-friendly. Furthermore, it has been successfully applied to determine VSCs expressed as hydrogen sulfide in breath samples (2 L and 250 mL) as proof of concept. The limit of detection can be improved by increasing the exposition time, if necessary.

##### **AgNPs-Nylon colorimetric solid sensor optimization**

The strong interaction between sulfur group and noble metal NPs is well known [307], this interaction could result in changes on the plasmonic resonance band of NPs as thus solution colour. Firstly, the response variation of AgNPs and AuNPs as a function of  $S^{-2}$  addition was evaluated in solution. It must be taken into account that  $H_2S$  is a weak acid with  $pK_a$  for the first and second protonation of 6.88 and 14.15 respectively. Then at pH 7 (corresponding to the pH of the silver and gold dispersions) the two forms  $H_2S$  and  $SH^-$  are present.

As it was expected, changes in the plasmonic resonance band were observed. As sulphide concentrations increased, the AgNPs plasmon band shifted towards higher wavelengths and the solution changed from yellow to brown colour, indicating the AgNPs aggregation (**Figure 4.2.1A**). These results were in accordance with those provided by Baalousha et al [308]. In the case of AuNPs, no band shift is observed, probably due to their stability (**Figure 4.2.1B**). Therefore, this study continued with AgNPs.

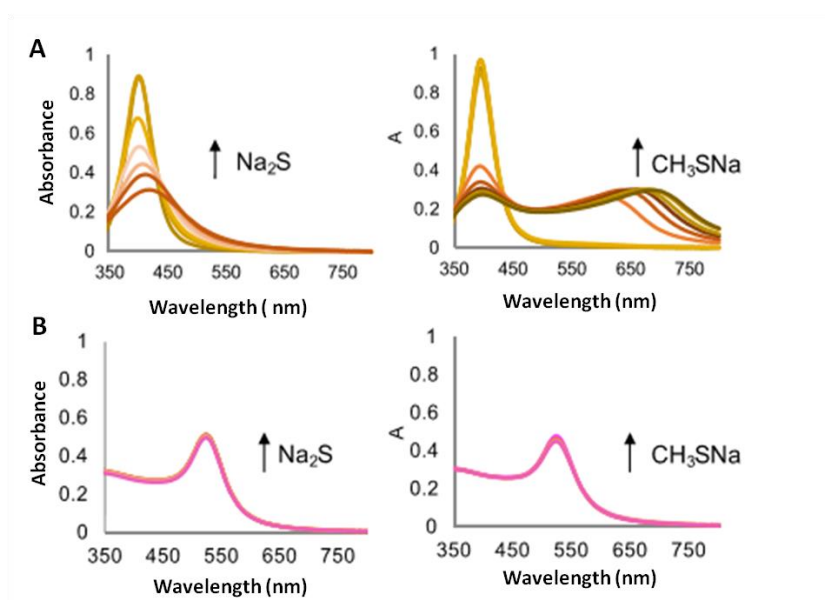


**Figure 4.2.1** Response analysis of the spherical citrate-AgNPs of 20 nm in solution for Na<sub>2</sub>S and NaCH<sub>3</sub>S (registered after 20 seconds of each addition) at final concentration between 0-10000 ppb for (A) and citrated-AuNPs in solution for (B) at the same concentrations than those indicated in (A).

To support the theory of aggregation of AgNPs in the presence of sulfides, fractograms by asymmetrical flow field-flow fractionation (AF4) coupled on line with dynamic light scattering (DLS) detector and the batch DLS data were obtained (**Figure 4.2.2**). An increase in the hydrodynamic diameter was achieved when the sulfide was added to citrate capped AgNPs.



## Chapter 4. Results and Discussion

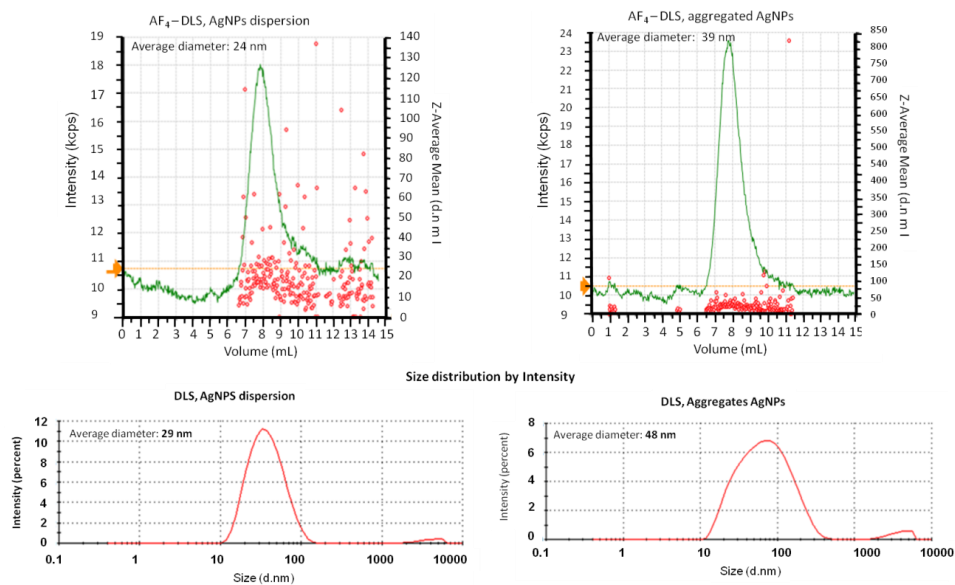


**Figure 4.2.2** Fractograms obtained with dynamic light scattering (DLS) detector and batch DLS measurements of dispersions of citrate-capped AgNPs in absence and presence of sulfide.

The second step was the retention of AgNPs on a solid membrane in order to get an easy-handling device. For this purpose three types of different membrane materials were examined such as cellulose, fiberglass and nylon (**Figure 4.2.3**). A dispersion of AgNPs (200 $\mu$ L) was passed through the membrane. As can be seen, nylon showed the higher retention for the same amount than cellulose and glass fiber, measured through the absorbance of the plasmonic band of the resulting dispersion (see **Figure 4.2.4**).

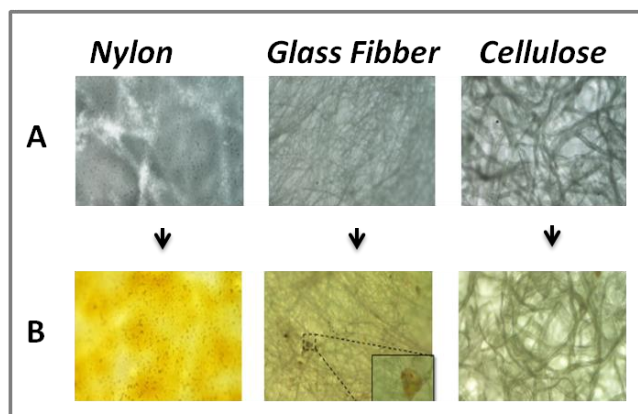


**Figure 4.2.3** Microscopy images of the membranes on nylon, glass fiber and cellulose membranes before (A) and after (B) retention of the AgNPs.

Different retention processes were studied: depositing the membrane in the dispersion or passing the nanoparticles through the membrane. The successful retention was performed with the last process (see section 3.3.2.2). Hence, the commercial AgNPs were directly retained on the membrane, without complex instrumentation or surface functionalization, avoiding chemical reagents and solvents.

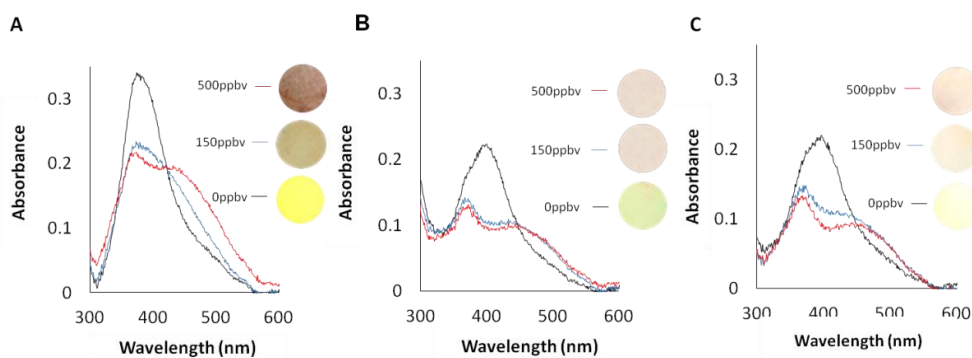


**Figure 4.2.4** AgNPs-coated membranes of A) Nylon, B) Glass fiber and C) Cellulose. The prepared membranes were exposed to different concentrations of  $H_2S$  (0, 150, 500 ppbv).

Different pore size nylon membranes were studied. The membranes with and without AgNPs were also characterized by Raman spectroscopy. The spectra are

shown in **Figure 4.2.5**. In the case of glass filter a strong fluorescence was observed and for cellulose no characteristic Raman peaks were observed.

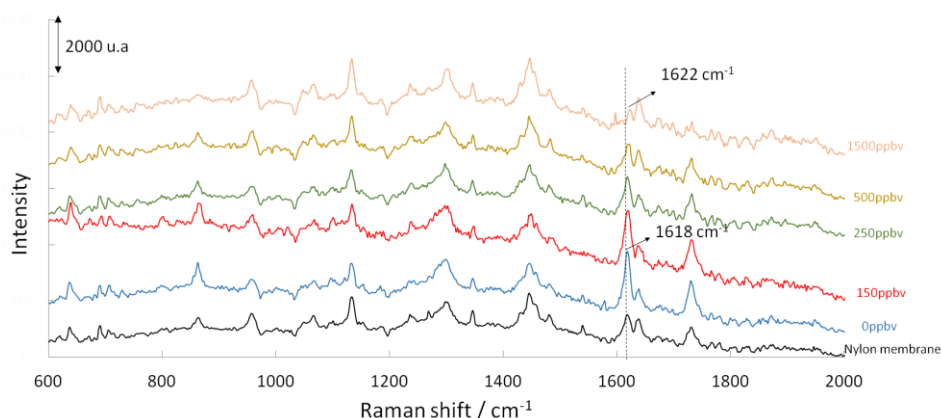


**Figure 4.2.5** Raman spectra of the nylon and AgNPs-nylon membranes after being exposed for 10 min to different  $H_2S$  concentrations (0, 150, 250, 500, 1500 ppbv).

For nylon membrane the Raman characteristic band is at  $1618\text{ cm}^{-1}$ , which corresponded to amide band that increases after AgNPs retention (**Figure 4.2.5**). Changes on the amide band of nylon nanofibers after AgNPs retention were indicative of the AgNPs bonded to nylon [127]. It was deduced that the retention compared with the other materials was improved due to the electropositive and electronegative charges of nylon and citrate capped AgNPs, respectively. On the other hand, Morales-Luckie et al. [309] also demonstrated the certainty of this electrostatic interaction between AgNPs and nylon. Nevertheless, we observed that some silver nanoparticles were deposited also in cellulose and glass fiber membranes, indicating that there was also a physical adsorption of the nanoparticles on the different substrates tested (**Figure 4.2.3**). Probably both types of retentions (physical and chemisorption) are involved in this case. Membrane responses were studied with the presence of sulfide compounds. In **Figures 4.2.3** and **4.2.4** the response can be assessed by visual inspection that the membranes change from yellow to orange/brown and the characteristic plasmon band at about 400-420 nm shifts to a higher wavelength ( $\sim 480\text{ nm}$ ) in the presence of volatile hydrogen sulphide. These changes were distinguishable and more significant through the use of nylon membranes and were clearly observed by diffuse reflectance spectrometry at concentrations of 150 and 500 ppbv in

comparison to those obtained in cellulose and fiberglass. By Raman spectrometry it was observed that in presence of  $H_2S$  the band of the C=O of the amide shift slightly to higher wavenumber from 1618 to 1622  $cm^{-1}$  (**Figure 4.2.5**). Sulphide groups on the AgNPs surface could change its electronegativity and this should affect the electrostatic interaction between AgNPs and the amide groups of the nylon membrane. In the next step, the size of the AgNPs was optimized. The AgNPs sizes tested were: (A) 10 nm, (B) 20 nm, and (C) 40 nm, which have a maximum plasmon band between 380–405 nm, 390–410 nm, and 405–425 nm, respectively. **Figure 4.2.6** shows the normalized spectra of the response of AgNPs in the presence of sulfides in solution and in the membrane. Using AgNPs of 20 nm, a linear relationship was found between the normalized absorbance at fixed wavelength and amounts of sulfide as low as 650  $\mu g$  (150 ppbv) in air (see **Figure 4.2.6**).

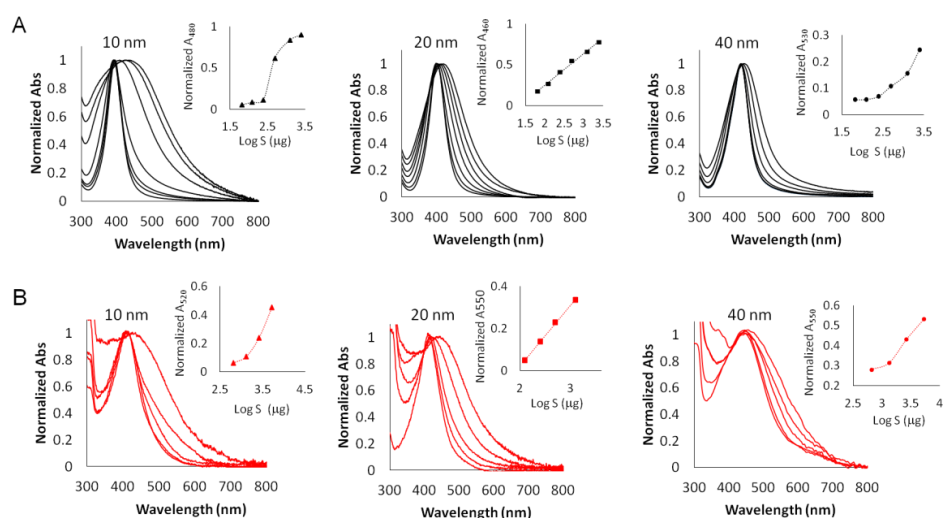


**Figure 4.2.6** Study of the response of the different sizes of AgNPs 10, 20, and 40 nm to sulfide (A) in solution and (B) using the membranes in air. The signal for several dispersions of AgNPs was registered after 20 s of the addition of aliquots of  $Na_2S$  to resulting amounts from 65 to 4925  $\mu g$  of sulfide. The membrane analytical responses were registered by diffuse reflectance after being exposed to  $H_2S$  for 10 min at amounts from 650 to 5251  $\mu g$  of sulfide.

Whereas, the sensitivities for 10 and 40 nm AgNPs nylon membranes were not sufficient to discriminate between amounts lower than 2500  $\mu g$  in air (500 ppbv).

Consequently, in subsequent experiments commercial citrate capped AgNPs of 20 nm (core size) were used.

Spectra without normalization for a dispersion of AgNPs of 20 nm is shown in **Figure 4.2.7**. The plasmon band broad at 550 nm, shift from 400 to 420 and decreased the maximum of absorbance from 0.9 to 0.3 as increased the amount of sulfide in both in solution and on the coated membrane.

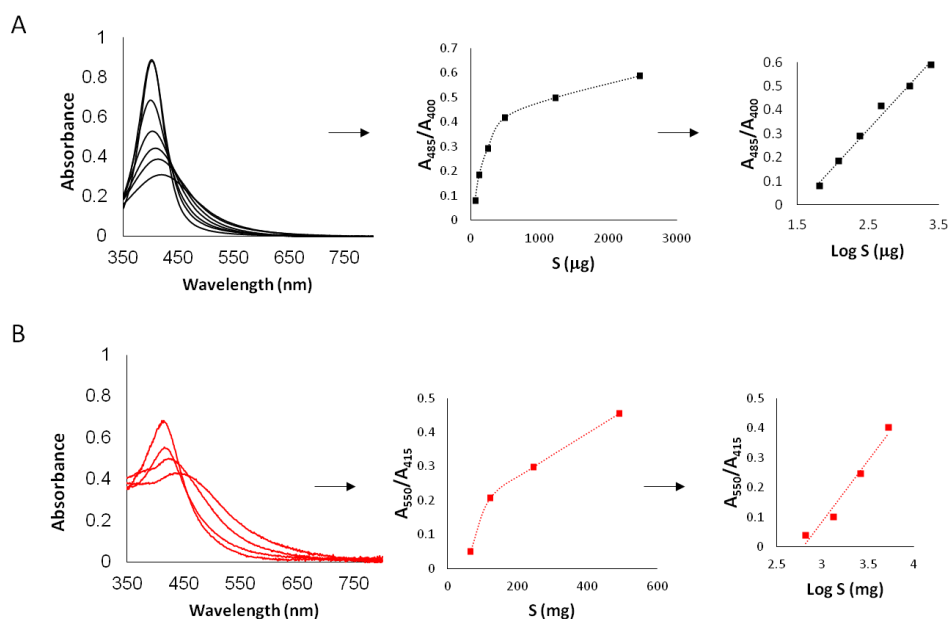


**Figure 4.2.7** Spectra registered for AgNPs of 20 nm with different amounts of sulfide and the dependence between them for sulfide quantification **(A)** in solution after the addition of  $\text{Na}_2\text{S}$  from 65 to 4925  $\mu\text{g}$  of sulfide and **(B)** coated on the membrane after being exposed to  $\text{H}_2\text{S}$  for 10 min at amounts from 650 to 5251  $\mu\text{g}$  to sulfide.

We also established a linear relationship by the quotient of absorbance at 550 nm and the maximum absorbance at 400 nm over the logarithm of the amount of sulfide.

On the other hand, the results obtained by SEM have an important role in the characterization, as well as for the solution, also for the sensor. **Figure 4.2.8A** shows the SEM images of the AgNPs dispersion before and after addition of the sulfide. On the other hand, the plasmonic membranes were observed before and after being exposed to  $\text{H}_2\text{S}$  by SEM (**Figure 4.2.8B**).

Based on the SEM images we observed silver nanoparticles had the same behaviour in solution and in membrane when sulphide is added. As an

explanation, some studies reported that the formation of  $\text{Ag}_2\text{S}$  nanostructures/bridges in presence of  $\text{H}_2\text{S}$  could also produce the destabilization of the monodisperse AgNP dispersion and promote their aggregation, besides to the influence of the cations in the reaction media [310].

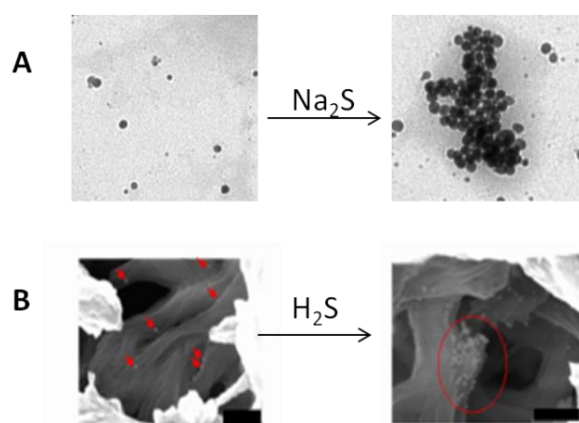


**Figure 4.2.8** Study of the behavior of AgNPs in presence of sulfide. **(A)** TEM images of a dispersion of AgNPs before and after addition of sulfide (250 ppb) in water, scale bar: 400 nm. **(B)** SEM images of the AgNP nylon membranes before and after being exposed to sulfide (250 ppbv), scale bar: 50 nm.

#### Quantification of generated $\text{H}_2\text{S}$ in atmospheres

The formation of the methylene blue was chosen as colorimetric reaction because it is widely used for the determination of dissolved sulphide in water since its introduction by Fischer in 1883 [300]. This method involves the reaction of this compound with N,N-Dimethyl-p-phenylene-diamine in presence of Fe(III) ions, giving rise to a characteristic blue coloration with a maximum at 670 nm, corresponding to the production of the heterocyclic thiazine dye. The amount of the generated  $\text{H}_2\text{S}$  from  $\text{Na}_2\text{S}$  and phosphoric acid was confirmed measuring the content of sulfide in the remaining solution after the generation of  $\text{H}_2\text{S}$  (for 10 min) into 2 L static dilution flasks and compared with a blank and a sulphide standard of 0.2 ppm. The remained solution contained less than 1% of the standard content obtained by mixing of 100  $\mu\text{L}$  of 2 0.5 ppm of standard (expressed as sulphide) and 100  $\mu\text{L}$  of phosphoric acid into the dilution flask. An example of the registers obtained is given in **Figure 4.2.9**.

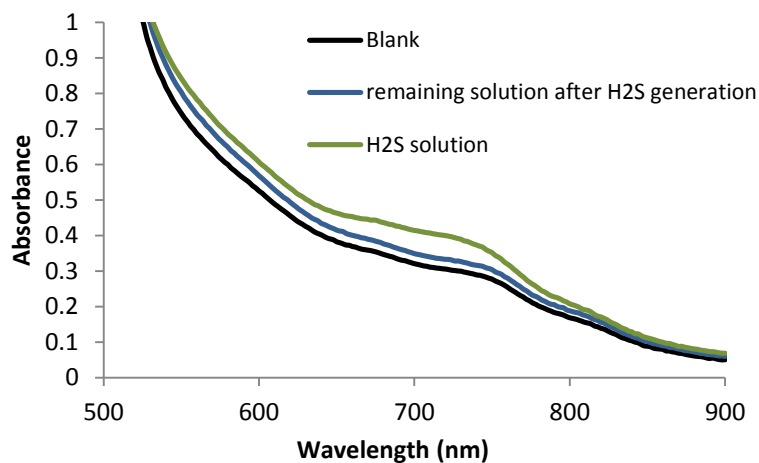


**Figure 4.2.9** Quantification of H<sub>2</sub>S volatilization in atmospheres by the methylene blue method. In green the signal corresponding to the aqueous mixture containing 0.2 ppm of sulphide, in blue its absorbance after its volatilization for 10 min in a static dilution flask of 2 L and in black a mixture without sulphide as a blank.

### Humidity

The influence of the humidity in AgNPs sensor response was also studied and percentages between 20 and 100% were tested. **Figure 4.2.10** shows that similar response was obtained from 50% humidity at conditions of room temperature (between 20–25 °C). The sensitivity decreased for the lower humidity assayed (20%). This work established the figures of merit provided by the sensor for atmospheres between 50–96% of humidity, but the sensor can work in other conditions by providing other different figures of merit.

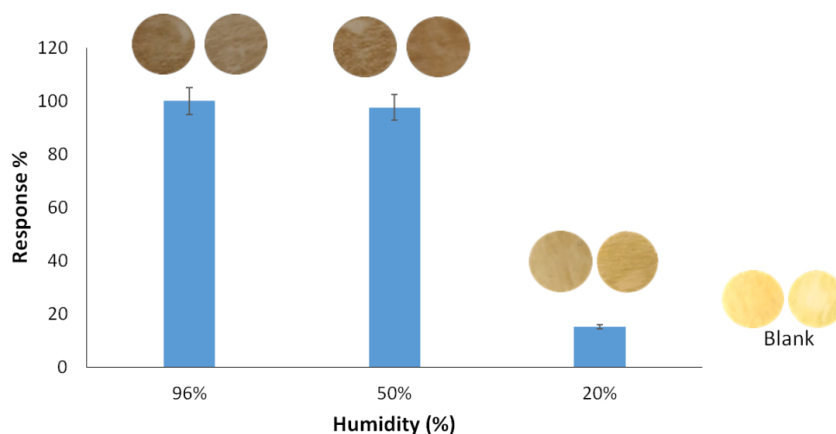


**Figure 4.2.10** Percentage of the response of the sensor and colour of the sensors obtained at different humidity 96%, 50% and 20% compared with the blank.

#### Glycerol effect in the sensor response

The membran responses were enhanced by coating them with glycerol, after being exposed to volatile sulphide compounds. The response increases two times in absorbance (**Figure 4.2.11**) after being coated with glycerol; the colour change could be related with its dielectric constant (37.4 instead of 78.5 for water). Besides that, the glycerol protected the surface membrane making possible to carry out the measurements hours/days after having obtained the response (for more information about glycerol effect, see stability of the plasmonic membranes).

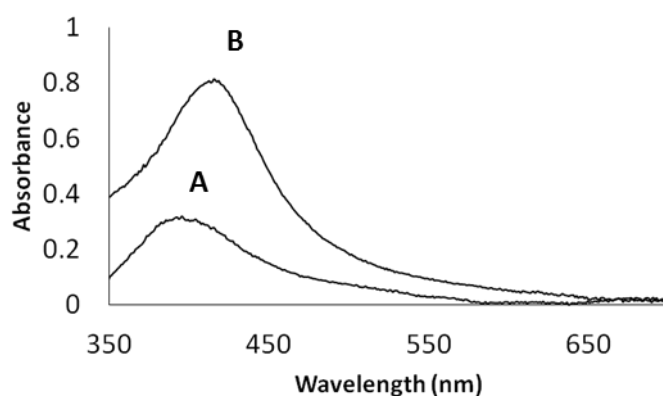


**Figure 4.2.11:** Sensors measured by diffuse reflectance before (A) and after (B) being coated with glycerol.



### **Influence of the commercial AgNPs batches in sensitivity and selectivity**

To study the influence of different commercial batches on the main analytical properties of the sensor such as the sensitivity or the concentration linear range, three different batches of citrate capped AgNPs were used for the preparation of plasmonic membranes. The slopes obtained for batches 1, 2 and 3 at H<sub>2</sub>S concentrations of 250, 500, 1000 and 1500 ppbv (n=3) were: 0.298±0.009 ppmv, 0.311±0.004 ppmv, 0.320 ± 0.003 ppmv, respectively. Therefore, we can conclude that non-significant differences were observed on the membrane responses prepared with different AgNPs batches.

The selectivity of the membrane was tested against possible volatile organic compounds that can be presented in breath samples and can act as interferences for halitosis estimation such as ethanol, acetone and ammonia (see **Figure 4.2.12**). It has been reported that these compounds can be found at high concentrations in breath and are related to several diseases. Ethanol at higher concentration of 20 ppbv is indicative of diabetes and hyperglycaemia, acetone between 300 - 500 ppbv is associated to lung cancer and 1000 - 4000 ppbv of ammonia is related to renal failure. Also, methanol, propanol, formaldehyde and toluene were associated to lung cancer at concentrations >100 ppbv and 10 ppbv for toluene [311]. The membranes were exposed to these compounds at 5000 ppbv and any change in color or shift of the plasmon band was observed.

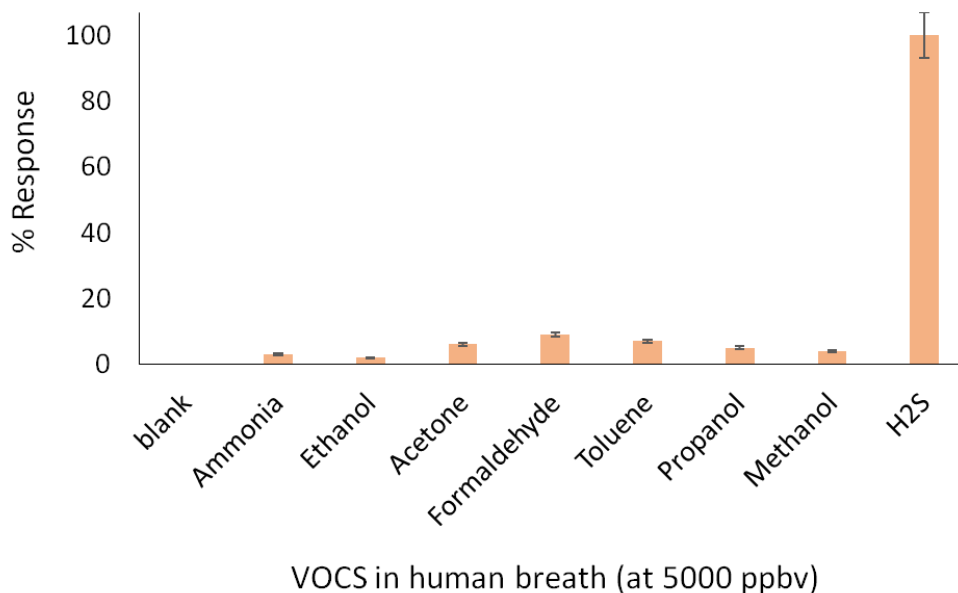


**Figure 4.2.12** Selectivity of the AgNPs plasmonic membrane against other VOCs in human breath of interest at concentration of 5000 ppbv.

#### AgNPs sensor stability

For the study of stability of the membranes they were stored in different conditions and for different times after which they were tested. **Figure 4.2.13** shows the results obtained under different temperature (4-25°C) and with different storage times. The membranes were stable for 30 days at 4 °C (at 35 days the sensor provided the color due to AgNP aggregation, and then it was damaged) while at room temperature the AgNPs aggregate in 1-2 week. In addition, coated membranes with glycerol were also tested in order to evaluate its effect on the plasmonic membrane stability. There are several works on the influence of glycerol on the stability of nanoparticles [312–314]. The sensors covered with glycerol before being used were washed with water, due to the stability that glycerol provides. Based on the results obtained we reported an evidence in which glycerol can be used to preserve AgNPs before being exposed to a sulfur atmosphere. They showed to be stable for at least 3 months in dark at 4 °C (**Figure 4.2.13**) and RSD % of the responses were in all cases  $\leq 10\%$ . If glycerol was used as preservative, previous the use of the membrane, it should be cleaned with water. In summary, the glycerol acts as a protective layer to fix the AgNPs, it can stabilize the monodisperse AgNPs and the membrane prepared today could

be used for H<sub>2</sub>S determination after 90 days at 4°C and also it can have stabilized the aggregated AgNPs obtained as a response and the membranes can be measured days/hours after their exposition to H<sub>2</sub>S.

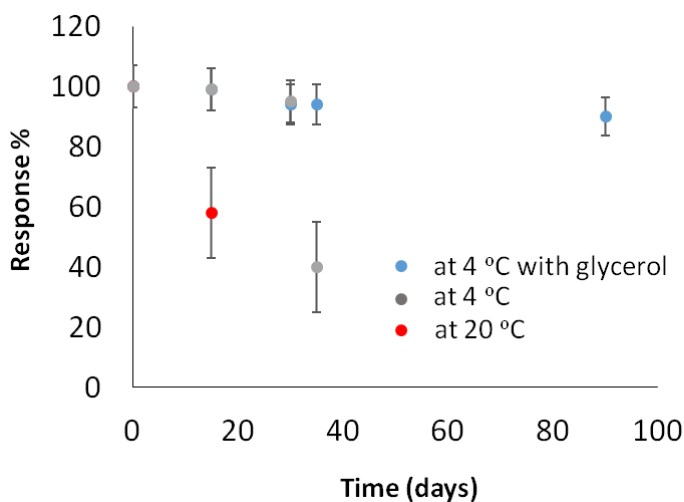


**Figure 4.2.13** Stability of the AgNPs plasmonic sensors over time. Comparison of the responses obtained for H<sub>2</sub>S at concentration of 250 ppbv using three membranes prepared the same day and the response of three membranes after several days of storage in different conditions; at 20° C, 4 °C and in absence/presence of glycerol.

### Analytical performance

The calibration curve was obtained from the ratio A<sub>550</sub> / A<sub>415</sub> against logS (ppbv) or by the signals of the normalized spectra at 550nm over the concentration of sulfide (**Figure 4.2.14**). Calibration curve tests were carried out between concentrations 150-2500ppbv, with the following results  $Abs_{550}/415 = (0.313 \pm 0.008) \log S - (0.60 \pm 0.02)$ ,  $R^2 = 0.998$ ,  $n = 36$  and  $Abs_{550norm} = (0.40 \pm 0.05) 10^{-3} S_{ppbv} - (0.01 \pm 0.03)$ ,  $R^2 = 0.99$ ,  $n = 8$ . The reaction time was chosen 10 minutes, but to achieve the necessary sensitivity according to the need for the type of test, more or less time can be left. The detection limit was measured by diffuse reflectance and calculated as  $3 S_{blank}/b$ , where  $b$  is the slope of the calibration curve and  $S_{blank}$  was the standard derivation of the intercept, it was 45 ppbv.

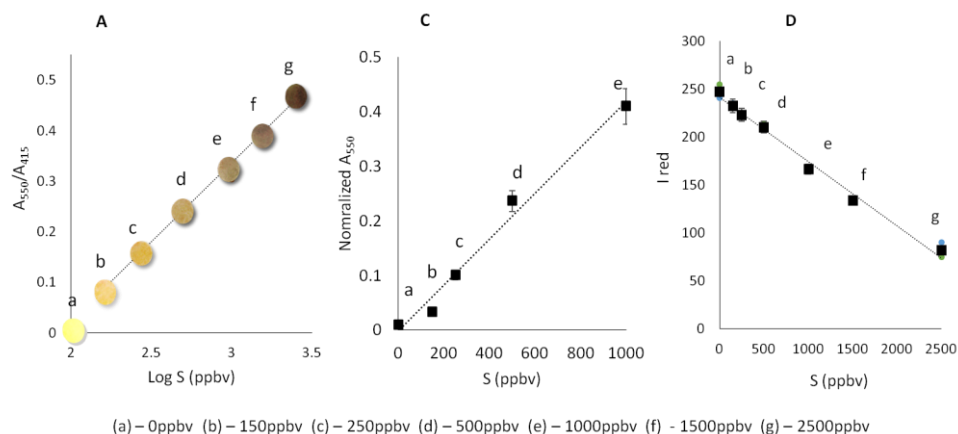


**Figure 4.2.14** Quantification of H<sub>2</sub>S using the plasmonic membrane: (A) Plotting of the  $A_{550}/A_{415}$  versus  $\text{Log } H_2S$  concentration (ppbv) with image membrane after being exposed 10 min to different concentrations of H<sub>2</sub>S. (C) Representation of the normalized spectra at 550 nm versus H<sub>2</sub>S in ppmv. (D) Representation of the RGB components (Red intensity value) versus H<sub>2</sub>S ppbv concentration.

The RSD % (intraday and interday) were 7% and 11%, respectively for  $n = 6$ . On the other hand, the calibration equation was obtained using the RGB colour model from the images obtained with a smartphone:  $I_{\text{red}} = (-0.067 \pm 0.003) S \text{ ppbv} + (241 \pm 3)$ ,  $R^2 = 0.990$  and  $n = 36$ . The spectra of the membranes can be measured in situ by using the GoSpectra dispositive coupled to a smartphone as it can be seen in **Figure 4.2.15** too.

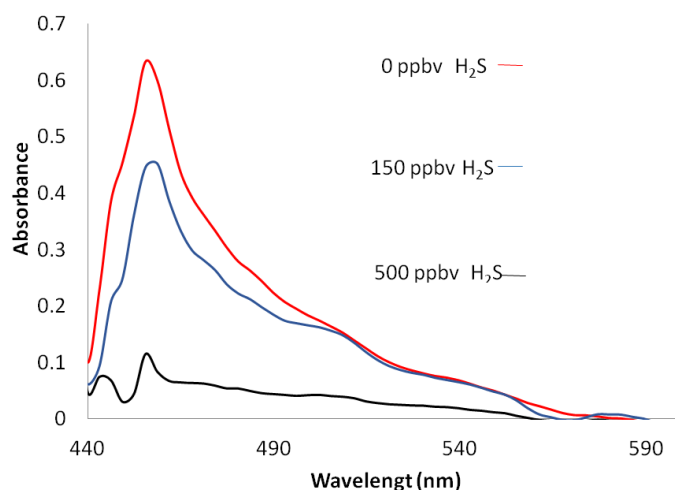


**Figure 4.2.15** Absorbance spectra by the reflection mode of the membranes using the GoSpectra accessory coupled to a smartphone iPhone 5s before and after being exposed to  $H_2S$  for 10 min.

#### AgNPs plasmonic membranes application to volatile sulfide detection

The plasmonic sensor was applied to determine volatile sulfides such as  $H_2S$  and also  $CH_3SH$  and  $(CH_3)_2S$  in atmospheres (**Figure 4.2.16**). The AgNPs plasmonic membrane for  $CH_3SH$  and  $(CH_3)_2S$  showed lower sensitivity than that achieved for  $H_2S$ . Consequently, at the levels present in breath samples, the membranes will be able to detect a halitosis problem by measuring the  $H_2S$  mainly.

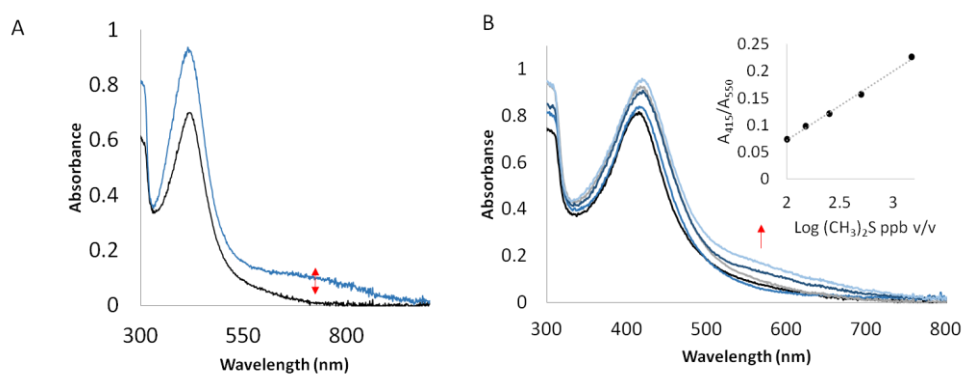


**Figure 4.2.16** Response of the plasmonic membranes to A)  $CH_3SH$  at 1000 ppb and B)  $(CH_3)_2S$  at concentration from 150, 250, 500, 1000, 1500 ppbv.

Recoveries were calculated using spiked samples. For which the breath samples of 2 healthy volunteers were enriched with H<sub>2</sub>S at different concentration levels 250, 300 and 500 ppbv. The results obtained were useful for the evaluation of recoveries (**see Table 4.2.1**).

In addition, the membrane was used to test the oral breath of 10 healthy volunteers (humidity percentages around 96 %). The concentrations of sulphur compounds found in the samples are shown in **Figure 4.2.17A**. The values obtained were below 250 ppbv, which is the lower level of sulphur levels that can be associated to periodontal and gingivitis diseases [315,316]. Finally, the concentration of sulphur compounds in breath samples of four volunteers who had intake allium vegetables (e.g. garlic) was determined. The data shown in **Figure 4.2.17B** indicated that there was an increase in sulphur concentration levels in the last case.

**Table 4.2.1** Determination of volatile sulphide in breath samples from two volunteers.

<b>Volunter 1</b>					<b>Volunter 2</b>			
<b>Diffuse reflectance</b>			<b>Digital imges</b>		<b>Diffuse reflectance</b>		<b>Digital images</b>	
<i>Spiked samples ppbv</i>	<i>Detect in breath ppbv</i>	<i>Recovery %</i>	<i>Detect in breath ppbv</i>	<i>Recovery %</i>	<i>Detect in breath ppbv</i>	<i>Recovery %</i>	<i>Detect in breath ppbv</i>	<i>Recovery %</i>
0	145	-	151	-	116	-	115	-
250	392	99	367	86	390	110	349	94
300	506	120	475	108	464	116	421	102
500	666	104	601	90	672	111	637	104

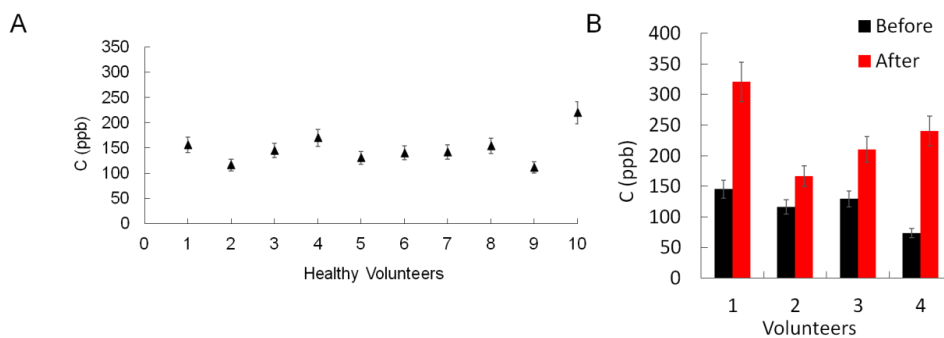


**Figure 4.2.17** Determination of volatile sulphide for A) ten volunteers ( $n=3$ ) and B) for four volunteers before and after food intake rich in allium vegetables (garlic).

As a proof of concept, we tested the collection of samples in small plastic bags to prove applicability of the method for sulfide quantification under different conditions of sampling. For the quantification, the air standards were generated into the static dilution bottles and transferred with a syringe into the bags containing the sensor (**Figure 4.2.18**). Exhaled air was taken by volunteers into plastic bags (250 mL) with AgNPs sensor, and after 10 min the membrane was removed and analyzed by diffuse reflectance spectrometry. The normalized absorbances at 550 nm obtained were interpolated on the calibration curve;  $\text{Abs norm. 550} = (0.35 \pm 0.03) [S, \text{ppmv}] + (0.111 \pm 0.015)$ ,  $R^2 = 0.99$ , ( $n = 3$ ) (**Figure 4.2.89B**). The sulfide concentration found was 110 ppbv (**Figure 4.2.18B in red**), which is a value below of 250 ppbv associated to periodontal and gingivitis diseases.



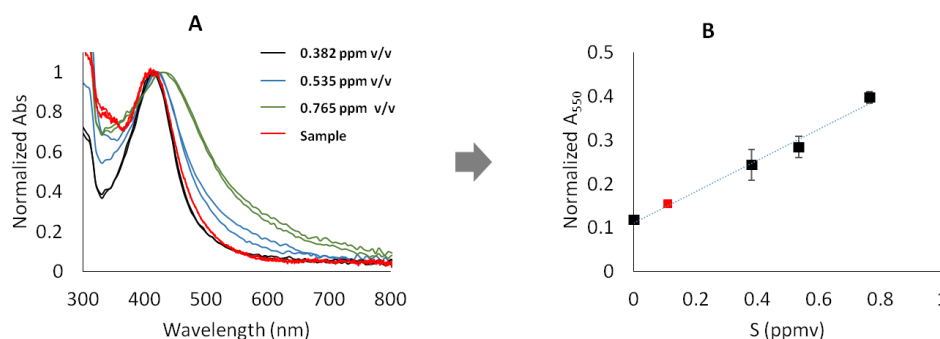


**Figure 4.2.18** Normalized absorbance spectra obtained for sulfide air standards generated into the static volumetric flask and transferred to the bags and normalized spectra of a breath sample (A). Normalized absorbance at 550 nm was over the concentration of sulfide for standards and a sample (B).

## Conclusions

In the present study we have proved that it is possible to obtain a solid-phase colorimetric sensor based on AgNPs retention on a nylon membrane. The mechanism of retention and aggregation of AgNPs has been confirmed by using UV-vis spectra, TEM, SEM, and Raman spectroscopy. The plasmonic membranes changed from yellow to orange/brown in the presence of hydrogen sulfide-like compounds at ppbv levels (LOD of 45 ppbv, 2L). It was observed that to improve sensitivity it can be achieved by leaving more sampling time. The particle size of the AgNPs affects the sensitivity and the concentration range of volatile sulfide compounds detection. The membranes were applied for the determination of volatile sulfide compounds in the exhaled breath of 10 healthy human volunteers.  $H_2S$  levels detected in exhaled human breath could serve as breath markers for some diseases such as halitosis. Their values were in the range of 70–210 ppbv, below the limit of periodontitis or gingivitis diagnostic (250 ppbv). A proof of concept employing a 250 mL of sample for testing halitosis was also carried out.

Contrary to existing methods in literature the proposed plasmonic sensor is accessible to the general population as well in economic terms due to its easy use. It should be noted that the preparation and use of the plasmonic sensor is free of toxic reagents, and finally this sensor is non-invasive and does not destroy the samples. They are stable in normal atmosphere and can be used directly to

determine selectively volatile sulfur compounds in 10 min. Therefore, the reported plasmonic membrane has proven as a new sustainable strategy with multiple possible applications for different types of matrices. In this sense, the following studies intend to demonstrate its validity also for cellular clinical trials. Finally, compared to the others methods, this strategy proposed is simple, stable, easy to use, affordable and has a competitive economic cost, mostly complying with the principles of sustainable analytical chemistry.

#### **4.2.2 Determination H<sub>2</sub>S in live cardiac cells samples using AgNPs multisensor sheet**

In the present work, a solid plasmonic colorimetric multisensory sheet adapted to a 96-well microplate has been manufactured to detect in vitro hydrogen sulfide (H<sub>2</sub>S) generated by biological samples. Such an approach will allow for low-cost, multi-sample testing. In this context and due to the interest of hydrogen sulfide emission by cardiac cells, we have developed and optimized a multisensory plate for in situ multi - analysis to determine the H<sub>2</sub>S emitted by cardiac cells under different clinical conditions (normoxia, ischemia / reperfusion) carried out in collaboration with the research group RETRACAR of the Hospital La Fe (Valencia, Spain).

#### **Optimization of the solid- phase colorimetric plasmonic sensor**

According to previous section, the AgNPs retained in the nylon membrane are aggregated in the presence of sulfides [317]. These studies corresponded to the development of an individual sensor of dimensions (diameter = 0.5cm) with 200µl citrate capped commercial AgNPs 20 nm retained. In order to scale the sensor to a 96-well multiwell system, individual sensors that individually matched to each of the wells can be used. However, in order to streamline and automate the procedure, the immobilization of the AgNPs on Nylon surfaces of size (7.5 x 10 cm) has been optimized. These sheets significantly improved the adaptation to the surface of the 96-well plate (**Figure 3.9 A in seccion 3.3.2**).

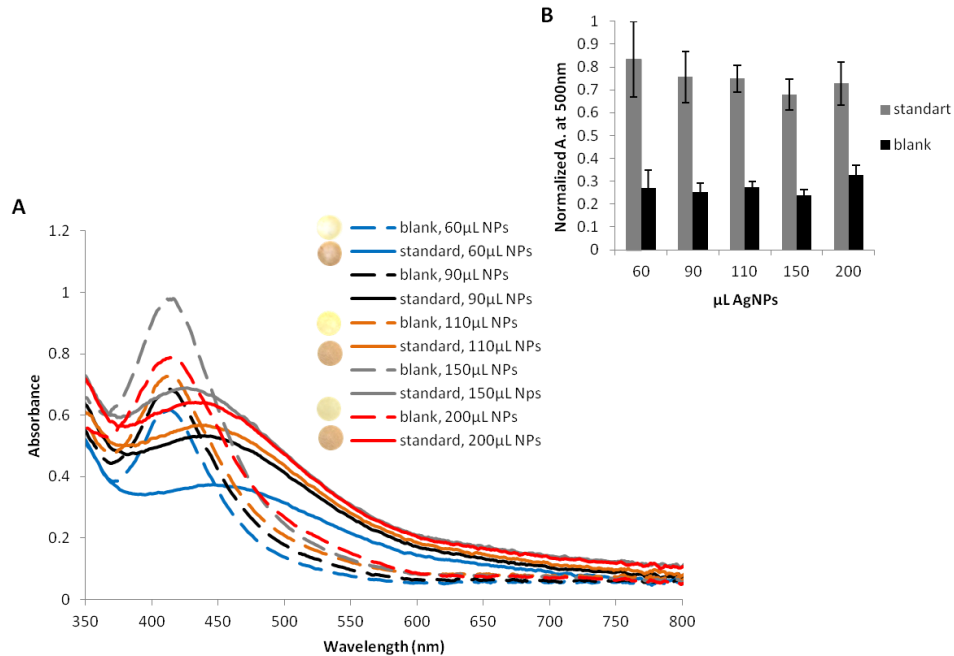


**Figure 4.2.19 A)** Plasmonic bands of the blanks (dashed line), and displacement of the plasmonic band in the presence of  $H_2S$  (2 mg/L) (continuous line) in both cases the test time was 2 hours. **Figure 4.2.19 B)** Analytical response of standard (gray color) and blank (black color) expressed with absorbance normalized at 500nm.

The sensor sensitivity and stability were studied by testing different volumes of AgNPs retained on the nylon plate. AgNPs tested volumes ranged from 60µl to 200µL. As we can see in **Figure 4.2.19 A**, the sensor with 60 µl of AgNPs lacked homogeneity, which led to lower precision (**Figure 4.19 B**), however, the analytical response was greater. A similar behaviour was observed in the case of 90 µL. The sensor with 200µl was also ruled out due to the instability observed during the test. As can be seen in **Figure 4.2.19 B** in the case of the blank, the plasmon band decreased due to possible agglomerations between them [318,319]. For future tests, the sensor with 110 µL ANPs was chosen, which gave a better response compared to sensors with 150 µL and 200 µL AgNPs and also good precision compared to 60 µL and 90 µL. Subsequently, the study of the influence of glycerol on the enhancement of the sensor response was performed (**Figure 4.2.20 A and B**). The precision study of the blank multisensory sheet with and without glycerol was carried out by measuring the diffuse reflectance of a plate with 14 and 24

sensors respectively. According to the results % RSD of the blank sensor was lower than 5%.

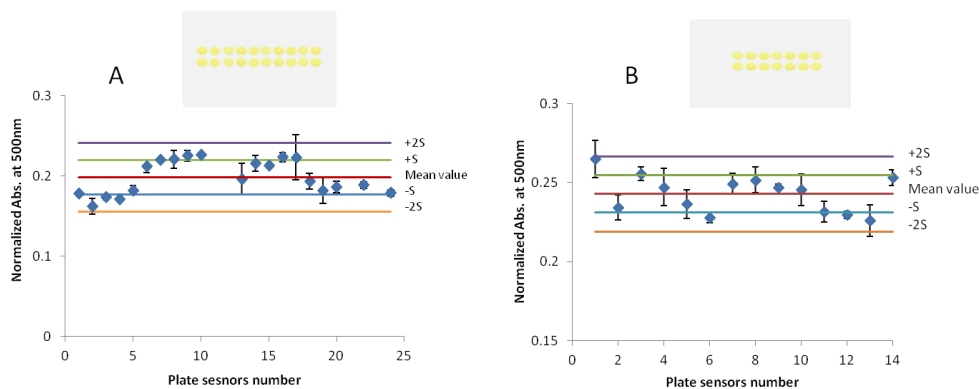


**Figure 4.2.20** Reproducibility of sensor along with the images of the distribution of the AgNPs sensors in the Nylon sheet plate **A)** Without glycerol. **B)** With glycerol.

The precision of the multisensory sheet preparation was evaluated by measuring the normalized absorbance at 500 nm by the diffuse reflectance of 3 multisensory sheets (with 14 sensors each plate) in the same conditions and the value of RSD% was lower than 7%. On the other hand, the results obtained showed improvement in the response of the membrane when coating it with glycerol after being exposed to the sulphur gases generated in the head spacing of the micro well cell, this agrees with the results obtained previously with the individual sensor (**Figure 4.2.20**). All tested sensors were prepared according to the Section 3.3.2.

**Figure 4.2.21** shows the images of the plasmonic sensors along with normalized spectra after exposition to  $\text{H}_2\text{S}$  from 0-25  $\mu\text{M}$ . For quantitative analysis the sensors after being exposed to the  $\text{H}_2\text{S}$  were measured by means of diffuse reflectance, however a semi-quantitative analysis can be performed with the naked eye.

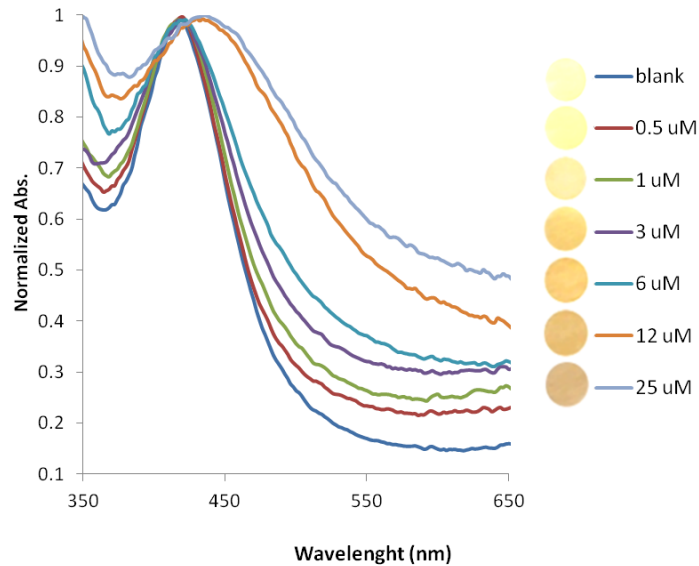


**Figure 4.2.21** Normalized Vis spectra of different  $H_2S$  concentration detected by AgNPs multisensor sheet.

The calibration equation, employing diffuse reflectance, was obtained by representing the normalized absorbance at 500nm vs. the concentration of hydrogen sulphide. **Table 4.2.2** shows the analytical parameters like linear range, sensitivity, precision and the limit of detection (LOD). They were calculated for the  $H_2S$  response by using diffuse reflectance under incubator conditions (temperature  $-37^\circ C$ , humidity- 95%) for 8 hours. The LOD was calculated as  $3S_{\text{blank}}/b$ , where  $b$  is the slope of the calibration curve and  $S_{\text{blank}}$  is the standard deviation of the absorbance of 10 blanks and was  $0.13\mu M$ . The precision of the analysis was also evaluated. The intraday precision RSD (%) was evaluated at a concentration of  $8\mu M$ . The interday precision was obtained comparing the response of the sensors prepared in three different days under identical condition, using the same analyte concentration as in the intraday test. The interday and intraday precision values were 4% and 8% respectively. RSD (%) values indicated that the proposed multisensory sheet is a precise device for practical applications.

**Table 4.2.2** Figures of merit obtained using the AgNPs sensor for H<sub>2</sub>S detection under following condition: temperature at 37°C with 95% atmosphere humidity for 8 hours.

Analyte	Trial time (hours)	Linearity (y=a+bx)			Linear Interval (μM)	RSD% (n=3)		LOD μM
		a±s <sub>a</sub>	b±s <sub>b</sub>	R <sup>2</sup>		intraday	interday	
H <sub>2</sub> S	8	-0.0051± 0.0016	0.0410± 0.0004	0.99	0.34 - 8	4	8	0.13

### Cellular sample analysis

In summary, these solid-phase plasmonic colorimetric sensor sheets were prepared using citrate capped AgNPs of 20 nm immobilized on Nylon sheet of pore sizes 0.22μm and following the optimal conditions mentioned above they were applied to detect H<sub>2</sub>S in biological samples such as cells. Firstly, the selectivity study of the method was carried out, which indicated that the culture itself does not produce any type of interference in the sensor response, so its response is attributable to the emissions by the cells. The tests on real samples were used using human AC-10 cardiomyocytes at a temperature of 37°C and in an atmosphere of 95% humidity and 20% O<sub>2</sub>, so previously necessary tests have been carried out to ensure that the correct operation of the sensor is carried out. On the other hand, the AC-10 culture with a density of 100,000 cells per well was optimized as the appropriate condition for carrying out the rest of the experiments. The stability of the sensor to the standard cell culture (DMEM with 3 mg/mL glucose, 2.5 mM L-glutamine and 10% fetal bovine serum) was also studied. Cell culture assays were performed in the 96-well plates (**Figure 4.2.22**).

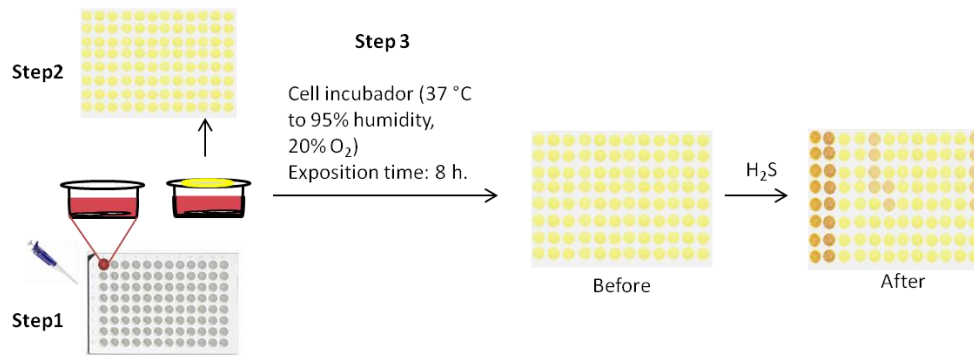


**Figure 4.2.22** Cells or standard assays steps and multisensor sheet image before and after exposure to different H<sub>2</sub>S concentrations.

Normoxia, Ischemia-Reperfusion (**I/R**) assays in human cardiomyocytes cultured *in vitro* was carried out by the Retracar group (ISLa Fe), in which the AgNPs device was used to measure the H<sub>2</sub>S levels produced after cell damage. **Figure 4.2.23 A** shows the Normoxia y I/R process where 100,000 AC-10s were seeded per well in a 96-well multiwell plate. Once the cells adhered to the surface of the well, the standard culture medium (DMEM with 3 mg / ml glucose, 2.5 mM L-glutamine and 10% fetal bovine serum) was replaced by means of ischemia (DMEM with 0 mg / ml of glucose, 4 mM L-glutamine and 0% fetal bovine serum) and the plate was transferred to a low O<sub>2</sub> atmosphere (1%) and the detection device was incorporated into the well. After 7 hours of ischemia, the culture medium was changed to a standard culture medium and the normoxia atmosphere was recovered (20% O<sub>2</sub>, 3 mg/ml glucose). Cells were cultured under these conditions (reperfusion) for 1 hour after which the device was removed for further reading. The results obtained indicate that cardiomyocytes subjected to ischemia-reperfusion produce sulfide molecules, detectable by the multisensory. As seen in **Figure 4.2.23 B**, O<sub>2</sub> deprivation causes increased levels of sulfide secreted by cardiomyocytes. The results demonstrated that the 96-well multiwell plate, I/R assay and the sensor were successfully optimized to achieve the target.

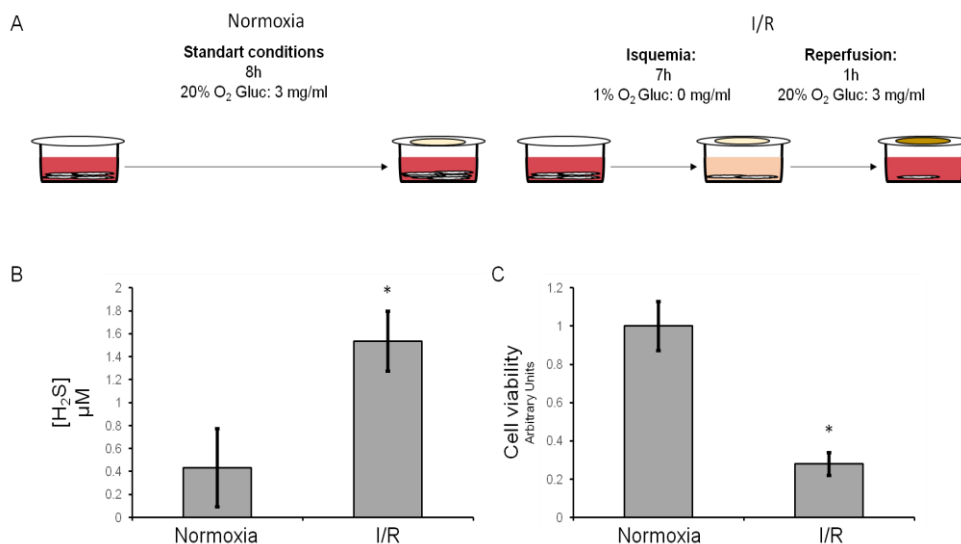


**Figure 4.2.23** Ischemia-reperfusion model in AC10 analyzed using AgNps multisensors sheets. **A)** Experimental design used. **B)** Quantification of H<sub>2</sub>S values produced by AC10 under different culture conditions. The bars represent the mean and standard deviation of 3 independent experiments. **C)** Cell viability of AC10 under different culture conditions. The bars represent the mean and standard deviation of 3 independent experiments. \* <math>p < .05</math> t-student paired test.

### Characterization of the multisensory sheet by the hexagon tool

A quantitative evaluation of the multisensory performance has been carried out using the hexagon tool proposed by our group [32,33] in order to demonstrate its benefits in reference to sustainable analytical chemistry. By means of a 0-4 score scale summarized in a hexagon pictogram, the analytical performance, associated risks, sustainability, environmental impact and annual economic cost of the proposed multisensory sheet have been evaluated. In this paper, the multisensory sheet was compared with recent analytical methods for detecting H<sub>2</sub>S in cell matrices found in the scientific literature. The results obtained are represented in **Figure 4.2.24**. Initially, a AgNPs based plasmonic sensor was proposed by our research group [317] for the in situ detection of H<sub>2</sub>S (see **Figure 4.2.24a**). Taking into account the basis of this solid-phase colorimetric sensor, the present multisensory sheet has been suggested as an improved alternative of the analytical characteristics of the single Ag NPs sensor, as indicated in **Figure 4.2.24b**. When comparing both hexagon pictograms, it can be observed that the



figures of merit FM-1 of the multisensory sheet show a lower penalization score due to the possibility to perform a quicker multianalysis (96 versus a single sensor) and the enhancement of the limit of detection (0.13  $\mu\text{M}$  versus 5  $\mu\text{M}$  for individual sensor).

The characteristics of the proposed multisensory sheet were compared to the sensor devices proposed in the literature, that is, a nano metal-organic fluorescence probe [320], a Ag nanoplate-coated paper assay [321] and a fluorescent chemosensor [322]. The results of the comparative study within the hexagon tool are shown in **Figure 4.2.24 c, d and e**. Mainly, it was observed that the proposed multisensory sheet showed potential analytical advantages since it is quicker to prepare (3 min.) and offers 96 simultaneous analyses without sample treatment. It was also easily handled and portable. All these features were missing in the other sensor devices, leading to a higher penalization score. In addition to this, the associated risks considered when using reagents and solvents by the sensor devices in **Figure 4.2.24 c, d and e** were noticeably high, which makes the multisensory sheet an optimal choice. Regarding sustainability, the nano metal-organic probe [320] and the multisensory sheet were the better options when considering the environmental impact due to the low carbon footprint estimation and the reduced amount of generated wastes in comparison to the other sensor devices in **Figure 4.2.24 d and e**. Finally, the annual economic cost associated with the analytical procedures was calculated taking into account the criteria indicated in the previous paper [33]. The instrumentation cost for absorbance measurement of the plasmonic band and the lack of additional reagents needed within the multisensory sheet suggested this colorimetric sensor was a low cost option that could be a potential candidate for  $\text{H}_2\text{S}$  in situ detection.

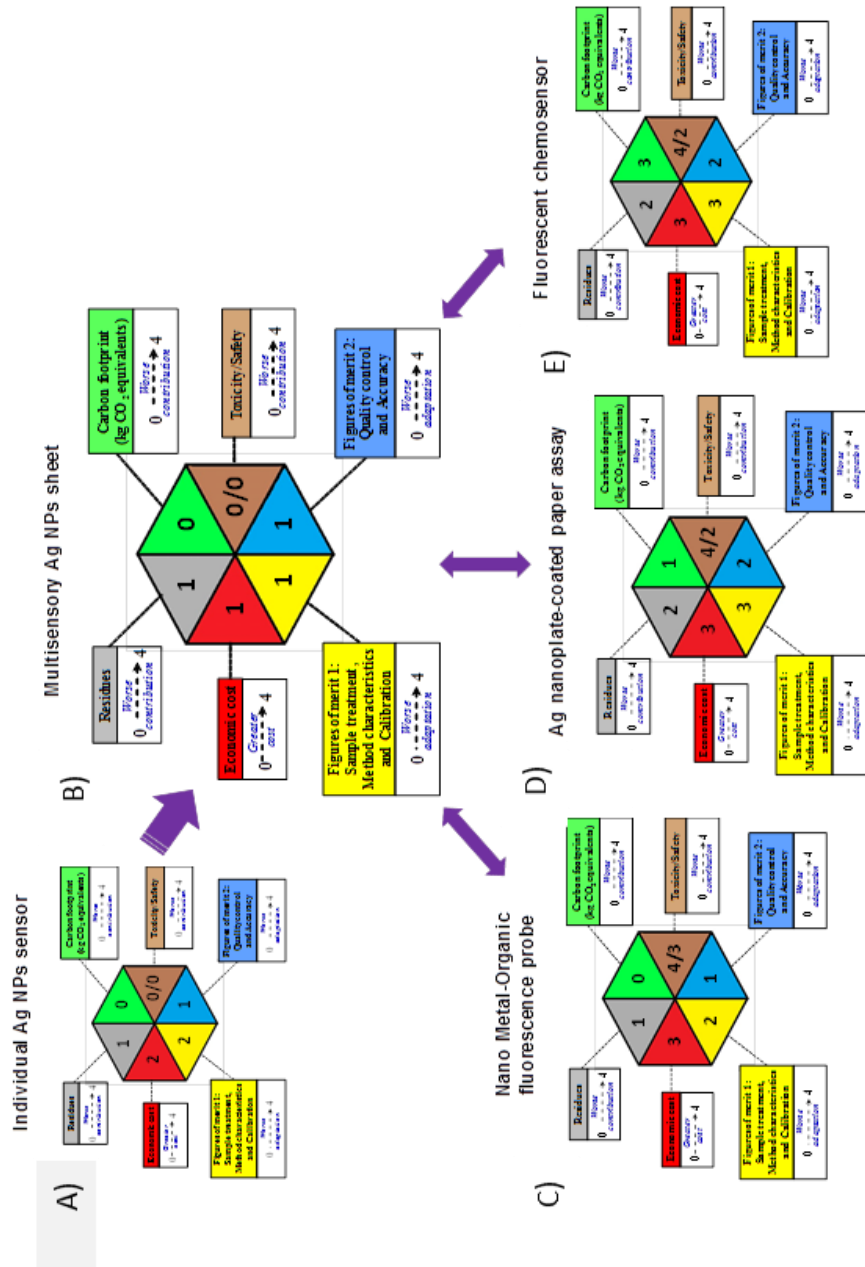


**Figure 4.2.24** Hexagon pictograms of several H<sub>2</sub>S detection using different analytical sensors: **A)** nylon-supported AgNPs plasmonic assay, **B)** 96-well nylon-supported AgNPs multisensory sheet, **C)** nano metal-organic fluorescence probe, **D)** Ag nanoplate-coated paper assay and **E)** fluorescent chemosensor.

## Conclusions

In the present study we have developed a simple method to prepare a solid-phase colorimetric multisensor (up to 96 devices) for detection of H<sub>2</sub>S in biological samples by in-vitro analysis. This approach is based on the retention of AgNPs in a nylon plate, adaptable to 96 microwells, which allows the performance of multi-analytes. Aside from simplicity in fabrication, it is also quick to prepare, and the manufacturing cost is very low. The sensor plate is prepared in 3 min, achieving in such a short time a plate of 96 silver nanoparticle sensors, for a multi-analysis or for several individual analytes. Additionally, an overall quantitative evaluation of the analytical performance of the AgNPs multisensory sheet by means of the hexagon tool shows that it offers advantages such as high sensibility, better sustainability and lower economic cost than other recent analytical methods found in the literature. According to the results obtained, it can be concluded that the developed approach is adequate for in-situ multi analysis monitoring of H<sub>2</sub>S in cardiomyocytes, is energy-efficient, it does not require sample pre-treatment, it is portable, rapid and easily handled by non-specialized personal and offers the advantage of simultaneous analysis with high sensibility for determination of hydrogen sulphide in biological samples such as cells, and also applicable for other types of matrices such as plasma or saliva. Those characteristics contributed to sustainable analytical chemistry.

### **4.2.3 Fast Blue B functionalized silica-polymer composite to evaluate 3,5-dihydroxyhydrocinnamic acid as biomarker of gluten intake**

Celiac disease is an immune-mediated systemic disorder elicited by gluten and related prolamines present in genetically susceptible individuals. The actual treatment is a strict and lifelong gluten-free diet. However, compliance with the

gluten-free diet is not always adequate and many food products contain low concentrations of gluten. As a consequence, the determination of dietary transgressions is a challenge for patients, physicians and dietitians. Alkylresorcinols (AR) have been proposed as sensitive and specific biomarkers of gluten consumption. Herein, the objective of this section was to evaluate silica – polymer composites doped with fast blue B (FB) colorimetric reagent to estimate AR in biological samples. The proposed colorimetric device was synthesized by immobilizing FB into PDMS/TEOS composite. The assay was based on the spontaneous release of FB to the solution containing AR (3,5-dihydroxyhydrocinnamic acid, DHCA, as target analytes) and the formation of the azo complex that can be measured at 520 nm. The response was evaluated with UV-vis spectroscopic measurements and a chromatographic technique (in-tube SPME-CapLC-DAD) to isolate the DHCA signal.

### **FB-doped membrane composition**

FB-doped PDMS membranes were synthesized by embedding the colorimetric reagent inside the polymeric network (PDMS). The colorimetric reaction can occur in the membrane or in the solution depending on the colorimetric reagent, target analytes, sample matrix and the polymeric composition. Taking into account the nature of the colorimetric reagent and application to aqueous matrices, the premise was that FB would be released to the solution and forms the derivative compound with the AR, which can be measured by UV-vis. In addition, this release can be favoured by adding to the polymeric matrix modifiers to improve the diffusion towards the solution. Thus, the first step was the study of the polymeric composition. In this work, FB-doped PDMS-polymeric membranes were compared with FB-doped-TEOS- and C18-PDMS membranes in order to evaluate the FB diffusion. **Figure 4.2.25A** shows the schematic representation of the procedure carried out to evaluate the membranes.

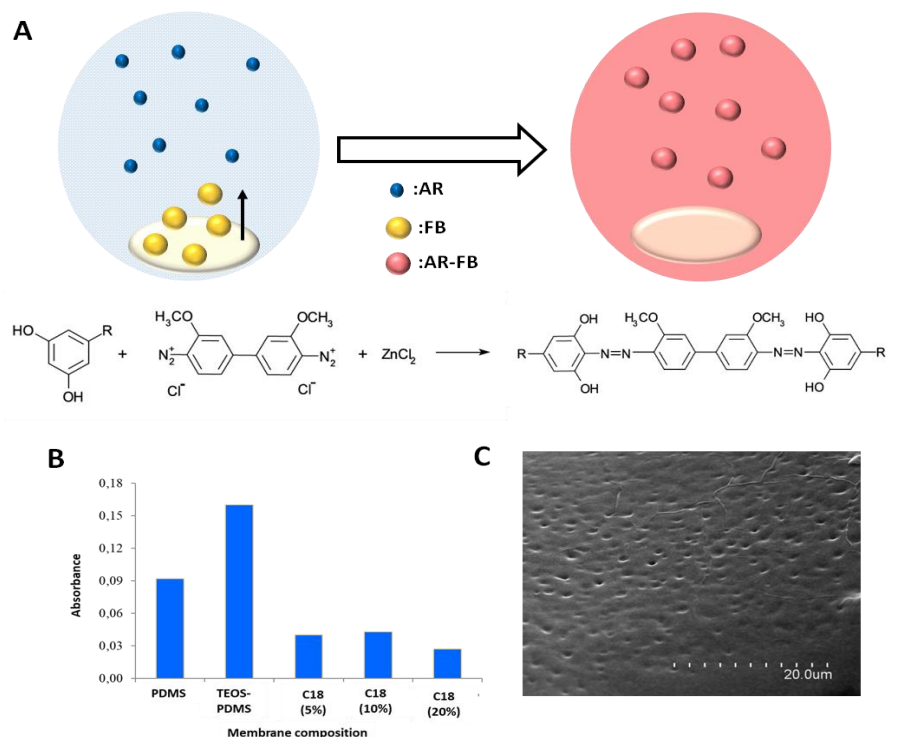


**Figure 4.2.25** A) Schematic diagram of the proposed device and chemical reaction between AR and FB reagent B) Variation of the response as a function of the membrane composition C) SEM micrographs of the FB-doped sensing membranes.

As it was expected, the polymeric membrane, in contact with the AR solution, gave rise to a coloured redish solution produced by the azocompound formed. **Figure 4.2.25 B** depicts the analytical response as a function of the composition (**Table 3.3.1**). It should be noted that the analysis time was 15 min. FB-doped PDMS membranes, released the chromogenic reagent to form the derivative. In previous work, our group has demonstrated that the reagent released can be favoured by increasing the polarity of the membrane, and this aim, TEOS was studied as matrix modifiers. As can be seen in **Figure 4.2.25 B**, the presence of TEOS in the polymeric matrix resulted in an increase of the response, due to the increase on the diffusion velocity of FB from the membrane to the solution. To prove this, C18 was used as an apolar modifier. As can be seen, the response decreased with the presence of C18 and this decrease was a function of the percentage of C18. These results indicated that FB release depended on the polarity of the polymeric matrix. TEOS improved FB release since diffusion kinetic

was facilitated. Indeed, the response obtained with the FB-doped-PDMS-TEOS membrane was comparable with the response obtained in conventional solution derivatization reaction (see **Figure 4.2.26**).

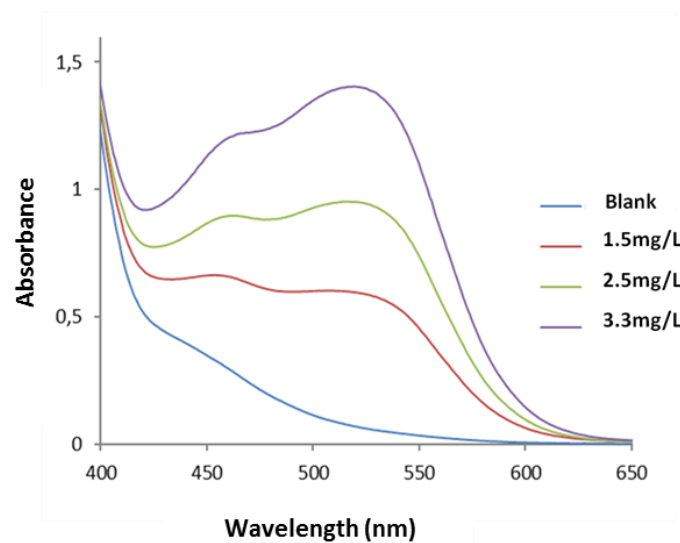


**Figure 4.2.26** Variation of the response as a function of the concentration obtained with the conventional solution derivatization reaction.

#### Analytical response of FB-doped membrane to AR

Firstly, the analytical response was evaluated as a function of AR concentration in solution. For this aim, the sensing membranes were immersed in AR solutions at concentration levels up to 4.4 mg/L. As it was expected, the results indicated an increase on the absorbance when the AR concentration increased. The working concentration interval was from 1 to 5 mg/L with a LOD of 0.35 mg/L. However, for practical applications, and in particular for AR determination in biological samples concentration range can be variable and in some cases, such as patients with gluten free diets, very low concentration level can be found. Therefore, a previous SPE procedure was evaluated in an attempt to cover lower concentration ranges.

Preconcentration and clean-up was accomplished with SPE using C18 cartridges. For this aim compounds, two AR were studied as a function of their polarity, PR

and DHCA taking into account the apolar hydrocarbon chain and the carboxylic acid functional group, respectively. The results indicated that the recovery was quantitative for PR (extraction efficiency =91%) when using methanol and water as conditioning solvents. However, in the case of DHCA, it was necessary to include a conditions step with 1 mL sodium acetate ( $\text{NaCH}_3\text{COO}$  at pH 5,00) in order to extract the non-ionic form of DHCA and therefore to reach an adequate recovery. Alternatively, 0,1 M HCl showed quantitative extraction recoveries for DHCA, and the use of one of the other was determined by the urine matrix (see application to urine samples section) Taking into account, that the potential application of the proposed membranes is the detection of metabolites from gluten intake, DHCA was chosen for further experiments.

Once the conditioned step was established, the volume of sample processed was studied. With this in mind, sample volume (2-10 mL) was studied. **Figure 4.2.27 A** shows the response variation as a function of sample volume processed ( $V_{\text{elution}}=0,5$  mL). As can be seen, the analytical response increased as a function of the processed volume. These results indicated that the sensitivity can be modulated by processing different volumes. Detection limits for 2, 5 and 10 mL were 120, 60 and 10  $\mu\text{g/L}$ , respectively, which is of special interest to apply the methodology given the variability of the AR contents in real samples. In this work and as a proof of concept, 5 mL were chosen for further experiments. Reaction time can be also related with the sensitivity, however, in this case, reaction times higher than 10 min provided a constant response (see **Figure 4.2.27 B**).

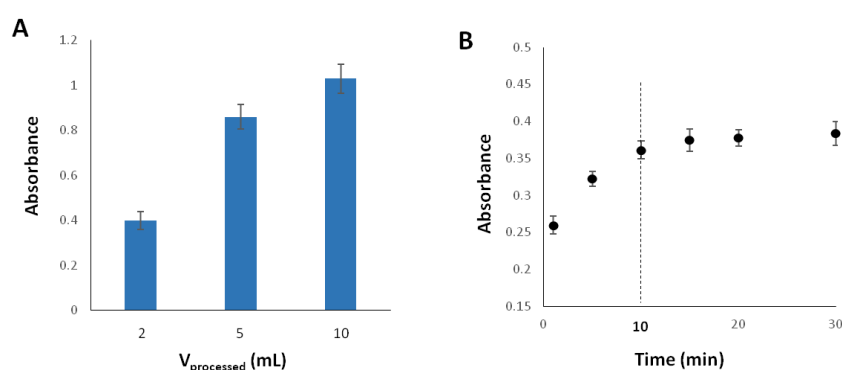


**Figure 4.2.27 A)** Variation of the response as a function processed volume in SPE y **B)** Study of the reaction time.

**Figure 4.2.28 A** shows the variation of the membrane response as a function of the concentration when SPE was used previous to the spectroscopic response. As can be seen, the combination of SPE and the sensing membranes allowed the determination of the DHCA in the concentration range from 0.2 to 1 mg/L. In addition, a semiquantitative analysis can be also carried out by visual inspection since the FB delivery to the AR solution caused an intense colorimetric shift from pale yellow to orange-red (**Figure 4.2.28 A** inset).

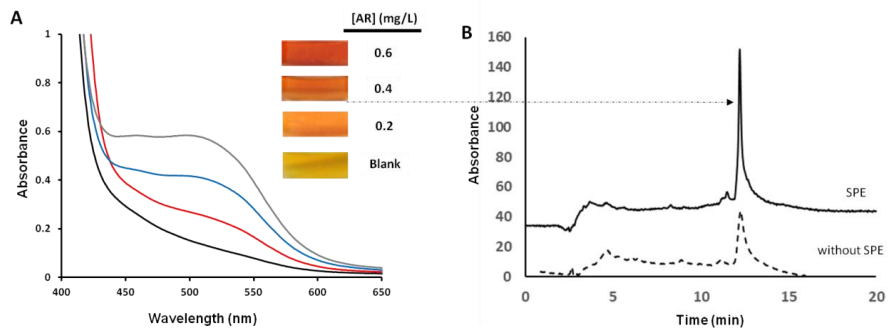


**Figure 4.2.28 A)** Spectra variation as a function of the concentration **B)** Chromatograms obtained for the derivative formed with the sensing membranes with and without SPE.

The potential application of the proposed devices was demonstrated for biological samples, in particular, urine samples. Therefore, isolation of the FB-AR response was mandatory. For this aim, chromatographic analysis of the membrane response was monitored. **Figure 4.2.28 B**, depicts the chromatograms obtained after the exposure of the target analyte to the sensing membrane by processing the sample with SPE and without that step. As can be seen, the derivative provided a chromatographic response at a retention time of 11,5 min, which can be used to monitor the response obtained the sensing membranes, isolating the DHCA signal from other potential compounds in urine samples in order to correlate it with the gluten intake.

#### Analytical parameters

The use of DHCA as biomarker to evaluate the gluten intake is a tricky issue, since the content can vary as a function of the intake, patient and sampling conditions,



among others. Therefore, sensitivity is a key parameter in order to adapt the procedure to the needs of the analysis. The proposed sensing membranes combined with SPE allowed the detection of the target analyte at different concentration level taking into account the processed sample volume, and at the same time the clean-up step reduced the potential interfering species in the urine sample. The calibration curve established for the proposed procedure using 5 mL as sample volume is shown in **Table 4.2.3**.

Under these conditions, the LOD was 60  $\mu\text{g/L}$  (see **Table 4.2.3**). Sensitivity of the chromatographic signal obtained for the isolated derivate was also evaluated. In this case, the LOD was 50  $\mu\text{g/L}$  when processing 5 mL of samples in the SPE cartridge and subsequent injection in the chromatographic system. It should be noted that in this case, the calibration showed a good linearity in the working concentration interval between 0.2 and 1.0  $\text{mg/L}$  (see **Table 4.2.3**). In addition, and as mentioned before LOD of 120 and 10  $\mu\text{g/L}$  can be achieved if 2 or 10 mL of sample are processed, respectively. Therefore, the procedure could be adapted to the patient state in terms of gluten intake.

Precision was evaluated for the spectroscopic and the chromatographic responses by using the RSD values. **Table 4.2.3** summarizes these results. Interday precision was evaluated for six replicates. The RSD value for the spectroscopic responses was 7%, meanwhile for the chromatographic signals 6%. No significant differences were found between the spectroscopic and chromatographic measurements despite the differences in signal acquisition due to the retention time of the derivative specie in the chromatographic system. These results were in agreement with the kinetics of the derivatization reaction (**Figure 4.2.27B**), which showed a constant signal after 10 min. In order to guarantee the practical application of the proposed membranes, synthesis-to-synthesis precision was also evaluated. For this aim, FB-sensing membranes were synthesized in three different days, and the response was evaluated at a AR concentration level of 1  $\text{mg/L}$ . The RSD calculated with the spectroscopic readout was 15%, which indicated an adequate performance of the sensing membranes in terms of precision.

**Table 4.2.3** Analytical parameters obtained with sensor and chromatographic methods to determine AR in standard solution and extracted from real samples.

Analytical methods	Lineal range (mg/L)	Calibration curve			LOD ( $\mu\text{g/L}$ )	RSD (%)
		$y = a + bx$ (mg/L)				
		$a \pm S_a$	$b \pm S_b$	$R^2$		
Sensor	1-5	$0.017 \pm 0.01$	$0.42 \pm 0.02$	0.99	60	7
Chrom. method	0.2-1	$6 \pm 18$	$260 \pm 8$	0.999	50	6

### Application to estimate AR in urine samples

The real performance of the proposed sensing devices was tested for urine samples. Preliminary studies were carried out with samples taken from volunteers controlling the gluten intake during different days. **Figure 4.2.29A** and **Figure 4.2.29B** show a scheme of the SPE procedure and the response obtained to a urine samples and the same urine spiked with 0,8 mg/L of DHCA, respectively. The spectroscopic signals for urine and spiked urine samples are shown in **Figure 4.2.29C**. For this sample, the sensing membrane did not provide response, showing the absence of the target analyte, meanwhile the addition of DHCA to the samples resulted in the expected spectroscopic signal. Thus, the negative response indicated that DHCA was not detected at concentrations lower than 60  $\mu\text{g/L}$ , therefore, it could be assumed the absence of gluten intake.

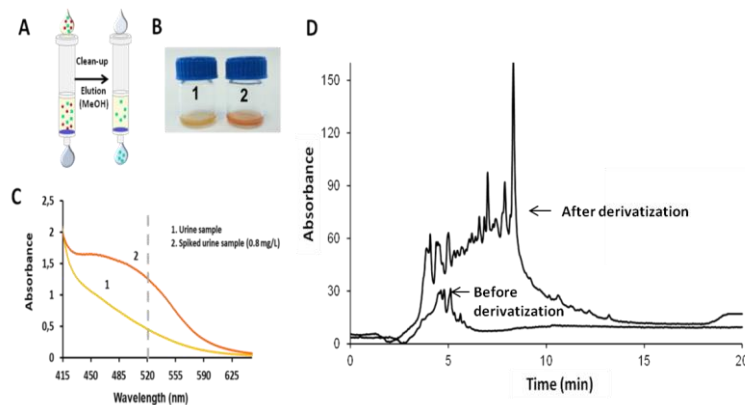


**Figure 4.2.29 A)** Schematic diagram of the SPE procedure, **B)** Image of the derivatized urine samples 1: sample and 2: spiked sample with DHCA 0.8 mg/L. **C)** Comparison of spectra obtained for that sample and spiked sample. **D)** Chromatograms obtained for a derivatized sample with and without derivatization.

Taking into account the previous results, the next step was to evaluate if the response obtained with the sensing membrane (spectroscopic and chromatographic responses) were correlated with the gluten intake. In this case, the spectroscopic measurements will be correlated with the total content of FB-derivatizable compounds meanwhile, the chromatographic response was correlated with the DHCA response. For these aim, three different samples taken in three different days were analysed. The first and third day there was gluten intake, meanwhile the second day, the gluten intake was suppressed. The three samples were analysed following the proposed procedure. After the SPE extraction and addition of the sensing membranes, the three samples provided a positive response, therefore a chromatographic analysis was performed. **Figure 4.2.30** compares the chromatograms obtained for the samples. As can be seen, in all cases, FB-derivatized compounds were eluted. However, DHCA was detected only when gluten intake took place, sample DAY1 and sample DAY3. In the case of sample DAY 2(no gluten intake), DHCA was not detected. These results indicated that DHCA could be an alternative biomarker to detect food transgressions in the context of gluten intake.

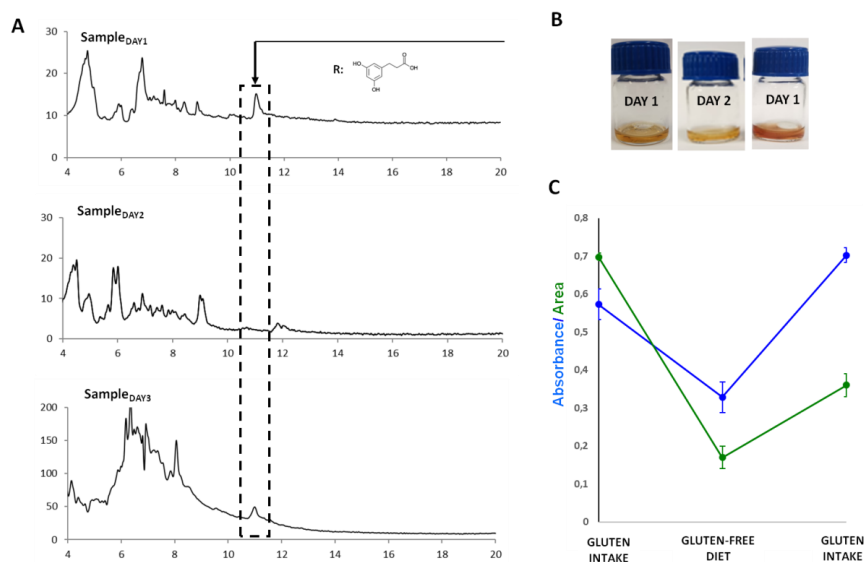


**Figure 4.2.30** A) Variation of the chromatographic profiles in the different sampling days (day 1: gluten intake, day 2: gluten-free diet and day 3: gluten intake), B) Images corresponding to the derivatized samples in the three sampling days, and C) Variation of the signal obtained with the spectroscopic measurements and the chromatographic measurements.

The comparison of the spectroscopic and chromatographic measurements revealed promising results for the use of the proposed sensing membranes. **Figure 4.2.30C** shows the variation of the total signal obtained with the spectroscopic measurements and it is compared with the variation of the chromatographic measurements as a function of the sampling days. As can be seen, the variation profile can be correlated with the gluten intake in both cases. The suppression of gluten intake in the diet, was translated into a decrease of the spectroscopic response, which was correlated with the decrease of the solution colour. The same way, the chromatographic peak at 11.5 min decreased with the suppression of gluten intake and increased again once a normal diet was established. It should be noted, that not only the chromatographic peak corresponding to DHCA decreased, but also, the complete chromatographic profile varied. Nevertheless, only DHCA peak was correlated with the gluten intake. With this in mind, and with the earlier discussed calibration equations, the corresponding concentrations to the responses were calculated. **Table 4.2.4** shows the results obtained for spectroscopic and chromatographic measurements.

**Table 4.2.4** Calculated concentrations for the spectroscopic and chromatographic responses

Sample	Gluten intake	[Total content] mg/L	[DHCA] mg/L
Day1	Yes	1.33±0.09	0.24±0.03
Day2	No	0.74±0.07	<LOD
Day3	Yes	1.63±0.12	0.11(<LOQ)

## Conclusions

In this present study work, a FB/doped PDMS/TEOS based membranes has been proposed as a sustainable tool to develop in-situ kits for detecting AR, taking into account the possibility to carry out a visual inspection analysis and the simplification of the derivatization procedure. The results indicated that spectroscopic analysis can be used as a screening tool to differentiate positive and negative samples. Meanwhile, the chromatographic assay was necessary to isolate the DHCA response in positive samples. Under the optimum experimental conditions, DHCA LOD was 60 ng/mL by adding a SPE step (C18 cartridges) prior to

the analysis. Precision was also tested, providing adequate results (RSD<7%). Preliminary studies in urine samples have shown successful results, showing that DHCA can be used as biomarker of gluten intake. The main advantages of the proposed methodology are the development of a pre-screening tool previous to the chromatographic analysis, and therefore the simplification of the dietary transgression evaluation which led to the improvement of the sustainability of the proposed method.

#### **4.2.4 Determination of antimicrobials in invasive medical devices by in-tube solid phase microextraction as preconcentration tool: application to endotracheal tubes**

The use of invasive medical devices, such as endotracheal tubes (ETT), for patients in intensive care unit is often necessary. However, the biofilm formation can result in ventilator associated infections and, therefore in such cases the treatment with antimicrobial agents is required. Meropenem is a widely used antimicrobial for the treatment of these infections. These treatments are not always effective, in fact, in-vitro studies have demonstrated the difficulty of antimicrobials to penetrate into the biofilm, however in-vivo studies of the effect of these compounds is a trend, mostly because of the complexity of pulmonary samples extracted from ETTs. Therefore, the objective of this study was to evaluate IT-SPME-CapLC-DAD to determine meropenem in ETTs in order to estimate the penetration capability into the biofilm. Firstly, the analytical performance of in-tube SPME-CapLC-DAD showed satisfactory results for estimation of meropenem in terms of sensitivity (LOD= 1 µg/L) and precision (RSD<10%). The extraction of meropenem from the ETTs was also studied. Direct extraction, stir assisted extraction (SAE) ultrasound extraction (UAE) extraction were tested. The results indicated similar recovery results, and thus, direct extraction was chosen for simplicity. Finally, samples from ETTs used for critically ill patients with different antimicrobial treatments were analysed with successful results. The proposed methodology can be a potential alternative to determine meropenem in invasive medical devices, and in particular in ETTs, taking into account that the pulmonary antimicrobial concentrations for meropenem (2-30 mg/L).

### Study of the preconcentration step

As mentioned in the introduction section, IT-SPME allows the preconcentration of the analytes into the internal surface of the capillary column through the interactions established between the coating and the compounds of the sample. Next, analytes retained during the load step can be desorbed by the mobile phase and transferred to the analytical column. The amount of analyte extracted depends on several parameters, such as the length of the extraction loop or the volume of sample processed. Therefore, firstly, these parameters were optimized. The study of the processed volume was carried out by processing different volumes of a meropenem solution (0.75  $\mu\text{g}/\text{mL}$ ). **Figure 4.2.31A** shows the variation of the analytical response as a function of the processed volume. As can be observed, an enhancement of the analytical signal was achieved by increasing the volume of processed sample. However, volumes higher than 500  $\mu\text{L}$  did not improve the analytical response. These results were in accordance with the basis of the IT-SPME, since this technique is not an exhaustive extraction technique. Generally, when the volume of processed sample is increased, an enhancement of the analytical signal is observed due the amount of analyte retained in the coating is higher. Nevertheless, when the equilibrium is reached, higher volumes did not improve the analytical response. Thus, a volume of 500  $\mu\text{L}$  was used for further experiments.

The length of the capillary columns was also studied. As can be seen in **Figure 4.2.31B**, the area of the chromatographic peak increased with the length of the capillary column, and this can be explained by the increment on the extractive phase in the system. An increase on the capillary length would lead to an enhancement on the analytical response; however, it would be also associated with an increase on the system pressure. Therefore, 60 cm was selected as the optimum capillary length. The flow rate and nature of the coating were also evaluated. **Figures 4.2.31C and D** show the results obtained with different flow rates and capillary coatings, respectively. As can be seen, there were not significant differences when using different flow, thus 9  $\mu\text{L}/\text{seg}$  was chosen for further experiments. Contrary to this, the nature of the coating is a key parameter in the preconcentration process. As it was expected TRB-35 provided the higher analytical response (see **Figure 4.2.31D**). It should be noted, that the percentage of diphenyl groups endows high polarity to the inner surface of the capillary coating, hence the affinity of meropenem towards the coating can be also

improved. Therefore, the selected IT-SPME conditions were: TRB-35 capillary column (60 cm), processed volume 500  $\mu\text{L}$  and flow rate 9  $\mu\text{L}/\text{seg}$ .

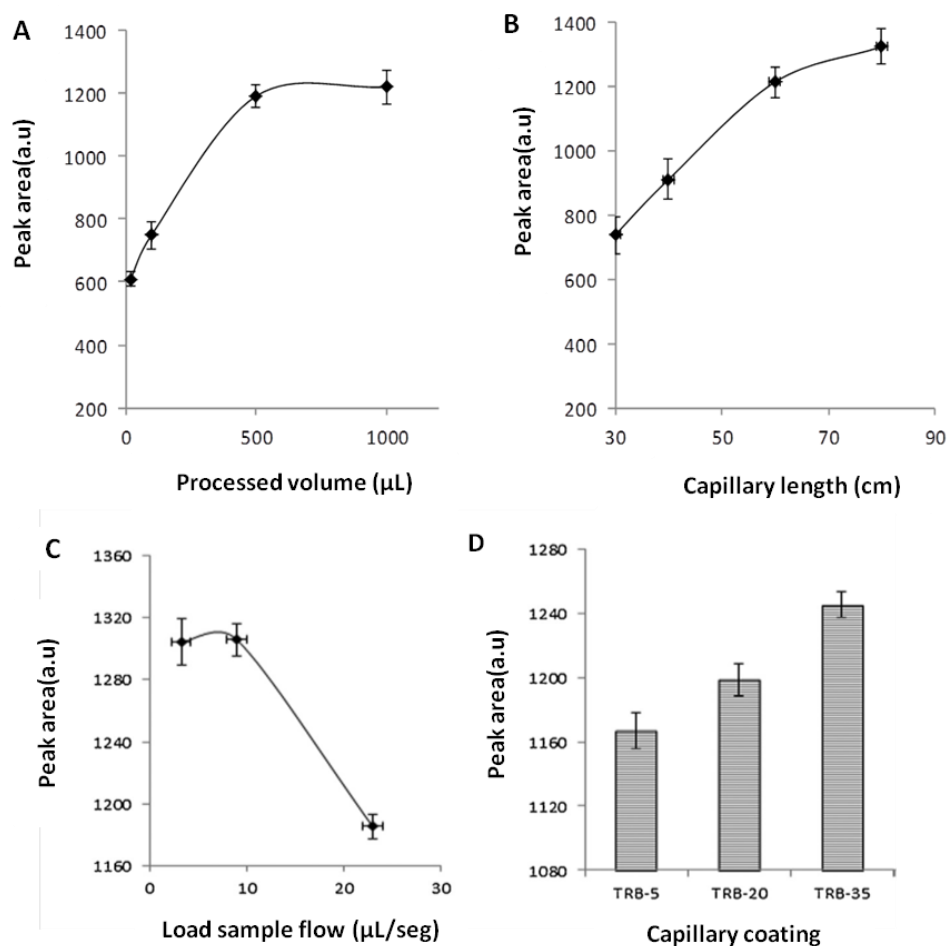


**Figure 4.2.31** Analytical response (peak area) obtained as function of the **A)** processed volume, **B)** capillary columns length, **C)** Sample processed flow and **D)** capillary coating. [Meropenem] = 0.5  $\mu\text{g}/\text{mL}$ . Mobile phase ACN:water in gradient elution mode:  $t = 0$  min acetonitrile:10% during 10 min, increased to 15% from 11 min to 13 min, and then from 14 min to 15 min-10% acetonitrile. Mobile phase flow rate was 8  $\mu\text{L}/\text{min}$ .

### Study of meropenem extraction from the ETTs

Following the procedures described in **section 3.4.2**, the ETTs controls spiked with meropenem were analysed by using direct DE, UAE and VAE. The percentages of recovery obtained using the proposed extraction methodologies were  $92\pm 5$ ,  $87\pm 4$  and  $95\pm 7\%$  for DI, UAE and VAE, respectively (0.5  $\mu\text{g}/\text{mL}$  meropenem was processed using as extraction time 5 min). The results showed that the three procedures provided satisfactory recovery values, however, DE and VAE were the procedures that provided higher recoveries. Therefore, the extraction kinetics for DE and VAE were also studied. The results indicated that quantitative extraction,  $91\pm 6\%$ , can be achieved with SAE with an extraction time of 1 min. However, the percentage of recovery with DE at 1 min was  $65\pm 5\%$ . Therefore, stir assisted extraction (water as extracting solvent and 1 min as extraction time) was the procedure chosen to extract meropenem for ETTs, taking into account the recovery values, the simplicity of the procedure, the elimination of hazardous solvents consumption and the low energy required to carry out the extraction.

### Analytical performance

Calibration equation, linear working range, LOD, LOQ and precision data are shown in **Table 4.2.5**. The results indicated satisfactory analytical performance in the lineal range 0.01-1  $\mu\text{g}/\text{mL}$ . The LOD and LOQ were experimentally determined as the analyte concentration that provided a signal-to-noise ratio of 3 and 10, respectively. The LOD was 0.003  $\mu\text{g}/\text{mL}$  and LOQ 0.01 was  $\mu\text{g}/\text{mL}$ . These results demonstrated the great potential of IT-SPME-CapLC-DAD for the determination of meropenem in ETTs, since it can be detected at ultra-trace level, and so remaining concentrations of the antimicrobial in the biofilm can be detected. It should be noted that these values were lower than the LODs provided by previously reported studies as can be seen in **Table 1.7**. Therefore, the proposed procedure can be used to determine residual concentrations of antimicrobials.

By another hand, precision of the proposed procedure was studied. This parameter was evaluated by RSD. Intra- and inter-day RSD were 1% and 4%, respectively (see **Table 4.2.5**). Thus, the precision was satisfactory for practical applications. **Figure 4.2.32A** shows the chromatograms obtained at different concentration levels.



**Table 4.2.5** Figures of merit obtained for the determination of meropenem by in-tube SPME-CapLC-DAD.

Analyte	Linear range ( $\mu\text{g/mL}$ )	Calibration curve		$R^2$	LOD ( $\mu\text{g/mL}$ )	LOQ ( $\mu\text{g/mL}$ )	RSD%	
		$y = a + bx$	$b$ ( $\mu\text{g/mL}$ )				Intraday (n=3)	Interday (n=6)
Meropenem	0.01-1	$23 \pm 6$	$1627 \pm 13$	0.99	0.003	0.01	1	4

### Analysis of samples from ETTs

Five ETTs tubes from patients with meropenem treatment were analysed following the optimized extraction procedure, VAE and subsequent analysis by IT-SPME-CapLC-DAD. The confirmation of the meropenem identification was carried out not only with the retention times, but also the by means of the UV-vis spectra of the chromatographic peaks in samples and the comparison with the spectra of meropenem standard solutions. By way of example, **Figure 4.2.32 B** shows the chromatogram obtained for a sample compared with a standard of meropenem ( $0.5\mu\text{g/mL}$ ) and the UV-vis spectra of the peak at  $t_R = 7.9$  min, corroborating the identification of meropenem. **Table 4.2.6** summarizes the results obtained for the analysis of the five ETTs tubes. As can be seen, meropenem was detected in three of the samples ETTs from patients treated with meropenem (ETT2, ETT3 and ETT5) at a concentration level 41, 33 and 80 ng/mL. This low amount of analyte in the ETT could be explained due the inability of the antibiotic to penetrate inside the mature biofilm. RSD values for samples were <12%. As it was expected, in samples ETT1 and ETT4, meropenem was not detected, as these patients were not treated with the antimicrobial.

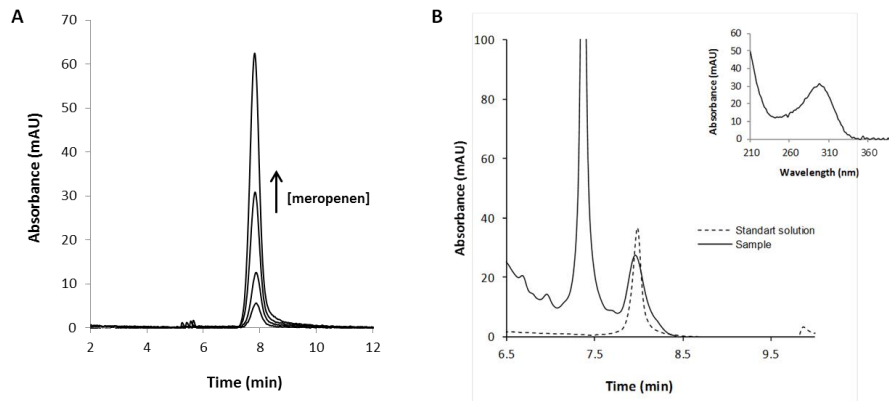


**Figure 4.2.32** **A)** Chromatograms obtained for increasing concentrations of meropenem: 0.1, 0.2, 0.5 and 1  $\mu\text{g/mL}$ . **B)** Chromatograms obtained for a sample extracted from the ETTs and a standard solution (0.5  $\mu\text{g/mL}$ ). Inset. Spectrum of the meropenem found in the ETT sample VAE: 1 min using water as extraction solvent under stirring. In-tube SPME conditions: TRB-35 capillary column (60 cm) processed volume = 500  $\mu\text{L}$  and flow 9  $\mu\text{L/seg}$ . Chromatographic conditions: mobile phase ACN:water in gradient elution mode:  $t=0$  min acetonitrile:10% during 10 min, increased to 15% from 11 min to 13 min, and then from 14 min to 15 min -10% acetonitrile. Mobile phase flow rate was 8  $\mu\text{L/min}$ .

**Table 4.2.6** Found concentrations and recovery values calculated for meropenem in samples from ETTs from patient in ICU.

Samples ETTs	Found concentrations ( $\mu\text{g/mL}$ )	Recovery %
ETT 1	<LOD	96 $\pm$ 3
ETT 2	0.041 $\pm$ 0.005	103 $\pm$ 5
ETT 3	0.033 $\pm$ 0.002	95 $\pm$ 4
ETT 4	<LOD	94 $\pm$ 6
ETT 5	0.08 $\pm$ 0.003	98 $\pm$ 4

### Conclusions

Quantifying the concentration of antibiotic in invasive medical devices can give information about its capability to penetrate into the biofilm and, therefore, the efficacy offered in the treatment of the infection. In this work, a new methodology has been proposed in order to determine the concentration of meropenem in endotracheal tubes from patients in intensive care unit who were treated with this antibiotic. For this purpose, an IT-SPME coupled to CapLC-DAD has been evaluated as an innovative tool to determine antimicrobial in invasive medical devices. Previously, the extraction of meropenem from the medical devices has been optimized using stir assisted extraction. The application of the proposed procedure has given rise to very low detection limits (3 ng/mL) and satisfactory precision (RSD <12%). The performance of the proposed methodology has been demonstrated by the analysis of samples from ETTs tubes in patients with meropenem treatment. Meropenem was found at concentrations of ng/mL. Validation of the procedure was carried out by a recovery study. The recovery values showed satisfactory results (94-103%). The new approach proposed in this work has proved to be an alternative not only because the sensitivity and precision, but also owing to the simplicity, cost efficiency, analysis time, and thus, its sustainability.

### 4.3 Food sample

Taking into account the need to develop sustainable analytical tools for food analysis, in this section PDMS based sensing membranes were developed to determine  $\text{NH}_3$ ,  $\text{NO}_2^-$  and  $\text{NO}_3^-$  in meat and vegetable samples.

#### 4.3.1 Ionic-liquid doped polymeric composite as passive colorimetric sensor for meat freshness as a use case

A composite containing 1,2-naphthoquinone-4-sulfonic acid sodium salt (NQS) embedded in an ionic liquid (IL)-PDMS-TEOS-SiO<sub>2</sub>NPs polymeric matrix was proposed. The selected IL was 1-methyl-3-octylimidazolium hexafluorophosphate (OMIM-PF<sub>6</sub>). It was demonstrated that ILs chemical additives inside PDMS influenced the sol-gel porosity. The analytical response for ammonia atmospheres was studied based on the sampling time (between 0.5 and 312 h), temperature (25°C and 4°C) and sampling volume (between 0.022 and 2 L) by means of diffuse reflectance measurements and also by RGB. RGB measurements were made from sensor images taken with a smartphone. Flexible calibration was possible, adapting it to the sampling time, temperature and sampling volume needed for its application. Calibration linear slopes (mA vs ppmv) between 1.7 and 467 ppm/v were obtained for ammonia as a function of the several studied conditions. Those slopes were between 48 and 91 % higher than those achieved with sensors without ILs. The practical application of this sensing device was demonstrated for the analysis of meat packaging environments, being a potential cost-effective candidate for in situ meat freshness analysis. In addition, the selectivity of the sensor was verified in reference to other compounds of the family emitted by meat products, such as sulfides. Homogeneity of the ammonia atmosphere was tested by using two sensors placed in two different positions inside the packages.

### Characterizing the response of the PDMS/TEOS-NQS/SiO<sub>2</sub>/IL sensing membranes

The ILs doping effect into the polymeric matrix depended on the combination of the IL and the polymeric network. As the membrane properties for analyte detection can be tuned by cationic and anionic modifications, three different ILs were tested to assess the influence of the presence of cations and anions on the detection performance. The sol-gel matrix developed satisfactorily when OMIM-PF<sub>6</sub> and 4MBP PF<sub>6</sub> were used in percentages up to 9%. Nevertheless, the PDMS membrane doping with BMIM OSU did not lead to adequate gelation. Hence, OMIM-PF<sub>6</sub> and 4MBP PF<sub>6</sub> were selected for further experiments. Different percentages of OMIMPF<sub>6</sub> were studied. As can be observed, the analytical response of the membrane depended on the proportion of OMIMPF<sub>6</sub> (Figure 4.3.1).

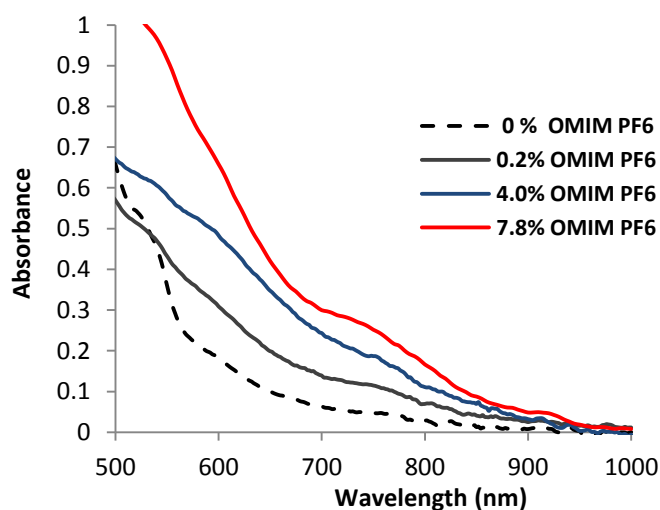


**Figure 4.3.1** Variation of the analytical response of NH<sub>3</sub> (20 ppmv at 8 hours) in atmospheres as a function of OMIM-PF<sub>6</sub> mass proportion in the polymeric matrix.

## Chapter 4. Results and Discussion

Optical microscopy and SEM images were performed to characterize the membranes (see **Figure 4.3.2**). Comparison of microscopy images and micrographs, without and with OMIM-PF<sub>6</sub>, we observed that the presence of IL in the sensing membrane increased the spongy structure, which led to an improvement in the analytical response. These results are in agreement with the results in **Figure 4.3.1**. The observed pore size was about 8-30 μm.

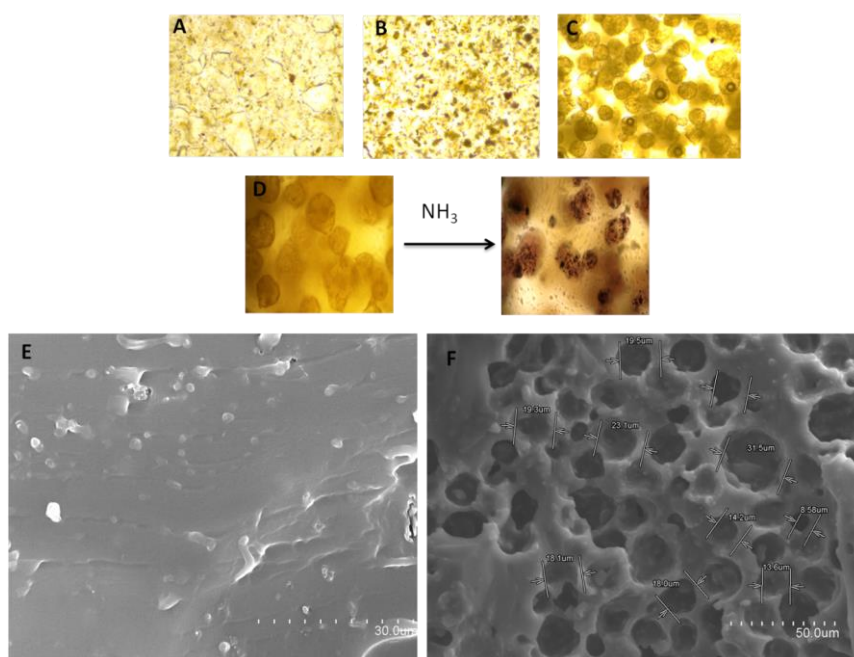


**Figure 4.3.2** Optical microscope images (magnification 10) of sensing membranes **A)** without OMIM-PF<sub>6</sub> **B)** with 0.2 % OMIM-PF<sub>6</sub> **C)** with 7.8 % OMIM-PF<sub>6</sub> and **D)** scheme of the sensing membrane (7.8 % IL) before and after the exposure to NH<sub>3</sub> with the optimum sensing membrane (magnification 50). **E)** SEM micrograph of the transversal cut of the polymeric membrane without IL **F)** SEM micrograph of the transversal cut of the polymeric membrane containing 7.8 % IL and porous measurements.

**Figure 4.3.3 A, B and C** show the sensing scheme of the membrane before and after ammonia exposition, the TEM micrographs of the inner membrane surface and their bright-field optical microscopy photographs, respectively. ILs as chemical additives influenced the sol-gel porosity basically because of the interactions between the components of the polymeric matrix.

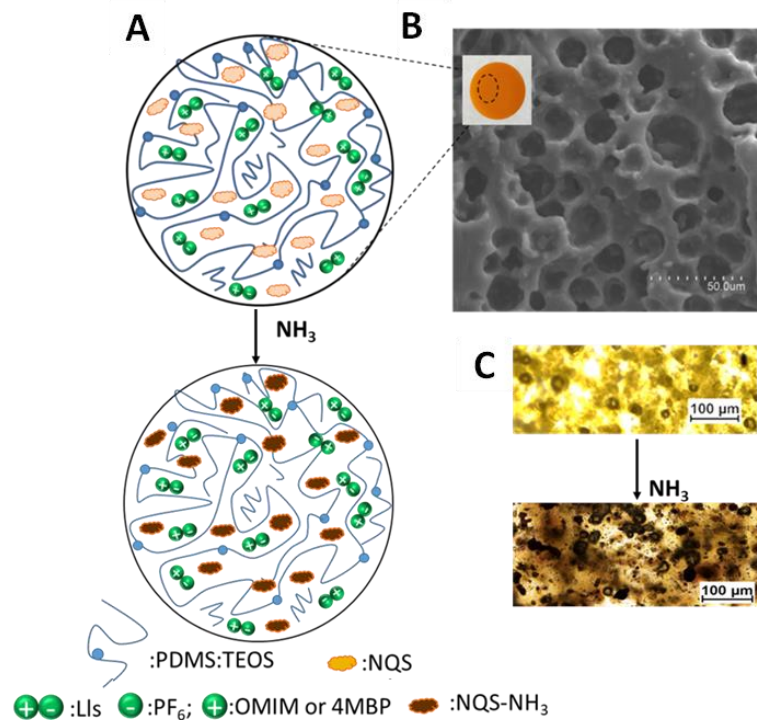


**Figure 4.3.3 A)** Schematic diagram of the sensing membrane composition and its response. **B)** SEM micrograph of the transversal cut of the polymeric membrane containing 7.8 % IL. **C)** Bright-field microscopy photographs of 10x magnification obtained for sensing membrane before and after ammonia exposition.

Simultaneous H-bonds between  $\text{PF}_6$  and silica matrix together with imidazolium groups  $\pi$ - $\pi$  stacking [295] when using OMIM- $\text{PF}_6$  gave rise to a high porosity membrane, which can improve the efficiency of the material for sensing purposes (see **Figure 4.3.2 and 4.3.3**). As it can be seen (**Figure 4.3.1**), analytical response increased as a function of the IL load due to the increase on the permeability. In all cases the response was higher in the presence of ILs. It is worth mentioning that higher contents of ILs did not allow the proper gelation of the polymeric matrix. The influence of the cation in the sensing performance was also studied and the results with pyridinium and imidazolium based ILs were compared. There were not significant differences in the analytical response and precision, showing that the performance of the sensing membrane is mainly governed by the anion. Therefore, imidazolium based sensing membrane was selected for further experiments.

The kinetics of the reaction between  $\text{NH}_3$  and the IL-NQS-PDMS device was investigated. The kinetic data were obtained by recording the absorbance of the device at different exposure times for several concentrations, at 25°C and for a sampling volume of 2 L. The results obtained are shown in **Figure 4.3.4**. The effect of the ammonia concentration on the reaction rate corresponded to a pseudo-first-order kinetics (tested up to 24 h). The slopes of the linear regressions  $\text{Ln}(\text{mA})$  vs  $t(\text{h})$  can be used as a measure of the initial reaction rate, being  $0,024 \pm 0.003 \text{ h}^{-1}$  ( $n=6$ ). A linear relationship existed between the obtained slopes of the linear interval (mA vs  $t$ ) for each assayed concentration and the sampling time (h) with a slope of 5.61 ppm/v (see **Figure 4.3.4**).



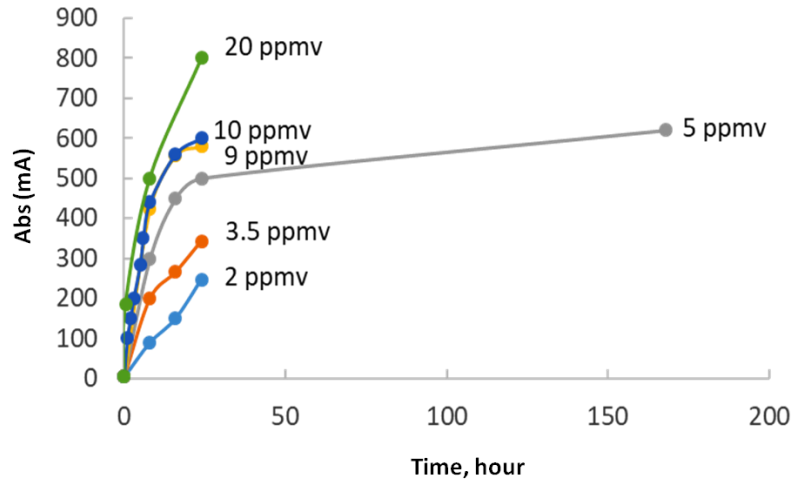


**Figure 4.3.4** Variation of the sensing response of  $\text{NH}_3$  at several levels of concentration (ppmv) as a function of the exposure time with OMIM- $\text{PF}_6$ -NQS-PDMS/TEOS- $\text{SiO}_2$  NPs.

**Figure 4.3.5** shows the results corresponding to 10 ppmv analyte concentration for several sampling times, which were compared with those obtained by using the firstly developed PDMS/TEOS-NQS-SiO<sub>2</sub>NPs sensor [112,113]. The absolute value of the analytical response increased, obtaining an evident improvement in the response of the sensor. As shown in **Figure 4.3.5**, the IL-NQS-PDMS sensor showed significant colour change in one hour due to the presence of ammonia whereas the reference sensor without IL gave response after 3 hours. Langmuir and Freundlich adsorption isotherms were examined to illustrate the nature of the interaction between the hybrid material and ammonia. The correlation coefficients ( $R^2$ ) indicated that the adsorption can be better demonstrated by the Langmuir isotherm ( $R^2 > 0.95$ ) compared to the Freundlich model ( $R^2 < 0.85$ ).  $1/A$  ( $A$  is absorbance, which is related with the adsorbed ammonia in the sensor) vs  $1/\text{ammonia ppmv}$  was plotted for 8 and 24h and the slopes were: 11.373 and 5.612 ppmv, respectively. These results can suggest that the analytes were adsorbed on homogeneous adsorption sites of the sensor, considering a chemisorption mechanism.

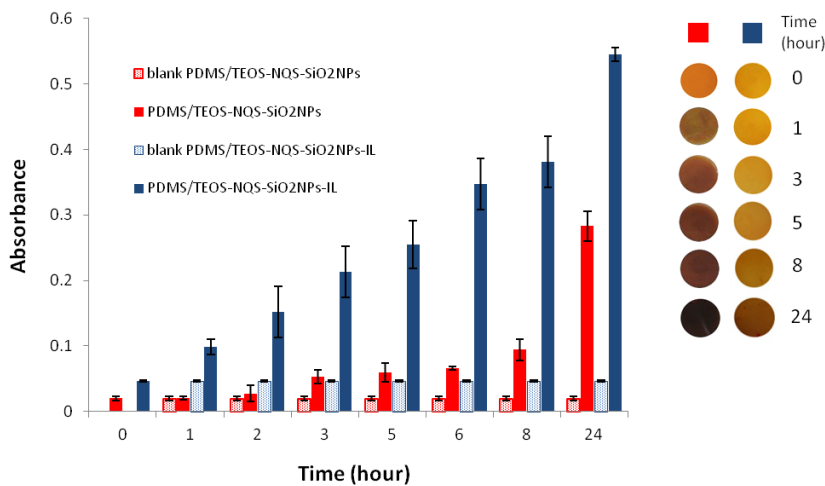


**Figure 4.3.5** Variation of the sensing response of NH<sub>3</sub> (ppmv) as a function of the exposition time with PDMS/TEOS-NQS- SiO<sub>2</sub> NPs (red columns) and PDMS/TEOS-NQS- SiO<sub>2</sub> NPs-OMIM-PF<sub>6</sub> (blue columns).

## Chapter 4. Results and Discussion

Other studies related with the estimation of the loaded ammonia mass by the sensor were carried out. We worked with the hypothesis that if the absorbance is the same for given sensors at several tested conditions, the loaded ammonia mass will be the same. Low ammonia concentrations were tested after a high sampling time of 312 h (Volume 2L, 25°C) for achieving a high load: 0.25, 0.5 and 1 ppmv, which presented mA values at 590 nm of 432, 397 and 497, respectively. Other studies related with the estimation of the loaded ammonia mass by the sensor were carried out.

The high absorbance value obtained for 0.25 ppmv can be in accordance with a high ammonia load percentage in reference to the ammonia atmosphere. We established 100 % arbitrarily, corresponding to 0.35  $\mu\text{g}$  in the ammonia atmosphere and from this value we established the approximate amounts ( $\mu\text{g}_{\text{adsorbed}}$ ) for all experiments carried out with standards ( $\mu\text{g}_{\text{standard}}$ ).

Straight lines were obtained for all experiments by plotting  $1/\mu\text{g}_{\text{adsorbed}}$  vs  $1/\mu\text{g}_{\text{standard}}$  considering Langmuir isotherm. It is important to note that several batches of sensors were employed and very different sampling times for a testing period of more than a year at 25°C and 2L as a sampling volume and ammonia concentrations between 0.25 and 20 ppmv. **Figure 4.3.6** shows the relationship between the obtained slopes of the abovementioned straight lines vs sampling times and an insert with their values for each time. These results indicated that the proposed sensor can be of utility for very different sampling times and several working ranges of concentrations.

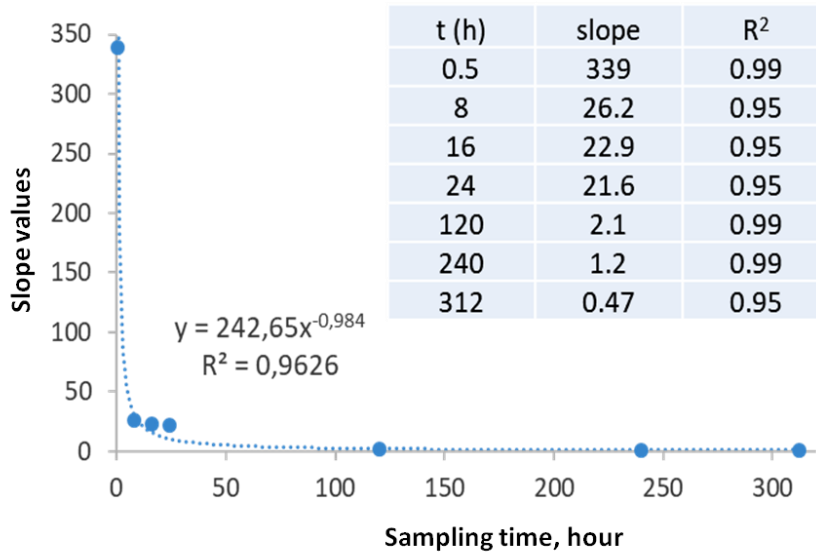


**Figure 4.3.6** Relationship between the obtained slopes of the straight lines  $1/\mu g_{adsorbed}$  vs  $1/\mu g_{standard}$  considering Langmuir isotherm vs sensor sampling times for several concentrations and an insert with their values for each time.

### Stablishing analytical parameters from the response of the sensor

In previous section, the influence of the sampling time on the ammonia sensor response has been demonstrated. In order to stablish the calibration data, the influence of the sampling volume was also tested. **Table 4.3.1** gives the linearity achieved at several conditions, mA at 590 nm vs ammonia concentration (ppmv) was considered. The response of the sensor was dependent on sampling time as it can be seen in **Table 4.3.1**, showing that very different sampling times can be employed and it was also dependent on the sample volume, which indicated its mass nature. The achieved sensitivities were higher than those achieved by the composite without ILs, for example for 2L and 8h and 24h the slopes were 5.3 and 20.3 ppm/v, which only represented 11% and 21 %, respectively, of the values shown in **Table 4.3.2** for the composite containing ILs.

**Table 4.3.1** Parameters of linear regressions (mA vs ppmv) for gaseous standards of ammonia, methylamine and dimethylamine for several sampling volumes and sampling times, under 25 °C.

Analyte	Time (h)	Volume (L)	Slope	R <sup>2</sup>	Working range (ppmv)/n=5
Ammonia	1.5	2	8.80	0.996	2-20
	8	2	47.33	0.990	2-10
	8	2	45.60	0.990	2-10
	16	2	92.24	0,990	2-10
	16	2	97.10	0.980	2-10
	24	2	91.90	0.990	2-10
	24	2	92.50	0.990	2-10
	120	2	161.43	0.980	0.5-5
	240	2	467	0.980	0.25-3
	1.5	0.36	1.70	0.990	2-20
Methylamine	240	0.1	5.64	0.990	2-50
	1	2	36.22	0.990	2-20
	1.5	2	45.42	0.990	2-20
	24	2	67,22	0.980	2-10
	24	2	66,50	0.990	2-10
	1.5	2	17.46	0.990	2-20
Dimethylamine	1.5	2	17.46	0.990	2-20

Results were evaluated considering a non-exposed IL-NQS-PDMS sensor as a blank reference sensor. In addition to ammonia, various amines were tested. Each sensor was placed in several vials with a volume of 22 mL as shown in **Figure 4.3.7**, and ammonia or amines were added (100  $\mu$ L of concentrated solution) the responses were immediate (**Figure 4.3.7A, B**) and diffuse reflectance measurements were carried out (**Figure 4.3.7C, D**). The sensing membrane was capable of discriminating between primary and secondary amines giving rise to different colours due to NQS reaction with amino groups. In addition, to the colour responses, the absorption spectra in the range between 500-900 nm evidenced a noticeably different profile for the analytes between them and in comparison with the absorption profile of the blank sensor. Methylamine and dimethylamine were also assayed at 2 L and several sampling times for linearity study obtaining adequate results, (see **Table 4.3.1**).

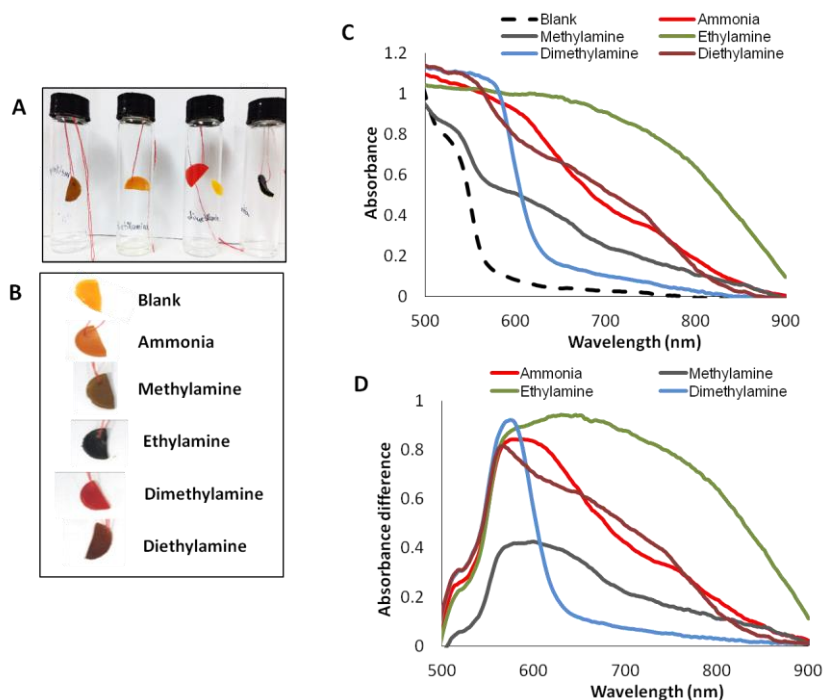


**Figure 4.3.7 A)** NQS sensor exposed to several atmospheres of ammonia and primary and secondary amines in a 22 mL vial **B)** Selective colour response depending on the chemical nature of the amine **C)** Sensors absorbance spectra including a blank sensor **D)** Spectra difference between ammonia and each amine response in relation to the blank sensor.

Sensor precision was evaluated from twenty five batches of sensors (precision achieved 8 % expressed as % RSD) for a testing period of more than a year and obtained by ten operators. The precision for sensor were between 6 and 8 % for inter and intra-day measurements (n= 30 for each one), respectively. The slopes of two replicates of the calibration graphs shown in **Table 4.3.2** were statistically compared by linear regression (n=8), due to very different values are achieved in function of sampling volume and sampling time. The equation was  $y = (-7\pm 4) + (1.1\pm 0.1)x$  being  $R^2 = 0.994$  and then, the replicate slopes are statistically the same at 95 % confidence level. This value indicated that a good precision was achieved. Experimental work was also carried out on the study of PDMS/TEOS-NQS-OMIM-PF<sub>6</sub> sensing membrane selectivity. During putrefaction of the meat, in addition to ammonia and amines, other gaseous compounds such as hydrogen sulfide (H<sub>2</sub>S) will also be released. Volatile sulfide compounds are emitted significantly during meat spoilage [323]. Subsequently, the influence of H<sub>2</sub>S on the PDMS- based sensor response has been tested against sulfide standards (**Figure 8 A,C**). Among the volatile compounds emitted during meat spoilage, H<sub>2</sub>S can be considered as an additional indicator of chicken decay [323]. To assess the influence of sulphide compound on the PDMS- TEOS- NQS- IL sensor response, sulphide standards of 1, 3 and 5 ppmv were prepared in a 100 mL plastic bag. The standards were kept under refrigeration conditions (4 °C) during 10 days. The evolution of the sensor colour was registered by taking a photo with a smartphone and quantified by the registration of diffuse reflectance.

## Chapter 4. Results and Discussion

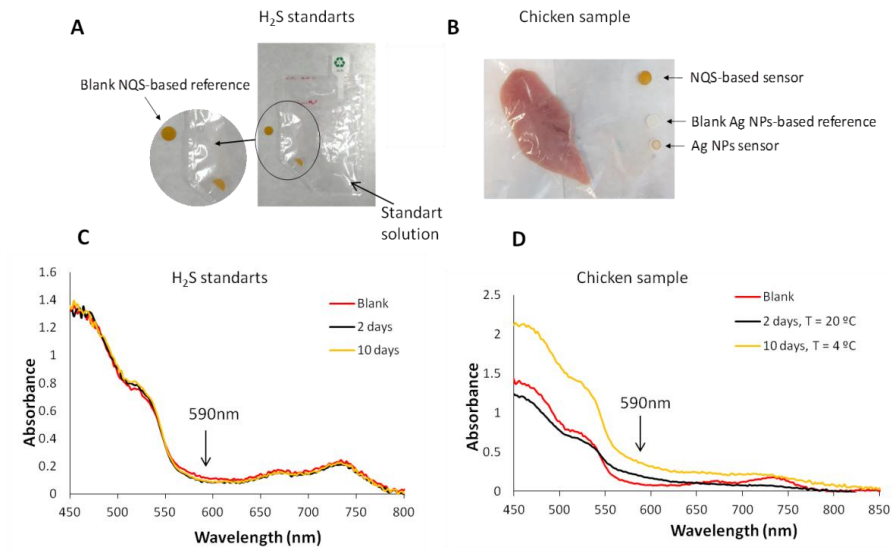


**Figure 4.3.8** **A)** NQS-based sensor exposed to sulphide standards prepared in a 100 mL plastic bag **B)** Chicken sample atmosphere in a 100 mL plastic bag in which the NQS-based and the AgNPs sensors were exposed **C)** NQS-based sensor absorption spectra stored for 10 days at 4 °C in the presence of H<sub>2</sub>S standards (1,3,5 ppmv) **D)** NQS-based sensor absorption spectra stored for 2 days at 20 °C and 10 days at 4 °C in the presence of the chicken sample.



As shown in **Figure 4.3.8A**, the NQS-based sensor preserved its original orange colour despite the presence of H<sub>2</sub>S atmosphere. It was concluded that no remarkable difference between the blank and the sampling NQS-based sensors was obtained (**Figure 4.3.8A**). Other experiment was carried out regarding real meat sample. 0.5 kg of chicken slice was introduced in a 100 mL plastic bag (**Figure 4.3.8B**) in the presence of the IL-NQS-PDMS sensor in addition to a solid plasmonic sensor developed by the MINTOTA research group for the determination of volatile sulfide compounds [111] as previously described. Two experiments were conducted: on the one hand, chicken sample was preserved at room temperature (20 °C) and refrigeration conditions (4 °C) during 2 and 10 days, respectively. Both sensors give signals as it is observed in **Figure 4.3.8B**, the responses for the PDMS-TEOS-NQS-IL sensors at the assayed conditions of conservation are given in **Figure 4.3.8D**. It was concluded that the proposed NQS-TEOS-NQS-IL sensor selectively reacted with ammonia and shows no interference in the presence of sulfur compounds, which is in accordance with the selectivity of the NQS reagent for amino groups.

### Application of the sensor to packed meat samples

For sensor application in packaged meat samples it was important to study the sensor coverage and package humidity influence in sensor response. Several covering configurations of the sensor were addressed. A full covering of the IL-NQS-PDMS sensor with lab film dramatically reduced sensor response by up to 93%, while a medium coverage setting offers a response of around 70%. An intermediate situation was found when a dotted film covered the sensor response (30% absorbance at 590 nm).

Additionally, the influence of humidity on the sensor response was experimentally tested (see section 3.4). The several relative humidity values (%HR) found for prepared standards were 75% (nitrogen), 78% (indoor air) and 88% (saturated water air). Finally, the sensor was taken and measured by diffuse reflectance spectroscopy. All experiments for humidity study were made at room temperature (20 °C). **Figure 4.3.9** shows the sensor response obtained at the humidity conditions indicated previously in comparison with the reference blank sensor.

## Chapter 4. Results and Discussion

The humidity of several meat samples atmosphere was also measured with the probe of the Thermo-Hygrometer when meat samples were preserved in a 100 mL plastic bag under refrigeration conditions at 4 °C (see **Figure 3.10B**). It was determined that meat under packaging conditions shows an average of  $87 \pm 3$  % relative humidity when preserved in refrigeration conditions for several days. Similar humidity values were found when using ammonia standards.

Relative humidity measurements at the indoor of the laboratory were carried out, giving values of  $51 \pm 6$  % (n=3). Blank sensor presented the same response between 51 and 88 % humidity conditions (see **Figure 4.3.9**). Therefore, the results presented in this work are satisfactory guidelines for detecting meat freshness.



**Figure 4.3.9** Sensor responses when exposed to a 20 ppmv ammonia atmosphere at 75 and 88 % humidity conditions compared to the reference blank sensor (left), which presented the same response between 51 and 88 % humidity conditions.

As we can see in Table 4.3.2, the calibration curves also depended on the volume of the container. For ammonia at 240 hours in 2L of volume, the slope had a value almost 100 times higher than for 0.1L volume. Another factor that affected the sensor response was temperature. Decreasing percentages smaller than 45 % for slopes of the calibration straight lines were obtained at refrigerate conditions of 4°C with respect to responses at 25°C depending of sampling time and sampling volume. This finding established that the calibration must be carried out considering sampling volume, sampling time and temperature. Another factor that also influenced the sensitivity of the sensor was the different porosity of the two faces of the sensor. A different porosity of the sensor faces was found when measurements were made with light microscope, as can be seen in Figure 4.3.10A. Two equivalent experiments were performed in which the sensor was adhered to the Tupper cover by the porous and non-porous side, respectively, and

the porous side showed better sensitivity and then this side was exposed for future experiments (Figure 4.3.10B). It should be noted that no difference was observed between the spectra of the blank sensor faces. The IL-NQS-PDMS sensor was applied to monitor the freshness of 0.5 kg of chicken slices under refrigerated conditions for 10 days. The meat sample was packed in a commercial rectangular shaped Tupper with 100 mL of free space between the meat and the tupperware lid. The IL-NQS-PDMS sensor was divided into two equivalent semicircles and stickled by the non-porous side at the Tupperware cover thanks to the adhesive composition properties of PDMS (**Figure 4.3.11A**).

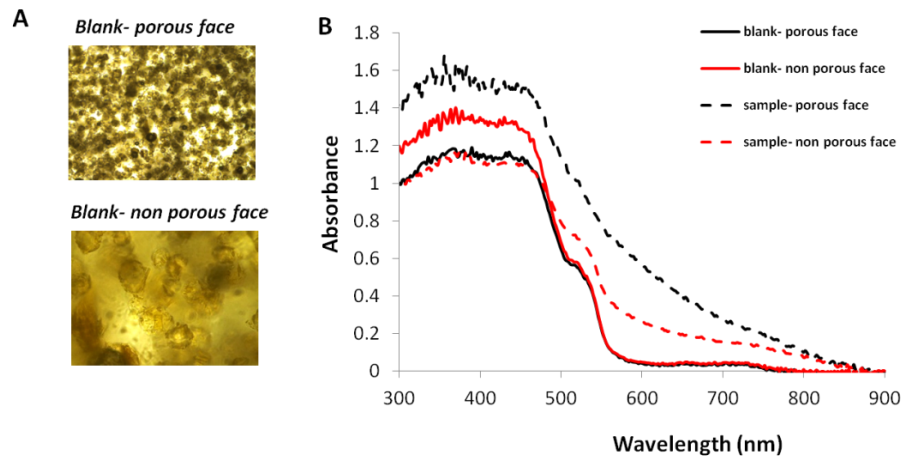


**Figure 4.3.10** Optical microscope images of the porous using (up) a  $\times 10$  objective and non-porous face (down) using a  $\times 50$  objective of the sensor (**A**). Sensor spectra for porous and non-porous face for chicken meat and blank samples under refrigerated conditions for 10 days (**B**).

## Chapter 4. Results and Discussion

The evolution of the sensor colour during 10 days was analysed by taking photos of the sensor and registering the RGB coordinates. The % R coordinate was found to be the most sensitive and, thus, the one employed for the analysis. The percentage of the R coordinate for both halves of the sensor showed similar values as indicated in **Figure 4.3.11B**. Therefore, it can be concluded that a homogeneous atmosphere is generated inside the Tupper.

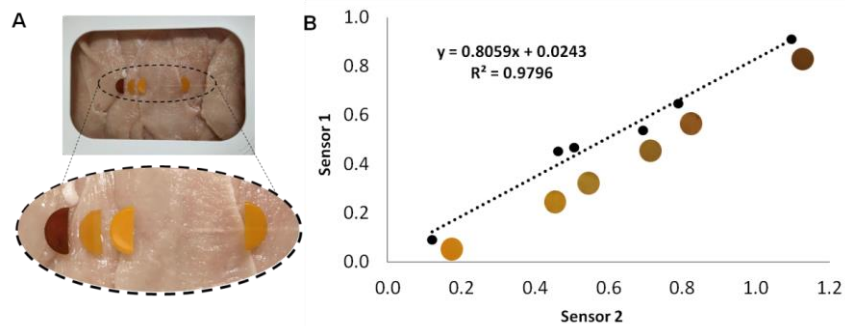


**Figure 4.3.11** Two half circles of the IL-NQS-PDMS sensor stucked at the tupperware lid and the reference sensors are placed at the lid on the outside part **(A)** Sensor evolution of the % R coordinate during 10 days when the meat sample is kept under refrigeration conditions **(B)**.

For quantitation purposes, calibration curves of 100 mL ammonia gaseous standards (10, 20 and 50 ppmv) were obtained by means of the % R coordinate analysis of the sensors image inside a plastic bag (see inset in **Figure 4.3.12A**) during 10 days at 4°C. The average of the % R coordinate for the reference blank standard (sensor outside the plastic bag) is  $56\% \pm 4$ . This value remains constant for the rest of the standards employed, that is,  $57\% \pm 4$ ,  $57\% \pm 5$  and  $59\% \pm 3$  for 10 ppmv, 20 ppmv and 50 ppmv, respectively. The variation of the % R for 10 and 50 ppmv with time was shown in **Figure 4.3.12A**, an increase in the sensor response was observed with time in accordance with the described behaviour of the sensor. After 10 days, the sensors were extracted from the plastic bag and the absorption spectrum was registered by diffuse reflectance measurements. The differences between the absorption profile of the 50 ppmv ammonia standard and meat atmosphere and sensor blank after 10 days of analysis were shown in **Figure 4.3.12B**, which indicated by the spectrum profile that the meat freshness is mainly related with ammonia in accordance with data given in the introduction section. **Figure 4.3.12C** shows the colour of the sensors with time for standards and meat sample. The footprint of the sample was not the same as those obtained for the standards, this can be in accordance with the progressive liberation of the ammonia from the meat. The quantification of the sensor response in the meat sample after 10 days at 4°C was computed by processing diffuse reflectance signal and RGB analysis of the sensor image taken by a smartphone using the corresponding calibration equations. A linear relationship was found between the absorbance (mA) and the percentage of red coordinate (%R), being the linear regression given by the equation  $\%R = (-0.0211 \pm 0.004) x + (53.5 \pm 0.7)$  with  $R^2 = 0.96$ . The ammonia content was found to be  $20 \pm 4 \mu\text{g}/\text{kg}$  and  $18 \pm 3 \mu\text{g}/\text{kg}$  per sample by using the calibration curves given in **Table 4.3.2**, respectively. According to human sensory evaluation based on colour and odor features [288] and after 10 days storage time, the meat freshness status was ascribed as putrid.

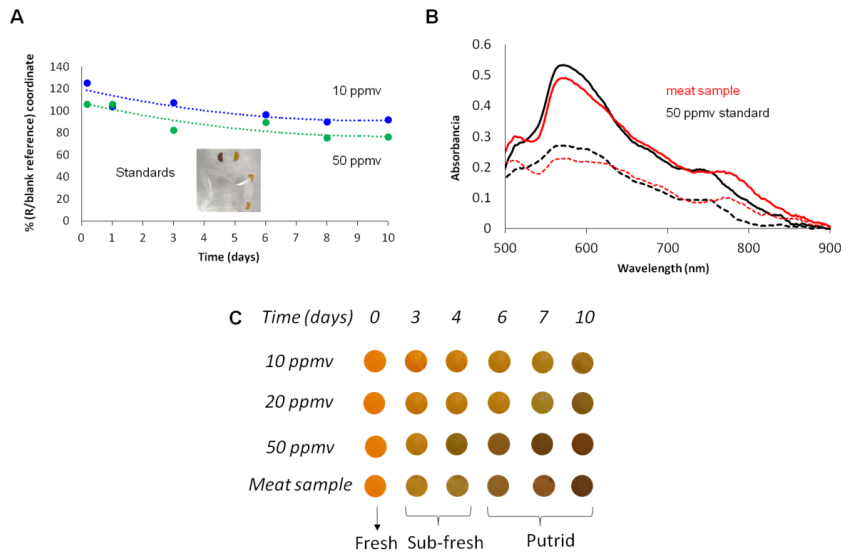


**Figure 4.3.12** **A)** Ammonia gaseous standard calibration curves inside a 100 mL plastic bag for 10 ppmv (blue), and 50 ppmv (green); insert: sensors placed inside a 100 mL plastic bag of gaseous standards. The reference sensors (blank and concentrated) for obtaining the images are located outside the bag. **B)** Difference absorption profile between the 50 ppmv ammonia standard and the atmosphere meat (both half's of the sensor) and blank reference sensor at the beginning (dotted line) and after 10 days (solid line) of analysis. **C)** Images of the evolution of the sensor colour obtained for standards and meat sample with time and meat freshness status divided into three groups: fresh, sub-fresh and putrid.

**Table 4.3.2** Calibration curves at 4°C and 10 days obtained when plotting the concentration of the ammonia standards of 10, 20 and 50 ppmv in 100 mL as a function of diffuse reflectance measurements at 590 nm and percentage of the R coordinate, respectively.

Calibration curve	Slope	Slope uncertainty	Intercept	Intercept uncertainty	R <sup>2</sup>
Diffuse reflectance vs ppmv	2.9	0.3	-0.014	0.012	0.99
%R coordinate vs ppmv	-0.12	0.01	53.8	0.3	0.992

## Conclusions

The paper contributes to develop new sustainability strategies to sensor and material science fields, a new synthetic strategy for preparing colorimetric solid sensors that incorporates ILs is investigated, with the hypothesis that ILs can provide changes in the composite morphology, which permit achieve more sensitive sensors. The mass nature of the sensor was demonstrated and kinetic parameters were established. Its adsorption capacity was better described by the Langmuir isotherm and results suggested that the analytes were adsorbed on homogeneous adsorption sites of the sensor, considering a chemisorption mechanism. Other contribution is in the subject of calibration of passive sensor. Flexible calibration was possible in function of the sampling time, temperature and sampling volume. It is shown that the IL-NQS-PDMS sensor is capable of discriminating between primary and secondary amino groups in atmospheres. PDMS is one of the most employed polymers since it shows low manufacturing cost, easy fabrication, optical transparency, low toxicity, non-flammability, flexible/stretchability and gas permeability. The fact that the NQS colorimetric derivatizing reagent is entrapped by using a sol-gel process can be considered as a smart strategy to develop responsive colorimetric sensing devices. This promising sensing platform has been successfully implemented for the determination of primary and secondary amines [111–113]. However, upon the exposure to ammonia or ammonium, these sensing platforms have shown low performance. In the present paper, the sensitivity of the sensing membrane has been increased by adding the IL. It can be considered as a green, rapid and inexpensive method for analytical purposes [120].

Therefore, the employment of PDMS-NQS-IL sensor could be a new potential green and cost-effective alternative to in-situ analysis of meat freshness in reference to that published [285–288] and then this paper contributes to sustainable analytical chemistry. Reference [287] shows also a colorimetric sensor, its response is due to pH changes instead of a nucleophilic reaction between amine groups and NQS. Then, IL-NQS-PDMS sensor can improve the selectivity of the ammonia quantification liberated from the meat sample. It is only shown that the presence of sulfide does not interfere in the sensor ammonia response.

### 4.3.2 New approach for Griess reaction based on reagent stabilization on PDMS membranes and ZnNPs as reducing of nitrates. Application to waters from canned and fresh vegetable samples

In the present work, a new approach was developed for the Griess reaction (previously studied in section 4.1.2 for environmental samples) based on the use of PDMS detection membranes doped with Griess reagents to determine nitrite and/or nitrate in water of fresh and canned vegetables. Griess reagents were entrapped in confined PDMS and IL compounds. The influence of some doping compounds on the properties of PDMS membranes, such as TEOS, and / or IL, was studied. The addition of TEOS to the membrane improved the hydrophilic character of the membrane [111]. OMIM-PF<sub>6</sub>, which is hydrophobic and insoluble in water, was used and confined in the organic polymeric matrix (PDMS-TEOS), giving the membrane a spongy structure, which led to increased sensitivity of the sensor. Firstly, optimization and response studies of PDMS/TEOS-SiO<sub>2</sub>NPs-SA-NEDD-OMIMPF<sub>6</sub> were performed; the results obtained are described in section 4.1.2. In PDMS/TEOS-OMIM-PF<sub>6</sub> membrane the SA/NEDD reagents are stable over time and could be released to a solution to carry out the derivatization reaction, giving satisfactory results in 5 min. To apply the procedure to nitrate, dispersed ZnNPs were used. ZnNPs dispersed in CTAB-SDS surfactant mixture was required to increase control over the nitrate reduction reaction to nitrite, which was with a satisfactory result within 3 minutes (**Figure 4.1.8**). Analytical responses were obtained by measuring absorbance or using RGB components of digital images. Results indicated good precision (RSD <8%) and good stability of the sensing membrane. The detection limit reached was 0.01 and 0.50 mg/L for nitrite and nitrate, respectively (**Table 4.3.3**). The practical application of the sensors was demonstrated through the analysis of different environmental waters (section 4.1.2), and waters of canned vegetables and fresh vegetables, which will be studied in this section.

Regarding to the liquid of the canned and the boiled water obtained from vegetables, two different samples of two different green leaves vegetables were analyzed. The samples were diluted in order to be analyzed. The concentrations of



nitrate found in the samples are shown in **Table 4.3.3**. The accuracy of the method was evaluated by spiking the samples with different nitrate concentrations. For all the concentrations studied the recoveries were about 100 % with relative errors lower than 10%. Based on these results we can conclude that no matrix effect was observed in these samples and the concentration can be directly determined by using external calibration. Validation of this methodology was carried out by comparing the results with those obtained using an ISE electrode for nitrate and UV-vis spectrometry methods [180]. For a level of significance of 95%, there were no statistically differences between the results of both methods. The found concentrations in the liquids from canned vegetables and boiled fresh vegetables were lower than those established in the CE legislation [324] that establish a maximum of 2000 mg of nitrate per Kg of vegetable. These results indicated the consumption of the liquid from canned vegetables or from the boiled water from fresh vegetables can result in a high source of nitrates in the diet. The results obtained between fresh and canned vegetables were similar.

**Table 4.3.3** Found concentrations in canned and fresh food green vegetables. Recoveries corresponding to samples fortified with standard nitrate solution (5 mg/L).

Food Samples		Found concentración NO <sub>3</sub> <sup>-</sup> (mg/L) (n=3)		Recovery (%) *
		Method A	Method C	
Canned food	Chard	1103 ±60	1210±90	103.9 ±0.4
	Spinach	810 ± 40	-	107.3±0.2
Fresh food	Chard	1600±100	1700±70	93.0±0.4
	Spinach	990±40	980±70	104.0±0.5

Method A - nitrate detection using the sensor \* Recovery values for method A; Method C - nitrate detection using  $\text{NO}_3^-$  ISE electrode.

### Conclusions

The proposed method was based on the detection of nitrate and nitrite analytes in waters of canned and fresh vegetable samples by doping PDMS/TEOS-IL sensing membrane with Griess reagents. As has been mentioned before the reagents of the Griess reaction were unstable outside the membrane, being stable for more than 3 months inside the synthesized composite. SA-NEED reagents doped on the sensor were diffused into the aqueous solution by performing nitrite derivatization. In the case of nitrate, the dispersion of ZnNPs was used as a reducing agent. ZnNPs dispersions were stable at room temperature for more than 3 months, as well as Griess reagent in the PDMS-TEOS-OMIM- $\text{PF}_6$  support. The analytical response was obtained by measuring the absorbance or RGB coordinates of the sensing membrane image. The results were satisfactory reached at the detection limit of 0.01 and 0.5 mg/L for nitrite and nitrate, respectively, and with good precision (RSD <8%). Based on these results a quick assay for quantitative determination of nitrate or nitrite in real samples has been developed. Nitrite was directly determined by using the Griess reagent membranes while nitrate required the reduction step with ZnNPs. Waters from canned and fresh vegetables were directly processed and any sample treatment was required. The advantages of the proposed method with respect other reported in the literature are related to the portability, low cost and short analysis time. The results indicated that the method would be very competitive in the routine in-situ analysis for food waters samples and it is a contribution to sustainable analytical chemistry.

#### **4.4 Forensic sample**

In this section, organic gunshot residues (OGSR) were analysed in order to obtain complementary information about these samples, strengthening the probative value of the forensic sample. Diphenylamine was selected as the issues related to false positives and negatives can be resolved by combined inorganic gunshot residues (IGSR) and OGSR analysis.

##### **4.4.1 Estimating diphenylamine in gunshot residues from a new tool for identifying both Inorganic and organic residues in the same sample**

In this section a method involving the collection and determination of OGSR and IGSR on hands using on-line IT-SPME-CapLC-DAD and scanning electron microscopy coupled to energy dispersion X-ray (SEM-EDX), respectively, for quantifying both residues was developed. The main objective was the determination of DPA in the hands of shooting as organic residue for gunshot. Due to DPA remains at low amounts on hands after discharge a firearm, factors such as the nature and length of the extractive phase and volume of sample processed have been investigated and optimized to achieve high sensitivity. Prior to chromatographic analysis, the procedure of DPA extraction from hands was also optimized. For this purpose, several samplers, assisted-extractions and solvents have been tested. The best extraction efficiency was achieved by using dry cotton swab followed by vortex-assisted extraction with water in a few seconds. Under the optimum conditions, the analytical performance has been successfully achieved. Satisfactory LOD (0.3 ng) and precision (RSD intra-day 9%) were obtained. The utility of the described approach was tested by analyzing several samples of shooter hands. DPA was found in the 81% of the samples analyzed. A complementary analysis of inorganic gunshot residues by SEM-EDX and optical microscopy was carried out. Both analyses provide a significant evidence of firearm discharge for forensic investigations.

### Optimization of the IT-SPME and chromatographic conditions

First of all, the DPA extraction by IT-SPME was optimized, as well as the subsequent chromatographic analysis. Initially, two mobile phase compositions were tested in isocratic mode, 60:40 and 70:30 ACN: H<sub>2</sub>O (v/v). According to the results obtained (**Figure 4.4.1A**), both mobile phases were suitable for desorbing the DPA from the extractive capillary. However, a decrease in retention time and narrower peaks were achieved with increasing ACN and flow. In the course of this study, we found DPA residues in blanks of nanopure water after analysis when using isocratic elution with 70% of ACN. Therefore, a gradient elution program with 100% ACN for 4 min as a cleaning solvent was used to elute the DPA retained in the extractive capillary.

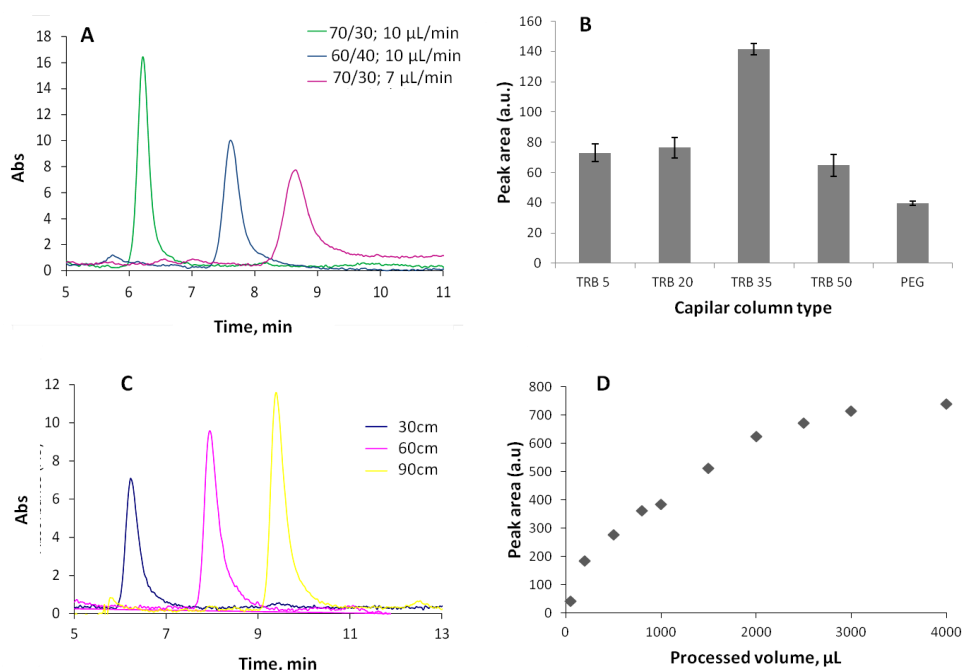


**Figure 4.4.1** Effect of **A)** acetonitrile percentage and flow of mobile phase (800 μL at 7 ng/mL, TRB-35, 30 cm) **B)** nature of the extractive phase (800 μL at 5 ng/mL, capillary length 30 cm, optimum mobile phase) **C)** capillary length (800 μL, 5 ng/mL, TRB-35, optimum mobile phase) and **D)** sample volume processed (5 ng/mL, TRB-35, capillary length 90 cm, optimum mobile phase) on the DPA retention in IT-SPME.

IT-SPME was performed using a capillary column as the loop of the injection valve. The analytes were extracted during sample loading and were transferred to the analytical column with the mobile phase by changing the valve position. This configuration is advantageous in order to achieve LODs required for detecting DPA deposited on shooter hands. Several trials were performed to achieve extraction optimization. The extraction of DPA was optimized by evaluating the extractive phase, the column capillary length and the injected sample volume. As an extractive phase, 5 types of columns capillary were studied: TRB 5, 20, 35, 50 and PEG.

According to the results obtained, the best analytical response (mean peak area) was obtained with TRB35 capillary (**Figure 4.4.1B**). This suggested that higher percentage of diphenyl groups in the extractive phase led to increase on the analytical response. It can be deduced that extraction involved  $\pi$ - $\pi$  interactions with DPA, through two aromatic rings. Nevertheless, TRB-50 resulted in a decrease on the analytical response, this effect was in accordance with the increment on the polarity of the extractive phase and so, the affinity towards the DPA decreased ( $\log K_{ow} = 3.5$ ). The same effect occurred with the PEG capillary due to its high polarity. Hence, the TRB-35 capillary column was selected for further experiments. The next step was the study of the capillary length. Capillary columns with lengths 30, 60, 90 cm were tested under the optimal conditions. **Figure 4.4.1C** shows the increase in the analytical response as a function of the capillary length. Thus, the amount of analyte extracted also increased. The analytical response was improved 40% and 47% with 60 and 90 cm capillary columns, respectively, compared to the 30 cm. Capillaries experimented longer than 90 cm did not improve analytical response. Therefore, the 90cm TRB-35 capillary column was selected as the optimal length for future trials.

Sample volumes up to 4 mL (5 ng/mL of DPA) were studied (**Figure 4.4.1D**). Based on the results obtained, a notable increase in the analytical response was observed as a function of sample volume up to 2 mL.

The signal increased very slightly from 2 to 4 mL and 2 mL was chosen as the optimum sample volume for further experiments. However, it was found that the swabs used in the present study absorbed about 125  $\mu\text{L}$  of contact solution. According to this observation, further experiments were carried out by processing 1800  $\mu\text{L}$  remaining in vial. The extraction efficiencies of the proposed methodology were estimate by comparing the amount of analyte extracted, which is the amount of the analyte transferred to the analytical column, with the total amount of analyte passed through the optimum extraction capillary. The amount of analyte extracted was established from the peak areas in the resulting chromatograms and from the calibration equations constructed through the direct injection of 72  $\mu\text{L}$  of standard solutions of the analyte. This volume was the inner volume of the TRB-35 capillary of 90 cm used for IT-SPME. The extraction efficiency obtained was 7%, which is in accordance with those reported for this technique [37,325]. In addition, the solution removed from the swab was filtered with a Nylon filter (0.45  $\mu\text{M}$ ), to confirm that no remaining fiber from the swab passed onto the column. However, the analyte was not observed because it was retained on the nylon filter. Therefore, the samples were not filtered prior to injection. Finally, a clean-up step was applied with 120  $\mu\text{L}$  of nanopure.

### **Study of DPA extraction optimization**

The procedure for the extraction of DPA from the collector was optimized by choosing the appropriate procedure. For this aim, non-assisted, ultrasound-assisted and vortex-assisted extraction of the analyte from a cotton swab, which is commonly used as collector, was tested. To test this, 3  $\mu\text{l}$  of 10  $\mu\text{g}/\text{mL}$  DPA working solution (prepared in ACN to favor evaporation) was spread on a glass slide. After it was air evaporated to dryness, a dry cotton swab was used to extract DPA from the slide. A tip of the cotton swab was introduced into a vial containing 2 mL of water under the three abovementioned conditions for 5 min. As can be seen in the **Figure 4.4.2A** the vortex assisted extraction results were better compared to non-assisted extraction and ultrasound-assisted in terms of both analytical response (peak area) and RSD. So the vortex extraction was chosen for the next tests.

## Chapter 4. Results and Discussion

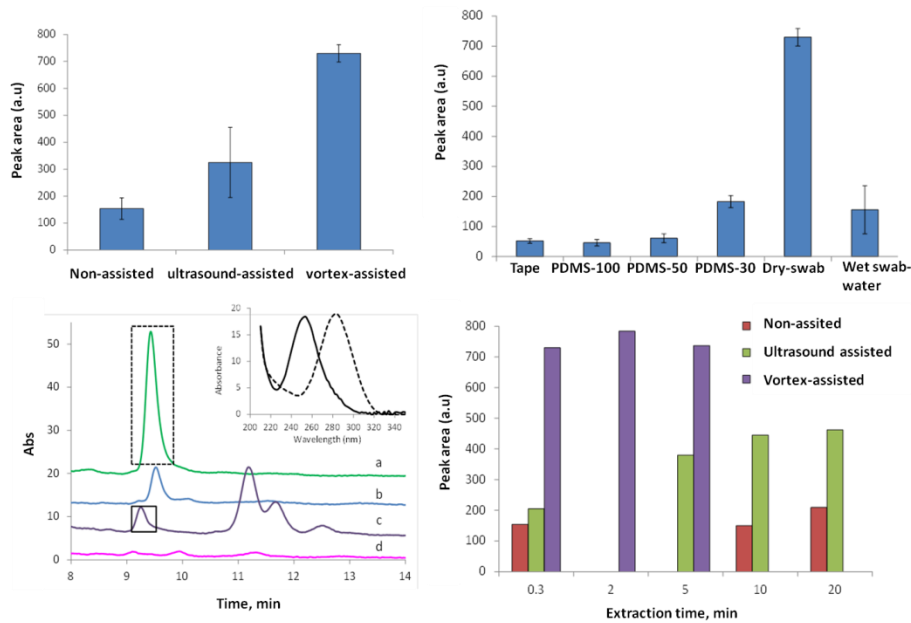


**Figure 4.4.2** Comparison of peak areas obtained for standard solution ( $3\mu\text{L}$  of  $10\mu\text{g/mL}$  in  $2\text{ mL}$  of water,  $15\text{ ng/mL}$ ) with different **A)** extraction modalities **B)** sample collectors **C)** extraction time and **D)** effect of solvents to wet cotton swab (at  $10\text{ ng/mL}$ ) together with normalized spectra (inset) of DPA (black dashed line) and unknown compound (black solid line).

On the other hand, several sampling tools were also tested and optimized for DPA collection from shooter hands. For which,  $3\mu\text{L}$  of a  $10\mu\text{g/mL}$  DPA standard solution was poured onto a glass slide, allowing it to evaporate in the air, then solid DPA was collected with various sampling tools and put in contact with  $2\text{ mL}$  of water in vortex conditions. **Figure 4.4.2B** compares the mean peak areas of DPA extracted from slides and the RSDs to determine the suitability of the several sampling devices tested: adhesive tape lift, PDMS-based device of several PDMS:TEOS proportions (100:0, 50:50 and 70:30), dry cotton swab and wet cotton swab with non-skin-toxic solvents such as water, acetone and ethanol.

According to the 24 European Chemicals Agency (ECHA) database [326] methanol and acetonitrile were not used due to their harmfulness and toxicity in contact with the skin, respectively.

The dry cotton swab provided the highest analytical response with satisfactory precision. The adhesive tape lift, showed an analytical response about 14 times lower than the dry cotton swab. Similar peak area loss was observed with pure PDMS-based device. However, low analytical response was achieved when the TEOS proportion increased in the composition device. In the case of PDMS:TEOS (30:70) device, the analytical response was improved 4 times, compared with the response with pure PDMS device. This effect can be attributed to the increment of the device hydrophilicity as a function of the TEOS amount, suggesting the improvement of analyte extraction from device to the aqueous solution. The analytical response was decreased when using the moistened swab with water and ethanol, comparing with the dry swab, a decrease in the response was observed by 80% and 97% respectively, Probably the wet swab spread the analyte on the surface of the slide and the value RSD > 30% so high also showed it. When acetone was used as the extraction solvent, no DPA was detected, but a small peak was observed at a retention time slightly less than that of the analyte (**Figure 4.4.2C**). As can be confirmed by the spectra depicted in the box in **Figure 4.4.2C**, this peak could be differentiated from the analyte peak by retention time and spectrum and could correspond to some compound from a cotton swab. Based on the results obtained, a dry cotton swab was chosen as the best collector for DPA samples from shooters hands for further work.

Similar to the sampler optimization, peak areas of DPA were compared against different extraction times under selected conditions: 20 s, 1, 2 and 5 min, as shown in **Figure 4.4.2D**. Longer times were not tested due to the discomfort with the manual vortex.

No significant differences on peak areas were observed at several extraction times. Additionally, long times for non-assisted and ultrasound-assisted extraction was also studied in order to investigate the improvement of analytical response but neither extraction was as satisfactory as vortex assisted. Therefore, 20 seconds was selected as the assisted vortex extraction time to extract the DPA from the hands to the proper level and in a short time.



The capacity of three solvents to extract the DPA analyte from cotton swabs was investigated: acetonitrile, ethanol, and water. Mixtures of Water/ACN and Water/Ethanol (90:10) and 100 % water were tested. A 51% and 85% of decrease on peak area was observed when ethanol and ACN, respectively, was included in extraction solvent (**Figure 4.4.3**). Probably, the analyte was not retained on the IT-SPME capillary column. Moreover, high peaks were observed at a retention time slightly lower than the analyte. In the analysis of the DPA standard solution these peaks were not detected, suggesting that they were due to compounds extracted from cotton. Note that ethanol was the solvent which extracted more amount of interfering compounds. However, water offered the best results in terms of extraction and reduced interferences, as well as green solvent. Therefore, water was chosen as optimum extraction solvent.

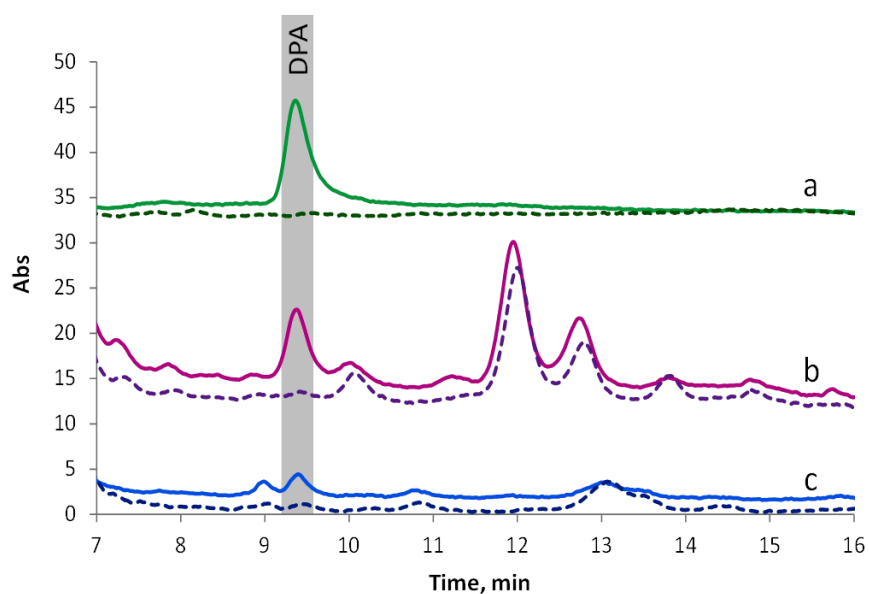


**Figure 4.4.3** Chromatograms of blanks (dashed lines) and standard solution of 5 ng/mL DPA (solid lines) obtained with different extraction solvents: water (**a**), 90:10 water: ethanol (**b**) and 90:10 water: acetonitrile (**c**).

## Analytical performance

Relevant analytical parameters such as calibration equations, linear working range, limit of detection (LOD), limit of quantification (LOQ) and precision are shown in **Table 4.4.1**, both standard solution and DPA extraction from hand samples. Satisfactory linearity within the tested concentrations was achieved. The LODs and LOQs were calculated experimentally from solutions containing concentrations providing signal/noise of 3 and 10, respectively. LODs and LOQs for DPA extracted from hand samples were 0.15 ng/mL and 0.5 ng/mL, respectively.

**Table 4.4.1** Analytical parameters obtained with the proposed method to determine DPA in standard solutions and extracted from real samples.

Matrix	Linear range (ng/mL)	Calibration curve $y = a + bx$ (ng/mL)			Precision (n=4, 15 ng/mL)		LOD (ng/mL)	LOQ (ng/mL)
		$a \pm s_a$	$b \pm s_b$	$R^2$	RSD <sub>intra-day</sub> (%)	RSD <sub>inter-day</sub> (%)		
Standard solutions	0.15 - 50	-7 ± 57	144 ± 2	0.999	5	10	0.05	0.15
Hand samples	0.5 - 25	-13 ± 24	49.2 ± 1.7	0.994	9	14	0.15	0.5

The results obtained regarding precision (%RSD) were satisfactory with values of 9% and 15% for intra- and inter-day respectively. The precision of the retention times was also estimated obtaining acceptable RSD values of 1.5% and 2.5% for intra and inter-day, respectively (n=3,15 ng/mL). Satisfactory results for the study in solution were obtained as depicted in Table 3. To test the efficiency of DPA extraction from the samples, the peaks obtained from the extraction of DPA from cotton swabs were compared with the peak from the standard solution injected directly, taking into account the same DPA concentrations (5 ng/mL) in two cases. The extraction efficiency estimated was  $37 \pm 5\%$ . A recovery was valued using spiked samples, obtaining following value  $108 \pm 16\%$ .

### **Samples analysis**

Several samples collected from hands of police officers before and after shooting test were analyzed by the proposed and optimized procedure. Samples collected before shooting served as blanks. The samples were analyzed without identification of volunteers. **Figure 4.4.4** shows the chromatograms for shooter (sample 2A) and non-shooter hand samples and UV-Vis spectra of standard and sample. Although unknown compounds were extracted from shooter hands, DPA was identified in samples by the concordance between retention time (9.4 min) and UV-Vis spectra of standard DPA and the suspect peak in the chromatogram of the sample. Taking into account the chromatography of a blank showed no peak interferences in the retention time of DPA (**Figure 4.4.4**).

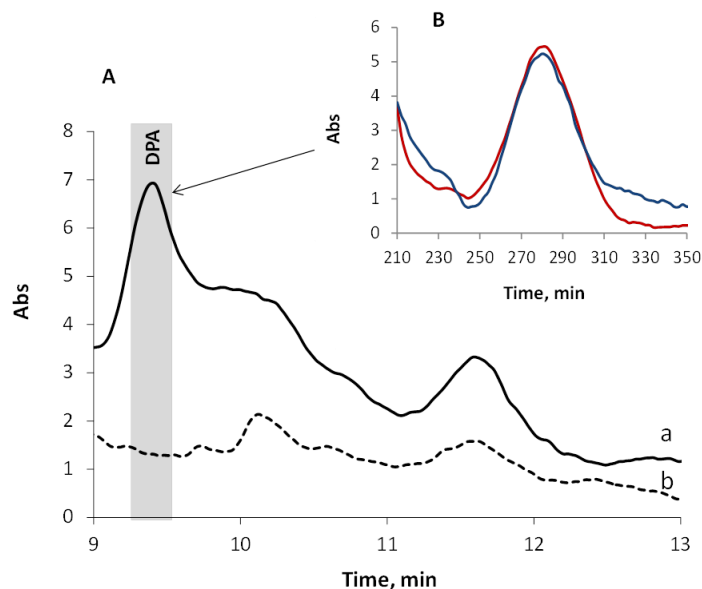


**Figure 4.4.4 (A)** Chromatograms obtained for sample 2A (black solid line) and blank of non-shooter hand (black dashed line). **(B)** DPA spectra found (blue line) in reference to the library of the standard (red line).

**Table 4.4.2** shows the samples screened and the quantification results. With a total of twenty one swab samples and six tape kit samples, DPA was found and quantified in seventeen swab samples (81% of all swab samples analyzed) and, as can be expected due to tape lift was worth sampler, three tape samples produced a signal above LOQ but DPA was not detected in the other three. In the literature, few studies of DPA are focused in hands and LODs reported are higher to that provided by the proposed method (**see Table 1.10**). In this work, the amount of DPA found in hands exceeded LOQ, providing forensic evidence for the presence of DPA. The paired t test was used to evaluate statistically differences between both hands of a shooter, left and right. The  $\alpha$  value obtained at 95% significant level was higher than 0.05 ( $\alpha=0.232$ ). From these results, we can conclude that the results from both hands were statistically equivalent.

**Table 4.4.2** Samples screened, quantification results of DPA on hands determined by optimized extraction procedure followed by in-tube SPME-CapLC-DAD. \*Tape lift kit samples quantified by regression equation 14 times lower than regression equation by cotton swab. \*\* On shooters hands.

Police officer	Sample	Hand	Number of shots	Concentration (ng)
<b>A</b>	1 A	left	25	4.4
	2 A	right		3.8
<b>B</b>	3 B	left	12	2.7
	4 B	right		1.9
<b>C</b>	5 C	left	25	3.0
	6 C	right		3.8
<b>D</b>	7 D	left	25	2.8
	8 D	right		< LOD
<b>E</b>	9 E	left	25	2.5
	10 E	right		3.2
<b>F</b>	11 F	left	25	16.5
	12 F	right		13.4
<b>G</b>	13 G	left	25	< LOD
	14 G	right		< LOD
<b>H</b>	15 H	left	25	4.9
	16 H	right		< LOD
<b>I</b>	17 I	left	25	8.4
	18 I	right		9.5
<b>J</b>	19 J	left	25	8.0
	20 J	right		4.3
<b>K*</b>	21 K	left	25	< LOD
	22 K	right		< LOD
<b>L</b>	23 L	left and right	25	1.4
<b>M*</b>	24 M	left and right	25	3.6
<b>N*</b>	25 N	left and right	25	6.6
<b>O*</b>	26 O	left and right	25	6.9
<b>P*</b>	27 P	left and right	25	< LOD

### IGSR particles identification

As can be seen in Figure 3, the presence of GSR particles from cotton swabs can be confirmed by naked eye and microscopically before chromatographic analysis. Clean fibers of cotton swab can be seen after sampling a non-shooter hand (**Figure 4.4.5A**). Nevertheless, gunpowder particles with typical spherical shape and size up to 20  $\mu\text{m}$  [327] were observed between cotton fibers (see red circles) after sampling a shooter hand (**Figure 4.4.5B**). It should be noted that this microscopic analysis was not destructive allowing subsequent DPA chromatographic analysis.

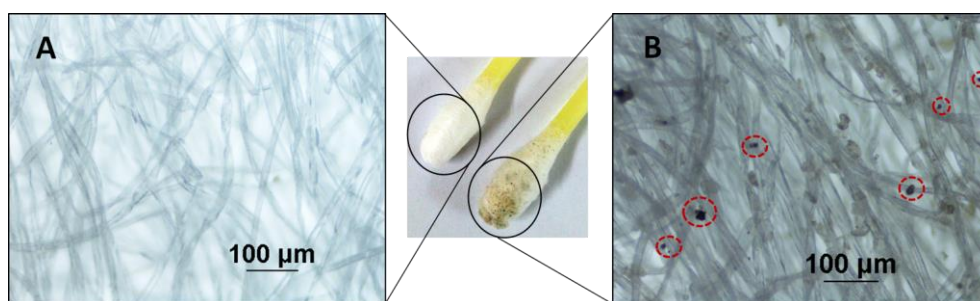


**Figure 4.4.5** Visual and microscopy (10x magnification) inspection of cotton swab after sampling a non-shooter hand (**A**) and after sampling a shooter hand (**B**).

**Figure 4.4.6** shows the same cotton sample (sample 2A) shown in **Figure 4.4.5** but characterized by SEM/EDX after DPA extraction. This was possible due to the presence of some gunpowder particles remaining on the cotton swabs after the DPA was extracted. **Figure 4.4.6** shows a typical IGSR particle with a spherical shape and 38  $\mu\text{m}$  size in accordance with References [260,328]. As can be observed in the elemental analysis, the predominant elements were Ba (46%) and Sb (44%), as reported in the literature for IGSRs [258]. Both inorganic and organic compounds were identified on shooters hands by SEM/EDX and chromatography, respectively. Hence, the presence of GSRs on the hands of shooters was confirmed.

The other aim of this work was to examine the morphology and elemental composition and distribution of GSR particles collected with the lift tape kits, the typical police collector. Only particles which can be identified as GSR by their composition and morphology were selected for SEM/EDX analysis. Roughly 6–7 particles per sample were studied as can be seen in Table 5. As reported by Bailey et al.[327], this number of particles is approximately equivalent to the particles that can be recovered on a shooter's hand at a forensic scene. A portion between 3–40% of the total surface of the sample was explored to find this number of particles, depending on the sample. **Figures 4.4.7** and **4.4.8** show the morphology and elemental data of particles found on adhesive tapes collected after shooting. Most of the particles observed were spherical. Less than 20% of particles found had an irregular shape, probably due to being distorted after shooting.

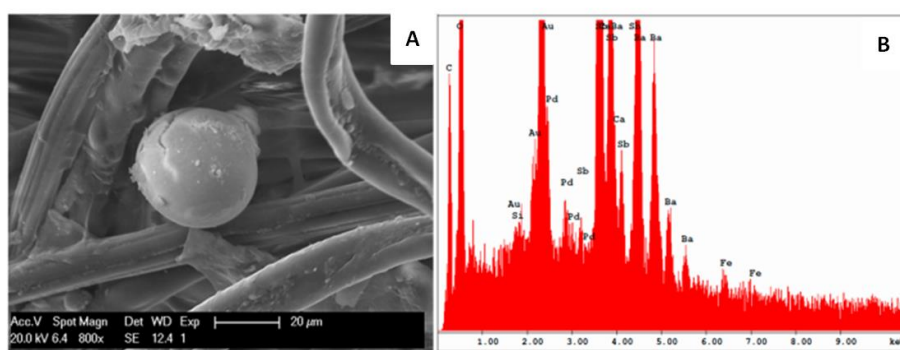


**Figure 4.4.6 A)** SEM image and **B)** Energy dispersion X-ray EDX spectra of inorganic gunshot residue found on a swab sample (sample 2A) after shooting.

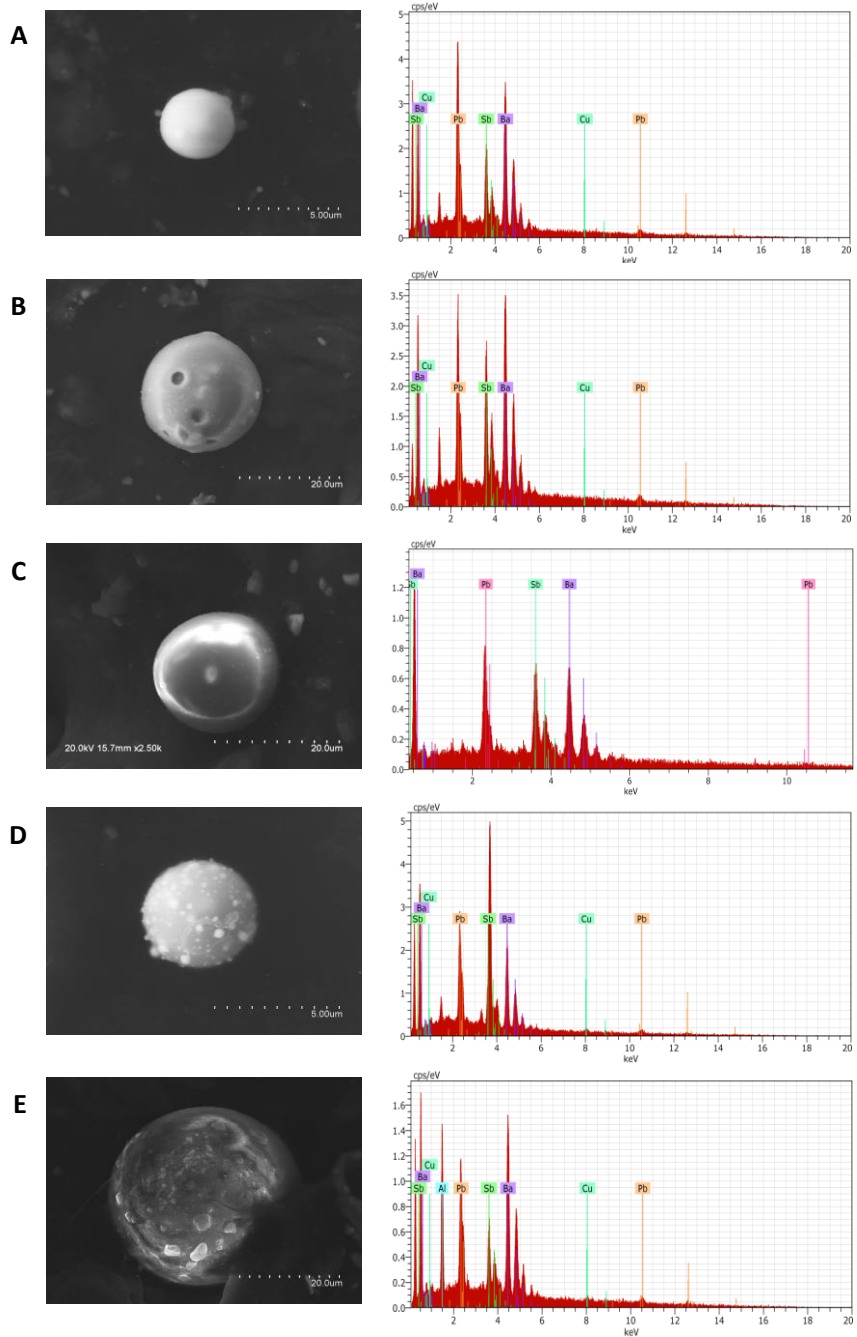


**Figure 4.4.7** SEM images (left) and EDX spectra (right) of non-spherical particles found on tapes used to collect GSRs after shooting a pistol: sample 22K.2 (A), sample 25N.3(B), sample 21K.1 (C), sample 25N.2 (D).



As shown, particles had different surfaces such as smooth, bumpy or covered with craters with or without a metallic shine. More than 60% of the particles found had a smooth surface. Their morphology was an effect of conditions taking place during the firing. Particles can be perforated, capped, broken or stemmed. Results of the SEM/EDX analysis of GRS particles found on the tapes from shooters' hands are displayed in **Table 4.4.3**.

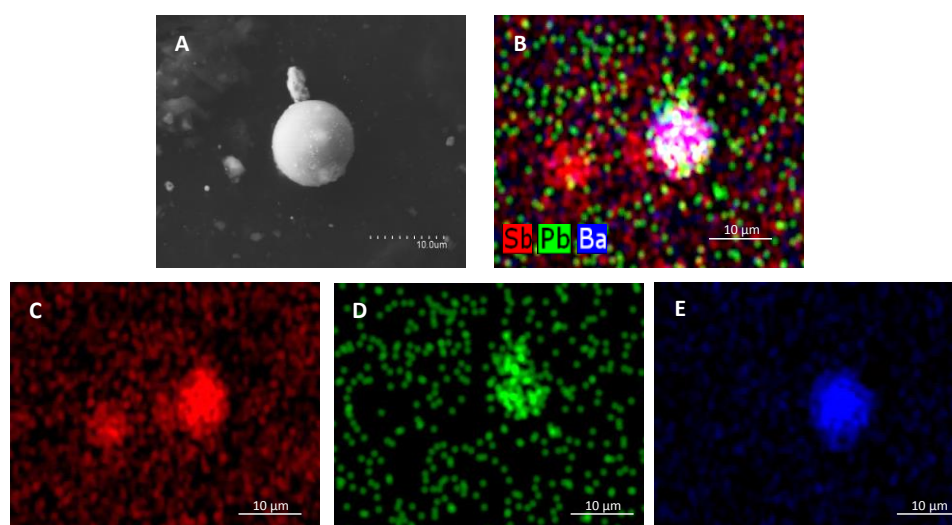


**Figure 4.4.8 (A)** SEM image **(B)** overlay X-ray map of singles X-ray of Sb **(C)**; Pb **(D)** and Ba **(E)** of particle found on a tape used to collect GSR on hands after shooting.

As observed in **Table 4.4.4**, most of the particles had the characteristic elemental composition of GSRs, which was mainly based on Pb, Sb, and Ba; 35 particles contained on average 61% Ba, 30% of Sb, and 9% Pb, and other two particles contained 95% Pb and 97% Sb, probably from bullets, shells or cartridges. Moreover, some particles also contained other elements such as Al, Cu, and Fe at trace levels. About 66% of samples contained traces of Cu, 20% Al, and 3% Fe, while 12% of them contained both Al and Cu. However, these minority elements cannot be considered evidence of firing a gun. Even though these particles had similar elemental composition, their size varied over a range from 3 to 30 µm according to the bibliography [258,260].

**Table 4.4.3** Summary of shape, surface, and elemental composition of GRS particles found on tape lift kits from shooter hands.

	GSR particle	Shape	Surface	Elemental composition (%)					
				Major			Minor/Trace		
				Ba	Sb	Pb	Cu	Al	Fe
<b>21K</b>	21K.1	Irregular	Nonmetallic bumpy	62.5	33.2	4.3	x		
	21K.2	Spherical	Nonmetallic smooth	62.4	25.7	11.9	x		
	21K.3	Spherical	Nonmetallic bumpy	65.9	18.8	15.3	x		
	21K.4	Spherical	Nonmetallic bumpy	46.8	40.2	13.0	x		
	21K.5	Spheroidal	Nonmetallic smooth	65.7	14.8	19.5	x		
	21K.6	Spherical	Nonmetallic smooth	87.5	11.1	1.4	x		
	21K.7	Spherical	Nonmetallic bumpy	58.4	28.8	12.8	x		
<b>22K</b>	22K.1	Spherical	Metallic smooth	61.5	33.5	5.0	x		
	22K.2	Irregular	Metallic bumpy	98.8	0.7	0.5			
	22K.3	Spherical	Nonmetallic smooth	48.0	37.3	14.7			
	22K.4	Spherical	Metallic smooth	57.0	37.1	5.9	x		
	22K.5	Spherical	Metallic smooth	61.8	32.7	5.5	x		
	22K.6	Spherical	Metallic smooth	79.0	16.8	4.2	x		
	22K.7	Spherical	Nonmetallic with hollows	50.6	33.4	16.0	x		
<b>24M</b>	24M.1	Spherical	Metallic smooth	63.0	34.8	2.1			
	24M.2	Spherical	Metallic smooth	63.2	30.6	6.3			
	24M.3	Spherical	Nonmetallic smooth	0.0	96.7	3.3		x	
	24M.4	Spherical	Metallic smooth	60.4	37.2	2.3		x	
	24M.5	Spherical	Nonmetallic smooth	51.1	34.5	14.3	x	x	
	24M.6	Spherical	Metallic smooth	69.2	20.3	10.5	x	x	
	24M.7	Spherical	Metallic smooth	54.8	37.3	7.9	x	x	

	<b>25N.1</b>	<b>Spherical</b>	<b>Metallic smooth</b>	<b>68.8</b>	<b>24.7</b>	<b>6.4</b>		<b>x</b>
<b>25N</b>	25N.2	Irregular	Nonmetallic bumpy	72.0	17.8	10.2	x	
	25N.3	Spheroidal	Metallic bumpy	63.3	30.0	6.7		
	25N.4	Spherical	Metallic smooth	53.0	39.7	7.4	x	
	260.1	Spherical	Metallic smooth	63.6	34.2	2.2		
	260.2	Spherical	Metallic smooth	61.7	35.2	3.0		x
	260.3	Irregular	Nonmetallic smooth	40.0	33.8	26.2		
<b>260</b>	260.4	Spherical	Metallic smooth	0.3	4.9	94.9	x	
	260.5	Spherical	Metallic smooth	62.7	31.2	6.3		
	260.6	Spherical	Metallic smooth	50.6	35.8	13.6		
	27P.1	Spherical	Nonmetallic bumpy	53.5	38.3	8.2	x	x
	27P.2	Spherical	Nonmetallic bumpy	57.4	30.9	11.7	x	
<b>27P</b>	27P.3	Spherical	Nonmetallic smooth	60.2	36.9	2.9	x	
	27P.4	Spherical	Nonmetallic smooth	57.6	30.9	11.5	x	
	27P.5	Spheroidal	Nonmetallic bumpy	48.9	30.7	20.5	x	
	27P.6	Spherical	Nonmetallic bumpy	61.3	31.7	7.0	x	

Spatial distribution of the Sb, Pb, and Ba of GSR particles shown in Table 5 was observed by X-ray mapping using colors to represent the elemental distribution. In this case, Sb appears red, Pb is green, and Ba is blue. **Figure 4.4.8** shows the X-ray mapping of sample 21K together with its corresponding SEM image. Figure 9B gives the merging of Figure 9C–E. As can be seen, the GSR particle presented the three elements Sb, Ba, and Pb together. Thus, these mapping results were in accordance with the previous elemental composition studied (**Table 4.4.3**). The results obtained by SEM/EDX can be considered as indicative of IGSR particles on shooters hands.

## Conclusions

This work proposed the sampling of gunshot residues on shooters' hands using dry cotton swabs followed by vortex-assisted extraction with water over a short time (20s). Aqueous samples were directly processed in the miniaturized IT-SPME-CapLC-DAD system for on-line clean-up and preconcentration of the sample and for quantization of the amount of diphenylamine as targeted organic residue. It is worth mentioning that non-toxic solvents and low-cost materials were employed. The efficiencies of the IT-SPME were tested for several compositions and lengths of the extractive phase, as well as sample volume processed in order to improve the sensitivity.

The highest analytical responses were obtained for the longest TRB-35 capillaries (90 cm) were more likely due to  $\pi$ - $\pi$  interactions and 1.8 mL of processed volume. The proposed approach is a rapid, green, and cost-effective option for detecting DPA on the hands of shooters contributing to sustainable analytical chemistry.

The sustainability of an analytical method is governed by minimization of toxic solvents, reduction of wastes, and employment of energy-efficient and cost-effective methodologies, but also on maintaining the reliability of the performance parameters, such as sensitivity, precision, and accuracy [329,330]. In two previous papers [297] our group demonstrated that IT-SPME-CapLC-DAD achieves the minimization of the sample pre-treatment step, analysis time, and wastes, the reduction of the analysis costs, and thus, improvement of the analytical and environmental performance. Satisfactory LOD (0.3 ng) and precision (RSD intra-day = 9%, RSD inter-day = 14%) were achieved. In order to test the utility of the method for real cases, several shooters' hands were sampled by dry cotton swabs and processed by IT-SPME-CapLC-DAD. The results showed that DPA was found and quantified in 81% of samples. Additionally, IGSRs inspection of swab samples was carried out by optical microscopy in order to confirm the presence of gunshot residues on shooters hands, which were analyzed by SEM-EDS after DPA extraction. Furthermore, some shooters' hands were sampled by a tape lift kit, which is the typical police sampler, but DPA extraction was fourteen times lesser than that achieved by the dry cotton swab sampler. Morphology, elemental composition, and distribution of the IGSRs particles were also studied. Then, improved results were obtained by the proposed sampling method as indicated above. If organic compounds are detected in combination with inorganic compounds, higher probative value can be achieved, and false positives/negatives can also be reduced for discriminating shooters hands.

In this work, a sensitive chromatographic method to detect the organic compound DPA can be combined with IGSR analysis by SEM-EDS in order to obtain valuable evidence of GSRs deposited on hands of a suspected shooter. Therefore, the proposed method is helpful to determine whether a person has fired a gun in a forensic investigation.



## **CHAPTER. 5 GENERAL CONCLUSIONS**





This Thesis focuses on the study of new analytical strategies to improve sustainability in the qualitative and/or quantitative analysis of different matrices such as environmental, biological, food and forensic. The matrices have an impact role in the designs of the analytical methods. For this purpose, sustainable analytical methodologies have been developed and improved contributing to Sustainable Analytical Chemistry. Thus, the analytical methodologies studied in this Thesis have been based on miniaturization, automatization and in situ analysis.

**In tube solide phase microextraction:** (IT-SPME) technique can be implemented on line with the chromatographic system, reducing the analysis time, energy consumption, the amount of solvents and waste generated. On the other hand, the miniaturization of chromatographic technique entails a significant increase in sensitivity and a lower consumption of solvents, therefore being more environmentally sustainable. Consequently, the use of methodologies based on the coupling of IT-SPME to CapLC is an interesting option that, on the one hand, allowed pre-treatment and cleaning of samples online and in a single step, which means an automation of the analytical process, and on the other, achieved more selectivity and sensitivity with less environmental impact.

Using the **IT-SPME-CapLC-DAD** technique, different analytes of interest have been determined such as biocides, OGSR, antibiotics and AR in the following matrices environmental, forensic and biological respectively.

**Environmental matrix:** Herbicides such as diuron and irgarol-1051 have been determined in environmental water samples. Satisfactory analytical parameters have been obtained with this technique. The LODs were 0.015 and 0.2  $\mu\text{g/L}$  for irgarol-1051 and diuron, respectively, which allowed us to perform the analysis according to the quality standards established by European regulations. In addition, this technique was also evaluated in terms of environmental performance, by calculating the carbon footprint, being a quantitative indicator of the environmental compatibility of a methodology. By comparing the methods for the determination of irgarol-1051 and diuron in **Table 4.1.2** shows that the carbon footprint varied significantly according to the pretreatment of the sample and the separation/detection technique. Therefore, IT- SPME as a sample pretreatment is a sustainable and environmentally friendly technique to estimate irgarol-1051 and diuron in environmental water samples. It has been applied to evaluate water samples from different ports of the Valencian Community, obtaining values below

the detection limit and establishing that these water masses accomplished the European directive.

**Biological matrices:** Quantifying the concentration of antibiotics in invasive medical devices can provide information about capability to penetrate biofilm. Meropenem has been determined in mucous membranes of the endotracheal tubes providing information on the efficacy offered in the treatment of infection. In the case of meropenem determination the application of the proposed technique has given rise to very low detection limits (3 ng/mL) and satisfactory precision (RSD <4%). The performance of the proposed methodology has been demonstrated by analyzing real samples using ETT tubes in patients previously treated with meropenem. Meropenem was found at concentrations of ng/mL. The recovery values showed satisfactory results (94-103%). The proposed method has proven to be a sustainable alternative not only due to its sensitivity and precision, but also due to its simplicity, cost-effectiveness, and analysis time.

**Forensic matrix:** The IT-SPME-CapLC-DAD used to determine DPA in shooting hands has achieved the minimization of the pretreatment step of the sample, the analysis time and the waste, the reduction of the analysis costs and, therefore, the improvement of analytical and environmental performance. A satisfactory LOD (0.3 ng) and precision (intraday RSD = 9%, intraday RSD = 14%) have been obtained. The utility of the described approach was tested by analyzing several samples of shooters' hands. Diphenylamine was found and quantified in 81% of the samples analyzed together with inorganic residues.

In all the cases mentioned using IT-SPME CapLC we have achieved satisfactory results not only in terms of detection limit and precision but also in terms of sustainability.

**Optical devices for in situ analysis** have been also proposed in this Thesis. PDMS doped composites and nylon based supports have been developed. These devices have some interesting properties, such as low cost, portability, low power consumption, and ease of use. These properties make them especially attractive from the point of view of sustainable Analytical Chemistry.

In this Thesis, the sensors developed have been based on two types of support: **PDMS based supports** doped following several strategies for controlling parameters as permeability, hidrofobocity, sensitivity or selectivity and **Nylon**

**support** where the dispersion of AgNP or ZnNPs has been retained. Derivatization reagents have been incorporated thereby avoiding the need to prepare unstable solutions.

Through in situ analysis, using optical sensors, different analytes of interest have been determined such as nitrite and nitrate in environmental and food matrices, H<sub>2</sub>S in biological matrices and NH<sub>3</sub> in food matrix.

**Environmental matrix:** PDMS-TEOS-OMIM-PF<sub>6</sub> sensing device doped with Griess reagent (SA-NEDD) has been proposed to determine nitrites and nitrates (previously reduced to nitrites by means of ZnNPs-(CTAB-SDS) dispersion or ZnNPs supported-nylon) in environmental waters. The results obtained have been satisfactory with limits of detection of 0.01 and 0.5 mg/L for nitrite and nitrate, respectively, and with limits of detection good precision (RSD <8%). Based on these results, rapid tests have been carried out to quantitatively determine nitrates or nitrites in real samples such as water. ZnNP dispersions were used as reducing agent, since ZnNPs present non-toxicity compared to other reducing known in the literature. Environmental water samples were processed directly without requiring any pretreatment, as it is established within the principles of sustainability in analytical chemistry. The advantages of the proposed method with respect to other reports in the literature are related to portability, low cost, and short analysis time. The satisfactory results indicated that the method can be very competitive in routine on-site analysis for different matrices of water samples.

**Biological matrices:** AgNPs–nylon individual sensing device and AgNPs–nylon multisensor (up to 96 devices) have been proposed to determine H<sub>2</sub>S in breath and cardiomyocyte cells samples. The final results obtained have been satisfactory with limits of detection of 45 ppbv and 0.13 μM for, breath and cardiomyocyte cells respectively, and with values of RSD <10% in both cases. In addition, this technique using AgNPs multisensory sheet has been also evaluated in terms of sustainable analytical chemistry, by means of the hexagon tool that shows that it offers advantages such as high sensibility, better sustainability and lower economic cost than other recent analytical methods found in the literature.

Alkylresorcinols as sensitive and specific biomarkers of gluten consumption can provide important information for the treatment of celiac disease. With this objective, PDMS-SiO<sub>2</sub> composite doped with FB colorimetric reagent was evaluated to estimate alkylresorcinols in biological samples such as urine. The

response was evaluated with UV-vis spectroscopic measurements and a chromatographic technique (in-tube SPME coupled to Capillary LC-DAD detection) to isolate the DHCA signal. Satisfactory results in terms of LOD and precision have been achieved in both cases. Under the optimum experimental conditions, detection limit of DHCA has been 60 ng/mL and RSD <7%. Satisfactory results have been obtained in studies of urine samples showing that DHHC can be used as a biomarker of gluten intake. The main advantages of the proposed methodology are the development of a pre-selection tool previous to the chromatographic analysis, and therefore the simplification of the dietary transgression evaluation.

**Food matrices:** A composite membrane containing 1,2-naphthoquinone-4-sulfonic acid sodium salt (NQS) embedded in an ionic liquid (IL)-polydimethylsiloxane (PDMS)-tetraethyl orthosilicate (TEOS)-SiO<sub>2</sub> nanoparticles (NPs) polymeric matrix is proposed. It is demonstrated that ILs chemical additives of PDMS influenced the sol-gel porosity. The sensor analytical performance for ammonia atmospheres has been tested as a function of sampling time (between 0.5 and 312 h), temperature (25 °C and 4 °C) and sampling volume (between 2L and 22 mL) by means of diffuse reflectance measurements and RGB measurements too. Flexible calibration was possible, adapting it to the sampling time, temperature and sampling volume needed for its application. Calibration linear slopes (mA vs ppmv) between 1.7 and 467 ppmv were obtained for ammonia in function of the several studied conditions. Those slopes were between 48 and 91% higher than those achieved with sensors without ILs. The practical application of this sensing device was demonstrated for the analysis of meat packaging environments, being a potential cost-effective candidate for in situ meat freshness analysis. NQS provided selectivity in reference to other family compounds emitted from meat products, such as sulphides. After 10 days at 4 °C ammonia liberated by the assayed meat was  $20 \pm 4 \mu\text{g}/\text{kg}$  and  $18 \pm 3 \mu\text{g}/\text{kg}$ , quantified by using diffuse reflectance and %R measurements, respectively. Homogeneity of the ammonia atmosphere was tested by using two sensors placed in two different positions inside the packages.

Furthermore, the PDMS/TEOS-NEDD-SA-OMIMPF<sub>6</sub> sensor proposed for nitrate determination is also suitable for quantifying the waters of food samples such as spinach and chard food analysis. As it has been mentioned previously for environmental water samples, the LODs values and precision obtained have been

## Chapter 5. General Conclusions

satisfactory, being the proposed sensing device a potential candidate for detecting harming concentration for human health.



## REFERENCES

## References

- [1] Maja, R. Fowkes, Planetary Forecast: The Roots of Sustainability in the Radical Art of the 1970s, *Third Text*. 23 (2009) 669–674.  
<https://doi.org/10.1080/09528820903189277>.
- [2] WCED (World Commission on Environment and Development),, 1987. *Our Common Future*. Oxford University Press, Oxford., (n.d.).
- [3] C.J. Barrow, *Caring for the earth: A strategy for sustainable living*, published by IUCN (World Conservation Union), UNEP (United Nations Environment Programme) and WWF (World Wide Fund for Nature). (London, Earthscan, 1991, pp. 228, £9.95 p/b), *J. Int. Dev.* 5 (1993) 352–352. <https://doi.org/10.1002/jid.3380050320>.
- [4] J. Brugmann, Who can deliver sustainability? Municipal reform and the sustainable development mandate, *Third World Plann. Rev.* (1994).  
<https://doi.org/10.3828/twpr.16.2.x761215601u2n52m>.
- [5] I.M. Herremans, R.E. Reid, Developing Awareness of the Sustainability Concept, *J. Environ. Educ.* 34 (2002) 16–20.  
<https://doi.org/10.1080/00958960209603477>.
- [6] J.D. Marshall, M.W. Toffel, Framing the elusive concept of sustainability: A sustainability hierarchy, *Environ. Sci. Technol.* (2005).  
<https://doi.org/10.1021/es040394k>.
- [7] EEA (European Environmental Agency). Glossary. Available from:<[http://glossary.eea.eu.int/EEA\\_Glossary/](http://glossary.eea.eu.int/EEA_Glossary/)>; 7 June, (2004).
- [8] US Environmental Protection Agency (EPA). Available from: <<http://www.epa.gov/>>; 1 June, (2004).
- [9] Remanufacturing. Available from:<<http://www.ciwmb.ca.gov/WPIE/remanugact/>>; 2 November, (2005).
- [10] Eco-ef fi ciency conference. Available from: <<http://www.eco-ef fi ciency conf.org/content/home.de fi nitions.shtml>>; 13 July, (2004).
- [11] UNEP, United Nation Environment Programme, Division of Technology, Industry, and Economics (UNEP DTIE). Cleaner production (CP) activities. Available from: <<http://www.uneptie.org/>>; 2 June, (2004).
- [12] global.pdf reporting initiative, <[www.globalreporting.org](http://www.globalreporting.org)>;9 October200, (n.d.).



## References

- [13] ONG.pdf F, Arnold MB. The power of environmental partnership. Forth Worth: Dryden Press; 1994., (n.d.).
- [14] Centre for Environmental Training and International Consulting. Available from: <<http://www.centric.at/index2.html>>; 29 March, (2005).
- [15] Gogaladze K. Cleaner production in Georgia. In: Barsonyi K, Zilahy G, editors. Clean products and processes: abstract booklet. Second meeting of the NATO/CCMS pilot study clean products and processes e phase II, May 2e6, 2004; Budapest (Hungary)., (2004).
- [16] G. Kaur, K. Uisan, K.L. Ong, C.S. Ki Lin, Recent Trends in Green and Sustainable Chemistry & Waste Valorisation: Rethinking Plastics in a circular economy, *Curr. Opin. Green Sustain. Chem.* 9 (2018) 30–39. <https://doi.org/10.1016/j.cogsc.2017.11.003>.
- [17] M. Eissen, J.O. Metzger, E. Schmidt, U. Schneidewind, 10 Years after Rio- Concepts on the Contribution of Chemistry to a Sustainable Development, *Angew. Chemie Int. Ed.* 41 (2002) 414–436. [https://doi.org/10.1002/1521-3773\(20020201\)41:3<414::AID-ANIE414>3.0.CO;2-N](https://doi.org/10.1002/1521-3773(20020201)41:3<414::AID-ANIE414>3.0.CO;2-N).
- [18] P. Glavič, R. Lukman, Review of sustainability terms and their definitions, *J. Clean. Prod.* 15 (2007) 1875–1885. <https://doi.org/10.1016/j.jclepro.2006.12.006>.
- [19] M.A. Gonzalez, R.L. Smith, A methodology to evaluate process sustainability, *Environ. Prog.* 22 (2003) 269–276. <https://doi.org/10.1002/ep.670220415>.
- [20] J.O. Metzger, M. Eissen, Concepts on the contribution of chemistry to a sustainable development. *Renewable raw materials, Comptes Rendus Chim.* 7 (2004) 569–581. <https://doi.org/10.1016/j.crci.2003.12.003>.
- [21] D. Hjeresen, Green Chemistry: Environment, Economics, and Competitiveness, *Corp. Environ. Strateg.* 9 (2002) 259–266. [https://doi.org/10.1016/S1066-7938\(02\)00068-4](https://doi.org/10.1016/S1066-7938(02)00068-4).
- [22] A. Halpaap, J. Dittkrist, Sustainable chemistry in the global chemicals and waste management agenda, *Curr. Opin. Green Sustain. Chem.* (2018). <https://doi.org/10.1016/j.cogsc.2017.11.001>.
- [23] C. Blum, D. Bunke, M. Hungsberg, E. Roelofs, A. Joas, R. Joas, M. Blepp, H.-C. Stolzenberg, The concept of sustainable chemistry: Key drivers for the transition towards sustainable development, *Sustain. Chem. Pharm.* 5

## References

- (2017) 94–104. <https://doi.org/10.1016/j.scp.2017.01.001>.
- [24] M. de la Guardia, S. Garrigues, Chapter 1. An Ethical Commitment and an Economic Opportunity, in: RSC Green Chem., 2011: pp. 1–12. <https://doi.org/10.1039/9781849732963-00001>.
- [25] L.A. Wright, S. Kemp, I. Williams, 'Carbon footprinting': towards a universally accepted definition, Carbon Manag. 2 (2011) 61–72. <https://doi.org/10.4155/cmt.10.39>.
- [26] B. Trost, The atom economy--a search for synthetic efficiency, Science (80-. ). 254 (1991) 1471–1477. <https://doi.org/10.1126/science.1962206>.
- [27] R.A. Sheldon, Fundamentals of green chemistry: Efficiency in reaction design, Chem. Soc. Rev. (2012). <https://doi.org/10.1039/c1cs15219j>.
- [28] I.K. Adu, H. Sugiyama, U. Fischer, K. Hungerbühler, Comparison of methods for assessing environmental, health and safety (EHS) hazards in early phases of chemical process design, Process Saf. Environ. Prot. 86 (2008) 77–93. <https://doi.org/10.1016/j.psep.2007.10.005>.
- [29] G. Rebitzer, T. Ekvall, R. Frischknecht, D. Hunkeler, G. Norris, T. Rydberg, W.-P. Schmidt, S. Suh, B.P. Weidema, D.W. Pennington, Life cycle assessment, Environ. Int. 30 (2004) 701–720. <https://doi.org/10.1016/j.envint.2003.11.005>.
- [30] D.W. Pennington, J. Potting, G. Finnveden, E. Lindeijer, O. Jolliet, T. Rydberg, G. Rebitzer, Life cycle assessment Part 2: Current impact assessment practice, Environ. Int. 30 (2004) 721–739. <https://doi.org/10.1016/j.envint.2003.12.009>.
- [31] P.M. Nowak, P. Kościelniak, M. Tobiszewski, A. Ballester-Caudet, P. Campíns-Falcó, Overview of the three multicriteria approaches applied to a global assessment of analytical methods, TrAC Trends Anal. Chem. 133 (2020) 116065. <https://doi.org/10.1016/j.trac.2020.116065>.
- [32] M.C. Prieto-Blanco, A. Ballester-Caudet, F.J. Souto-Varela, P. López-Mahía, P. Campíns-Falcó, Rapid evaluation of ammonium in different rain events minimizing needed volume by a cost-effective and sustainable PDMS supported solid sensor, Environ. Pollut. 265 (2020) 114911. <https://doi.org/10.1016/j.envpol.2020.114911>.
- [33] A. Ballester-Caudet, P. Campíns-Falcó, B. Pérez, R. Sancho, M. Lorente, G. Sastre, C. González, A new tool for evaluating and/or selecting analytical

## References

- methods: Summarizing the information in a hexagon, *TrAC - Trends Anal. Chem.* (2019). <https://doi.org/10.1016/j.trac.2019.06.015>.
- [34] M.A.A. y M. Ambiente, Guía para el cálculo de la huella de carbono y para la elaboración de un plan de mejora de una organización, *Gob. España.* (2015).
- [35] H. Kataoka, A. Ishizaki, Y. Nonaka, K. Saito, Developments and applications of capillary microextraction techniques: A review, *Anal. Chim. Acta.* (2009). <https://doi.org/10.1016/j.aca.2009.09.032>.
- [36] C. Silva, C. Cavaco, R. Perestrelo, J. Pereira, J.S. Câmara, Microextraction by packed Sorbent (MEPS) and solid-phase microextraction (SPME) as sample preparation procedures for the metabolomic profiling of urine, *Metabolites.* (2014). <https://doi.org/10.3390/metabo4010071>.
- [37] Y. Moliner-Martinez, R. Herráez-Hernández, J. Verdú-Andrés, C. Molins-Legua, P. Campíns-Falcó, Recent advances of in-tube solid-phase microextraction, *TrAC - Trends Anal. Chem.* (2015). <https://doi.org/10.1016/j.trac.2015.02.020>.
- [38] K. Belay, Advanced Analytical Microextraction Techniques and Their Applications: A Review, *J. Biol.* (2016).
- [39] M.A. Jeannot, F.F. Cantwell, Solvent microextraction into a single drop, *Anal. Chem.* (1996). <https://doi.org/10.1021/ac960042z>.
- [40] Y. He, H.K. Lee, Liquid-Phase Microextraction in a Single Drop of Organic Solvent by Using a Conventional Microsyringe, *Anal. Chem.* (1997). <https://doi.org/10.1021/ac970242q>.
- [41] R. Jain, R. Singh, Microextraction techniques for analysis of cannabinoids, *TrAC - Trends Anal. Chem.* (2016). <https://doi.org/10.1016/j.trac.2016.03.012>.
- [42] A. Zgoła-Grzeškowiak, T. Grzeškowiak, Dispersive liquid-liquid microextraction, *TrAC - Trends Anal. Chem.* (2011). <https://doi.org/10.1016/j.trac.2011.04.014>.
- [43] M. Rezaee, Y. Assadi, M.R. Milani Hosseini, E. Aghaee, F. Ahmadi, S. Berijani, Determination of organic compounds in water using dispersive liquid-liquid microextraction, *J. Chromatogr. A.* (2006). <https://doi.org/10.1016/j.chroma.2006.03.007>.

## References

- [44] S. Pedersen-Bjergaard, K.E. Rasmussen, Liquid-liquid-liquid microextraction for sample preparation of biological fluids prior to capillary electrophoresis, *Anal. Chem.* (1999). <https://doi.org/10.1021/ac990055n>.
- [45] K.E. Rasmussen, S. Pedersen-Bjergaard, Developments in hollow fibre-based, liquid-phase microextraction, *TrAC - Trends Anal. Chem.* (2004). [https://doi.org/10.1016/S0165-9936\(04\)00105-0](https://doi.org/10.1016/S0165-9936(04)00105-0).
- [46] V. Sharifi, A. Abbasi, A. Nosrati, Application of hollow fiber liquid phase microextraction and dispersive liquid-liquid microextraction techniques in analytical toxicology, *J. Food Drug Anal.* (2016). <https://doi.org/10.1016/j.jfda.2015.10.004>.
- [47] C.L. Arthur, J. Pawliszyn, Solid Phase Microextraction with Thermal Desorption Using Fused Silica Optical Fibers, *Anal. Chem.* (1990). <https://doi.org/10.1021/ac00218a019>.
- [48] R. Eisert, J. Pawliszyn, Automated In-Tube Solid-Phase Microextraction Coupled to High-Performance Liquid Chromatography, *Anal. Chem.* (1997). <https://doi.org/10.1021/ac970319a>.
- [49] K. Mizuno, H. Kataoka, Analysis of urinary 8-isoprostane as an oxidative stress biomarker by stable isotope dilution using automated online in-tube solid-phase microextraction coupled with liquid chromatography-tandem mass spectrometry, *J. Pharm. Biomed. Anal.* (2015). <https://doi.org/10.1016/j.jpba.2015.04.020>.
- [50] A. Masiá, Y. Moliner-Martinez, M. Muñoz-Ortuño, Y. Pico, P. Campíns-Falcó, Multiresidue analysis of organic pollutants by in-tube solid phase microextraction coupled to ultra-high performance liquid chromatography-electrospray-tandem mass spectrometry, *J. Chromatogr. A.* (2013). <https://doi.org/10.1016/j.chroma.2013.07.019>.
- [51] J. Pan, Y. Huang, L. Liu, Y. Hu, G. Li, A novel fractionized sampling and stacking strategy for online hyphenation of solid-phase-based extraction to ultra-high performance liquid chromatography for ultrasensitive analysis, *J. Chromatogr. A.* (2013). <https://doi.org/10.1016/j.chroma.2013.09.082>.
- [52] X.-Y. Liu, Y.-S. Ji, H.-X. Zhang, M.-C. Liu, Highly sensitive analysis of substituted aniline compounds in water samples by using oxidized multiwalled carbon nanotubes as an in-tube solid-phase microextraction medium, *J. Chromatogr. A.* (2008). <https://doi.org/10.1016/j.chroma.2008.10.034>.

## References

- [53] Y. Moliner-Martínez, P. Serra-Mora, J. Verdú-Andrés, R. Herráez-Hernández, P. Campíns-Falcó, Analysis of polar triazines and degradation products in waters by in-tube solid-phase microextraction and capillary chromatography: An environmentally friendly method, *Anal. Bioanal. Chem.* (2015). <https://doi.org/10.1007/s00216-014-8366-7>.
- [54] M. Zarejousheghani, M. Möder, H. Borsdorf, A new strategy for synthesis of an in-tube molecularly imprinted polymer-solid phase microextraction device: Selective off-line extraction of 4-nitrophenol as an example of priority pollutants from environmental water samples, *Anal. Chim. Acta.* (2013). <https://doi.org/10.1016/j.aca.2013.08.038>.
- [55] A.R. Chaves, M.E. Costa Queiroz, In-tube solid-phase microextraction with molecularly imprinted polymer to determine interferon alpha 2a in plasma sample by high performance liquid chromatography, *J. Chromatogr. A.* (2013). <https://doi.org/10.1016/j.chroma.2013.10.018>.
- [56] Y. Hu, C. Song, G. Li, Fiber-in-tube solid-phase microextraction with molecularly imprinted coating for sensitive analysis of antibiotic drugs by high performance liquid chromatography, *J. Chromatogr. A.* (2012). <https://doi.org/10.1016/j.chroma.2012.09.029>.
- [57] Y. Moliner-Martínez, H. Prima-Garcia, A. Ribera, E. Coronado, P. Campíns-Falcó, Magnetic in-tube solid phase microextraction, *Anal. Chem.* (2012). <https://doi.org/10.1021/ac301660k>.
- [58] R. González-Fuenzalida, Y. Moliner-Martínez, H. Prima-Garcia, A. Ribera, P. Campíns-Falcó, R. Zaragoza, Evaluation of Superparamagnetic Silica Nanoparticles for Extraction of Triazines in Magnetic in-Tube Solid Phase Microextraction Coupled to Capillary Liquid Chromatography, *Nanomaterials.* (2014). <https://doi.org/10.3390/nano4020242>.
- [59] Y. Moliner-Martínez, Y. Vitta, H. Prima-Garcia, R.A. González-Fuenzalida, A. Ribera, P. Campíns-Falcó, E. Coronado, Silica supported Fe<sub>3</sub>O<sub>4</sub> magnetic nanoparticles for magnetic solid-phase extraction and magnetic in-tube solid-phase microextraction: Application to organophosphorous compounds Microextraction Techniques, *Anal. Bioanal. Chem.* (2014). <https://doi.org/10.1007/s00216-013-7379-y>.
- [60] Y. Moliner-Martínez, R. Herráez-Hernández, C. Molins-Legua, P. Campíns-Falcó, Improving analysis of apolar organic compounds by the use of a capillary titania-based column: Application to the direct determination of faecal sterols cholesterol and coprostanol in wastewater samples, *J.*

- Chromatogr. A. (2010). <https://doi.org/10.1016/j.chroma.2010.05.001>.
- [61] N. Jornet-Martínez, M. Muñoz-Ortuño, Y. Moliner-Martínez, R. Herráez-Hernández, P. Campíns-Falcó, On-line in-tube solid phase microextraction-capillary liquid chromatography method for monitoring degradation products of di-(2-ethylhexyl) phthalate in waters, *J. Chromatogr. A.* (2014). <https://doi.org/10.1016/j.chroma.2014.04.074>.
- [62] M. Muñoz-Ortuño, A. Argente-García, Y. Moliner-Martínez, J. Verdú-Andrés, R. Herráez-Hernández, M.T. Picher, P. Campíns-Falcó, A cost-effective method for estimating di(2-ethylhexyl)phthalate in coastal sediments, *J. Chromatogr. A.* (2014). <https://doi.org/10.1016/j.chroma.2013.11.018>.
- [63] Y. Fan, Y.Q. Feng, S.L. Da, Z.G. Shi, Poly (methacrylic acid-ethylene glycol dimethacrylate) monolithic capillary for in-tube solid phase microextraction coupled to high performance liquid chromatography and its application to determination of basic drugs in human serum, *Anal. Chim. Acta.* (2004). <https://doi.org/10.1016/j.aca.2004.07.052>.
- [64] C. Cháfer-Pericás, R. Herráez-Hernández, P. Campíns-Falcó, In-tube solid-phase microextraction-capillary liquid chromatography as a solution for the screening analysis of organophosphorus pesticides in untreated environmental water samples, *J. Chromatogr. A.* (2007). <https://doi.org/10.1016/j.chroma.2006.11.105>.
- [65] H. Kataoka, M. Itano, A. Ishizaki, K. Saito, Determination of patulin in fruit juice and dried fruit samples by in-tube solid-phase microextraction coupled with liquid chromatography-mass spectrometry, *J. Chromatogr. A.* (2009). <https://doi.org/10.1016/j.chroma.2009.03.017>.
- [66] P. Campíns-Falcó, J. Verdú-Andrés, A. Sevillano-Cabeza, C. Molins-Legua, R. Herráez-Hernández, New micromethod combining miniaturized matrix solid-phase dispersion and in-tube in-valve solid-phase microextraction for estimating polycyclic aromatic hydrocarbons in bivalves, *J. Chromatogr. A.* (2008). <https://doi.org/10.1016/j.chroma.2008.09.074>.
- [67] L.P. Melo, R.H.C. Queiroz, M.E.C. Queiroz, Automated determination of rifampicin in plasma samples by in-tube solid-phase microextraction coupled with liquid chromatography, *J. Chromatogr. B Anal. Technol. Biomed. Life Sci.* (2011). <https://doi.org/10.1016/j.jchromb.2011.06.041>.
- [68] T. Li, J. Xu, J.H. Wu, Y.Q. Feng, Liquid-phase deposition of silica nanoparticles into a capillary for in-tube solid-phase microextraction

## References

- coupled with high-performance liquid chromatography, *J. Chromatogr. A.* (2009). <https://doi.org/10.1016/j.chroma.2009.01.076>.
- [69] M. Sun, J. Feng, Y. Bu, C. Luo, Highly sensitive copper fiber-in-tube solid-phase microextraction for online selective analysis of polycyclic aromatic hydrocarbons coupled with high performance liquid chromatography, *J. Chromatogr. A.* (2015). <https://doi.org/10.1016/j.chroma.2015.07.024>.
- [70] R.A. González-Fuenzalida, E. López-García, Y. Moliner-Martínez, P. Campíns-Falcó, Adsorbent phases with nanomaterials for in-tube solid-phase microextraction coupled on-line to liquid nanochromatography, *J. Chromatogr. A.* (2016). <https://doi.org/10.1016/j.chroma.2016.01.009>.
- [71] M.C. Prieto-Blanco, Y. Moliner-Martínez, P. López-Mahía, P. Campíns-Falcó, Ion-pair in-tube solid-phase microextraction and capillary liquid chromatography using a titania-based column: Application to the specific lauralkonium chloride determination in water, *J. Chromatogr. A.* (2012). <https://doi.org/10.1016/j.chroma.2012.05.099>.
- [72] Y. Vitta, Y. Moliner-Martínez, P. Campíns-Falcó, A.F. Cuervo, An in-tube SPME device for the selective determination of chlorophyll a in aquatic systems, *Talanta.* (2010). <https://doi.org/10.1016/j.talanta.2010.05.069>.
- [73] D. Ishii, K. Asai, K. Hibi, T. Jonokuchi, M. Nagaya, A study of micro-high-performance liquid chromatography. I. Development of technique for miniaturization of high-performance liquid chromatography, *J. Chromatogr. A.* (1977). [https://doi.org/10.1016/S0021-9673\(00\)99351-8](https://doi.org/10.1016/S0021-9673(00)99351-8).
- [74] R.P.W. Scott, P. Kucera, Mode of operation and performance characteristics of microbore columns for use in liquid chromatography, *J. Chromatogr. A.* 169 (1979) 51–72. [https://doi.org/10.1016/0021-9673\(75\)85032-1](https://doi.org/10.1016/0021-9673(75)85032-1).
- [75] C.E.D. Nazario, M.R. Silva, M.S. Franco, F.M. Lanças, Evolution in miniaturized column liquid chromatography instrumentation and applications: An overview, *J. Chromatogr. A.* 1421 (2015) 18–37. <https://doi.org/10.1016/j.chroma.2015.08.051>.
- [76] G.J. Johnson, *Encyclopedia of Analytical Science* (2nd edition) 2005421 Edited by Paul Worsfold, Alan Townshend and Colin Poole. *Encyclopedia of Analytical Science* (2nd edition) . Amsterdam: Elsevier Academic Press 2005. 10 vols., ISBN: 0 12 764199 9 £2,950, \$4,570 , Ref. Rev. (2005). <https://doi.org/10.1108/09504120510632723>.

## References

- [77] J. Šesták, D. Moravcová, V. Kahle, Instrument platforms for nano liquid chromatography, *J. Chromatogr. A.* (2015). <https://doi.org/10.1016/j.chroma.2015.07.090>.
- [78] R. DeKosky, Developing Chemical Instrumentation for Environmental Use in the Late Twentieth Century: Detecting Lead in Paint Using Portable X-Ray Fluorescence Spectrometry, *Ambix.* 56 (2009) 138–162. <https://doi.org/10.1179/174582309X441408>.
- [79] N. Jornet-Martínez, Y. Moliner-Martínez, C. Molins-Legua, P. Campíns-Falcó, Trends for the Development of In Situ Analysis Devices, in: *Encycl. Anal. Chem.*, 2017. <https://doi.org/10.1002/9780470027318.a9593>.
- [80] C. Turner, Sustainable analytical chemistry-more than just being green, *Pure Appl. Chem.* (2013). <https://doi.org/10.1351/PAC-CON-13-02-05>.
- [81] A.M. Nightingale, A.D. Beaton, M.C. Mowlem, Trends in microfluidic systems for in situ chemical analysis of natural waters, *Sensors Actuators B Chem.* 221 (2015) 1398–1405. <https://doi.org/10.1016/j.snb.2015.07.091>.
- [82] S.K. Pandey, K.H. Kim, K.T. Tang, A review of sensor-based methods for monitoring hydrogen sulfide, *TrAC - Trends Anal. Chem.* (2012). <https://doi.org/10.1016/j.trac.2011.08.008>.
- [83] M.M.F. Choi, P. Hawkins, Development of an optical hydrogen sulphide sensor, in: *Sensors Actuators, B Chem.*, 2003. [https://doi.org/10.1016/S0925-4005\(03\)00030-3](https://doi.org/10.1016/S0925-4005(03)00030-3).
- [84] N. Donato, D. Aloisio, S.G. Leonardi, G. Neri, Ink-Jet Printed Colorimetric Sensor for the Determination of Fe(II), *IEEE Sens. J.* 15 (2015) 3196–3200. <https://doi.org/10.1109/JSEN.2014.2379216>.
- [85] A. Hulanicki, S. Glab, F. Ingman, Chemical sensors definitions and classification, *Pure Appl. Chem.* (1991). <https://doi.org/10.1351/pac199163091247>.
- [86] M.E. Stewart, C.R. Anderton, L.B. Thompson, J. Maria, S.K. Gray, J.A. Rogers, R.G. Nuzzo, Nanostructured plasmonic sensors, *Chem. Rev.* (2008). <https://doi.org/10.1021/cr068126n>.
- [87] K.H. Su, Q.H. Wei, X. Zhang, J.J. Mock, D.R. Smith, S. Schultz, Interparticle coupling effects on plasmon resonances of nanogold particles, *Nano Lett.* (2003). <https://doi.org/10.1021/nl034197f>.



## References

- [88] S. Eustis, M.A. El-Sayed, Why gold nanoparticles are more precious than pretty gold: Noble metal surface plasmon resonance and its enhancement of the radiative and nonradiative properties of nanocrystals of different shapes, *Chem. Soc. Rev.* (2006). <https://doi.org/10.1039/b514191e>.
- [89] J. Homola, Surface plasmon resonance sensors for detection of chemical and biological species, *Chem. Rev.* (2008). <https://doi.org/10.1021/cr068107d>.
- [90] I. Caelen, A. Kalman, L. Wahlström, Biosensor-Based Determination of Riboflavin in Milk Samples, *Anal. Chem.* (2004). <https://doi.org/10.1021/ac034876a>.
- [91] A.D. Taylor, J. Ladd, Q. Yu, S. Chen, J. Homola, S. Jiang, Quantitative and simultaneous detection of four foodborne bacterial pathogens with a multi-channel SPR sensor, *Biosens. Bioelectron.* (2006). <https://doi.org/10.1016/j.bios.2006.03.012>.
- [92] G.A.J. Besselink, R.P.H. Kooyman, P.J.H.J. Van Os, G.H.M. Engbers, R.B.M. Schasfoort, Signal amplification on planar and gel-type sensor surfaces in surface plasmon resonance-based detection of prostate-specific antigen, *Anal. Biochem.* (2004). <https://doi.org/10.1016/j.ab.2004.05.009>.
- [93] P.P. Dillon, S.J. Daly, B.M. Manning, R. O'Kennedy, Immunoassay for the determination of morphine-3-glucuronide using a surface plasmon resonance-based biosensor, *Biosens. Bioelectron.* (2002). [https://doi.org/10.1016/S0956-5663\(02\)00182-3](https://doi.org/10.1016/S0956-5663(02)00182-3).
- [94] Y. Li, J.L. Hye, R.M. Corn, Detection of protein biomarkers using RNA aptamer microarrays and enzymatically amplified surface plasmon resonance imaging, *Anal. Chem.* (2007). <https://doi.org/10.1021/ac061849m>.
- [95] N. Jornet-Martínez, M. González-Béjar, Y. Moliner-Martínez, P. Campíns-Falcó, J. Pérez-Prieto, Sensitive and selective plasmonic assay for spermine as biomarker in human urine, *Anal. Chem.* (2014). <https://doi.org/10.1021/ac404165j>.
- [96] H. Kawazumi, K.V. Gobi, K. Ogino, H. Maeda, N. Miura, Compact surface plasmon resonance (SPR) immunosensor using multichannel for simultaneous detection of small molecule compounds, in: *Sensors Actuators, B Chem.*, 2005. <https://doi.org/10.1016/j.snb.2004.11.069>.
- [97] E. Mauriz, A. Calle, J.J. Manclús, A. Montoya, A.M. Escuela, J.R. Sendra,

## References

- L.M. Lechuga, Single and multi-analyte surface plasmon resonance assays for simultaneous detection of cholinesterase inhibiting pesticides, *Sensors Actuators, B Chem.* (2006). <https://doi.org/10.1016/j.snb.2006.04.085>.
- [98] E. Mauriz, A. Calle, L.M. Lechuga, J. Quintana, A. Montoya, J.J. Manclús, Real-time detection of chlorpyrifos at part per trillion levels in ground, surface and drinking water samples by a portable surface plasmon resonance immunosensor, *Anal. Chim. Acta.* (2006). <https://doi.org/10.1016/j.aca.2005.12.069>.
- [99] A.R. Ferhan, L. Guo, X. Zhou, P. Chen, S. Hong, D.H. Kim, Solid-phase colorimetric sensor based on gold nanoparticle-loaded polymer brushes: Lead detection as a case study, *Anal. Chem.* (2013). <https://doi.org/10.1021/ac4001817>.
- [100] B. Heli, E. Morales-Narváez, H. Golmohammadi, A. Ajji, A. Merkoçi, Modulation of population density and size of silver nanoparticles embedded in bacterial cellulose: Via ammonia exposure: Visual detection of volatile compounds in a piece of plasmonic nanopaper, *Nanoscale.* (2016). <https://doi.org/10.1039/c6nr00537c>.
- [101] A. Colombelli, M. Serri, M. Mannini, R. Rella, M.G. Manera, Volatile Organic Compounds sensing properties of TbPc2 thin films: Towards a plasmon-enhanced opto-chemical sensor, *Sensors Actuators, B Chem.* (2017). <https://doi.org/10.1016/j.snb.2017.05.183>.
- [102] D.D. Liana, B. Raguse, J. Justin Gooding, E. Chow, Recent advances in paper-based sensors, *Sensors (Switzerland).* (2012). <https://doi.org/10.3390/s120911505>.
- [103] W. Zhao, M.M. Ali, S.D. Aguirre, M.A. Brook, Y. Li, Paper-based bioassays using gold nanoparticle colorimetric probes, *Anal. Chem.* (2008). <https://doi.org/10.1021/ac801008q>.
- [104] N. Lopez-Ruiz, V.F. Curto, M.M. Erenas, F. Benito-Lopez, D. Diamond, A.J. Palma, L.F. Capitan-Vallvey, Smartphone-based simultaneous pH and nitrite colorimetric determination for paper microfluidic devices, *Anal. Chem.* (2014). <https://doi.org/10.1021/ac5019205>.
- [105] S. Chaiyo, W. Siangproh, A. Apilux, O. Chailapakul, Highly selective and sensitive paper-based colorimetric sensor using thiosulfate catalytic etching of silver nanoplates for trace determination of copper ions, *Anal. Chim. Acta.* (2015). <https://doi.org/10.1016/j.aca.2015.01.042>.

## References

- [106] T. Eaidkong, R. Mungkarndee, C. Phollookin, G. Tumcharern, M. Sukwattanasinitt, S. Wacharasindhu, Polydiacetylene paper-based colorimetric sensor array for vapor phase detection and identification of volatile organic compounds, *J. Mater. Chem.* (2012). <https://doi.org/10.1039/c2jm16273c>.
- [107] T. Soga, Y. Jimbo, K. Suzuki, D. Citterio, Inkjet-printed paper-based colorimetric sensor array for the discrimination of volatile primary amines, *Anal. Chem.* (2013). <https://doi.org/10.1021/ac402070z>.
- [108] J. Chang, H. Li, T. Hou, F. Li, Paper-based fluorescent sensor for rapid naked-eye detection of acetylcholinesterase activity and organophosphorus pesticides with high sensitivity and selectivity, *Biosens. Bioelectron.* (2016). <https://doi.org/10.1016/j.bios.2016.07.022>.
- [109] C. Sicard, C. Glen, B. Aubie, D. Wallace, S. Jahanshahi-Anbuhi, K. Pennings, G.T. Daigger, R. Pelton, J.D. Brennan, C.D.M. Filipe, Tools for water quality monitoring and mapping using paper-based sensors and cell phones, *Water Res.* (2015). <https://doi.org/10.1016/j.watres.2014.12.005>.
- [110] J.A. Osorio Saraz, I. de F. Ferreira Tinoco, R.S. Gates, K.S. Oliveira Rocha, O.L. Zapata Marín, A simple methodology to measure ammonia flux generated in naturally ventilated poultry houses, *Rev. Colomb. Ciencias Pecu.* (2015).
- [111] N. Jornet-Martínez, Y. Moliner-Martínez, R. Herráez-Hernández, C. Molins-Legua, J. Verdú-Andrés, P. Campíns-Falcó, Designing solid optical sensors for in situ passive discrimination of volatile amines based on a new one-step hydrophilic PDMS preparation, *Sensors Actuators B Chem.* 223 (2016) 333–342. <https://doi.org/10.1016/j.snb.2015.09.097>.
- [112] A. Argente-García, M. Muñoz-Ortuño, C. Molins-Legua, Y. Moliner-Martínez, P. Campíns-Falcó, A solid device based on doped hybrid composites for controlling the dosage of the biocide N-(3-aminopropyl)-N-dodecyl-1,3-propanediamine in industrial formulations, *Talanta.* 147 (2016) 147–154. <https://doi.org/10.1016/j.talanta.2015.09.051>.
- [113] M. Muñoz-Ortuño, A. Argente-García, Y. Moliner-Martínez, C. Molins-Legua, P. Campíns-Falcó, Polydimethylsiloxane composites containing 1,2-naphthoquinone 4-sulphonate as unique dispositive for estimation of casein in effluents from dairy industries, *Anal. Chim. Acta.* 873 (2015) 31–37. <https://doi.org/10.1016/j.aca.2015.02.057>.
- [114] J. Le Bideau, L. Viau, A. Vioux, Ionogels, ionic liquid based hybrid materials,

## References

- Chem. Soc. Rev. (2011). <https://doi.org/10.1039/c0cs00059k>.
- [115] K.D. Clark, C. Zhang, J.L. Anderson, Sample preparation for bioanalytical and pharmaceutical analysis, *Anal. Chem.* (2016). <https://doi.org/10.1021/acs.analchem.6b02935>.
- [116] M.P. Singh, R.K. Singh, S. Chandra, Ionic liquids confined in porous matrices: Physicochemical properties and applications, *Prog. Mater. Sci.* (2014). <https://doi.org/10.1016/j.pmatsci.2014.03.001>.
- [117] S. V. Muginova, D.A. Myasnikova, S.G. Kazarian, T.N. Shekhovtsova, Applications of ionic liquids for the development of optical chemical sensors and biosensors, *Anal. Sci.* (2017). <https://doi.org/10.2116/analsci.33.261>.
- [118] A.I. Horowitz, M.J. Panzer, Poly(dimethylsiloxane)-supported ionogels with a high ionic liquid loading, *Angew. Chemie - Int. Ed.* (2014). <https://doi.org/10.1002/anie.201405691>.
- [119] M.C. Prieto-Blanco, N. Jornet-Martinez, J. Verdú-Andrés, C. Molíns-Legua, P. Campíns-Falcó, Quantifying both ammonium and proline in wines and beer by using a PDMS composite for sensing, *Talanta.* (2019). <https://doi.org/10.1016/j.talanta.2019.02.001>.
- [120] N.J.-M. P. Campíns-Falco, Y. Moliner-Martínez, R. Herráez-Hernández, C. Molíns-Legua, J. Verdú-Andrés, Passive device for in situ detection and/or determination of amines in gases. Grant number : ES2519891B1. Application number: P201300436. Titular Entity: 2735- Universidad de Valencia. PCT: PCT/ ES2014/000077 (granted 2020), EP 14795283.2. Extended Patent, 2020.
- [121] A.A. Elbashir, A.A. Ahmed, S.M. Ali Ahmed, H.Y. Aboul-Enein, 1,2-naphthoquinone-4-sulphonic acid sodium salt (NQS) as an analytical reagent for the determination of pharmaceutical amine by spectrophotometry, *Appl. Spectrosc. Rev.* (2012). <https://doi.org/10.1080/05704928.2011.639107>.
- [122] P.C. Falcó, C.M. Legua, A.S. Cabeza, R.P. Serrano, Derivatization of amphetamine and methamphetamine with 1,2-naphthoquinone 4-sulfonic acid into solid-phase extraction cartridges. Determination of amphetamine in pharmaceutical and urine samples, *Analyst.* (1997). <https://doi.org/10.1039/a701134b>.
- [123] A.A. Elbashir, A.H.E. Elwagee, Spectrophotometric determination of

## References

- pyrimethamine (PYM) in pharmaceutical formulation using 1,2-naphthoquinone-4-sulfonate (NQS), *J. Assoc. Arab Univ. Basic Appl. Sci.* (2012). <https://doi.org/10.1016/j.jaubas.2011.12.003>.
- [124] D. Giustarini, I. Dalle-Donne, R. Colombo, A. Milzani, R. Rossi, Adaptation of the griess reaction for detection of nitrite in human plasma, *Free Radic. Res.* (2004). <https://doi.org/10.1080/10715760400017327>.
- [125] D. Li, Y. Ma, H. Duan, W. Deng, D. Li, Griess reaction-based paper strip for colorimetric/fluorescent/SERS triple sensing of nitrite, *Biosens. Bioelectron.* (2018). <https://doi.org/10.1016/j.bios.2017.08.008>.
- [126] T.H. Cheng, S. Bin Lin, L.C. Chen, H.H. Chen, Studies of the antimicrobial ability and silver ions migration from silver nitrate-incorporated electrospun nylon nanofibers, *Food Packag. Shelf Life.* (2018). <https://doi.org/10.1016/j.fpsl.2018.03.003>.
- [127] Z. Xu, S. Mahalingam, J.L. Rohn, G. Ren, M. Edirisinghe, Physio-chemical and antibacterial characteristics of pressure spun nylon nanofibres embedded with functional silver nanoparticles, *Mater. Sci. Eng. C.* (2015). <https://doi.org/10.1016/j.msec.2015.06.003>.
- [128] J. Pla-Tolós, Y. Moliner-Martínez, C. Molins-Legua, P. Campíns-Falcó, Solid glucose biosensor integrated in a multi-well microplate coupled to a camera-based detector: Application to the multiple analysis of human serum samples, *Sensors Actuators B Chem.* 258 (2018) 331–341. <https://doi.org/10.1016/j.snb.2017.11.069>.
- [129] S.K. Vashist, T. van Oordt, E.M. Schneider, R. Zengerle, F. von Stetten, J.H.T. Luong, A smartphone-based colorimetric reader for bioanalytical applications using the screen-based bottom illumination provided by gadgets, *Biosens. Bioelectron.* (2015). <https://doi.org/10.1016/j.bios.2014.08.027>.
- [130] C.A. Chaplan, H.T. Mitchell, A.W. Martinez, Paper-based standard addition assays, *Anal. Methods.* (2014). <https://doi.org/10.1039/c4ay00205a>.
- [131] K. Su, Q. Zou, J. Zhou, L. Zou, H. Li, T. Wang, N. Hu, P. Wang, High-sensitive and high-efficient biochemical analysis method using a bionic electronic eye in combination with a smartphone-based colorimetric reader system, *Sensors Actuators, B Chem.* (2015). <https://doi.org/10.1016/j.snb.2015.04.052>.
- [132] K. Su, X. Qiu, J. Fang, Q. Zou, P. Wang, An improved efficient biochemical

## References

- detection method to marine toxins with a smartphone-based portable system—Bionic e-Eye, *Sensors Actuators, B Chem.* (2017).  
<https://doi.org/10.1016/j.snb.2016.02.092>.
- [133] M.Y. Jia, Q.S. Wu, H. Li, Y. Zhang, Y.F. Guan, L. Feng, The calibration of cellphone camera-based colorimetric sensor array and its application in the determination of glucose in urine, *Biosens. Bioelectron.* (2015).  
<https://doi.org/10.1016/j.bios.2015.07.072>.
- [134] M.R. Bladergroen, Y.E.M. Van Der Burgt, Solid-Phase Extraction Strategies to Surmount Body Fluid Sample Complexity in High-Throughput Mass Spectrometry-Based Proteomics, *J. Anal. Methods Chem.* (2015).  
<https://doi.org/10.1155/2015/250131>.
- [135] K.H. Lam, Z. Cai, H.Y. Wai, V.W.H. Tsang, M.H.W. Lam, R.Y.H. Cheung, H.X. Yu, P.K.S. Lam, Identification of a new Irgarol-1051 related s-triazine species in coastal waters, *Environ. Pollut.* (2005).  
<https://doi.org/10.1016/j.envpol.2005.01.014>.
- [136] I. Omae, General aspects of tin-free antifouling paints, *Chem. Rev.* (2003).  
<https://doi.org/10.1021/cr030669z>.
- [137] K.H. Lam, H.Y. Wai, K.M.Y. Leung, V.W.H. Tsang, C.F. Tang, R.Y.H. Cheung, M.H.W. Lam, A study of the partitioning behavior of Irgarol-1051 and its transformation products, *Chemosphere.* (2006).  
<https://doi.org/10.1016/j.chemosphere.2005.11.006>.
- [138] K. V. Thomas, M. McHugh, M. Waldock, Antifouling paint booster biocides in UK coastal waters: Inputs, occurrence and environmental fate, *Sci. Total Environ.* (2002). [https://doi.org/10.1016/S0048-9697\(01\)01153-6](https://doi.org/10.1016/S0048-9697(01)01153-6).
- [139] A. Scarlett, P. Donkin, T.W. Fileman, R.J. Morris, Occurrence of the antifouling herbicide, Irgarol 1051, within coastal-water seagrasses from Queensland, Australia, *Mar. Pollut. Bull.* (1999).  
[https://doi.org/10.1016/S0025-326X\(99\)00003-X](https://doi.org/10.1016/S0025-326X(99)00003-X).
- [140] L.W. Hall, J.M. Giddings, K.R. Solomon, R. Balcomb, An ecological risk assessment for the use of Irgarol 1051 as an algaecide for antifoulant paints, *Crit. Rev. Toxicol.* (1999).
- [141] K. V. Thomas, M. McHugh, M. Hilton, M. Waldock, Increased persistence of antifouling paint biocides when associated with paint particles, *Environ. Pollut.* (2003). [https://doi.org/10.1016/S0269-7491\(02\)00343-3](https://doi.org/10.1016/S0269-7491(02)00343-3).

## References

- [142] M.E. Callow, J.A. Finlay, A simple method to evaluate the potential for degradation of antifouling biocides, *Biofouling*. (1995). <https://doi.org/10.1080/08927019509378299>.
- [143] M.V. Fernandez, P.R. Gardinali, Risk assessment of triazine herbicides in surface waters and bioaccumulation of Irgarol and M1 by submerged aquatic vegetation in Southeast Florida, *Sci. Total Environ.* (2016). <https://doi.org/10.1016/j.scitotenv.2015.09.035>.
- [144] I. Ferrer, D. Barceló, Identification of a new degradation product of the antifouling agent Irgarol 1051 in natural samples, in: *J. Chromatogr. A*, 2001. [https://doi.org/10.1016/S0021-9673\(01\)01068-8](https://doi.org/10.1016/S0021-9673(01)01068-8).
- [145] S. Giacomazzi, N. Cochet, Environmental impact of diuron transformation: A review, *Chemosphere*. (2004). <https://doi.org/10.1016/j.chemosphere.2004.04.061>.
- [146] pedro gerardo prieto Bejarano, 2013/39/EU Directive of the Parliament and of the Council of 12 August 2013 amending Directives 2000/60/EC and 2008/105/EC as regards priority substances in the field of water policy. *Official Journal of the European Union L 226/1*, (2008). <http://ir.obihiro.ac.jp/dspace/handle/10322/3933>.
- [147] M.I. Pinto, H.D. Burrows, G. Sontag, C. Vale, J.P. Noronha, Priority pesticides in sediments of European coastal lagoons: A review, *Mar. Pollut. Bull.* (2016). <https://doi.org/10.1016/j.marpolbul.2016.06.101>.
- [148] N.C. Maragou, N.S. Thomaidis, M.A. Koupparis, Optimization and comparison of ESI and APCI LC-MS/MS methods: A case study of Irgarol 1051, Diuron, and their degradation products in environmental samples, *J. Am. Soc. Mass Spectrom.* (2011). <https://doi.org/10.1007/s13361-011-0191-z>.
- [149] C.C. Kaonga, K. Takeda, H. Sakugawa, Antifouling agents and Fenitrothion contamination in seawater, sediment, plankton, fish and selected marine animals from the Seto Inland Sea, Japan, *Geochem. J.* (2015). <https://doi.org/10.2343/geochemj.2.0327>.
- [150] J.J. Heo, U.J. Kim, J.E. Oh, Simultaneous quantitative analysis of four isothiazolinones and 3-iodo-2-propynyl butyl carbamate in hygienic consumer products, *Environ. Eng. Res.* (2019). <https://doi.org/10.4491/eer.2018.144>.
- [151] H. Singer, S. Jaus, I. Hanke, A. Lück, J. Hollender, A.C. Alder, Determination

## References

- of biocides and pesticides by on-line solid phase extraction coupled with mass spectrometry and their behaviour in wastewater and surface water, *Environ. Pollut.* (2010). <https://doi.org/10.1016/j.envpol.2010.06.013>.
- [152] I. Giráldez, E. Chaguaceda, M. Bujalance, E. Morales, Determination of five booster biocides in seawater by stir bar sorptive extraction-thermal desorption-gas chromatography-mass spectrometry, *J. Chromatogr. A.* (2013). <https://doi.org/10.1016/j.chroma.2012.11.017>.
- [153] Á. Sánchez-Rodríguez, Z. Sosa-Ferrera, J.J. Santana-Rodríguez, Applicability of microwave-assisted extraction combined with LC-MS/MS in the evaluation of booster biocide levels in harbour sediments, *Chemosphere.* (2011). <https://doi.org/10.1016/j.chemosphere.2010.09.064>.
- [154] D.A. Lambropoulou, V.A. Sakkas, T.A. Albanis, Headspace solid phase microextraction for the analysis of the new antifouling agents Irgarol 1051 and Sea Nine 211 in natural waters, *Anal. Chim. Acta.* (2002). [https://doi.org/10.1016/S0003-2670\(02\)00600-1](https://doi.org/10.1016/S0003-2670(02)00600-1).
- [155] D.A. Lambropoulou, V.A. Sakkas, T.A. Albanis, Determination of antifouling compounds in marine sediments by solid-phase microextraction coupled to gas chromatography-mass spectrometry, *J. Chromatogr. A.* (2003). [https://doi.org/10.1016/S0021-9673\(03\)01022-7](https://doi.org/10.1016/S0021-9673(03)01022-7).
- [156] D. LAMBROPOULOU, T. ALBANIS, Application of solvent microextraction in a single drop for the determination of new antifouling agents in waters, *J. Chromatogr. A.* (2004). [https://doi.org/10.1016/s0021-9673\(04\)01353-6](https://doi.org/10.1016/s0021-9673(04)01353-6).
- [157] A. Saleh, N. Sheijooni Fumani, S. Molaei, Microfunnel-supported liquid-phase microextraction: Application to extraction and determination of Irgarol 1051 and diuron in the Persian Gulf seawater samples, *J. Chromatogr. A.* (2014). <https://doi.org/10.1016/j.chroma.2014.06.057>.
- [158] L.C. Marube, S.S. Caldas, K.L. Soares, E.G. Primel, Dispersive liquid-liquid microextraction with solidification of floating organic droplets for simultaneous extraction of pesticides, pharmaceuticals and personal care products, *Microchim. Acta.* (2015). <https://doi.org/10.1007/s00604-015-1507-7>.
- [159] A. Kurunc, S. Ersahin, B.Y. Uz, N.K. Sonmez, I. Uz, H. Kaman, G.E. Bacalan, Y. Emekli, Identification of nitrate leaching hot spots in a large area with contrasting soil texture and management, *Agric. Water Manag.* (2011). <https://doi.org/10.1016/j.agwat.2011.01.010>.



## References

- [160] D.A. Lashof, D.R. Ahuja, Relative contributions of greenhouse gas emissions to global warming, *Nature*. (1990). <https://doi.org/10.1038/344529a0>.
- [161] M. Ward, R. Jones, J. Brender, T. de Kok, P. Weyer, B. Nolan, C. Villanueva, S. van Breda, Drinking Water Nitrate and Human Health: An Updated Review, *Int. J. Environ. Res. Public Health*. 15 (2018) 1557. <https://doi.org/10.3390/ijerph15071557>.
- [162] European Communities. COUNCIL DIRECTIVE 98/83/EC of 3 November 1998 on the quality of water intended for human consumption. *Official Journal of the European Communities*, 05.12.98, 320/32, (1998). <http://journal.unair.ac.id/download-fullpapers-ln522cc87c61full.pdf>.
- [163] <https://www.epa.gov/ground-water-and-drinking-water/table-regulated-drinking-water-contaminants>, (n.d.).
- [164] Background document for development of WHO Guidelines for Drinking-water Quality. Nitrate and nitrite in drinking-water. Fourth edition. [www.who.int/water\\_sanitation\\_health/dwq/.../nitratenitrite.pdf](http://www.who.int/water_sanitation_health/dwq/.../nitratenitrite.pdf), (n.d.). <https://doi.org/10.16194/j.cnki.31-1059/g4.2011.07.016>.
- [165] European Union. DIRECTIVE 2006/118/EC OF THE EUROPEAN PARLIAMENT AND OF THE COUNCIL of 12 December 2006 On the protection of groundwater against pollution and deterioration. *Official Journal of the European Union*, 27.12.2006, 372/19, (2006).
- [166] <https://www.boe.es/eli/es/rd/2007/12/07/1620/con>, (n.d.).
- [167] Q.-H. Wang, L.-J. Yu, Y. Liu, L. Lin, R. Lu, J. Zhu, L. He, Z.-L. Lu, Methods for the detection and determination of nitrite and nitrate: A review, *Talanta*. 165 (2017) 709–720. <https://doi.org/10.1016/j.talanta.2016.12.044>.
- [168] P. Griess, Bemerkungen zu der Abhandlung der HH. Weselsky und Benedikt „Ueber einige Azoverbindungen“, *Berichte Der Dtsch. Chem. Gesellschaft*. 12 (1879) 426–428. <https://doi.org/10.1002/cber.187901201117>.
- [169] S. Bocanegra-Rodríguez, N. Jornet-Martínez, C. Molins-Legua, P. Campíns-Falcó, Delivering Inorganic and Organic Reagents and Enzymes from Zein and Developing Optical Sensors, *Anal. Chem*. 90 (2018) 8501–8508. <https://doi.org/10.1021/acs.analchem.8b01338>.
- [170] P. Rattanarat, W. Dungchai, D.M. Cate, W. Siangproh, J. Volckens, O. Chailapakul, C.S. Henry, A microfluidic paper-based analytical device for rapid quantification of particulate chromium, *Anal. Chim. Acta*. 800 (2013)

## References

- 50–55. <https://doi.org/10.1016/j.aca.2013.09.008>.
- [171] P.S. Ellis, A.M.H. Shabani, B.S. Gentle, I.D. McKelvie, Field measurement of nitrate in marine and estuarine waters with a flow analysis system utilizing on-line zinc reduction, *Talanta*. (2011). <https://doi.org/10.1016/j.talanta.2010.12.028>.
- [172] H.P. Hansen, F. Koroleff, Determination of nutrients, in: *Methods Seawater Anal. Third, Complet. Revis. Ext. Ed.*, 2007. <https://doi.org/10.1002/9783527613984.ch10>.
- [173] B.C. Madsen, Utilization of flow injection with hydrazine reduction and photometric detection for the determination of nitrate in rain-water, *Anal. Chim. Acta*. (1981). [https://doi.org/10.1016/S0003-2670\(01\)93594-9](https://doi.org/10.1016/S0003-2670(01)93594-9).
- [174] S. Wang, K. Lin, N. Chen, D. Yuan, J. Ma, Automated determination of nitrate plus nitrite in aqueous samples with flow injection analysis using vanadium (III) chloride as reductant, *Talanta*. (2016). <https://doi.org/10.1016/j.talanta.2015.06.031>.
- [175] K. Lin, P. Li, J. Ma, D. Yuan, An automatic reserve flow injection method using vanadium (III) reduction for simultaneous determination of nitrite and nitrate in estuarine and coastal waters, *Talanta*. (2019). <https://doi.org/10.1016/j.talanta.2018.11.077>.
- [176] C. Martinez-Cisneros, Z. Da Rocha, A. Seabra, F. Valdés, J. Alonso-Chamarro, Highly integrated autonomous lab-on-a-chip device for on-line and: In situ determination of environmental chemical parameters, *Lab Chip*. (2018). <https://doi.org/10.1039/c8lc00309b>.
- [177] B.M. Jayawardane, S. Wei, I.D. McKelvie, S.D. Kolev, Microfluidic paper-based analytical device for the determination of nitrite and nitrate, *Anal. Chem.* (2014). <https://doi.org/10.1021/ac5013249>.
- [178] L. Merino, Development and validation of a method for determination of residual nitrite/nitrate in foodstuffs and water after zinc reduction, *Food Anal. Methods*. (2009). <https://doi.org/10.1007/s12161-008-9052-1>.
- [179] E. Murray, E.P. Nesterenko, M. McCaul, A. Morrin, D. Diamond, B. Moore, A colorimetric method for use within portable test kits for nitrate determination in various water matrices, *Anal. Methods*. (2017). <https://doi.org/10.1039/c6ay03190k>.
- [180] Rice E. W., Baird R. B., Eaton A. D. and Clesceri L. S. (Standard Methods for

## References

- the examination of Water and Wastewater). Métodos normalizados para análisis de aguas potables y residuales. (17ed) Madrid: Diaz de Santos, (2012).
- [181] Y.J. Xue, H. Gao, Q.C. Ji, Z. Lam, X. Fang, Z. Lin, M. Hoffman, D. Schulz-Jander, N. Weng, Bioanalysis of drug in tissue: Current status and challenges, *Bioanalysis*. (2012). <https://doi.org/10.4155/bio.12.252>.
- [182] A. Vertes, V. Hitchins, K.S. Phillips, Analytical challenges of microbial biofilms on medical devices, *Anal. Chem.* (2012). <https://doi.org/10.1021/ac2029997>.
- [183] J.N. Wilking, V. Zaboradaev, M. De Volder, R. Losick, M.P. Brenner, D.A. Weitz, Liquid transport facilitated by channels in *Bacillus subtilis* biofilms, *Proc. Natl. Acad. Sci. U. S. A.* (2013). <https://doi.org/10.1073/pnas.1216376110>.
- [184] P. Ramírez, M. Gordón, A. Soriano, S. Gil-Perotin, V. Marti, E.M. Gonzalez-Barbera, M.T. Sanchez-Aguilar, J.A. Simal, J. Bonastre, Assessment of the in vivo formation of biofilm on external ventricular drainages, *Eur. J. Clin. Microbiol. Infect. Dis.* (2013). <https://doi.org/10.1007/s10096-013-1895-8>.
- [185] A.K. Epstein, A.I. Hochbaum, P. Kim, J. Aizenberg, Control of bacterial biofilm growth on surfaces by nanostructural mechanics and geometry, *Nanotechnology*. (2011). <https://doi.org/10.1088/0957-4484/22/49/494007>.
- [186] K.M. Papp-Wallace, A. Endimiani, M.A. Taracila, R.A. Bonomo, Carbapenems: Past, Present, and Future, *Antimicrob. Agents Chemother.* 55 (2011) 4943–4960. <https://doi.org/10.1128/AAC.00296-11>.
- [187] A.S.L. Mendez, V. Weisheimer, T.P. Oppe, M. Steppe, E.E.S. Schapoval, Microbiological assay for the determination of meropenem in pharmaceutical dosage form, *J. Pharm. Biomed. Anal.* 37 (2005) 649–653. <https://doi.org/10.1016/j.jpba.2004.11.030>.
- [188] L. Huang, J. Haagensen, D. Verotta, P. Lizak, F. Aweeka, K. Yang, Determination of meropenem in bacterial media by LC–MS/MS, *J. Chromatogr. B.* 961 (2014) 71–76. <https://doi.org/10.1016/j.jchromb.2014.05.002>.
- [189] S. Bompadre, L. Ferrante, M. De Martinis, L. Leone, Determination of meropenem in serum by high-performance liquid chromatography with column switching, *J. Chromatogr. A.* 812 (1998) 249–253.

## References

[https://doi.org/10.1016/S0021-9673\(98\)00249-0](https://doi.org/10.1016/S0021-9673(98)00249-0).

- [190] M. Carlier, M. Noe, J.A. Roberts, V. Stove, A.G. Verstraete, J. Lipman, J.J. De Waele, Population pharmacokinetics and dosing simulations of cefuroxime in critically ill patients: non-standard dosing approaches are required to achieve therapeutic exposures, *J. Antimicrob. Chemother.* 69 (2014) 2797–2803. <https://doi.org/10.1093/jac/dku195>.
- [191] M. Beumier, G. Casu, M. Hites, L. Seyler, F. Cotton, J.-L. Vincent, F. Jacobs, F. Taccone,  $\beta$ -lactam antibiotic concentrations during continuous renal replacement therapy, *Crit. Care.* 18 (2014) R105. <https://doi.org/10.1186/cc13886>.
- [192] R. Denooz, C. Charlier, Simultaneous determination of five  $\beta$ -lactam antibiotics (cefepim, ceftazidim, cefuroxim, meropenem and piperacillin) in human plasma by high-performance liquid chromatography with ultraviolet detection, *J. Chromatogr. B.* 864 (2008) 161–167. <https://doi.org/10.1016/j.jchromb.2008.01.037>.
- [193] F. Mattioli, C. Fucile, V. Del Bono, V. Marini, A. Parisini, A. Molin, M.L. Zuccoli, G. Milano, R. Danesi, A. Marchese, M. Polillo, C. Viscoli, P. Pelosi, A. Martelli, A. Di Paolo, Population pharmacokinetics and probability of target attainment of meropenem in critically ill patients, *Eur. J. Clin. Pharmacol.* 72 (2016) 839–848. <https://doi.org/10.1007/s00228-016-2053-x>.
- [194] M.A. Pfaller, R.N. Jones, A review of the in vitro activity of meropenem and comparative antimicrobial agents tested against 30,254 aerobic and anaerobic pathogens isolated world wide, *Diagn. Microbiol. Infect. Dis.* 28 (1997) 157–163. [https://doi.org/10.1016/S0732-8893\(97\)00065-5](https://doi.org/10.1016/S0732-8893(97)00065-5).
- [195] G.K. McEvoy, Dose adjustment in renal impairment: Response from AHFS Drug Information, *BMJ.* 331 (2005) 293.1. <https://doi.org/10.1136/bmj.331.7511.293>.
- [196] A.S. Mendez, M. Steppe, E.E. Schapoval, Validation of HPLC and UV spectrophotometric methods for the determination of meropenem in pharmaceutical dosage form, *J. Pharm. Biomed. Anal.* 33 (2003) 947–954. [https://doi.org/10.1016/S0731-7085\(03\)00366-2](https://doi.org/10.1016/S0731-7085(03)00366-2).
- [197] M. Ehrlich, F. Daschner, K. Kümmerer, Rapid antibiotic drug monitoring; *J. Chromatogr. B Biomed. Sci. Appl.* 751 (2001) 357–363. [https://doi.org/10.1016/S0378-4347\(00\)00504-1](https://doi.org/10.1016/S0378-4347(00)00504-1).

## References

- [198] H. Elkhaili, S. Niedergang, D. Pompei, L. Linger, D. Leveque, F. Jehl, High-performance liquid chromatographic assay for meropenem in serum, *J. Chromatogr. B Biomed. Sci. Appl.* 686 (1996) 19–26. [https://doi.org/10.1016/S0378-4347\(96\)00205-8](https://doi.org/10.1016/S0378-4347(96)00205-8).
- [199] E. Brendel, M. Zschunke, I. Meineke, High-performance liquid chromatographic determination of cefonicid in human plasma and urine, *J. Chromatogr. B Biomed. Appl.* 339 (1985) 359–365.
- [200] Y. Mrestani, R. Neubert, F. Nagel, Capillary zone electrophoresis determination of meropenem in biological media using a high sensitivity cell., *J. Pharm. Biomed. Anal.* 20 (1999) 899–903.
- [201] J.M. Serrano, M. Silva, Rapid and sensitive determination of aminoglycoside antibiotics in water samples using a strong cation-exchange chromatography non-derivatisation method with chemiluminescence detection, *J. Chromatogr. A.* 1117 (2006) 176–183. <https://doi.org/10.1016/j.chroma.2006.03.086>.
- [202] K. Ikeda, K. Ikawa, N. Morikawa, M. Miki, S.-I. Nishimura, M. Kobayashi, High-performance liquid chromatography with ultraviolet detection for real-time therapeutic drug monitoring of meropenem in plasma, *J. Chromatogr. B.* 856 (2007) 371–375. <https://doi.org/10.1016/j.jchromb.2007.05.043>.
- [203] Y.-W. Chou, Y.-H. Yang, J.-H. Chen, C.-C. Kuo, S.-H. Chen, Quantification of meropenem in plasma and cerebrospinal fluid by micellar electrokinetic capillary chromatography and application in bacterial meningitis patients, *J. Chromatogr. B.* 856 (2007) 294–301. <https://doi.org/10.1016/j.jchromb.2007.06.015>.
- [204] S.G. Wicha, C. Kloft, Simultaneous determination and stability studies of linezolid, meropenem and vancomycin in bacterial growth medium by high-performance liquid chromatography, *J. Chromatogr. B.* 1028 (2016) 242–248. <https://doi.org/10.1016/j.jchromb.2016.06.033>.
- [205] M. Carlier, V. Stove, J.J. De Waele, A.G. Verstraete, Ultrafast quantification of  $\beta$ -lactam antibiotics in human plasma using UPLC–MS/MS, *J. Chromatogr. B.* 978–979 (2015) 89–94. <https://doi.org/10.1016/j.jchromb.2014.11.034>.
- [206] E. Çubuk Demiralay, D. Koç, Y.D. Daldal, G. Alsancak, S.A. Ozkan, Determination of chromatographic dissociation constants of some carbapenem group antibiotics and quantification of these compounds in

- human urine, *Biomed. Chromatogr.* 28 (2014) 660–666.  
<https://doi.org/10.1002/bmc.3085>.
- [207] S.E. Briscoe, B.C. McWhinney, J. Lipman, J.A. Roberts, J.P.J. Ungerer, A method for determining the free (unbound) concentration of ten beta-lactam antibiotics in human plasma using high performance liquid chromatography with ultraviolet detection, *J. Chromatogr. B.* 907 (2012) 178–184. <https://doi.org/10.1016/j.jchromb.2012.09.016>.
- [208] E. Dailly, R. Bouquié, G. Deslandes, P. Jolliet, R. Le Floch, A liquid chromatography assay for a quantification of doripenem, ertapenem, imipenem, meropenem concentrations in human plasma: Application to a clinical pharmacokinetic study, *J. Chromatogr. B.* 879 (2011) 1137–1142. <https://doi.org/10.1016/j.jchromb.2011.03.038>.
- [209] M. Cohen-Wolkowicz, N.R. White, A. Bridges, D.K. Benjamin, A.D.M. Kashuba, Development of a liquid chromatography–tandem mass spectrometry assay of six antimicrobials in plasma for pharmacokinetic studies in premature infants, *J. Chromatogr. B.* 879 (2011) 3497–3506. <https://doi.org/10.1016/j.jchromb.2011.09.031>.
- [210] B.C. McWhinney, S.C. Wallis, T. Hillister, J.A. Roberts, J. Lipman, J.P.J. Ungerer, Analysis of 12 beta-lactam antibiotics in human plasma by HPLC with ultraviolet detection, *J. Chromatogr. B.* 878 (2010) 2039–2043. <https://doi.org/10.1016/j.jchromb.2010.05.027>.
- [211] T. Ohmori, A. Suzuki, T. Niwa, H. Ushikoshi, K. Shirai, S. Yoshida, S. Ogura, Y. Itoh, Simultaneous determination of eight  $\beta$ -lactam antibiotics in human serum by liquid chromatography–tandem mass spectrometry, *J. Chromatogr. B.* 879 (2011) 1038–1042. <https://doi.org/10.1016/j.jchromb.2011.03.001>.
- [212] K. Kameda, K. Ikawa, K. Ikeda, N. Morikawa, A. Nakashima, H. Ohge, T. Sueda, HPLC method for measuring meropenem and biapenem concentrations in human peritoneal fluid and bile: application to comparative pharmacokinetic investigations., *J. Chromatogr. Sci.* 48 (2010) 406–11.
- [213] M. Phillips, K. Gleeson, J.M.B. Hughes, J. Greenberg, R.N. Cataneo, L. Baker, W.P. McVay, Volatile organic compounds in breath as markers of lung cancer: A cross-sectional study, *Lancet.* (1999). [https://doi.org/10.1016/S0140-6736\(98\)07552-7](https://doi.org/10.1016/S0140-6736(98)07552-7).
- [214] Y.Y. Broza, S. Khatib, A. Gharra, A. Krilaviciute, H. Amal, I. Polaka, S.

## References

- Parshutin, I. Kikuste, E. Gasenko, R. Skapars, H. Brenner, M. Leja, H. Haick, Screening for gastric cancer using exhaled breath samples, *Br. J. Surg.* (2019). <https://doi.org/10.1002/bjs.11294>.
- [215] M.K. Nakhleh, H. Amal, H. Awad, A. Gharra, N. Abu-Saleh, R. Jeries, H. Haick, Z. Abassi, Sensor arrays based on nanoparticles for early detection of kidney injury by breath samples, *Nanomedicine Nanotechnology, Biol. Med.* (2014). <https://doi.org/10.1016/j.nano.2014.06.007>.
- [216] World Health Organization (WHO) Concise International Chemical Assessment Document 53, Hydrogen sulfide: Human health aspects; WHO, Geneva, Switzerland, (2003).
- [217] S. De Geest, I. Laleman, W. Teughels, C. Dekeyser, M. Quirynen, Periodontal diseases as a source of halitosis: A review of the evidence and treatment approaches for dentists and dental hygienists, *Periodontol.* 2000. (2016). <https://doi.org/10.1111/prd.12111>.
- [218] S. Corrao, Halitosis: New insight into a millennial old problem, *Intern. Emerg. Med.* (2011). <https://doi.org/10.1007/s11739-011-0541-7>.
- [219] S. Yokoyama, M. Ohnuki, K. Shinada, M. Ueno, F.A. Clive Wright, Y. Kawaguchi, Oral malodor and related factors in Japanese senior high school students, *J. Sch. Health.* (2010). <https://doi.org/10.1111/j.1746-1561.2010.00512.x>.
- [220] A.C. Donaldson, M.P. Riggio, H.J. Rolph, J. Bagg, P.J. Hodge, Clinical examination of subjects with halitosis, *Oral Dis.* (2007). <https://doi.org/10.1111/j.1601-0825.2006.01248.x>.
- [221] M. Baharvand, Z. Maleki, S. Mohammadi, K. Alavi, E.J. Moghaddam, Assessment of oral malodor: A comparison of the organoleptic method with sulfide monitoring, *J. Contemp. Dent. Pract.* (2008). <https://doi.org/10.5005/jcdp-9-5-76>.
- [222] E. Iwanicka-Grzegorek, J. Michalik, J. Kepa, M. Wierzbicka, M. Aleksinski, E. Pierzynowska, Subjective patients' opinion and evaluation of halitosis using halimeter and organoleptic scores, in: *Oral Dis.*, 2005. <https://doi.org/10.1111/j.1601-0825.2005.01101.x>.
- [223] A. Tangerman, E.G. Winkel, The portable gas chromatograph OralChroma™: A method of choice to detect oral and extra-oral halitosis, in: *J. Breath Res.*, 2008. <https://doi.org/10.1088/1752-7155/2/1/017010>.

## References

- [224] N. Dhalla, S. Patil, K.K. Chaubey, I.S. Narula, The detection of BANA micro-organisms in adult periodontitis before and after scaling and root planing by BANA-Enzymatic TM test kit: An in vivo study, *J. Indian Soc. Periodontol.* (2015). <https://doi.org/10.4103/0972-124X.154167>.
- [225] J. Zhou, M. Ikram, A.U. Rehman, J. Wang, Y. Zhao, K. Kan, W. Zhang, F. Raziq, L. Li, K. Shi, Highly selective detection of NH<sub>3</sub> and H<sub>2</sub>S using the pristine CuO and mesoporous In<sub>2</sub>O<sub>3</sub>@CuO multijunctions nanofibers at room temperature, *Sensors Actuators, B Chem.* (2018). <https://doi.org/10.1016/j.snb.2017.08.200>.
- [226] Drager-Tubes & CMS Handbook; [https://www.draeger.com/Library/Content/tubeshandbook\\_br\\_9092086\\_en.pdf](https://www.draeger.com/Library/Content/tubeshandbook_br_9092086_en.pdf), accessed February 14, 2019., (2019) 9092086.
- [227] N. Alagirisamy, S.S. Hardas, S. Jayaraman, Novel colorimetric sensor for oral malodour, *Anal. Chim. Acta.* (2010). <https://doi.org/10.1016/j.aca.2009.11.064>.
- [228] S.M. Rosolina, T.S. Carpenter, Z.L. Xue, Bismuth-Based, Disposable Sensor for the Detection of Hydrogen Sulfide Gas, *Anal. Chem.* (2016). <https://doi.org/10.1021/acs.analchem.5b04489>.
- [229] Z. Zhang, Z. Chen, S. Wang, C. Qu, L. Chen, On-site visual detection of hydrogen sulfide in air based on enhancing the stability of gold nanoparticles, in: *ACS Appl. Mater. Interfaces*, 2014. <https://doi.org/10.1021/am500564w>.
- [230] P. Ni, Y. Sun, H. Dai, J. Hu, S. Jiang, Y. Wang, Z. Li, Z. Li, Colorimetric detection of sulfide ions in water samples based on the in situ formation of Ag<sub>2</sub>S nanoparticles, *Sensors Actuators, B Chem.* (2015). <https://doi.org/10.1016/j.snb.2015.05.066>.
- [231] C. Dong, Z. Wang, Y. Zhang, X. Ma, M.Z. Iqbal, L. Miao, Z. Zhou, Z. Shen, A. Wu, High-Performance Colorimetric Detection of Thiosulfate by Using Silver Nanoparticles for Smartphone-Based Analysis, *ACS Sensors.* (2017). <https://doi.org/10.1021/acssensors.7b00257>.
- [232] S.D. Using, L. Acetate, T. Paper, Lead Acetate Test Paper Introduction ; [https://www.amazon.com/Precision-Laboratories-Lead-Acetate-paper/dp/B001DBH4DQ/ref=sr\\_1\\_3?ie=UTF8&qid=1440613832&sr=8-3&keywords=lead+acetate#productdescription-iframe](https://www.amazon.com/Precision-Laboratories-Lead-Acetate-paper/dp/B001DBH4DQ/ref=sr_1_3?ie=UTF8&qid=1440613832&sr=8-3&keywords=lead+acetate#productdescription-iframe), access on February 14, (2019).



## References

- [233] H. Kimura, Hydrogen sulfide: From brain to gut, *Antioxidants Redox Signal.* (2010). <https://doi.org/10.1089/ars.2009.2919>.
- [234] S.A. Karimi, N. Hosseinmardi, M. Janahmadi, M. Sayyah, R. Hajisoltani, The protective effect of hydrogen sulfide (H<sub>2</sub>S) on traumatic brain injury (TBI) induced memory deficits in rats, *Brain Res. Bull.* (2017). <https://doi.org/10.1016/j.brainresbull.2017.07.014>.
- [235] C.L. Hou, M.J. Wang, C. Sun, Y. Huang, S. Jin, X.P. Mu, Y. Chen, Y.C. Zhu, Protective Effects of Hydrogen Sulfide in the Ageing Kidney, *Oxid. Med. Cell. Longev.* (2016). <https://doi.org/10.1155/2016/7570489>.
- [236] G. Farrugia, J.H. Szurszewski, Carbon monoxide, hydrogen sulfide, and nitric oxide as signaling molecules in the gastrointestinal tract, *Gastroenterology.* (2014). <https://doi.org/10.1053/j.gastro.2014.04.041>.
- [237] J.L. Wallace, Physiological and pathophysiological roles of hydrogen sulfide in the gastrointestinal tract, *Antioxidants Redox Signal.* (2010). <https://doi.org/10.1089/ars.2009.2900>.
- [238] K. Qu, S.W. Lee, J.S. Bian, C.M. Low, P.T.H. Wong, Hydrogen sulfide: Neurochemistry and neurobiology, *Neurochem. Int.* (2008). <https://doi.org/10.1016/j.neuint.2007.05.016>.
- [239] P. Kamoun, M.-C. Belardinelli, A. Chabli, K. Lallouchi, B. Chadeaux-Vekemans, Endogenous hydrogen sulfide overproduction in Down syndrome, *Am. J. Med. Genet.* (2003). <https://doi.org/10.1002/ajmg.a.10847>.
- [240] A. Martelli, L. Testai, A. Marino, M. C. Breschi, F. Da Settimo, V. Calderone, Hydrogen Sulphide: Biopharmacological Roles in the Cardiovascular System and Pharmaceutical Perspectives, *Curr. Med. Chem.* (2012). <https://doi.org/10.2174/092986712801215928>.
- [241] G. Yang, L. Wu, B. Jiang, W. Yang, J. Qi, K. Cao, Q. Meng, A.K. Mustafa, W. Mu, S. Zhang, S.H. Snyder, R. Wang, H<sub>2</sub>S as a physiologic vasorelaxant: Hypertension in mice with deletion of cystathionine  $\gamma$ -lyase, *Science* (80-. ). (2008). <https://doi.org/10.1126/science.1162667>.
- [242] M. Fu, W. Zhang, L. Wu, G. Yang, H. Li, R. Wang, Hydrogen sulfide (H<sub>2</sub>S) metabolism in mitochondria and its regulatory role in energy production, *Proc. Natl. Acad. Sci. U. S. A.* (2012). <https://doi.org/10.1073/pnas.1115634109>.

## References

- [243] M. Hoffman, A. Rajapakse, X. Shen, K.S. Gates, Generation of DNA-damaging reactive oxygen species via the autoxidation of hydrogen sulfide under physiologically relevant conditions: Chemistry relevant to both the genotoxic and cell signaling properties of H<sub>2</sub>S, *Chem. Res. Toxicol.* (2012). <https://doi.org/10.1021/tx300066z>.
- [244] D. Boehning, S.H. Snyder, Novel neural modulators, *Annu. Rev. Neurosci.* (2003). <https://doi.org/10.1146/annurev.neuro.26.041002.131047>.
- [245] W.A. Pryor, K.N. Houk, C.S. Foote, J.M. Fukuto, L.J. Ignarro, G.L. Squadrito, K.J.A. Davies, Free radical biology and medicine: It's a gas, man!, *Am. J. Physiol. - Regul. Integr. Comp. Physiol.* (2006). <https://doi.org/10.1152/ajpregu.00614.2005>.
- [246] R. Wierzbicka, L. Eyer, R. Landberg, A. Kamal-Eldin, M. Franek, Development of antibodies for determination of alkylresorcinol metabolites in human urine and elucidation of ELISA cross-reactivity, *J. Immunol. Methods.* (2014). <https://doi.org/10.1016/j.jim.2014.07.007>.
- [247] C.H. Geerkens, A.E. Matejka, R. Carle, R.M. Schweiggert, Development and validation of an HPLC method for the determination of alk(en)ylresorcinols using rapid ultrasound-assisted extraction of mango peels and rye grains, *Food Chem.* (2015). <https://doi.org/10.1016/j.foodchem.2014.08.001>.
- [248] A.B. Ross, Analysis of alkylresorcinols in cereal grains and products using ultrahigh-pressure liquid chromatography with fluorescence, ultraviolet, and coulArray electrochemical detection, in: *J. Agric. Food Chem.*, 2012. <https://doi.org/10.1021/jf301332q>.
- [249] M. V. Lind, M.L. Madsen, J.J. Rumessen, H. Vestergaard, R.J. Gøbel, T. Hansen, L. Lauritzen, O.B. Pedersen, M. Kristensen, A.B. Ross, Plasma alkylresorcinols reflect gluten intake and distinguish between gluten-rich and gluten-poor diets in a population at risk of metabolic syndrome 1-3, *J. Nutr.* (2016). <https://doi.org/10.3945/jn.116.236398>.
- [250] R. Landberg, P. Åman, L.E. Friberg, B. Vessby, H. Adlercreutz, A. Kamal-Eldin, Dose response of whole-grain biomarkers: Alkylresorcinols in human plasma and their metabolites in urine in relation to intake, *Am. J. Clin. Nutr.* (2009). <https://doi.org/10.3945/ajcn.2008.26709>.
- [251] F.A. Bernal, L.L. Orduz-Diaz, C. Guerrero-Perilla, E.D. Coy-Barrera, Diazo coupling reaction of catechins and alkylresorcinols with diazotized sulfanilic acid for quantitative purposes in edible sources: Method development and validation, *Food Anal. Methods.* (2016).

## References

<https://doi.org/10.1007/s12161-015-0207-6>.

- [252] M. Marklund, R. Landberg, A. Andersson, P. Aman, A. Kamal-Eldin, Alkylresorcinol metabolites in urine correlate with the intake of whole grains and cereal fibre in free-living Swedish adults, *Br. J. Nutr.* (2013). <https://doi.org/10.1017/S0007114512000621>.
- [253] Y. Zhu, K.L. Shurlknight, X. Chen, S. Sang, Identification and pharmacokinetics of novel alkylresorcinol metabolites in human urine, new candidate biomarkers for whole-grain wheat and rye intake, *J. Nutr.* (2014). <https://doi.org/10.3945/jn.113.184663>.
- [254] R. Wierzbicka, H. Wu, M. Franek, A. Kamal-Eldin, R. Landberg, Determination of alkylresorcinols and their metabolites in biological samples by gas chromatography-mass spectrometry, *J. Chromatogr. B Anal. Technol. Biomed. Life Sci.* (2015). <https://doi.org/10.1016/j.jchromb.2015.07.009>.
- [255] K.D. Kochanek, S.L. Murphy, J. Xu, E. Arias, Deaths: Final data for 2017, *Natl. Vital Stat. Reports.* (2019).
- [256] J.A. Martin, B.E. Hamilton, S.J. Ventura, M.J.K. Osterman, E.C. Wilson, T.J. Mathews, Births: Final data for 2010, *Natl. Vital Stat. Reports.* (2012).
- [257] M.O. Salles, J. Naozuka, M. Bertotti, A forensic study: Lead determination in gunshot residues, *Microchem. J.* (2012). <https://doi.org/10.1016/j.microc.2011.10.004>.
- [258] A. Tarifa, J.R. Almirall, Fast detection and characterization of organic and inorganic gunshot residues on the hands of suspects by CMV-GC-MS and LIBS, *Sci. Justice.* (2015). <https://doi.org/10.1016/j.scijus.2015.02.003>.
- [259] E. Bernal Morales, A.L. Revilla Vázquez, Simultaneous determination of inorganic and organic gunshot residues by capillary electrophoresis, *J. Chromatogr. A.* (2004). <https://doi.org/10.1016/j.chroma.2004.10.083>.
- [260] O. Dalby, D. Butler, J.W. Birkett, Analysis of gunshot residue and associated materials - A review, *J. Forensic Sci.* (2010). <https://doi.org/10.1111/j.1556-4029.2010.01370.x>.
- [261] K.H. Chang, P.T. Jayaprakash, C.H. Yew, A.F.L. Abdullah, Gunshot residue analysis and its evidential values: A review, *Aust. J. Forensic Sci.* (2013). <https://doi.org/10.1080/00450618.2012.691546>.

## References

- [262] Z. Brožek-Mucha, Trends in analysis of gunshot residue for forensic purposes, *Anal. Bioanal. Chem.* (2017). <https://doi.org/10.1007/s00216-017-0460-1>.
- [263] M. Grima, M. Butler, R. Hanson, A. Mohameden, Firework displays as sources of particles similar to gunshot residue, *Sci. Justice.* (2012). <https://doi.org/10.1016/j.scijus.2011.04.005>.
- [264] A. Farokhchah, N. Alizadeh, Determination of diphenylamine residue in fruit samples using spectrofluorimetry and multivariate analysis, *LWT - Food Sci. Technol.* (2013). <https://doi.org/10.1016/j.lwt.2013.05.032>.
- [265] L.S. Blakey, G.P. Sharples, K. Chana, J.W. Birkett, Fate and Behavior of Gunshot Residue—A Review, *J. Forensic Sci.* (2018). <https://doi.org/10.1111/1556-4029.13555>.
- [266] G.L. Burlison, B. Gonzalez, K. Simons, J.C.C. Yu, Forensic analysis of a single particle of partially burnt gunpowder by solid phase micro-extraction-gas chromatography-nitrogen phosphorus detector, *J. Chromatogr. A.* (2009). <https://doi.org/10.1016/j.chroma.2009.03.074>.
- [267] H. Mei, Y. Quan, W. Wang, H. Zhou, Z. Liu, H. Shi, P. Wang, Determination of Diphenylamine in Gunshot Residue by HPLC-MS/MS, *J. Forensic Sci. Med.* (2016). <https://doi.org/10.4103/2349-5014.162808>.
- [268] Y. Tong, Z. Wu, C. Yang, J. Yu, X. Zhang, S. Yang, X. Deng, Y. Xu, Y. Wen, Determination of diphenylamine stabilizer and its nitrated derivatives in smokeless gunpowder using a tandem MS method, *Analyst.* (2001). <https://doi.org/10.1039/b010183o>.
- [269] M. Morelato, A. Beavis, A. Ogle, P. Doble, P. Kirkbride, C. Roux, Screening of gunshot residues using desorption electrospray ionisation-mass spectrometry (DESI-MS), *Forensic Sci. Int.* (2012). <https://doi.org/10.1016/j.forsciint.2011.10.030>.
- [270] G. Scherperel, G.E. Reid, R. Waddell Smith, Characterization of smokeless powders using nanoelectrospray ionization mass spectrometry (nESI-MS), *Anal. Bioanal. Chem.* (2009). <https://doi.org/10.1007/s00216-009-2689-9>.
- [271] J. Arndt, S. Bell, L. Crookshanks, M. Lovejoy, C. Oleska, T. Tulley, D. Wolfe, Preliminary evaluation of the persistence of organic gunshot residue, *Forensic Sci. Int.* (2012). <https://doi.org/10.1016/j.forsciint.2012.05.011>.
- [272] M. Morelato, A. Beavis, P. Kirkbride, C. Roux, Forensic applications of

## References

- desorption electrospray ionisation mass spectrometry (DESI-MS), *Forensic Sci. Int.* (2013). <https://doi.org/10.1016/j.forsciint.2013.01.011>.
- [273] D. Laza, B. Nys, J. De Kinder, A. Kirsch-De Mesmaeker, C. Moucheron, Development of a quantitative LC-MS/MS method for the analysis of common propellant powder stabilizers in gunshot residue, *J. Forensic Sci.* (2007). <https://doi.org/10.1111/j.1556-4029.2007.00490.x>.
- [274] P.I. Reed, K. Haines, P.L.R. Smith, F.R. House, C.L. Walters, GASTRIC JUICE N-NITROSAMINES IN HEALTH AND GASTRODUODENAL DISEASE, *Lancet.* (1981). [https://doi.org/10.1016/S0140-6736\(81\)90939-9](https://doi.org/10.1016/S0140-6736(81)90939-9).
- [275] J. Hsu, J. Arcot, N. Alice Lee, Nitrate and nitrite quantification from cured meat and vegetables and their estimated dietary intake in Australians, *Food Chem.* 115 (2009) 334–339. <https://doi.org/10.1016/j.foodchem.2008.11.081>.
- [276] European Union. COMMISSION REGULATION (EC) No 1881/2006 of 19 December 2006 Setting maximum levels for certain contaminants in foodstuffs. *Official Journal of the European Union*, 20.12.2006, 364/5, (2006).
- [277] H. Salehzadeh, A. Maleki, R. Rezaee, B. Shahmoradi, K. Ponnet, The nitrate content of fresh and cooked vegetables and their health-related risks, *PLoS One.* 15 (2020) e0227551. <https://doi.org/10.1371/journal.pone.0227551>.
- [278] G. Elmasry, D.F. Barbin, D.W. Sun, P. Allen, Meat Quality Evaluation by Hyperspectral Imaging Technique: An Overview, *Crit. Rev. Food Sci. Nutr.* (2012). <https://doi.org/10.1080/10408398.2010.507908>.
- [279] K. Mc Donald, D.W. Sun, Effect of evacuation rate on the vacuum cooling process of a cooked beef product, *J. Food Eng.* (2001). [https://doi.org/10.1016/S0260-8774\(00\)00158-8](https://doi.org/10.1016/S0260-8774(00)00158-8).
- [280] J. Cai, Q. Chen, X. Wan, J. Zhao, Determination of total volatile basic nitrogen (TVB-N) content and Warner-Bratzler shear force (WBSF) in pork using Fourier transform near infrared (FT-NIR) spectroscopy, *Food Chem.* (2011). <https://doi.org/10.1016/j.foodchem.2010.11.098>.
- [281] F. Tao, Y. Peng, Y. Li, K. Chao, S. Dhakal, Simultaneous determination of tenderness and *Escherichia coli* contamination of pork using hyperspectral scattering technique, *Meat Sci.* (2012). <https://doi.org/10.1016/j.meatsci.2011.11.028>.

## References

- [282] B.H. Kong, L.Z. Ma Meat science and technology Chinese Light Industry Press, Beijing, China (2003), (2003) 2003.
- [283] A.H. Lockwood, J.M. McDonald, R.E. Reiman, A.S. Gelbard, J.S. Laughlin, T.E. Duffy, F. Plum, The dynamics of ammonia metabolism in man. Effects of liver disease and hyperammonemia, *J. Clin. Invest.* (1979). <https://doi.org/10.1172/JCI109322>.
- [284] R.S. Singhal, P.R. Kulkarni, D. V Rege, *Handbook of Indices of Food Quality and Authenticity*, 1997. <https://doi.org/10.1533/9781855736474>.
- [285] G. Barandun, M. Soprani, S. Naficy, M. Grell, M. Kasimatis, K.L. Chiu, A. Ponzoni, F. Güder, Cellulose Fibers Enable Near-Zero-Cost Electrical Sensing of Water-Soluble Gases, *ACS Sensors*. (2019). <https://doi.org/10.1021/acssensors.9b00555>.
- [286] Z. Ma, P. Chen, W. Cheng, K. Yan, L. Pan, Y. Shi, G. Yu, Highly Sensitive, Printable Nanostructured Conductive Polymer Wireless Sensor for Food Spoilage Detection, *Nano Lett.* (2018). <https://doi.org/10.1021/acs.nanolett.8b01825>.
- [287] L. Cao, G. Sun, C. Zhang, W. Liu, J. Li, L. Wang, An Intelligent Film Based on Cassia Gum Containing Bromothymol Blue-Anchored Cellulose Fibers for Real-Time Detection of Meat Freshness, *J. Agric. Food Chem.* (2019). <https://doi.org/10.1021/acs.jafc.8b06493>.
- [288] J. Chen, J. Gu, R. Zhang, Y. Mao, S. Tian, Freshness evaluation of three kinds of meats based on the electronic nose, *Sensors (Switzerland)*. (2019). <https://doi.org/10.3390/s19030605>.
- [289] M. Valdez, S.K. Gupta, K. Lozano, Y. Mao, ForceSpun polydiacetylene nanofibers as colorimetric sensor for food spoilage detection, *Sensors Actuators, B Chem.* (2019). <https://doi.org/10.1016/j.snb.2019.126734>.
- [290] C. Ruiz-Capillas, F. Jiménez-Colmenero, Biogenic amines in meat and meat products, *Crit. Rev. Food Sci. Nutr.* (2005). <https://doi.org/10.1080/10408690490489341>.
- [291] J. Stadnik, Z.J. Dolatowski, Biogenic amines in meat and fermented meat products, *Acta Sci. Pol. Technol. Aliment.* (2010).
- [292] E. De Mey, G. Drabik-Markiewicz, H. De Maere, M.C. Peeters, G. Derdelinckx, H. Paelinck, T. Kowalska, Dabsyl derivatisation as an alternative for dansylation in the detection of biogenic amines in

## References

- fermented meat products by reversed phase high performance liquid chromatography, *Food Chem.* (2012).  
<https://doi.org/10.1016/j.foodchem.2011.07.124>.
- [293] V. Sirocchi, G. Caprioli, M. Ricciutelli, S. Vittori, G. Sagratini, Simultaneous determination of ten underivatized biogenic amines in meat by liquid chromatography-tandem mass spectrometry (HPLC-MS/MS), *J. Mass Spectrom.* (2014). <https://doi.org/10.1002/jms.3418>.
- [294] M.S. Steiner, R.J. Meier, C. Spangler, A. Duerkop, O.S. Wolfbeis, Determination of biogenic amines by capillary electrophoresis using a chameleon type of fluorescent stain, *Microchim. Acta.* (2009).  
<https://doi.org/10.1007/s00604-009-0247-y>.
- [295] J. Ruiz-Jiménez, M.D. Luque de Castro, Pervaporation as interface between solid samples and capillary electrophoresis, *J. Chromatogr. A.* (2006).  
<https://doi.org/10.1016/j.chroma.2006.01.081>.
- [296] K.H. Eom, K.H. Hyun, S. Lin, J.W. Kim, The meat freshness monitoring system using the smart RFID tag, *Int. J. Distrib. Sens. Networks.* (2014).  
<https://doi.org/10.1155/2014/591812>.
- [297] N. Jornet-Martínez, S. Bocanegra-Rodríguez, R.A. González-Fuenzalida, C. Molins-Legua, P. Campíns-Falcó, In Situ Analysis Devices for Estimating the Environmental Footprint in Beverages Industry, in: *Process. Sustain. Beverages*, 2019. <https://doi.org/10.1016/b978-0-12-815259-1.00009-4>.
- [298] Z. Li, K.S. Suslick, Portable Optoelectronic Nose for Monitoring Meat Freshness, *ACS Sensors.* (2016).  
<https://doi.org/10.1021/acssensors.6b00492>.
- [299] J. Pla-Tolós, Y. Moliner-Martínez, C. Molins-Legua, R. Herráez-Hernández, J. Verdú-Andrés, P. Campíns-Falcó, Selective and sensitive method based on capillary liquid chromatography with in-tube solid phase microextraction for determination of monochloramine in water, *J. Chromatogr. A.* 1388 (2015) 17–23. <https://doi.org/10.1016/j.chroma.2015.02.024>.
- [300] N.S. Lawrence, J. Davis, R.G. Compton, Analytical strategies for the detection of sulfide: A review, *Talanta.* (2000).  
[https://doi.org/10.1016/S0039-9140\(00\)00421-5](https://doi.org/10.1016/S0039-9140(00)00421-5).
- [301] P. Campíns-Falcó, J. Verdú-Andrés, A. Sevillano-Cabeza, R. Herráez-Hernández, C. Molins-Legua, Y. Moliner-Martínez, In-tube solid-phase microextraction coupled by in valve mode to capillary LC-DAD: Improving

## References

- detectability to multiresidue organic pollutants analysis in several whole waters, *J. Chromatogr. A.* (2010).  
<https://doi.org/10.1016/j.chroma.2010.01.018>.
- [302] G. Gatidou, A. Kotrikla, N.S. Thomaidis, T.D. Lekkas, Determination of the antifouling booster biocides irgarol 1051 and diuron and their metabolites in seawater by high performance liquid chromatography-diode array detector, *Anal. Chim. Acta.* (2005).  
<https://doi.org/10.1016/j.aca.2004.10.012>.
- [303] I. Ferrer, D. Barceló, Validation of new solid-phase extraction materials for the selective enrichment of organic contaminants from environmental samples, *TrAC - Trends Anal. Chem.* (1999).  
[https://doi.org/10.1016/S0165-9936\(98\)00108-3](https://doi.org/10.1016/S0165-9936(98)00108-3).
- [304] R.A. Gimeno, C. Aguilar, R.M. Marcé, F. Borrull, Monitoring of antifouling agents in water samples by on-line solid-phase extraction-liquid chromatography-atmospheric pressure chemical ionization mass spectrometry, *J. Chromatogr. A.* (2001). [https://doi.org/10.1016/S0021-9673\(01\)00619-7](https://doi.org/10.1016/S0021-9673(01)00619-7).
- [305] A. Shrivastava, V. Gupta, Methods for the determination of limit of detection and limit of quantitation of the analytical methods, *Chronicles Young Sci.* (2011). <https://doi.org/10.4103/2229-5186.79345>.
- [306] J.V.-A. A.I. Argente-García, N. Jornet-Martínez, P. Campíns-Falcó, R. Herráez-Hernández, Y. Moliner- Martínez, Colorimetric Sensor Based on Silver Nanoparticles for the Determination of Volatile Sulphur Compounds Field of the Invention. EP3467476A1,PCT/ES2017/070532, EPO, 20 December 2018. Application number: P20160040., 2018.
- [307] J.C. Love, L.A. Estroff, J.K. Kriebel, R.G. Nuzzo, G.M. Whitesides, Self-assembled monolayers of thiolates on metals as a form of nanotechnology, *Chem. Rev.* (2005). <https://doi.org/10.1021/cr0300789>.
- [308] M. Baalousha, K.P. Arkill, I. Romer, R.E. Palmer, J.R. Lead, Transformations of citrate and Tween coated silver nanoparticles reacted with Na<sub>2</sub>S, *Sci. Total Environ.* (2015). <https://doi.org/10.1016/j.scitotenv.2014.09.035>.
- [309] R.A. Morales-Luckie, V. Sánchez-Mendieta, O. Olea-Mejia, A.R. Vilchis-Nestor, G. López-Téllez, V. Varela-Guerrero, L. Huerta, J. Arenas-Alatorre, Facile solventless synthesis of a nylon-6,6/silver nanoparticles composite and its XPS study, *Int. J. Polym. Sci.* (2013).  
<https://doi.org/10.1155/2013/235850>.



## References

- [310] B.C. Reinsch, C. Levard, Z. Li, R. Ma, A. Wise, K.B. Gregory, G.E. Brown, G. V. Lowry, Sulfidation of silver nanoparticles decreases *Escherichia coli* growth inhibition, *Environ. Sci. Technol.* (2012). <https://doi.org/10.1021/es203732x>.
- [311] G. Konvalina, H. Haick, Sensors for breath testing: From nanomaterials to comprehensive disease detection, *Acc. Chem. Res.* (2014). <https://doi.org/10.1021/ar400070m>.
- [312] Q. Zhang, N. Li, J. Goebel, Z. Lu, Y. Yin, A systematic study of the synthesis of silver nanoplates: Is citrate a “magic” reagent?, *J. Am. Chem. Soc.* (2011). <https://doi.org/10.1021/ja2080345>.
- [313] M. Schütz, D. Steinigeweg, M. Salehi, K. Kömpe, S. Schlücker, Hydrophilically stabilized gold nanostars as SERS labels for tissue imaging of the tumor suppressor p63 by immuno-SERS microscopy, *Chem. Commun.* (2011). <https://doi.org/10.1039/c0cc05229a>.
- [314] D. Steinigeweg, S. Schlücker, Monodispersity and size control in the synthesis of 20–100 nm quasi-spherical silver nanoparticles by citrate and ascorbic acid reduction in glycerol–water mixtures, *Chem. Commun.* (2012). <https://doi.org/10.1039/c2cc33850e>.
- [315] H. Eid, Non surgical management of periodontitis related halitosis among adults, *Saudi J. Heal. Sci.* (2014). <https://doi.org/10.4103/2278-0521.134855>.
- [316] D.L.A. Fernandes, T.A. Rolo, J.A.B.P. Oliveira, M.T.S.R. Gomes, A new analytical system, based on an acoustic wave sensor, for halitosis evaluation, *Sensors Actuators, B Chem.* (2009). <https://doi.org/10.1016/j.snb.2008.10.037>.
- [317] Y.J. Ahn, Y.J. Lee, J. Lee, D. Lee, H.K. Park, G.J. Lee, Colorimetric detection of endogenous hydrogen sulfide production in living cells, *Spectrochim. Acta - Part A Mol. Biomol. Spectrosc.* (2017). <https://doi.org/10.1016/j.saa.2017.01.040>.
- [318] L. Sanjuan-Navarro, A. Boughbina-Portolés, Y. Moliner-Martínez, P. Campíns-Falcó, Aqueous dilution of noble NPS bulk dispersions: Modeling instability due to dissolution by af4 and stablishing considerations for plasmonic assays, *Nanomaterials.* (2020). <https://doi.org/10.3390/nano10091802>.
- [319] J. Li, Y. Lin, B. Zhao, Spontaneous agglomeration of silver nanoparticles

## References

- deposited on carbon film surface, *J. Nanoparticle Res.* (2002).  
<https://doi.org/10.1023/A:1021120723498>.
- [320] Y. Ma, H. Su, X. Kuang, X. Li, T. Zhang, B. Tang, Heterogeneous nano metal-organic framework fluorescence probe for highly selective and sensitive detection of hydrogen sulfide in living cells, *Anal. Chem.* (2014).  
<https://doi.org/10.1021/ac503622n>.
- [321] Y.J. Ahn, Y.G. Gil, Y.J. Lee, H. Jang, G.J. Lee, A dual-mode colorimetric and SERS detection of hydrogen sulfide in live prostate cancer cells using a silver nanoplate-coated paper assay, *Microchem. J.* (2020).  
<https://doi.org/10.1016/j.microc.2020.104724>.
- [322] G. Asaithambi, V. Periasamy, Hydrogen sulfide detection by ESIPT based fluorescent sensor: Potential in living cells imaging, *J. Photochem. Photobiol. A Chem.* (2019).  
<https://doi.org/10.1016/j.jphotochem.2018.10.013>.
- [323] Y. Salinas, J. V. Ros-Lis, J.L. Vivancos, R. Martínez-Mañez, M.D. Marcos, S. Aucejo, N. Herranz, I. Lorente, Monitoring of chicken meat freshness by means of a colorimetric sensor array, *Analyst.* (2012).  
<https://doi.org/10.1039/c2an35211g>.
- [324] Freeman, J. Van Rensburg, DIRECTIVE 2006/118/EC OF THE EUROPEAN PARLIAMENT AND OF THE COUNCIL of 12 December 2006 On the protection of groundwater against pollution and deterioration. *Official Journal of the European Union*, 27.12.2006, 372/19., *Oficial J. Eur. Union.* (2006).
- [325] P. Serra-Mora, Y. Moliner-Martínez, C. Molins-Legua, R. Herráez-Hernández, J. Verdú-Andrés, P. Campíns-Falcó, Trends in Online Intube Solid Phase Microextraction, *Compr. Anal. Chem.* (2017).  
<https://doi.org/10.1016/bs.coac.2017.01.002>.
- [326] European Chemicals Agency (ECHA). Available online:  
<https://echa.europa.eu/es/informationon-chemicals/registered-substances> accessed on 31 January ., (2019).
- [327] M.J. Bailey, K.J. Kirkby, C. Jeynes, Trace element profiling of gunshot residues by PIXE and SEM-EDS: a feasibility study, *X-Ray Spectrom.* (2009).  
<https://doi.org/10.1002/xrs.1142>.
- [328] A.J. Schwoeble, D.L. Exline, *Current Methods in Forensic Gunshot Residue Analysis*, 2000. <https://doi.org/10.1201/9781420042573>.

## References

- [329] A. Gałuszka, Z.M. Migaszewski, P. Konieczka, J. Namieśnik, Analytical Eco-Scale for assessing the greenness of analytical procedures, *TrAC - Trends Anal. Chem.* (2012). <https://doi.org/10.1016/j.trac.2012.03.013>.
- [330] J. Płotka-Wasyłka, A new tool for the evaluation of the analytical procedure: Green Analytical Procedure Index, *Talanta*. (2018). <https://doi.org/10.1016/j.talanta.2018.01.013>.



# **ANNEX**



## **A1. Abbreviations**





## Annex

ACN	Acetonitrile
AF4	Asymmetrical flow field-flow fractionation
AgNPs	Silver nanoparticles
AR	Alkylresorcinol
au	Absorbance units
AuNPs	Gold nanoparticles
CFP	Carbon footprint estimation
CMYK	Cyan, Magenta, Yellow and Key
CTAB	Cetyl Trimethyl Ammonium Bromide
DCA	3,4 - dichloroaniline
DCPMU	1-(3, 4-Dichlorophenyl)-3-methylurea
DCPU	3, 4-Dichlorophenylurea
DESI-MS	Desorption electrospray ionization-mass spectrometry
DHCA	3,5-dihydroxyhydrocinnamic acid
DLLME	Liquid-dispersive liquid microextraction
DLL-ME	Dispersive liquid-liquid microextraction
DPA	Diphenylamine
ECHA	European Chemicals Agency
EEA	Environmental Protection Agency
EHS	Health and safety index
EQS	Environmental quality standards
ETTs	Endotracheal tubes
FB	Fast blue B
GC	Gas chromatography
GHG	Greenhouse gases
GIMP	Image manipulation program
GSR	Gunshot residues
HFLPME	Hollow fiber liquid phase microextraction
HS-SPME	Headspace solid phase microextraction
HSV	Hue, Saturation, Value
i.d.	Internal diameter
ICLEI	International Council of Local Environmental Initiatives
ILs	Ionic liquids
IMS	Ion mobility spectrometry
IT-SPME	In-tube solid phase microextraction
IUPAC	International union of pure and applied chemistry

## Annex

LC	Liquid chromatography
LOD	Detection limit
LOQ	Limit quantification
LPME	Liquid phase microextraction
MAC	Maximum allowable concentrations
MAE	Microwave assisted extraction
MF-LPME	Microfunnel-supported liquid-phase microextraction
MNPs	Metallic nanoparticles
MS	Mass spectrometry
MS-MS	Tandem mass spectrometry
MWCNTs	Multi-walled carbon nanotubes
NanoLC	Liquid nanochromatography
NEDD	Naphthyl ethylenediamine dihydrochloride
nESI-MS	Nanoelectrospray ionization mass spectrometry
NPs	Nanoparticles
NQS	1,2-naphthoquinone-4-sulfonate
OGSR	Organic gunshot residue
OMIMPF6	1-methyl-3-octylimidazolium hexafluorophosphate
PDMS	Polydimethylsiloxane
PEG	Polyethylene glycol
PR	1.3 dihydroxy-5-pentylbenzene
RGB	Red, Green, Blue
SA	Sulphanilamide
SBSE	Stir bar sorptive extraction
SDME	Single drop microextraction
SDS	Sodium dodecyl sulfate
SEM	Scanning electron microscopy
SEM-EDX	Scanning electron microscopy coupled to energy dispersion X-ray
SiO <sub>2</sub> NPs	Silicon dioxide nanoparticles
TD-GC-MS	Thermal desorption gas chromatography-mass spectrometry
TEM	Transmission electron microscopy
TEOS	Tetraethyl orthosilicate
TRB-20	20% diphenyl-95% polydimethylsiloxane
TRB-35	35% diphenyl-95% polydimethylsiloxane
TRB-5	5% diphenyl-95% polydimethylsiloxane
TRB-50	50% diphenyl-95% polydimethylsiloxane
TVBN	Volatile basic nitrogen
UHPLC	Ultra high pressure liquid chromatography

Annex

VAE	Vortex assisted extraction
VOCs	Volatile organic compounds
VSCs	Volatile sulfure compounds



## **A2. List of Figures**



Annex

<b>Figure 1.1 Weight of sustainability in different scientific areas expressed in percentages with respect to the total publications that contain this item. Web of Science source by searching sustainability (December 2020).</b> .....	<b>3</b>
<b>Figure 1.2 Sustainable systems: principles and approaches.</b> .....	<b>5</b>
<b>Figure 1.3 Evolution of the citation number of published papers in Web of Science for matching the search terms “sustainable chemistry” in a period of 12 years (December 2020).</b> .....	<b>10</b>
<b>Figure 1.4 Evolution of the number of citation in Web of Science for matching the search sustainable analytical chemistry for the last 12 years (December 2020).</b> .....	<b>13</b>
<b>Figure 1.5 Sustainable analytical chemistry scheme</b> .....	<b>14</b>
<b>Figure 1.6 Pictogram to evaluate and quantify the sustainability of an analytical procedure (Figures of merit 1: Sample treatment, method characteristics and calibration. Figures of merit 2: Quality control and Accuracy).</b> .....	<b>16</b>
<b>Figure 1.7. Schematic representation of the draw/eject configuration.</b> .....	<b>18</b>
<b>Figure 1.8. Schematic representation of the in- valve IT-SPME system.</b> .....	<b>18</b>
<b>Figure 1.9 Schematic representation of a IT-SPME system in circulation mode with two valves.</b> .....	<b>19</b>
<b>Figure 1.10 Schematic representation of in-situ and off-line analysis.</b> .....	<b>23</b>
<b>Figure 1.11 Number of publications in Web of Science for matching the following search term “sensors” and “in-situ analysis” in the 2000-2020 periods.</b> .....	<b>24</b>
<b>Figure 1.12 In-situ devices classification with some of their characteristics.</b>	<b>25</b>
<b>Figure 1.13 A) PDMS, B) TEOS, C) OMIMPF<sub>6</sub> structures</b> .....	<b>28</b>
<b>Figure 1.14 Derivatization reactions A) Reaction of NQS in the presence of primary, secondary amines or ammonia in an alkaline medium. B) Griess reaction in the presence of nitrites. C) Chemical reaction between AR and FB reagent.</b> .....	<b>30</b>
<b>Figure 1.15 Structure of Nylon</b> .....	<b>31</b>
<b>Figure 1.16 Number of publication evolution in Web of Science on Smartphone used with analytical applications.</b> .....	<b>32</b>

## Annex

Figure 1.17 Diuron and irgarol-1051 chemical structure with their main degradation products DCPU (3, 4-Dichlorophenylurea), DCPMU (1-(3, 4-Dichlorophenyl)-3-methylurea), DCA (3,4 - dichloroaniline) and M1 (2-methylthio-4-tert-butylamino-6-amino-s-triazine) respectively. ....	35
Figure 1.18 Chemical structure of meropenem. ....	43
Figure 1.19. A) DHCA and B) PR structures. ....	53
Figure 1.20 Chemical structure of DPA. ....	56
Figure 3.1 A) Cary 60 UV-Vis Spectrophotometer with B) Remote Diffuse Reflectance Accessory (DRA) accessory. ....	79
Figure 3.2 Optical microscopy ECLIPSE E200LED MV. ....	80
Figure 3.3 SEM - Hitachi S-4800. ....	80
Figure 3.4 CapLC-DAD system, Agilent 1200 Series with binary pump. ....	81
Figure 3.5 Steps for PDMS /TEOS-SiO <sub>2</sub> NPs-SA-NEDD-ILs sensing devices preparation. ....	83
Figure 3.6 Steps for PDM/TEOS-ILs-NQS-SiO <sub>2</sub> NPs sensing devices preparation. ....	84
Figure 3.7 A) Zn NPs in different proportions of surfactants A – CTAB 30% - SDS 70%; B – SDS 100%; C- CTAB 70% - SDS 30%. B) ZnNPs sensor preparation scheme. ....	85
Figure 3.8 Scheme of AgNPs sensor preparation ....	86
Figure 3.9 AgNPs multisensory sheet preparation scheme. A) corresponds to the multisensory sheet with 96 sensors, B) – 36 sensors, C) – 16 sensors. ....	87
Figure 3.10 A) NH <sub>3</sub> and H <sub>2</sub> S standard atmospheres preparation steps B) Humidity measurement using termo-hygrometer device. ....	89
Figure 3.11 Collecting human oral breath samples process in image. ....	93
Figure 3.12 Chicken meat samples preparation in 2 different packaging A) plastic bag and B) tupper. ....	94
Figure 3.13 Schematic representation of in valve IT-SPME coupled to a CapLC system. A) Load position B) Inject position. ....	96
Figure 3.14 Steps for meropenem extraction and detection from ETTs. ....	97



Annex

Figure 3.15 Sampling, extraction and detection process for DPA from shooting hands. ....	97
Figure 3.16 Nitrite or Nitrate detection scheme using PDMS /TEOS-SiO <sub>2</sub> NPs-SA-NEDD-OMIM-PF <sub>6</sub> sensor, based on the Griess reaction. ....	103
Figure 3.17 Gaseous ammonia standards generation scheme in the static dilution glass flask. ....	104
Figure 3.18 Images of standard dilution flask (A) and plastic bag (B) with AgNPs sensors. ....	105
Figure 3.19 Cells or standard assays steps and multisensor sheet image before and after exposure to different H <sub>2</sub> S concentrations. ....	106
Figure 4.1.1. Variation of the analytical response with A) The percentage of diphenyl groups in the PDMS based extractive phase; B) the processed sample volume (2.5 µg/L of Irgarol-1051 and 25 µg/L of diuron). ....	110
Figure 4.1.2 A) Chromatogram obtained for a mixture of target analytes under the optimum conditions B) UV-vis spectrum of diuron and C) UV-vis spectrum of irgarol- 1051. ....	111
Figure 4.1.3 Chromatogram obtained for sample 1. Inset: UV-vis spectra of peak tr = 8.7 min corresponding to irgarol-1051. ....	116
Figure 4.1.4 SEM micrographs for (A) PDMS-TEOS and (B) PDMS-TEOS-OMIM-PF <sub>6</sub> solid sensors. ....	120
Figure 4.1.5 A) Analytical signals obtained with PDMS-TEOS and PDMS-TEOS- OMIMPF <sub>6</sub> membranes doped with SA and NEDD. B) Analytical response study for different sensor sizes. ....	120
Figure 4.1.6 A) Griess reaction time optimization employed PDMS sensing devices for 0.5mg/L nitrite concentration. B) Vis spectra of different NO <sub>2</sub> <sup>-</sup> solutions employing Griess reagents entrapped in PDMS membranes. ....	121
Figure 4.1.7. A) ZnNPs and Zn power in CTAB-SDS surfactant mixture. B) Intensity size distribution of the ZnNPs dispersed (in the 30%SDS - 70%CTAB). ....	123
Figure 4.1.8 A) ZnNPs amount optimization in the reduction reaction of nitrate (24mg/L) to nitrite B) Reduction reaction time optimization of nitrate (20mg/L) to nitrite C) Analytical responses comparison using ZnNPs-Nylon and ZnNPs-dispersion. ....	124

Annex

**Figure 4.2.1 Response analysis of the spherical citrate-AgNPs of 20 nm in solution for Na<sub>2</sub>S and NaCH<sub>3</sub>S (registered after 20 seconds of each addition) at final concentration between 0-10000 ppb for (A) and citrated-AuNPs in solution for (B) at the same concentrations than those indicated in (A)..... 130**

**Figure 4.2.2 Fractograms obtained with dynamic light scattering (DLS) detector and batch DLS measurements of dispersions of citrate-capped AgNPs in absence and presence of sulfide. .... 131**

**Figure 4.2.3 Microscopy images of the membranes on nylon, glass fiber and cellulose membranes before (A) and after (B) retention of the AgNPs. .... 132**

**Figure 4.2.4 AgNPs-coated membranes of A) Nylon, B) Glass fiber and C) Cellulose. The prepared membranes were exposed to different concentrations of H<sub>2</sub>S (0, 150, 500 ppbv). .... 132**

**Figure 4.2.5 Raman spectra of the nylon and AgNPs-nylon membranes after beingexposed for 10 min to different H<sub>2</sub>S concentrations (0, 150, 250, 500, 1500 ppbv). .... 133**

**Figure 4.2.6 Study of the response of the different sizes of AgNPs 10, 20, and 40 nm to sulfide (A) in solution and (B) using the membranes in air. The signal for several dispersions of AgNPs was registered after 20 s of the addition of aliquots of Na<sub>2</sub>S to resulting amounts from 65 to 4925 µg of sulfide. The membrane analytical responses were registered by diffuse reflectance after being exposed to H<sub>2</sub>S for 10 min at amounts from 650 to 5251 µg of sulfide. . 134**

**Figure 4.2.7 Spectra registered for AgNPs of 20 nm with different amounts of sulfide and the dependence between them for sulfide quantification (A) in solution after the addition of Na<sub>2</sub>S from 65 to 4925 µg of sulfide and (B) coated on the membrane after being exposed to H<sub>2</sub>S for 10 min at amounts from 650 to 5251 µg to sulfide..... 135**

**Figure 4.2.8 Study of the behavior of AgNPs in presence of sulfide. (A) TEM images of a dispersion of AgNPs before and after addition of sulfide (250 ppb) in water, scale bar: 400 nm. (B) SEM images of the AgNP nylon membranes before and after being exposed to sulfide (250 ppbv), scale bar: 50 nm. .... 136**

Annex

**Figure 4.2.9** Quantification of H<sub>2</sub>S volatilization in atmospheres by the methylene blue method. In green the signal corresponding to the aqueous mixture containing 0.2 ppm of sulphide, in blue its absorbance after its volatilization for 10 min in a static dilution flask of 2 L and in black a mixture without sulphide as a blank. .... 137

**Figure 4.2.10** Percentage of the response of the sensor and colour of the sensors obtained at different humidity 96%, 50% and 20% compared with the blank. .... 138

**Figure 4.2.11:** Sensors measured by diffuse reflectance before (A) and after (B) being coated with glycerol. .... 138

**Figure 4.2.12** Selectivity of the AgNPs plasmonic membrane against other VOCs in human breath of interest at concentration of 5000 ppbv..... 140

**Figure 4.2.13** Stability of the AgNPs plasmonic sensors over time. Comparison of the responses obtained for H<sub>2</sub>S at concentration of 250 ppbv using three membranes prepared the same day and the response of three membranes after several days of storage in different conditions; at 20<sup>o</sup> C, 4 <sup>o</sup>C and in absence/presence of glycerol. .... 141

**Figure 4.2.14** Quantification of H<sub>2</sub>S using the plasmonic membrane: (A)Ploting of the A550/A415 versus Log H<sub>2</sub>S concentration (ppbv) with image membrane after being exposed 10 min to different concentrations of H<sub>2</sub>S. (C) Representation of the normalized spectra at 550 nm versus H<sub>2</sub>S in ppmv. (D) Representation of the RGB components (Red intensity value) versus H<sub>2</sub>S ppbv concentration. .... 142

**Figure 4.2.15** Absorbance spectra by the reflection mode of the membranes using the GoSpectra accessory coupled to a smartphone iPhone 5s before and after being exposed to H<sub>2</sub>S for 10 min..... 143

**Figure 4.2.16** Response of the plasmonic membranes to A) CH<sub>3</sub>SH at 1000 ppb and B) (CH<sub>3</sub>)<sub>2</sub>S at concentration from 150, 250, 500, 1000, 1500 ppbv. .... 143

**Figure 4.2.17** Determination of volatile sulphide for A) ten volunteers (n=3) and B) for four volunteers before and after food intake rich in allium vegetables (garlic). .... 146

Annex

**Figure 4.2.18** Normalized absorbance spectra obtained for sulfide air standards generated into the static volumetric flask and transferred to the bags and normalized spectra of a breath sample (A). Normalized absorbance at 550 nm was over the concentration of sulfide for standards and a sample (B)..... 147

**Figure 4.2.19** A) Plasmonic bands of the blanks (dashed line), and displacement of the plasmonic band in the presence of H<sub>2</sub>S (2 mg/L) (continuous line) in both cases the test time was 2 hours. **Figure 4.2.20** B) Analytical response of standard (gray color) and blank (black color) expressed with absorbance normalized at 500nm..... 149

**Figure 4.2.20** Reproducibility of sensor along with the images of the distribution of the AgNPs sensors in the Nylon sheet plate A) Without glycerol. B) With glycerol. .... 150

**Figure 4.2.21** Normalized Vis spectra of different H<sub>2</sub>S concentration detected by AgNPs multisensor sheet..... 151

**Figure 4.2.22** Cells or standard assays steps and multisensor sheet image before and after exposure to different H<sub>2</sub>S concentrations..... 153

**Figure 4.2.23** Ischemia-reperfusion model in AC10 analyzed using AgNps multisensors sheets. A) Experimental design used. B) Quantification of H<sub>2</sub>S values produced by AC10 under different culture conditions. The bars represent the mean and standard deviation of 3 independent experiments. C) Cell viability of AC10 under different culture conditions. The bars represent the mean and standard deviation of 3 independent experiments. \* <p .05 t-student paired test. .... 154

**Figure 4.2.24** Hexagon pictograms of several H<sub>2</sub>S detection using different analytical sensors: A) nylon-supported AgNPs plasmonic assay, B) 96-well nylon-supported AgNPs multisensory sheet, C) nano metal-organic fluorescence probe, D) Ag nanoplate-coated paper assay and E) fluorescent chemosensor. .... 156

**Figure 4.2.25** A) Schematic diagram of the proposed device and chemical reaction between AR and FB reagent B) Variation of the response as a function of the membrane composition C) SEM micrographs of the FB-doped sensing membranes..... 159

**Figure 4.2.26** Variation of the response as a function of the concentration obtained with the conventional solution derivatization reaction. .... 160

Annex

Figure 4.2.27 A) Variation of the response as a function processed volume in SPE y B) Study of the reaction time. .... 161

Figure 4.2.28 A) Spectra variation as a function of the concentration B) Chromatograms obtained for the derivative formed with the sensing membranes with and without SPE. .... 162

Figure 4.2.29 A) Schematic diagram of the SPE procedure, B) Image of the derivatized urine samples 1: sample and 2: spiked sample with DHCA 0.8 mg/L. C) Comparison of spectra obtained for that sample and spiked sample. D) Chromatograms obtained for a derivatized sample with and without derivatization..... 164

Figure 4.2.30 A) Variation of the chromatographic profiles in the different sampling days (day 1: gluten intake, day 2: gluten-free diet and day 3: gluten intake), B) Images corresponding to the derivatized samples in the three sampling days, and C) Variation of the signal obtained with the spectroscopic measurements and the chromatographic measurements. .... 165

Figure 4.2.31 Analytical response (peak area) obtained as function of the A) processed volume, B) capillary columns length, C) Sample processed flow and D) capillary coating. [Meropenem] = 0.5 $\mu$ g/mL. Mobile phase ACN:water in gradient elution mode: t = 0 min acetonitrile:10% during 10 min, increased to 15% from 11 min to 13 min, and then from 14 min to 15 min-10% acetonitrile. Mobile phase flow rate was 8  $\mu$ L/min. .... 169

Figure 4.2.32 A) Chromatograms obtained for increasing concentrations of meropenem: 0.1, 0.2, 0.5 and 1  $\mu$ g/mL. B) Chromatograms obtained for a sample extracted from the ETTs and a standard solution (0.5  $\mu$ g/mL). Inset. Spectrum of the meropenem found in the ETT sample VAE: 1 min using water as extraction solvent under stirring. In-tube SPME conditions: TRB-35 capillary column (60 cm) processed volume = 500 $\mu$ L and flow 9 $\mu$ L/seg. Chromatographic conditions: mobile phase ACN:water in gradient elution mode: t=0 min acetonitrile:10% during 10 min, increased to 15% from 11 min to 13 min, and then from 14 min to 15 min -10% acetonitrile. Mobile phase flow rate was 8 $\mu$ L/min. .... 172

Figure 4.3.1 Variation of the analytical response of NH<sub>3</sub> (20 ppmv at 8 hours) in atmospheres as a function of OMIM-PF<sub>6</sub> mass proportion in the polymeric matrix..... 175

**Figure 4.3.2** Optical microscope images (magnification 10) of sensing membranes A) without OMIM-PF<sub>6</sub> B) with 0.2 % OMIM-PF<sub>6</sub> C) with 7.8 % OMIM-PF<sub>6</sub> and D) scheme of the sensing membrane (7.8 % IL) before and after the exposure to NH<sub>3</sub> with the optimum sensing membrane (magnification 50). E) SEM micrograph of the transversal cut of the polymeric membrane without IL F) SEM micrograph of the transversal cut of the polymeric membrane containing 7.8 % IL and porous measurements..... 176

**Figure 4.3.3** A) Schematic diagram of the sensing membrane composition and its response. B) SEM micrograph of the transversal cut of the polymeric membrane containing 7.8 % IL. C) Bright-field microscopy photographs of 10x magnification obtained for sensing membrane before and after ammonia exposition..... 177

**Figure 4.3.4** Variation of the sensing response of NH<sub>3</sub> at several levels of concentration (ppmv) as a function of the exposure time with OMIM-PF<sub>6</sub>-NQS-PDMS/TEOS-SiO<sub>2</sub> NPs..... 179

**Figure 4.3.5** Variation of the sensing response of NH<sub>3</sub> (ppmv) as a function of the exposition time with PDMS/TEOS-NQS- SiO<sub>2</sub> NPs (red columns) and PDMS/TEOS-NQS- SiO<sub>2</sub> NPs-OMIM-PF<sub>6</sub> (blue columns). ..... 180

**Figure 4.3.6** Relationship between the obtained slopes of the straight lines  $1/\mu\text{g}_{\text{adsorbed}}$  vs  $1/\mu\text{g}_{\text{standard}}$  considering Langmuir isotherm vs sensor sampling times for several concentrations and an insert with their values for each time. .... 182

**Figure 4.3.7** A) NQS sensor exposed to several atmospheres of ammonia and primary and secondary amines in a 22 mL vial B) Selective colour response depending on the chemical nature of the amine C) Sensors absorbance spectra including a blank sensor D) Spectra difference between ammonia and each amine response in relation to the blank sensor. .... 184

**Figure 4.3.8** A) NQS-based sensor exposed to sulphide standards prepared in a 100 mL plastic bag B) Chicken sample atmosphere in a 100 mL plastic bag in which the NQS-based and the AgNPs sensors were exposed C) NQS-based sensor absorption spectra stored for 10 days at 4 °C in the presence of H<sub>2</sub>S standards (1,3,5 ppmv) D) NQS-based sensor absorption spectra stored for 2 days at 20 °C and 10 days at 4 °C in the presence of the chicken sample..... 186

**Figure 4.3.9** Sensor responses when exposed to a 20 ppmv ammonia atmosphere at 75 and 88 % humidity conditions compared to the reference blank sensor (left), which presented the same response between 51 and 88 % humidity conditions. .... 188

**Figure 4.3.10** Optical microscope images of the porous using (up) a x10 objective and non-porous face (down) using a x50 objective of the sensor (A). Sensor spectra for porous and non-porous face for chicken meat and blank samples under refrigerated conditions for 10 days (B)..... 189

**Figure 4.3.11** Two half circles of the IL-NQS-PDMS sensor stucked at the tupperware lid and the reference sensors are placed at the lid on the outside part (A) Sensor evolution of the % R coordinate during 10 days when the meat sample is kept under refrigeration conditions (B). .... 190

**Figure 4.3.12** A) Ammonia gaseous standard calibration curves inside a 100 mL plastic bag for 10 ppmv (blue), and 50 ppmv (green); insert: sensors placed inside a 100 mL plastic bag of gaseous standards. The reference sensors (blank and concentrated) for obtaining the images are located outside the bag. B) Difference absorption profile between the 50 ppmv ammonia standard and the atmosphere meat (both half's of the sensor) and blank reference sensor at the beginning (dotted line) and after 10 days (solid line) of analysis. C) Images of the evolution of the sensor colour obtained for standards and meat sample with time and meat freshness status divided into three groups: fresh, sub-fresh and putrid. .... 192

**Figure 4.4.1** Effect of A) acetonitrile percentage and flow of mobile phase (800  $\mu$ L at 7 ng/mL, TRB-35, 30 cm) B) nature of the extractive phase (800  $\mu$ L at 5 ng/mL, capillary length 30 cm, optimum mobile phase) C) capillary length (800  $\mu$ L, 5 ng/mL, TRB-35, optimum mobile phase) and D) sample volume processed (5 ng/mL, TRB-35, capillary length 90 cm, optimum mobile phase) on the DPA retention in IT-SPME. .... 198

**Figure 4.4.2** Comparison of peak areas obtained for standard solution (3 $\mu$ L of 10  $\mu$ g/mL in 2 mL of water, 15 ng/mL) with different A) extraction modalities B) sample collectors C) extraction time and D) effect of solvents to wet cotton swab (at 10 ng/mL) together with normalized spectra (inset) of DPA (black dashed line) and unknown compound (black solid line). .... 201

Annex

**Figure 4.4.3 Chromatograms of blanks (dashed lines) and standard solution of 5 ng/mL DPA (solid lines) obtained with different extraction solvents: water (a), 90:10 water: ethanol (b) and 90:10 water: acetonitrile (c). ..... 203**

**Figure 4.4.4 (A) Chromatograms obtained for sample 2A (black solid line) and blank of non-shooter hand (black dashed line). (B) DPA spectra found (blue line) in reference to the library of the standard (red line). ..... 206**

**Figure 4.4.5 Visual and microscopy (10x magnification) inspection of cotton swab after sampling a non-shooter hand (A) and after sampling a shooter hand (B). ..... 208**

**Figure 4.4.6 A) SEM image and B) Energy dispersion X-ray EDX spectra of inorganic gunshot residue found on a swab sample (sample 2A) after shooting. .... 209**

**Figure 4.4.7 SEM images (left) and EDX spectra (right) of non-spherical particles found on tapes used to collect GSRs after shooting a pistol: sample 22K.2 (A), sample 25N.3(B), sample 21K.1 (C), sample 25N.2 (D). ..... 210**







**Figure 4.4.8 (A) SEM image (B) overlay X-ray map of singles X-ray of Sb (C); Pb (D) and Ba (E) of particle found on a tape used to collect GSR on hands after shooting. .... 211**



### **A3. List of Tables**



Annex

Table 1.1 Summary of the principles and approaches in sustainability.....	5
Table 1.2 The 12 principles of Green Chemistry .....	11
Table 1.3 PDMS based capillary columns used in this Thesis.....	20
Table 1.4 General classification of LC systems taking into account the dimensions of the column and the flow. ....	21
Table 1.5 Concentrations limits of nitrate or nitrite established by different regulations.....	37
Table 1.6 Main analytical properties of different procedures described in the literature for NO <sub>2</sub> <sup>-</sup> /NO <sub>3</sub> <sup>-</sup> determination (*related with higher complexity of the parameter). ....	39
Table 1.7 Main analytical properties of different analytical methods proposed for Meropenem and other antimicrobials in the bibliography. ....	44
Table 1.8 Summary of existing methods for the in situ sulphide determination.....	49
Table 1.9 Previously proposed techniques for the determination of AR. ....	54
Table 1.10 Comparison of reported methods for DPA on a shooter's hands The method proposed in this work was also included for comparison (On-line in-tube solid phase microextraction coupled to capillary liquid chromatography with diode array detection (IT-SPME-CapLC-DAD). ....	58
Table 1.11 Concentrations limits of nitrate or nitrite established by different regulations.....	60
Table 1.12 Different procedures described in the literature for TVBM quantification in meat matrix. ....	64
Table 3.1 Summary of reagents with their commercial suppliers and GHS pictograms, were  - (GHS02) flammable,  - (GHS05) corrosive,  - (GHS06) toxic,  - (GHS07) harmful,  - (GHS08) health hazard,  - (GHS09) environmental hazard. ....	77
Table 3.2 Composition of PDMS/TEOS-FB sensing membrans.....	84
Table 3.3 Types of matrices and the analytes determined. ....	90
Table 3.4 Experimental conditions used in the analysis of different matrix by IT-SPME-Cap-DAD. ....	101

Annex

Table 3.5 Experimental conditions used in the in-situ analysis of compound by PDMS-sensor and AgNPs-sensor.....	102
Table 4.1.1 Analytical parameters obtained with the proposed method to determine diuron and irgarol-1051. ....	112
Table 4.1.2 Estimation of carbon footprints Kg CO <sub>2</sub> /100 samples of different analytical procedures proposed for antifouling biocides in water samples. ....	114
Table 4.1.3 Samples screened quantification results and recoveries from water samples determined by in-tube SPME-CapLC-DAD.....	117
Table 4.1.4. Figures of merit obtained using the different methodologies proposed for detection of nitrites and nitrates. <sup>(a)</sup> Assay carried out by adding the conventional Griess method <sup>(b)</sup> Assay performed by using the synthesized PDMS sensor and ZnNPs – dispersion. <sup>(c)</sup> Assay carried out by using PDMS sensor and ZnNPs-Nylon for reduction reaction. ....	126
Table 4.1.5 Detected concentrations of NO <sub>3</sub> <sup>-</sup> and NO <sub>2</sub> <sup>-</sup> in different water samples using PDMS sensor.....	127
Table 4.2.1 Determination of volatile sulphide in breath samples from two volunteers. ....	145
Table 4.2.2 Figures of merit obtained using the AgNPs sensor for H <sub>2</sub> S detection under following condition: temperature at 37°C with 95% atmosphere humidity for 8 hours.....	152
Table 4.2.3 Analytical parameters obtained with sensor and chromatographic methods to determine AR in standard solution and extracted from real samples. ....	164
Table 4.2.4 Calculated concentrations for the spectroscopic and chromatographic responses.....	166
Table 4.2.5 Figures of merit obtained for the determination of meropenem by in-tube SPME-CapLC-DAD. ....	171
Table 4.2.6 Found concentrations and recovery values calculated for meropenem in samples from ETTs from patient in ICU. ....	172
Table 4.3.1 Parameters of linear regressions (mA vs ppmv) for gaseous standards of ammonia, methylamine and dimethylamine for several sampling volumes and sampling times, under 25 ° C. ....	183

Annex

**Table 4.3.2 Calibration curves at 4°C and 10 days obtained when plotting the concentration of the ammonia standards of 10, 20 and 50 ppmv in 100 mL as a function of diffuse reflectance measurements at 590 nm and percentage of the R coordinate, respectively. .... 192**

**Table 4.3.3 Found concentrations in canned and fresh food green vegetables. Recoveries corresponding to samples fortified with standard nitrate solution (5 mg/L)..... 195**

**Table 4.4.1 Analytical parameters obtained with the proposed method to determine DPA in standard solutions and extracted from real samples..... 204**

**Table 4.4.2 Samples screened, quantification results of DPA on hands determined by optimized extraction procedure followed by in-tube SPME-CapLC-DAD. \*Tape lift kit samples quantified by regression equation 14 times lower than regression equation by cotton swab. \*\* On shooters hands. .... 207**

**Table 4.4.3 Summary of shape, surface, and elemental composition of GRS particles found on tape lift kits from shooter hands. .... 212**



## **A4. PhD contributions to publication**





## Annex

1. J. Pla- Tolós, P. Serra-Mora, **L. Hakobyan**, C. Molins-Legua, Y. Moliner- Martinez, P. Campins Falcó. A sustainable on-line CapLC method for quantifying antifouling agents like irgarol-1051 and diuron in water samples: Estimation of the carbon footprint. *Science of the Total Environment* 569-579,611-618, 2016. Impact Factor (2019): 6.551. Contribution 30%
2. **L. Hakobyan**, J. Plá - Tolos, Y. Moliner-Martinez, C. Molins-Legua, P. Campins-Falcó, Jesús Ruiz Ramos, Paula Ramirez - Galleymore. Determination of antimicrobials in invasive medical devices by in-tube solid phase microextraction as preconcentration tool: application to endotracheal tubes. *Journal of Pharmaceutical and Biomedical Analysis* 151(2018) 170-177. Impact Factor (2019): 3.209. Contribution 50%.
3. A. Argente-García, **L. Hakobyan**, C. Guillem, P. Campíns-Falcó, A new method for estimating diphenylamine in gunshot residues as a new tool for identifying both, inorganic and organic ones, in the same sample. *Separations* **2019**, 6, 16. Open Access. Contribution 50%.
4. N. Jornet-Martínez, **L. Hakobyan**, A. I. Argente-García, C. Molins-Legua, P. Campíns-Falcó, Nylon-Supported Plasmonic Assay Based on the Aggregation of Silver Nanoparticles: In Situ Determination of Hydrogen Sulfide-like Compounds in Breath Samples as a Proof of Concept. *Journal ACS Sensors*. **2019**, 4, 2164–2172. Impact Factor (2019): 6.944. Contribution 50%.
5. A. Ballester-Caudet, **L. Hakobyan**, Y. Moliner-Martinez\*, C. Molins-Legua, P. Campíns-Falcó, Ionic-liquid doped polymeric composite as passive colorimetric sensor for meat freshness as a use case. *Journal Talanta*. 2021, 223, 2, 121778. Impact Factor (2019): 5.339. Contribution 100%.
6. **L. Hakobyan**, Y. Moliner Martínez, C. Molins-Legua, P. Campíns-Falcó, New approach for Griess reaction based on reagent stabilization on PDMS membranes and ZnNPs as reductor of nitrates. Application to environmental waters and waters from canned and fresh vegetable samples. Submitted. Contribution 100%
7. **L. Hakobyan**, M.C. Prieto-Blanco, Maria Roca Llorens, C. Molins-Legua, M. Fuster-García, Y. Moliner-Martinez, P. Campins-Falcó,

Annex

Carmen Ribes-Koninckx, Fast Blue B Functionalized Silica-Polymer Composite to Evaluate DHHC as Biomarker of Gluten Intake. Submitted. Contribution 100%

8. **L. Hakobyan**, A. Ballester-Caudet, C. Molins-Legua, P. Campíns-Falcó, S. Tejedor, E. Peiró Moline, A. Dorronsoro, P. Sepulveda.  
Título: Colorimetric multiplatform for determination of endogenous H<sub>2</sub>S emitted by living cells: application to cardiomyocytes.  
Submitted. Contribution 100%